



HAL
open science

Interplay between cancer cells and cancer-associated fibroblasts in tumor invasion and metastasis formation

Youmna Marie Lyne Atieh

► **To cite this version:**

Youmna Marie Lyne Atieh. Interplay between cancer cells and cancer-associated fibroblasts in tumor invasion and metastasis formation. Cellular Biology. Université Pierre et Marie Curie - Paris VI, 2017. English. NNT : 2017PA066140 . tel-01635271

HAL Id: tel-01635271

<https://theses.hal.science/tel-01635271>

Submitted on 14 Nov 2017

HAL is a multi-disciplinary open access archive for the deposit and dissemination of scientific research documents, whether they are published or not. The documents may come from teaching and research institutions in France or abroad, or from public or private research centers.

L'archive ouverte pluridisciplinaire **HAL**, est destinée au dépôt et à la diffusion de documents scientifiques de niveau recherche, publiés ou non, émanant des établissements d'enseignement et de recherche français ou étrangers, des laboratoires publics ou privés.

Université Pierre et Marie Curie

Ecole doctorale : Complexité du Vivant

THESE DE DOCTORAT

Mention Biologie Cellulaire

Présentée par **Youmna Atieh**

Interplay between cancer cells and cancer-associated fibroblasts in tumor invasion and metastasis formation

Rôle des fibroblastes associés au cancer dans l'invasion tumorale

Dirigée par le **Pr. Danijela Matić Vignjević**

Présentée et soutenue publiquement le 4 juillet 2017

Jury

Pr. Fatima Mechta-Grigoriou

Présidente

Pr. Johanna Ivaska

Rapporteur

Dr. Olivier Destaing

Rapporteur

Dr. Alexandre Boissonnas

Examineur

Pr. Danijela Matić Vignjević

Directrice de thèse – membre invité

Outline

I.	Introduction.....	5
	Chapter 1: The gut – a model organ to study cell migration and tumorigenesis....	5
	Chapter 2: Overview on the basic principles of cell motility	7
	2.1. Migration on 2D substrates.....	8
	2.2. Integrins, mediators of the crosstalk between cells and the ECM.....	12
	2.3. Migration and invasion in 3D matrices.....	18
	Chapter 3: Cancer invasion and metastasis – when cells go wild	26
	3.1. Modes of cancer cell invasion	27
	3.2. Following gradients in cell motility.....	29
	Chapter 4: The tumor microenvironment	33
	4.1. The extracellular matrix – structural composition and architecture	34
	Chapter 5: Cancer-associated fibroblasts in tumor development	42
	5.1. Their origin(s).....	43
	5.2. At the primary site	44
	5.3. Reaching secondary organs.....	55
II.	Objectives and Hypotheses	60
III.	Results	61
	1. How do CAFs assist cancer cell invasion at the primary site?.....	61
	<i>Introduction</i>	61
	<i>Results</i>	62
	<i>Conclusion</i>	82
	2. Can cancer cells find the blood vessels alone or do they need a guide?	83
	<i>Introduction</i>	83
	<i>Method optimization</i>	84
	<i>Results</i>	87
	<i>Conclusion and perspectives</i>	90

3. What role do CAFs play in metastasis formation?	103
<i>Introduction</i>	103
<i>Method establishment</i>	104
<i>Results</i>	105
<i>Conclusion and perspectives</i>	108
IV. Discussion.....	109
V. Material and methods.....	119
1. <i>Cell Biology</i>	119
2. <i>Molecular biology and biochemistry</i>	127
3. <i>Animal experiments</i>	129
VI. References.....	134

Abbreviations

BM	Basement membrane
ECM	Extracellular matrix
HGF	Hepatocyte growth factor
FAK	Focal adhesion kinase
FN	Fibronectin
DOK1	Docking protein 1
ICAP1	Integrin cytoplasmic domain-associated protein 1
DAB1	Disabled homolog 1
DAB2	Disabled homolog 2
SHARPIN	SHANK-associated RH domain-interacting protein
MDGI	Mammary-derived growth inhibitor
CIB1	Calcium and integrin-binding protein 1
PKC α	Protein kinase C alpha
EGF	Epidermal growth factor
CMV	Cytomegalovirus
MMPs	Matrix metalloproteinases
WASP	Wiskott–Aldrich Syndrome protein
WIP	WASP-interacting protein WIP
EMT	Epithelial-mesenchymal transition
CTC	Circulating tumor cell
CXCR7	Chemokine receptor type 7
CXCL12	Chemokine ligand 12
SDF-1	Stromal derived factor-1
TNC	Tenascin C
GAG	Glycosaminoglycan
LOX	Lysyl-oxidase
DDR	Dimeric discoidin receptor
GPVI	Glycoprotein VI
LAIR	Leukocyte-associated immunoglobulin-like receptor

pFN	Plasma fibronectin
cFN	Cellular fibronectin
uPAR	Urokinase-type plasminogen activator receptor
α SMA	α -smooth muscle actin
PDGF	Platelet derived growth factor
PDGFR β	Platelet derived growth factor receptor β
CAF	Cancer-associated fibroblast
EndMT	Endothelial to mesenchymal transition
ASCs	Adipose derived stem cells
TGF- β	Transforming growth factor- β
T β R	TGF- β receptor
HGF	Hepatocyte growth factor
PI3K	Phosphatidylinositol 3-kinase
PCP	Planar cell polarity
Timp	Tissue inhibitor of metalloproteinases
LH	Lysyl hydroxylase
FAP	Fibroblast activation protein
JAK	Janus kinase
MLC	Myosin light chain
LIF	Leukemia inhibitory factor
FGF	Fibroblast growth factor
VEGF	Vascular endothelial growth factor
IGF-1	Insulin-like growth factor 1
MSC	Mesenchymal stem cell
FSP1	Fibroblast-specific protein 1

I. Introduction

Chapter 1: The gut – a model organ to study cell migration and tumorigenesis

The intestinal tract is comprised of two anatomically and functionally distinct segments: the small intestine and the colon (Figure I.1). In both cases, the intestinal epithelium is composed of a single layer of cells and is folded into a simple repetitive structure. Within the connective tissue are embedded the crypts, epithelial invaginations home to a population of self-renewing and multi-potent stem cells that persist for a life-time while constantly producing all differentiated cells of the intestinal epithelium (Clevers, 2013; Simons and Clevers, 2011). They first give rise to transit amplifying cells which expand rapidly as they move upwards along the inner surface of the crypt before emerging as mature and functional epithelial cells. In contrast to the flat surface of the colonic mucosa, the crypts of the small intestine give rise to villi, finger-like protrusions that project into the gut lumen (Radtke et al., 2006; Shyer et al., 2013) (Figure I.1). As the villi are essential to maximize the available absorptive surface area, this fundamental difference reflects the distinct functions of the colon and the small intestine. The villi are home to 6 types of differentiated specialized epithelial cells (Barker, 2014). Although the cellular composition of the intestinal epithelium varies between the colon and the small intestine, they both involve absorptive and secretory cell types (Barker, 2014; Radtke et al., 2006).

The basal surface of the epithelium is underlined by the basement membrane (BM), a thin and dense sheet mostly made of collagen VI and laminin (Glentis et al., 2014; LeBleu et al., 2007; Morrissey and Sherwood, 2015). It provides structural support for the epithelium, maintains cell polarity, and has a role in compartmentalization of the tissue by separating the epithelium from the stroma (LeBleu et al., 2007; Morrissey and Sherwood, 2015). The stroma contains nerves, blood and lymphatic vessels, and an extracellular matrix (ECM) mainly composed of collagen I fibers (Bosman et al., 1993; Chen and Huang, 2014). It is also home to many cell populations such as endothelial cells, pericytes, immune cells and fibroblasts, the latter being divided into two subpopulations: normal fibroblasts, which constitute the majority of the mesenchymal stroma, are evenly shed within the ECM. Myofibroblasts are almost exclusively located beneath

the crypts and play a role in gut organogenesis and homeostasis by producing growth factors, cytokines and ECM proteins (Tomasek et al., 2002) (Figure I.1).

With an intense self-renewal kinetic, the intestine is one of the most proliferative tissues in mammals (Radtke et al., 2006). Its particular architecture coupled with its homeostasis makes it a unique model to study many biological processes such as proliferation, migration and extrusion, as well as the coupling between these processes. Indeed, while cells are constantly migrating from the bottom of the crypt to the tip of the villus, mitosis only occurs within the crypts (Clevers, 2013) while cell extrusion and death will take place at the top of the villi (Eisenhoffer et al., 2012) (Figure I.1).

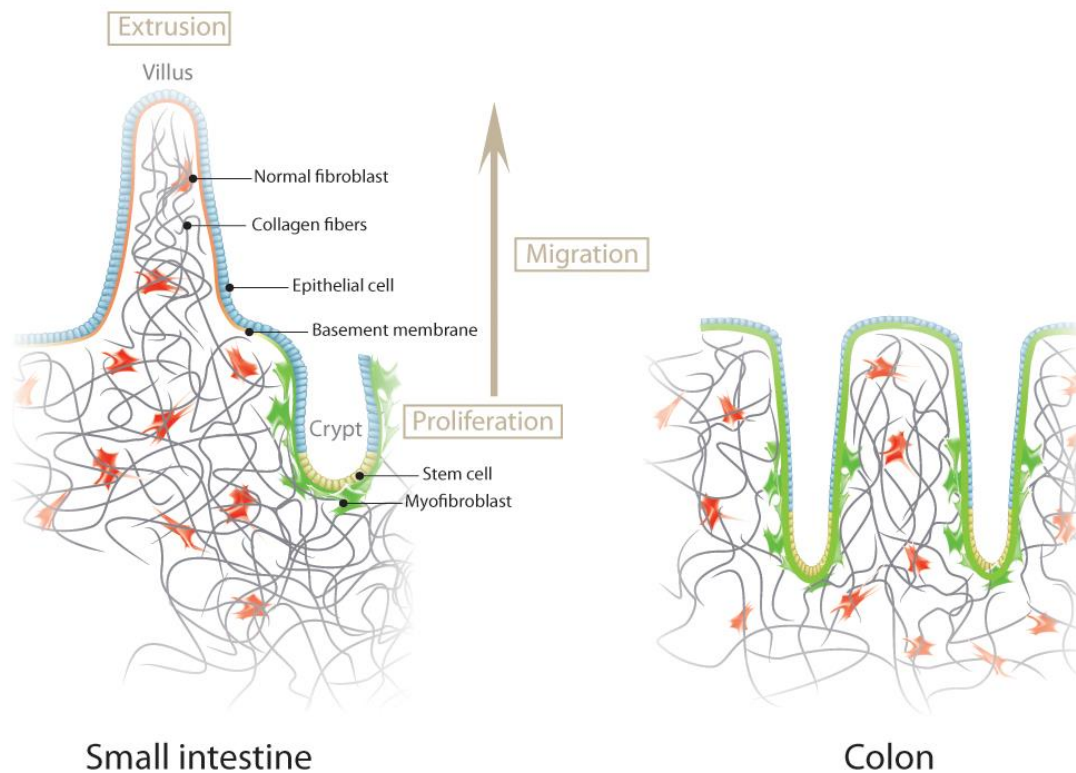


Figure I.1. The intestinal epithelium – architecture, composition and homeostasis

This stringent homeostatic maintenance sometimes falls short, leading to malignant transformations such as cancer. Colorectal cancer is one of the most common cancers worldwide with approximately 1.2 million cases every year (Ferlay et al., 2010). It is first induced when epithelial cells of the gut acquire mutations within components of the Wnt pathway (such as

APC and β -catenin) and lead to the development of dysplastic crypt foci followed by adenomas (Harada et al., 1999; Sansom et al., 2004). The transition from adenoma to carcinoma is often associated with activating mutations in the K-RAS pathway and inactivation of p53, SMAD4 and PTEN (Markowitz and Bertagnolli, 2009). Although this model suggests a cell-autonomous induction of adenomas, it has also been suggested that the tumorigenic capacity of individual cancer cells may be influenced by homeostatic signals derived from their microenvironment (Medema and Vermeulen, 2011; Vermeulen et al., 2010). Chronic inflammation of the intestine can predispose to cancer initiation in the gut of patients (Itzkowitz and Yio, 2004), and lead to a strong increase in polyp formation in *Apc*^{Min} mice (Tanaka et al., 2006). It has also been shown that dedifferentiation from mature epithelial cells to stem cells can easily occur in tumor settings and is under the influence of stromal myofibroblasts and their secretion of hepatocyte growth factor (HGF) (Vermeulen et al., 2010). Therefore, microenvironmental influences need to be placed within the scheme of events as it is now well established that environmental factors are an enabling characteristic promoting tumor initiation and growth (Hanahan and Weinberg, 2011).

Chapter 2: Overview on the basic principles of cell motility

Cell migration is a fundamental mechanism required for a multitude of biological processes which start at the developmental stage. As already described, intestinal homeostasis highly depends on the coordination of migration, proliferation and extrusion. Cell migration is also crucial for immune cells patrolling the organism and for tissue repair by epithelial and stromal cells. Thus, deregulation of the migration process leads to many pathologies including vascular disease, chronic inflammatory diseases and cancer.

During cancer progression, successful completion of the metastatic process is highly dependent on the ability of cancer cells to actively move, navigate through different environments and find their way by sensing external cues. Depending on the intrinsic contractility of the cells, the nature of the matrix (protein composition), its topography (compliance and dimensionality), as well as on the extracellular cues (gradients of growth factors and chemokines), cancer cells will adopt a specific migration mode that will allow them to move with minimal constraints (Friedl, 2004). Therefore, basic understanding of the mechanisms of different cell migration modes and the factors that drive them is crucial for preventing metastasis.

2.1. Migration on 2D substrates

Most of our knowledge on how cells move is grasped from *in vitro* studies using planar (2D) substrates and mesenchymal cells. In the early 1960s, Abercrombie provided the first description of a “locomotory organ” in moving fibroblasts that he dubbed the lamellipodium (Abercrombie, 1961). A large series of studies followed within the next 30 years further describing in detail the biochemical composition and dynamics of the protrusions driving this sort of mesenchymal movement. Although complex, cell migration can be described as a cycle of four discrete steps (Figure I.2): 1) cells initiate the migration cycle by polarizing and extending protrusions of the cell membrane towards the cue. These protrusions comprise large, broad lamellipodia and/or spike-like filopodia that are driven by the polymerization of actin filaments (Small et al., 2002); 2) protrusions are then stabilized by adhesions that link the actin cytoskeleton to the underlying matrix; 3) actomyosin contraction generates traction forces on the substrate; 4) finally, contractility also promotes the disassembly of adhesions at the cell rear to allow the cell to move forwards (Case and Waterman, 2015; Pollard and Borisy, 2003; Ridley et al., 2003). Because of the focus of my thesis, I will keep the introduction succinct and only go into a detailed description of the protrusions mediating cell-ECM adhesion.

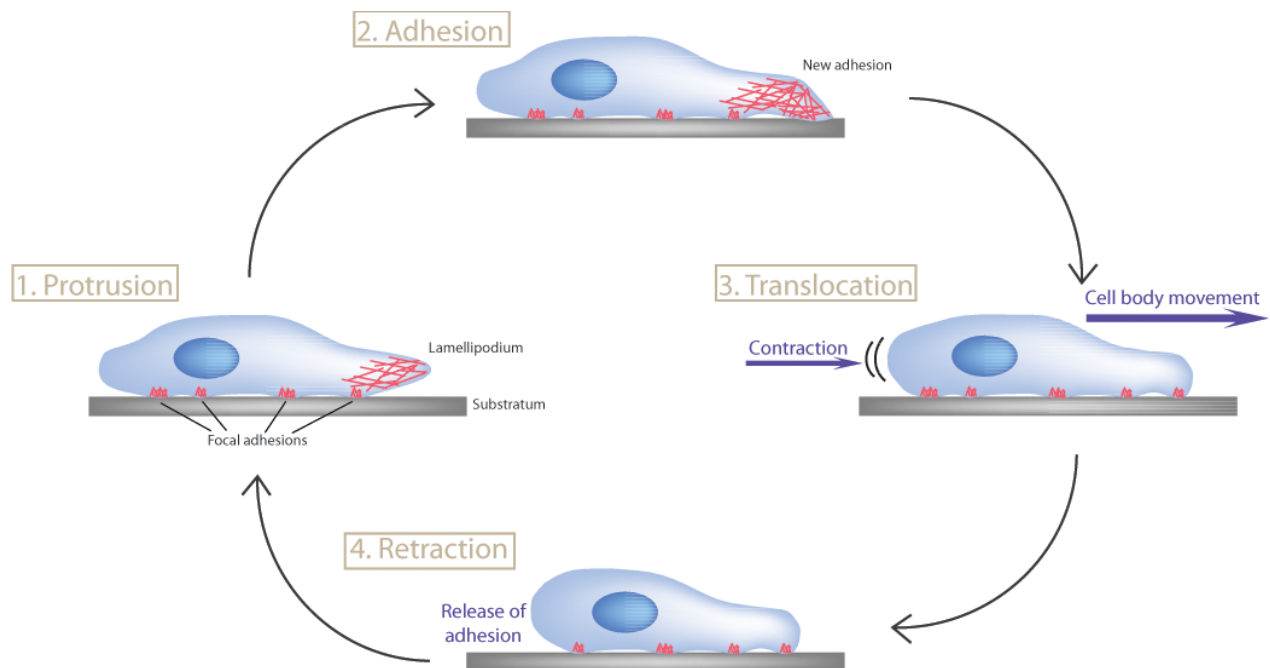


Figure I.2. The cell migration cycle on 2D substrates

2.1.1. Cell-matrix adhesions – composition of the adhesome

Cell-matrix adhesions were first identified by interference reflection microscopy as an area of close association with the substratum (Curtis, 1964; Izzard and Lochner, 1976). Later, by electron microscopy, they were characterized as electron-dense plaques associated with actin filament bundles (Abercrombie et al., 1971; Heath and Dunn, 1978).

The maturation of adhesion formation from nascent adhesions to fibrillar adhesions is a hierarchical process consisting of a sequential cascade of protein recruitment (Zaidel-Bar et al., 2004; Zamir and Geiger, 2001). So far, more than 180 adhesion-associated proteins have been identified, altogether called “adhesome” (Figure I.3) (Wozniak et al., 2004; Yamada and Geiger, 1997; Zaidel-Bar and Geiger, 2010; Zaidel-Bar et al., 2007a; Zamir and Geiger, 2001).

The adhesome is composed of different groups of proteins: adhesion receptors such as integrins and syndecans, proteins associated to actin (e.g. talin, vinculin and zyxin), adaptor proteins (e.g. paxillin), and signaling proteins (e.g. Src tyrosine kinase and the focal adhesion kinase FAK). Starting from the outside, focal adhesions are composed of an integrin extracellular layer followed by a signaling layer containing the cytoplasmic tails of integrins, FAK and paxillin, then an intermediate force-transduction layer containing talin and vinculin, and finally an upper actin-regulatory layer containing zyxin, vasodilator-stimulated phosphoprotein (VASP) and α -actinin (Figure I.3) (Kanchanawong et al., 2010). In addition, some proteins are transiently associated with focal adhesions and play regulatory roles such as the Rho family of GTPases, calcium-dependent protein calpain 2 and tyrosine phosphatases (Geiger and Yamada, 2011; Horton et al., 2016; Winograd-Katz et al., 2014). Integrin signaling regulates the activity of Rho GTPases (Rho, Rac and Cdc42) by recruiting guanine nucleotide exchange factors (GEFs) and GTPase activating proteins (GAPs) to the adhesome. In return, Rho GTPases dictate focal adhesion assembly and disassembly by regulating actin polymerization and actomyosin driven contractility (Figure I.3).

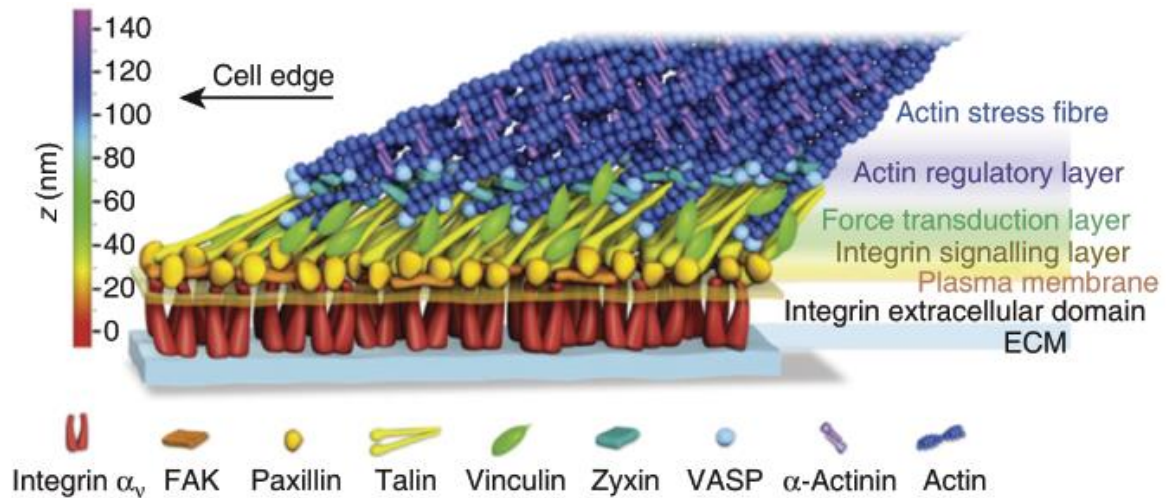


Figure I.3. Schematic model of the molecular architecture of focal adhesions (Adapted from Kanchanawong et al., 2010)

2.1.2. The adhesion continuum – from assembly to maturation and breakdown

As the cell advances, small adhesions of $0.25\mu\text{m}$ – or nascent adhesions – form in the lamellipodium, right behind the leading edge of the cell (Choi et al., 2008; Zaidel-Bar et al., 2003; Zaidel-Bar et al., 2004). These adhesions are myosin-independent and mediated by actin polymerization (Choi et al., 2008). The mechanism by which nascent adhesions are nucleated is still debated. To date, two models are proposed (see section 2.2.2 for a more detailed description): the first model suggests an outside-in sequence of events where integrin binding to the ECM leads to integrin activation by talin and clustering by vinculin (Figure I.4). Subsequently, other adhesome proteins bind to the cytoplasmic domain of integrins therefore connecting integrins to the actin cytoskeleton (Calderwood et al., 2002; Calderwood et al., 1999). This model is further supported by the observation of activated integrins near the leading edge of migrating cells where nascent adhesions are forming. Moreover, studies using ligand or anti-integrin antibodies coupled to beads have shown clustering of adhesion components around the beads indicating that integrins can recruit and activate components of the “adhesome” (Miyamoto et al., 1995). In the second model, assembly is initiated inside the cell by actin polymerization (Figure I.4). Vinculin binds the Arp2/3 complex and this pre-clustered complex associates with activated integrins leading to formation of nascent adhesions. Evidence for this model comes from the notion that the formation of nascent adhesions is abolished if actin

polymerization is inhibited (Choi et al., 2008) as well as by characterization of a direct and transient interaction of vinculin and FAK with the Arp2/3 complex (DeMali et al., 2002; Serrels et al., 2007). Importantly, these two models cannot be mutually exclusive as integrin clustering and actin polymerization and ligation exert positive feedback signals on each other and together stabilize nascent adhesions.

Nascent adhesions can either turnover rapidly or evolve into larger 1 μ m dot-like structures, focal complexes. Their formation requires the forward movement of the leading edge to pause, a phenomenon triggered by myosin II-dependent contractility (Choi et al., 2008). Focal complexes are therefore located slightly further back from the leading edge, at the lamellipodium-lamella interface (Nobes and Hall, 1995; Zaidel-Bar et al., 2003; Zaidel-Bar et al., 2004). Thus, initial adhesion is linked to actin polymerization in the lamellipodium through Rac activity, whereas myosin II activity through Rho exerted on actin in the lamellum contributes to the maturation of newly formed adhesions to focal complexes. The actin-cross-linking protein α -actinin has also been implicated in adhesion maturation as it is the earliest component detected in maturing adhesions. Its spatial organization suggests that it is crucial for orienting actin templates and linking actin filaments to adhesions (Choi et al., 2008; Rajfur et al., 2002). It has also been shown to compete with talin for the binding of the β tail of integrins and to transmit the cytoskeletal forces that trigger mechanotransduction and adhesion maturation (Choi et al., 2008; Rajfur et al., 2002; Roca-Cusachs et al., 2013a).

Within less than a minute of their formation, focal complexes either turnover, or undergo a force-dependent transformation into larger focal adhesions which are typically 2 μ m wide and 3-10 μ m long and reside both in central and peripheral regions, at the ends of actin- and myosin-associated stress fibers (Critchley, 2000; Zaidel-Bar et al., 2004). Until this point, all types of adhesions (nascent adhesions, focal complexes and focal adhesions) contain integrins, talin, vinculin, α -actinin, and paxillin (Choi et al., 2008; Zaidel-Bar et al., 2007b), as well as the tyrosine kinases Src and FAK. Tyrosine kinase activity (or tyrosine phosphatase inhibition) is crucial for tyrosine phosphorylation of focal adhesion proteins paxillin and FAK, and subsequent focal adhesion assembly (Chrzanowska-Wodnicka and Burridge, 1994; Geiger et al., 2001; Retta et al., 1996). Focal adhesions typically disassemble at the cell's rear. Alternatively, if maintained by high actomyosin contractility, focal adhesions can further mature into fibrillar adhesions.

Fibrillar adhesions are long-lived and elongated adhesions specialized in fibronectin (FN) matrix assembly and remodeling of the ECM (Zaidel-Bar et al., 2004; Zaidel-Bar et al., 2007b). They derive from the centripetal movement of focal adhesions and the concomitant loss of tyrosine kinases activity and phosphopaxillin (Geiger et al., 2001; Zaidel-Bar et al., 2007b). The typical components of fibrillary adhesions are extracellular FN fibrils, the FN receptor $\alpha 5\beta 1$ integrin and the cytoplasmic protein tensin (Pankov et al., 2000; Zamir and Geiger, 2001).

Of note, not all cells exhibit the full range of adhesion structures. The contractile nature of the cells, their migratory capacity, as well as the mechanical properties of the matrix (stiffness, dimensionality, fiber orientation), all determine the nature of adhesions (Cukierman et al., 2001; Discher et al., 2005; Geiger et al., 2009; Zamir and Geiger, 2001). Conversely, the nature of adhesions can also reflect on the contractile capacity of a cell. For example, fast migrating cells such as neutrophils and macrophages display small and highly dynamic adhesions (mostly nascent adhesions and focal complexes), while more contractile and slowly migrating fibroblasts are characterized by more prominent and stable focal adhesions and fibrillary adhesions, allowing them to assemble and shape the ECM.

2.2. Integrins, mediators of the crosstalk between cells and the ECM

Integrins are a family of heterodimeric receptors that mediate cell-matrix adhesions. In mammals, 18α and 8β -integrin genes encode polypeptides that combine to form $24\alpha\beta$ receptors (Hynes, 2002). Each α - or β -subunit is a typical type I transmembrane protein with the amino-terminus on the extracellular side and a single transmembrane domain that connects to a carboxy-terminal cytoplasmic tail (Hynes, 2002; Shattil et al., 2010). The amino-terminal domains of both α and β subunits assemble by non-covalent interactions to form a “head” and provide a ligand binding site to various matrix components. Through their short cytoplasmic tail, integrins interact with modules of the actin cytoskeleton as already described (section 2.1.1) (Hynes, 2002; Shattil et al., 2010). Binding specificity defines the nature of the heterodimer. For example, $\alpha 1\beta 1$ and $\alpha 2\beta 1$ integrins will bind to collagen, $\alpha 2\beta 1$, $\alpha 3\beta 1$, $\alpha 6\beta 1$ and $\alpha 6\beta 4$ will recognize laminin while FN will bind $\alpha 5\beta 1$, $\alpha v\beta 3$, $\alpha v\beta 5$, $\alpha 4\beta 1$ or $\alpha I I b\beta 3$ (Horton et al., 2016; Hynes, 2002). By connecting the actin cytoskeleton to the ECM, integrins convey the tension that is generated by the actin cytoskeleton through focal adhesions and fibrillar adhesions externally to the matrix (Schwartz, 2010; Sun et al., 2016).

2.2.1. Conformation and clustering of integrins

Cell anchorage and consequent migration, polarization and ECM assembly are all processes that depend on integrin activation. Integrin activation is the process during which integrin heterodimers switch from a bent to an open conformation. As integrin heterodimers open up, they also go from a low affinity to a high affinity state and become prone to easily bind ligands in the ECM although the bent form has been shown to engage ligands such as FN (Adair et al., 2005; Shattil et al., 2010). This evolution of conformations is concomitant with a lateral clustering of integrins into hetero-oligomers (Arnold et al., 2004; Shattil et al., 2010). Experiments from the lab of J. Spatz indicate that cells can sense the spacing of RGD-peptide functionalized nanoparticles and propose a universal length scale of 58-73nm that is optimal for integrin clustering, activation and subsequent cell adhesion, spreading and migration (Arnold et al., 2004). Thus, conformational change and clustering go hand in hand and are both likely to be important for integrin activation and function but their timing as well as their relative contribution to the activation process need to be further evaluated.

2.2.2. Balancing between activated and inactivated states – Integrin activation

The interaction of transmembrane domains of α - and β -subunits defines integrins' activity as their association maintains the low affinity state (Bouvard et al., 2013; Hughes et al., 1996; Luo et al., 2004; Shattil et al., 2010). Indeed, mutations within the transmembrane domain that reduce the $\alpha\beta$ -integrin association lead to integrin activation (Li et al., 2005; Luo et al., 2005; Partridge et al., 2005).

Integrin activation can be initiated both in the extracellular (outside-in) and intracellular (inside-out) compartments of the cell (Figure I.4), thus providing integrins a unique capacity to signal bidirectionally (Kim et al., 2003).

Inside-out activation

Inside-out signaling enables mechanotransduction from integrins to the ECM and back, to control cell adhesion, migration and ECM remodeling and assembly (Shattil et al., 2010). Inside-out activation is triggered at the cytoplasmic tail through the cooperative action of talin and kindlins with the β -subunit where talin recruitment is regulated through the activity of Rap1 GTPase (Calderwood et al., 2013; Lafuente et al., 2004; Pouwels et al., 2012; Shattil et al., 2010). The β -cytoplasmic subunit is characterized by two conserved motifs: the membrane-

proximal NPxY motif and the membrane-distal NxxY motif (Liu et al., 2000; Pouwels et al., 2012). Binding of talin to the cytoplasmic domain of β -integrin disrupts the salt bridge between the $\alpha\beta$ -cytoplasmic tails and probably reorients the transmembrane domains leading to integrin activation and increased affinity to extracellular ligands (Shattil et al., 2010; Tadokoro et al., 2003). This binding occurs through the N-terminal head of talin, more specifically through its F3 subdomain that contains a phosphotyrosine-binding (PTB) motif which recognizes the membrane-proximal NPxY β -subunit (Calderwood et al., 2003; Liu et al., 2000; Pouwels et al., 2012). Of note, binding of talin to integrins requires the PTB domain to be non-phosphorylated (Anthis et al., 2009; Oxley et al., 2008).

Although talin is important, it is unclear whether it is sufficient for integrin activation. Indeed, depletion of kindlins both in mice and cells has been shown to prevent integrin activation (Ma et al., 2008; Montanez et al., 2008; Moser et al., 2008). Kindlins interact with the membrane-distal NxxY motif of the β -subunit through their C-terminus head (Shattil et al., 2010). It is still unclear though how kindlins cooperate with talin to activate integrins. Do both proteins simultaneously bind to the β -cytoplasmic tail and together lead to integrin activation? Or does one of the proteins initially associate with the β -subunit, for example to trigger a signaling event or to displace an inhibitor, therefore allowing the second protein to bind and activate integrins (Shattil et al., 2010)? Of note, overexpression of kindlin-2 has been shown to interfere with β 1 integrin-talin binding suggesting that integrin activation through kindlins might be dependent on the nature of the integrin heterodimer (Harburger et al., 2009).

Finally, inside-out activation can also occur through the α -tail although this mechanism is still poorly described. As opposed to the β -cytoplasmic tail, the α -subunits present a highly conserved membrane-proximal domain and a variable distal domain (Liu et al., 2000; Rantala et al., 2011). This suggests that depending on their binding affinity, integrin regulators that act through the α -subunit will either regulate all of the different α -subunits at once or act in a heterodimer-specific manner. To date, RAPL (a regulator of cell adhesion and polarization enriched in lymphoid tissues) is the only protein that has been shown to activate integrins through their α tail. By specifically associating with the α L subunit of the α L β 2 heterodimer of lymphocytes, RAPL complements talin and regulates cell adhesion and interstitial migration (Ebisuno et al., 2010; Katagiri et al., 2003)

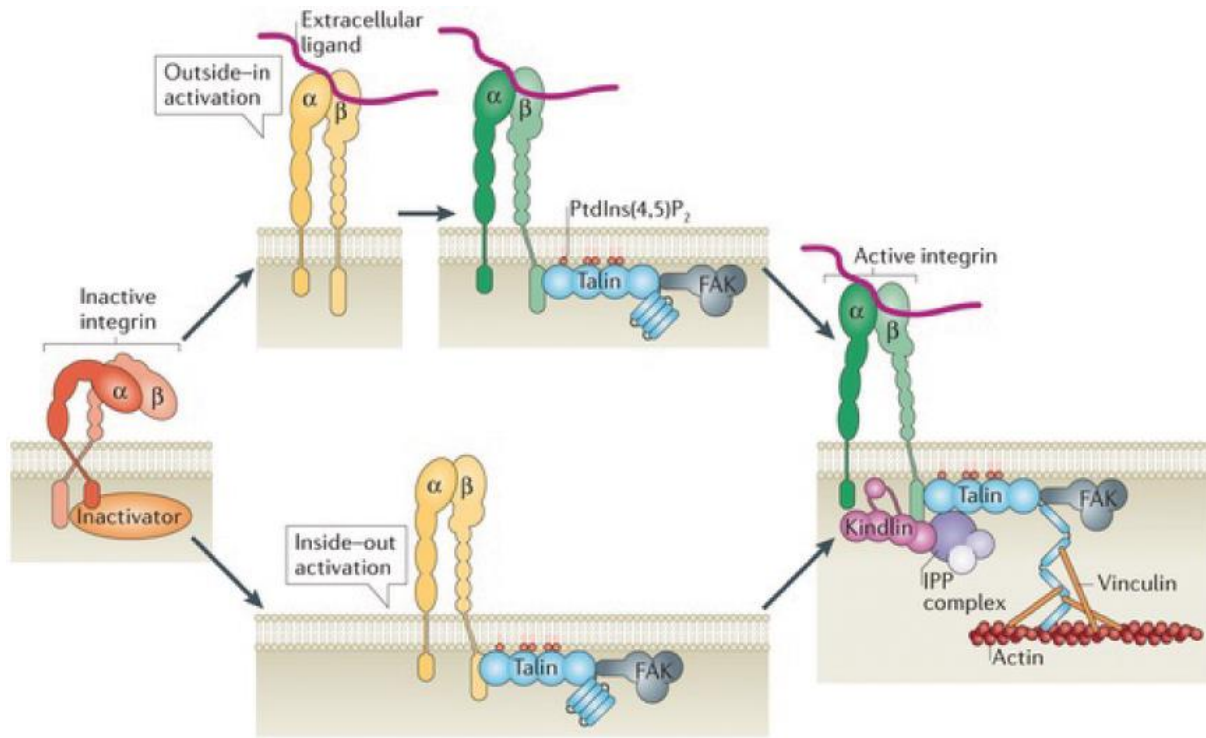


Figure I.4. Molecular pathways leading to integrin activation (Modified from Bouvard *et al.*, 2013)

Outside-in activation

The outside-in scenario requires initial binding of integrins to their extracellular ligands. This binding induces integrin conformational changes, and, because most ligands are multivalent, integrin clustering. Conformational changes are propagated across the plasma membrane, leading to alterations of the $\alpha\beta$ -transmembrane and cytoplasmic tails and subsequent intracellular signaling to control cell polarity, cytoskeletal structure and gene expression (Du *et al.*, 1991; Kim *et al.*, 2003; Shattil *et al.*, 2010).

Of note, although the two processes are conceptually separated, they are tightly linked as inside-out activation increases ligand binding and subsequent outside-in signaling while ligand binding and outside-in activation leads to the recruitment of cytoskeletal modules and inside-out signaling.

As the outside-in activation mechanism can also occur through integrin binding of monovalent ligands, it proposes that conformational changes precede integrin clustering. Similarly, the

inside-out activation model proposes that integrins undergo conformational changes before binding to the ECM and subsequent clustering. In fact, the only model suggesting concomitant clustering and conformational change is the outside-in activation model where integrins bind to multivalent ligands. It is therefore more likely that in most cases, conformational change of integrins precedes their clustering although both mechanisms are necessary for further maintenance of integrin activation.

2.2.3. Balancing between activated and inactivated states – Integrin inactivation

The general dogma has been that integrins actively go from an inactive to an active state while the inactive conformation is passively adopted by default. However, studies have identified and extensively described proteins that actively inhibit integrins and the malfunction of these proteins has been linked to developmental defects and disorders such as cancer (Bouvard et al., 2003; Calderwood et al., 2001; Peuhu et al., 2017). This indicates that the control of both integrin activation and inactivation is critical for optimal cell behavior (Bouvard et al., 2013).

Integrin inactivation through the β -subunit

Integrin inactivators can function through many mechanisms (Figure I.5) (Bouvard et al., 2013; Pouwels et al., 2012): they can compete with talin or kindlins by directly binding integrins' cytoplasmic tails. This is the case of filamins (Figure I.5.a), numb and the docking protein 1 (DOK1) (Figure I.5.c) that directly bind the membrane-proximal NPxY motif (Calderwood et al., 2003; Calderwood et al., 2001; Kiema et al., 2006) (Figure I.5). Tensins act through the same mechanism but as their expression correlates with fibrillar adhesion formation, it is tempting to hypothesize that tensins interfere with talin-integrin interaction towards the cell center, promoting the switch from focal adhesions to fibrillary adhesions (Calderwood et al., 2003; Katz et al., 2007). The integrin cytoplasmic domain-associated protein 1 (ICAP1) (Figure I.5.b), the disabled homolog 1 and 2 (DAB1 and DAB2) as well as Shc contain a PTB domain which binds the NxxY distal-domain and therefore competes with kindlins (Bouvard et al., 2003; Calderwood et al., 2003; Chang et al., 1997; Pouwels et al., 2012). Of these inactivators, some are tyrosine kinase dependent. For example, Shc and DOK1's binding to integrins greatly increases upon PTB phosphorylation by Src kinases (Oxley et al., 2008). As the tyrosine kinase Src also promotes focal adhesion assembly, its continuous activity supports the transition from focal adhesion to fibrillar adhesion.

Integrin inactivation through the α -subunit

Some inactivators can also bind the α -cytoplasmic tail although their mode of action is still poorly described. Because of the highly conserved WKxGFFKR domain on the α -tail, these inactivators should have the capacity to interact with and inhibit most integrins (Nevo et al., 2010; Rantala et al., 2011). The SHANK-associated RH domain-interacting protein SHARPIN for example has been shown to co-localize with inactive integrin ruffles at focal adhesions and affect cell spreading and migration, as well as collagen arrangement by stromal cells and ECM stiffness (Figure I.5.d) (Bouvard et al., 2013; Peuhu et al., 2017; Pouwels et al., 2012; Rantala et al., 2011). Some inactivators bind the α -subunit but inhibit the binding of talin and kindlin to the β -subunit (Nevo et al., 2010; Rantala et al., 2011). For example, overexpression of the mammary-derived growth inhibitor (MDGI) has been shown to reduce the kindlin- β 1 interaction and subsequent β 1 activation and cell adhesion (Figure I.5.d) (Nevo et al., 2010). The calcium and integrin-binding protein 1 (CIB1) is slightly different: it specifically recognizes the cytoplasmic tail of α II and opposes the binding of talin on the β -subunit (Naik et al., 1997; Yuan et al., 2006). Thus, it would seem that CIB1 does not bind the proximal-domain of α II like SHARPIN and MDGI and would rather associate with its unique distal-domain but this hypothesis has never been tested. Whether MDGI and CIB1 act through steric hindrance, by stabilizing the transmembrane association of the integrin heterodimers, or by recruiting inhibitors of the β -subunit, is still unknown (Pouwels et al., 2012).

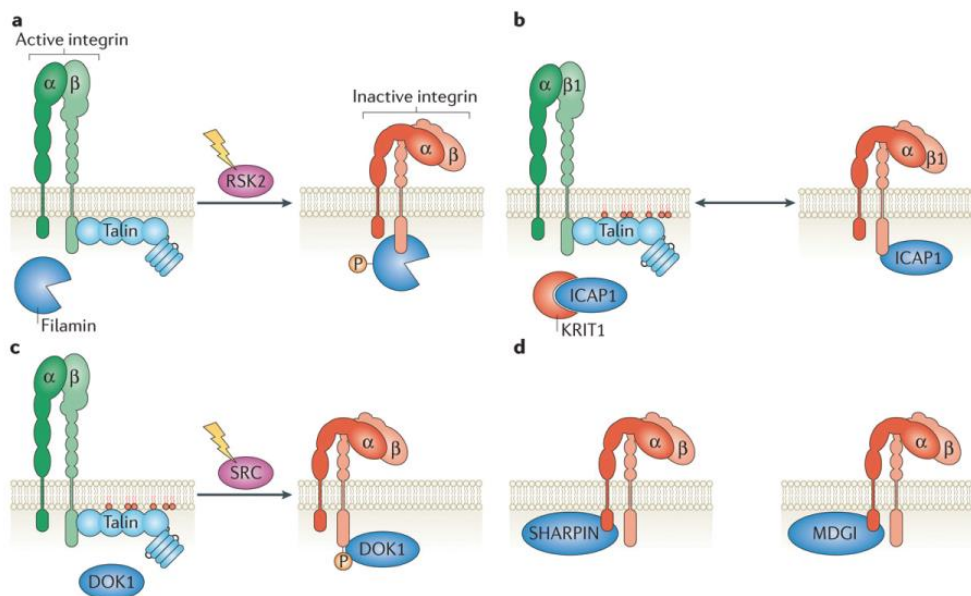


Figure I.5. Molecular pathways leading to integrin inactivation
(Adapted from Bouvard *et al.*, 2013)

Integrin inactivation through regulation of trafficking

Alternatively, integrin inactivators can affect the amount of cell surface integrins through the regulation of integrin trafficking. Of the latter mentioned β -tail binding inactivators, some can trigger integrin endocytosis in addition to their competition with talin and kindlin. The PTB-domain containing DAB2 and numb for example are both clathrin adaptors that have been shown to trigger endocytosis of integrins β 1 and β 3 respectively (Calderwood et al., 2003; Ezratty et al., 2009; Teckchandani et al., 2009). In addition to these clathrin adaptors, the protein kinase C alpha (PKC α) triggers recycling of integrin β 1 from the plasma membrane (Ng et al., 1999; Parsons et al., 2002). As PKC α and talin both bind the NPxY motif, PKC α probably affects the levels of inactive integrin heterodimers at the plasma membrane and their activation through outside-in signaling. Integrin inactivation can also occur via blockage of talin recruitment to the β -subunit. A recent study has shown that SHANK proteins have a high affinity for Rap1 and sequester it, thus limiting its bioavailability at the plasma membrane and blocking the recruitment of talin (Lilja et al., 2017). The case of α -tail binding regulators is simpler as the binding site of SHARPIN and MDGI is the same one at which Rab21 binds integrin heterodimers to induce their endocytosis (Pellinen et al., 2006). Thus, α -subunit inactivators can either recycle active integrins or inhibit integrin heterodimers at the cell surface but recycling of inactive integrins seems like an unlikely scenario.

Finally, similarly to the activation process, integrin inactivation can also be the result of outside-in signaling. For example, extracellular epidermal growth factor (EGF) stimulation induces interaction of the ribosomal protein S6 kinase 2 (RSK2) with the membrane-proximal domain of integrins β 1 and β 7 and triggers filamin recruitment and binding (Gawecka et al., 2012; Woo et al., 2004). In addition to its role in integrin inactivation through direct binding to the α -tail, MDGI also influences EGFR trafficking, thus participating to the outside-in inactivation of integrin β 1 (Nevo et al., 2009).

2.3. Migration and invasion in 3D matrices

In 2003 the Nature editor Allison Abbott published an editorial article entitled “Goodbye, flat Biology?” that highlighted the necessity of switching from 2D to 3D cell cultures (2003). There are many differences between a flat layer of cells and a complex three-dimensional tissue where cells connect, not only to each other, but also to a complex ECM in which they are embedded. These differences became increasingly clear when, in 1997, studies in the lab of Mina Bissell

showed that treatment of 3D cultures of breast cancer cells with antibodies against integrin $\beta 1$ reverted the cells' phenotype to normal, a result that was not observed in 2D cultures (Weaver et al., 1997). A follow-up study later showed that blocking of integrin $\beta 1$ led to a decrease in the signaling of EGFR and vice-versa, again this reciprocal interaction not being reproduced in 2D (Wang et al., 1998). Therefore, changing the way cells interact with their 3D environment can also alter their behavior. These studies further highlighted the differences in the integration of signaling pathways between 2D and 3D assays and it became evident that in some biological studies, 3D models recapitulate the complexity of *in vivo* behavior more faithfully.

2.3.1. Focal-adhesions in 3D matrices

Most of the studies characterizing cell-matrix adhesions are done using 2D cultures where the ECM proteins are only in contact with the ventral side of the cell. However, the formation and regulation of adhesions in 3D environments where cells are surrounded by the ECM could be completely different (Figure I.6). Studies on cells seeded on top of thick cell-derived matrices or embedded within a thin 3D matrix reveal the presence of discrete adhesion structures containing the same proteins as the ones of the adhesome (Figure I.6) (Cukierman et al., 2001; Hakkinen et al., 2011). However, *in vivo* studies have shown that focal adhesions are not detected in cells buried inside a thicker 3D matrix (Friedl et al., 1998; Petroll et al., 2003). These observations led to question the importance of focal adhesions and focal adhesion proteins in cells in 3D environments, especially as their expression level correlates with the metastatic potential of cancer cells (Barbazan et al., 2012; Hanada et al., 2005; Salgia et al., 1999; Yu and Luo, 2006). Later on, additional studies showed an inverse correlation between the dimensionality of the matrix and focal adhesion formation: in “2.5D” matrices where cells are sandwiched between 2 collagen layers, focal adhesions still form but are decreased in size and number (Fraley et al., 2010). Similarly, in a 3D collagen gel, increasing the distance of the cell from the substrate bottom correlates with the disappearance of adhesion aggregates until focal adhesion proteins are diffusely distributed in the cytoplasm of cells fully embedded in the matrix (Figure I.6) (Fraley et al., 2010; Geraldo et al., 2012). However, depletion of major focal adhesion proteins in these cells as well as blocking of integrin $\beta 1$ interfere with cell speed and persistence by affecting protrusion activity and deformation (Fraley et al., 2010). These observations suggest that focal adhesions do exist in cells embedded in a 3D matrix and they are critical for cellular traction motility but probably too small, and their lifetime too short, to be detected. Indeed, following the

study by Fraley *et al.*, Kubow and Horwitz performed experiments using a truncated cytomegalovirus (CMV) promoter which drives the expression of chimeric proteins in low levels thus reducing the cytoplasm background and allowing a better visualization of 3D adhesions (Kubow and Horwitz, 2011). Moreover, vinculin aggregates were detected in cellular protrusions of cancer cells and colocalized with collagen fibers (Geraldo *et al.*, 2012). Finally, the dimensionality of the matrix is not the only component to be taken into account when studying focal adhesion formation. Indeed, cells plated on soft 2D substrates display small aggregates of focal adhesion proteins similar to the ones observed in 3D (Fraley *et al.*, 2010; Geraldo *et al.*, 2012; Harunaga and Yamada, 2011; Kubow and Horwitz, 2011). This adds another layer of complexity to the system as the difference in the tension and elasticity of collagen gels, whether in 2D or 3D, also affects the formation of focal adhesions.

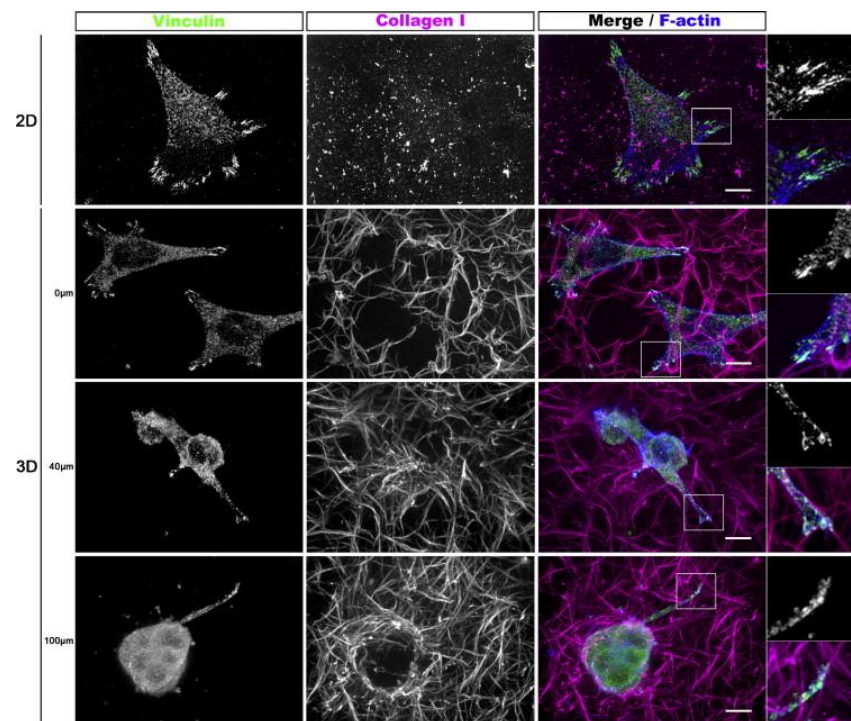


Figure I.6. Vinculin rich cell–matrix adhesions in HCT116 colon cancer cells. Immunofluorescence spinning disk images of HCT116 cells labeled with vinculin antibodies (green) and phalloidin for F-actin (blue) plated on TAMRA-labeled collagen I (magenta) coated-coverslips (2D) or embedded on TAMRA-labeled collagen I matrix (3D). 3D images correspond to x - y maximal projections of Z stacks of 8.8 μm , 15 μm and 16 μm , starting 0 μm , 40 μm and 100 μm away from the substrate bottom, respectively. Far right columns correspond to zoomed views of the boxed regions. Scale bar, 10 μm (Geraldo *et al.*, 2012)

2.3.2. The importance of invadopodia in 3D motility

Throughout the body, cells encounter different types of matrices, from the dense and tightly packed BM (Glentis et al., 2014) to the more loose ECM (see section 4.1). As these matrices differ in composition, structure and pore size, cells, and invading cancer cells in particular, sometimes need to create passageways in order to move (Poincloux et al., 2009; Sabeh et al., 2009; Wolf et al., 2009). Thus, 2D and 3D motility are fundamentally different in the sense that migration in 2D solely depends on adhesion assembly and disassembly, while invasion in 3D also relies on the ability of cells to degrade the barriers they come across or squeeze through matrix pores.

Matrix metalloproteinases mediating ECM degradation

The main proteins involved in matrix degradation are matrix metalloproteinases (MMPs). Through their catalytic site, MMPs cleave collagen fibers and facilitate cell migration through the ECM during development, wound healing and tumorigenesis (Edwards and Murphy, 1998; Egeblad and Werb, 2002). The presence of MMPs in tumors correlates with aggressiveness and poor prognosis (Jodele et al., 2006; Tetu et al., 2006; Zhang et al., 2008). To date, 25 MMPs have been identified in humans and are divided into two structural classes: soluble MMPs are secreted as inactive molecules that diffuse in the matrix, thus their enzymatic activity is not limited to the vicinity of the cell. Upon secretion, they get activated through cleavage by other proteases (Coussens et al., 2002; Egeblad and Werb, 2002; Overall and Kleifeld, 2006). In contrast, membrane-bound MMPs (or MT-MMPs) mediate localized ECM degradation at the cell surface. They get activated prior to their arrival to the cell surface by furin cleavage in the trans-Golgi (Poincloux et al., 2009; Yana and Weiss, 2000). In the context of cancer invasion and metastasis, membrane bound MMP14 (or MT1-MMP) is considered to be the major player (Castro-Castro et al., 2016; Hotary et al., 2006; Hotary et al., 2003). Besides cleaving all types of collagens as well as gelatin, FN and laminin, MT1-MMP is the only protease required for BM crossing while other MMPs are dispensable (Hotary et al., 2006). However, the function of MMPs is much wider than ECM cleavage and all MMPs have the ability to modulate cell motility by controlling many processes such as cleavage of cell adhesion molecules, growth-factor precursors, receptors tyrosine kinases and other proteases (Egeblad and Werb, 2002). MMPs also play an important role in stromal cell-mediated ECM remodeling, especially in the tumor stroma (see section 5.2.2).

Structure of invadopodia

In vitro, cancer cells cultured on top of an ECM develop finger-like actin-rich protrusions called invadopodia that degrade the underlying matrix (Chen, 1989; Weaver, 2006; Weaver, 2008). Similar protrusions, podosomes, are observed in a normal physiological situation, in immune cells, endothelial cells or smooth muscle cells (Buccione et al., 2004; Linder, 2007). Like focal adhesions, invadopodia and podosomes are defined as cell-matrix adhesion sites strongly associated with actin filaments and share most of the same proteins. However, focal adhesions are fundamentally different from invadopodia and podosomes by their architecture and dynamics (Albige-Rizo et al., 2009). While stress fibers anchored to focal adhesions show a tangential orientation with respect to the matrix, invadopodia and podosomes display an actin core perpendicular to the ECM (Albige-Rizo et al., 2009). Moreover, invadopodia and podosomes are characterized by a fast actin turnover necessary for their extension while focal adhesions, or at least the more stable focal adhesions, are slow cycling structures (Albige-Rizo et al., 2009; Destaing et al., 2003).

Podosomes and invadopodia also display different characteristics. On 2D matrices, while both structures accumulate at the ventral surface of cells into either isolated structures or circular rosettes, podosomes preferentially localize to cell periphery (Buccione et al., 2004; Linder, 2007). Moreover, podosomes are shallow protrusions in contrast to invadopodia that appear as long and thin projections protruding into the ECM (Figure I.7) (Lizarraga et al., 2009; Schoumacher et al., 2010; Weaver, 2008). Finally, podosomes are more dynamic structures with half-lives of 2-12min while invadopodia are more stable and can persist up to several hours (Buccione et al., 2004; Linder, 2007).

Of note, a new type of linear invadopodia has been recently described in invading cancer cells. As opposed to the classical invadopodia, linear invadopodia lay parallel to the matrix and are only induced by collagen I matrices upon TGF- β stimulation (Ezzoukhry et al., 2016; Juin et al., 2014). Interestingly, these protrusions are integrin independent and rely on the collagen I receptor Discoidin Domain Receptor I (DDR1) (see section 4.1.1). This notion is in line with a recent publication suggesting that fibroblasts apply mechanical forces on the matrix via DDR1 in an integrin and focal adhesion independent manner (Coelho et al., 2017).

Invadopodia were originally discovered in fibroblasts transformed by the *v-src* oncogene (Chen, 1989). Later, the ability to form such protrusions was shown to be a general property of many cancer cell lines (Gligorijevic et al., 2014; Gligorijevic et al., 2012; Kedrin et al., 2008; Monteiro et al., 2013; Poincloux et al., 2009; Schoumacher et al., 2010). Since the discovery, almost 30 years ago, of these “invasive feet”, it has been assumed that invadopodia are indispensable structures for cancer cell invasion of the basement membrane and the ECM. However, the existence of invadopodia in 3D matrices and *in vivo* has never been really demonstrated. Only one study in the lab of J. Condeelis using intravital imaging of breast cancer cells in mice reveals the presence of slow locomotion cells that exhibit protrusions with molecular, morphological and functional characteristics associated with invadopodia (Gligorijevic et al., 2014). These protrusions were mostly directed perpendicularly to blood vessels or collagen fibers and were associated with high MMP secretion, further pointing towards their role as invadopodia.

Structurally, invadopodia formation is driven by the nucleation of F-actin filaments through the Arp2/3 complex which is activated by the synergistic activity of cortactin and proteins of the Wiskott–Aldrich Syndrome protein (WASP) family, notably N-WASP (Artym et al., 2006; Gligorijevic et al., 2012; Linder et al., 1999; Weaver et al., 2002; Weaver et al., 2001). The WASP-interacting protein WIP directly binds N-WASP and cortactin and enhances their ability to activate the Arp2/3 complex (Kinley et al., 2003; Peterson et al., 2007). Membrane protrusion driving proteins of the BAR and F-BAR family are also essential for invadopodia formation as they activate the N-WASP-WIP complex as well as Cdc42, therefore promoting local actin polymerization at sites of membrane curvature (Albiges-Rizo et al., 2009; Cory and Cullen, 2007; Ho et al., 2004; Takano et al., 2008). All of these components are under the orchestration of small GTPases Rac and Cdc42: while Cdc42 activates F-BAR proteins and controls the N-WASP-Arp2/3 complex (Ho et al., 2004), Rac targets cortactin, leading to its phosphorylation and also allows WASP-Arp2/3 complex stabilization (Head et al., 2003). Finally, actin-elongation factors such as Ena/VASP family proteins and formin promote actin polymerization at the barbed ends of actin filaments. Although their expression does not affect the formation of invadopodia, they are necessary for maintaining the stability of the protrusion and for subsequent matrix degradation (Philippart et al., 2008).

Signals triggering invadopodia formation

The whole cascade of events leading to invadopodia formation is dependent on the activation of Src or the expression of oncogenic *v-src* as already mentioned (Chen, 1989; Destaing et al., 2011; Destaing et al., 2010). Src orchestrates the activity of many proteins involved in actin nucleation, polymerization and architecture: Src stimulates the Rac GTPase which, as already mentioned, regulates cortactin phosphorylation and the WASP-Arp2/3 complex (Head et al., 2003). The scaffold protein Tks5 is also a substrate of Src with N-WASP and cortactin and facilitates the formation of podosome and invadopodia rings (Courtneidge et al., 2005). As already mentioned, high Src activity supports the transition from focal adhesions to fibrillar adhesions. Coupled to its role in regulating actin nucleation and integrin-associated complexes, Src could therefore be the lead protein orchestrating all types of cell-matrix adhesions. This notion suggests that ECM contractility and degradation are tightly linked and interdependent processes.

In addition to Src, activation of the PKC family was shown to induce invadopodia in various normal and transformed cell types (Tatin et al., 2006). $\beta 1$ integrins are targets of PKC and their activation is necessary for Src-induced rosette assembly (Destaing et al., 2010). It has also been recently shown that MT1-MMP and the isoform αPKC_1 are co-upregulated and colocalize at invadopodia sites of breast cancer cells (Rosse et al., 2014).

Cell attachment to the substrate is also an important signal that triggers invadopodia formation which is therefore dependent on integrins as well as proteins of the focal adhesion family (Bowden et al., 1999; Mueller et al., 1999; Petropoulos et al., 2016). Upon binding to collagen or laminin, $\alpha 3\beta 1$ and $\alpha 6\beta 1$ become activated and induce recruitment of the protease seprase to invadopodia (Figure I.7), while $\alpha 5\beta 1$ is present at the base of protruding invadopodia and seems to support membrane attachment while the invadopodium is extending into the matrix (Mueller et al., 1999). As integrins also activate Rho family and focal adhesion proteins through outside-in signaling (see section 2.2.2), this highlights once more the invadopodia/focal adhesion activation link.

Finally, in addition to promoting focal adhesion formation, the rigidity of the substrate also increases the number and activity of invadopodia (see section 2.3.1) (Alexander et al., 2008; Enderling et al., 2008). This observation agrees with the increase in tissue rigidity noticed during

tumor progression (Paszek et al., 2005) and provides a possible explanation for the correlation between higher tissue density and increased risk of invasive behavior (Chen et al., 2006; Levental et al., 2009).

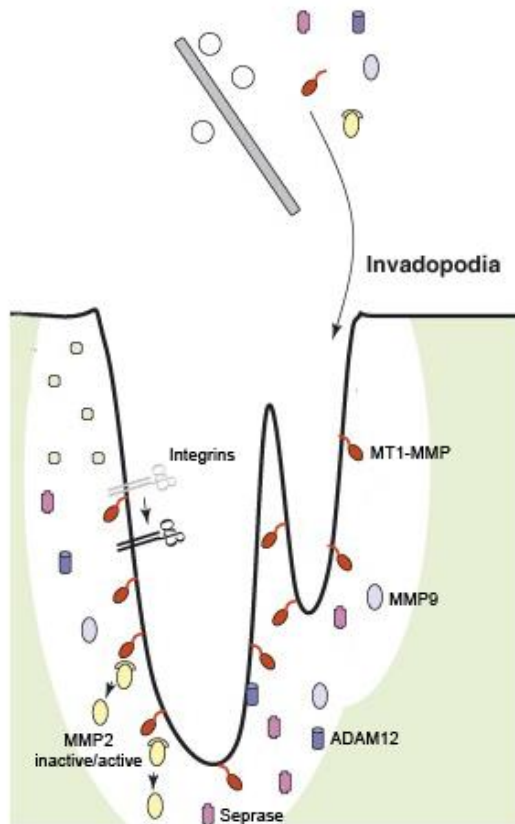


Figure I.7. Schematic representation of the molecular composition of invadopodia. (Adapted from Linder, 2007)

Coupling MMP delivery to invadopodia

The key feature of invadopodia is their ability to degrade matrices via the action of MMPs. It is believed that the rod-like shape of invadopodia allows focal delivery of MMPs. Sec8, a component of the exocyst complex, and the vesicular SNARE VMP-7, both have been shown to localize in invadopodia to control docking of MT1-MMP containing vesicles to the invadopodia plasma membrane (Poincloux et al., 2009; Sakurai-Yageta et al., 2008; Steffen et al., 2008). Evidence of the interaction of the exocyst complex with actin binding proteins of the cytoskeleton suggests that MMP delivery to invadopodia sites is also coupled with membrane protrusion and elongation of actin fibers (Figure I.7) (Sakurai-Yageta et al., 2008). Indeed, cortactin has been shown to regulate the secretion of major MMPs (MT1-MMP, MMP2 and MMP9) and is recruited to invadopodia before MT1-MMP suggesting that actin assembly precedes clustering of MMPs (Artym et al., 2006; Clark and Weaver, 2008; Clark et al., 2007).

However, depletion of MT1-MMP or inhibition of MMP activity also impairs the accumulation of actin and cortactin at the ventral surface of invasive cells, suggesting a positive feedback loop in which MMPs contribute to the initiation and maturation of invadopodia (Clark et al., 2007; Sakurai-Yageta et al., 2008; Steffen et al., 2008).

Chapter 3: Cancer invasion and metastasis – when cells go wild

Metastasis is a complex process that offers many challenges to cancer cells. In order to move from one tissue to another, they must go through and survive many inhospitable environments: the acquisition of genetic and epigenetic modifications in epithelial cells leads to a loss of polarity, overproliferation and formation of adenomas which later evolve into carcinomas (Hanahan and Weinberg, 2011). Carcinomas evolve from *in situ* to invasive when tumor cells acquire the capacity to breach the basement membrane they lie on. Then, cancer cells invade the surrounding stroma, and find their way to the circulation (Figure I.8) (Hanahan and Weinberg, 2011). Thousands of cancer cells are shed into the circulation but within 24h, less than 0.1% of them are viable due to the mechanical destruction caused by the high pressured blood flow and the immune surveillance (Fidler, 1970; Joyce and Pollard, 2009).

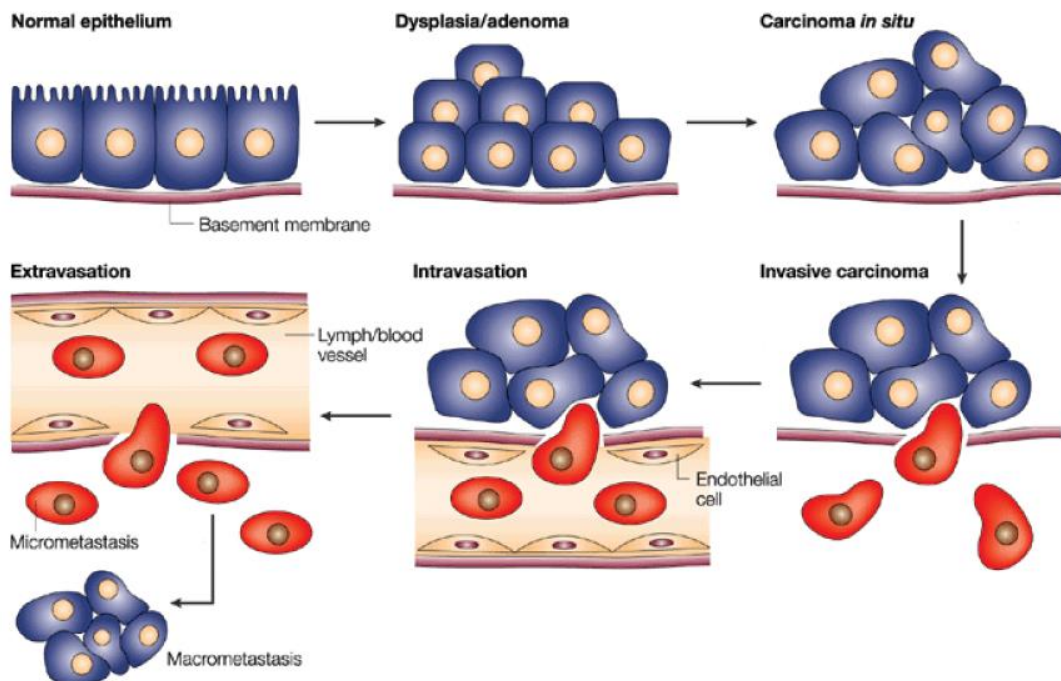


Figure I.8. The metastatic cascade (Adapted from Thiery *et al.*, 2002)

The remaining cells must then lodge into capillaries, survive, extravasate, seed and proliferate before they have clinical relevance meaning that overall, less than 0.01% of circulating tumor cells survive to produce metastases (Fidler, 1970). This makes the whole metastatic process highly selective for a very low number of cells and tumors. As a consequence, many efforts have been made towards understanding the difference between these 0.01% of metastatic cells and the millions of cancer cells in the tissue of origin that do not make it to secondary organs. Do they possess specific genetic traits that confer them resistance to the series of hostile environments they pass through (Hart and Easty, 1991; Ross et al., 2015)? Do they travel in group therefore providing support to each other (Aceto et al., 2014)? Or do they get sustenance from their microenvironment (Duda et al., 2010; Joyce and Pollard, 2009)?

3.1. Modes of cancer cell invasion

In vivo, invasive cancer cells migrate through a 3D environment that imposes physical constraints to their movement. The structural and chemical composition of the tissue environment regulates cell morphology and the mode of migration cancer cells adopt. Cells either migrate individually using amoeboid or mesenchymal migration, or collectively by migrating as cohesive multicellular units (Friedl and Wolf, 2010).

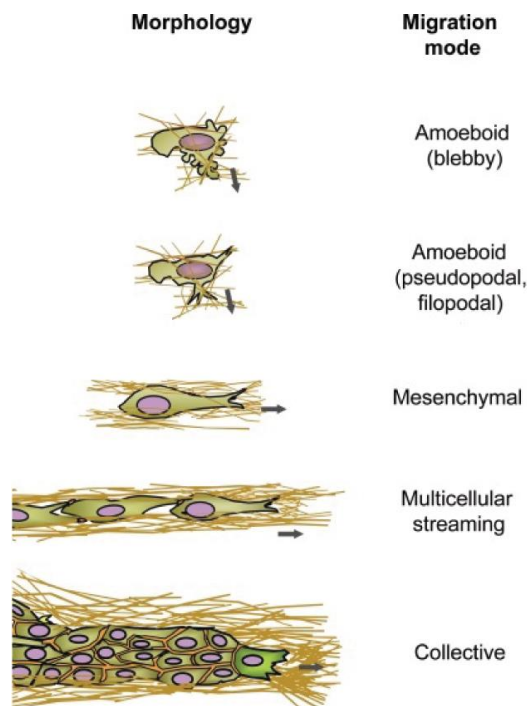


Figure I.9. Migration modes of invasive cancer cells (Adapted from Friedl and Wolf, 2010)

3.1.1. Single cell invasion

Mesenchymal migration is characteristic of elongated cells that depend on high levels of matrix adhesion and proteolysis (Figure I.9). In 3D collagen matrices, mesenchymal migration can be described as a cycle of 5 steps: 1) protrusion formation through polarization of an actin flow; 2) adhesion to the matrix through focal adhesions, force transmission through integrins and consequent collagen pulling and aligning; 3) local matrix proteolysis through MT1-MMP; 4) forward sliding of the cell body and nucleus squeezing through actomyosin contraction; 5) retraction of the cell rear forward to produce a path of remodeled collagen fibers (Friedl and Wolf, 2009). Thus, mesenchymal migration relies on the cells' ability to degrade the matrix they move into and is highly dependent on cell-matrix adhesion through integrins.

For a long time, it was assumed that the only way a cell can move through the ECM is to degrade it (Edwards and Murphy, 1998; Page-McCaw et al., 2007). This notion was challenged for the first time in 2008 when the lab of M. Sixt described a new mode of integrin-independent migration in leukocytes, referred to as amoeboid migration (Lammermann et al., 2008). Cells using an amoeboid type of migration are round, devoid of stress fibers and cell matrix adhesions (Figure I.9) (Friedl and Alexander, 2011; Lammermann et al., 2008; Wolf et al., 2013). They move by squeezing in between collagen fibers without degrading the matrix, using cortical actomyosin contractility for pushing their nucleus forward (Fackler and Grosse, 2008; Friedl and Alexander, 2011; Lammermann et al., 2008; Sanz-Moreno and Marshall, 2009; Wolf et al., 2013). In cancer cells, amoeboid migration can be adopted as a rescue mechanism when MMPs are inhibited which provides an explanation for the failure of drugs targeting MMPs in clinics (Wolf et al., 2013).

3.1.2. Collective invasion

Collective cell migration refers to a cohesive, multicellular group moving together (Friedl and Gilmour, 2009). Cells can establish weak or transient cell-cell contacts and independently generate traction forces on the matrix, thus migrating as a multicellular stream (Figure I.9). Alternatively, cells can move together as a cohesive group by maintaining cell-cell contacts (Friedl et al., 2012). In the latter mode of migration, the collectively moving cluster is driven by a leader cell that develops cell-matrix adhesion structures similarly to single migrating mesenchymal cells and thus degrades the matrix opening a path for the followers (Figure I.9) (Friedl and Gilmour, 2009; Friedl et al., 2012; Sahai, 2005). It has been shown that leader cells

can originate within the tumor itself following induction of basal epithelial genes such as cytokeratin-14 and p63 (Cheung et al., 2013). Leader cells could also come from the stromal fibroblasts and be of a mesenchymal nature (Clark and Vignjevic, 2015; Gaggioli et al., 2007; Labernadie et al., 2017).

3.1.3. Single vs collective mode in cancer progression

It was originally assumed that single cell invasion was the only mode adopted by cancer cells during metastasis. This view was driven by the notion that epithelial cells lose cell-cell junctions during cancer progression and undergo epithelial-mesenchymal transition (EMT) as they invade the surrounding stroma (Thiery, 2002). However, recent studies have suggested that carcinomas can also invade as a cohesive multicellular unit (Cheung et al., 2013; Nguyen-Ngoc et al., 2012; Plutoni et al., 2016) and heterogeneous circulating tumor cell (CTC) clusters were found to have an increased metastatic potential compared with single cells or homogeneous CTC clusters (Aceto et al., 2014). Furthermore, EMT was shown to be dispensable for the development of pancreatic cancer (Zheng et al., 2015), although targeting EMT cells in mice induced a better response to chemotherapy and overall survival. Altogether, these studies suggest that metastasis is mainly driven by collective invading clusters, while mesenchymal single cells, because of their low division rates (Gligorijevic et al., 2014), are more resistant to treatment and might eventually contribute to patient relapse.

3.2. Following gradients in cell motility

Cell motility is not a random process in the sense that cells at steady state do not actively migrate unless exposed to a gradient of extracellular cues that will promote an asymmetric activation of receptors and the generation of morphologically distinguishable cell front and back (King and Parsons, 2011). As cells tend to polarize their front towards the highest concentration of the cue, this implies that cell motility is driven by the establishment of gradients *in vivo* (Ladoux et al., 2016; Roca-Cusachs et al., 2013b). Cells respond to different extracellular cues such as chemokines and growth factors which can either be freely diffusing (chemotaxis) or tethered within the matrix (haptotaxis), as well as to physical and mechanical properties of the ECM (durotaxis), and to local electrical fields (galvanotaxis) (Figure I.10) (Haeger et al., 2015).

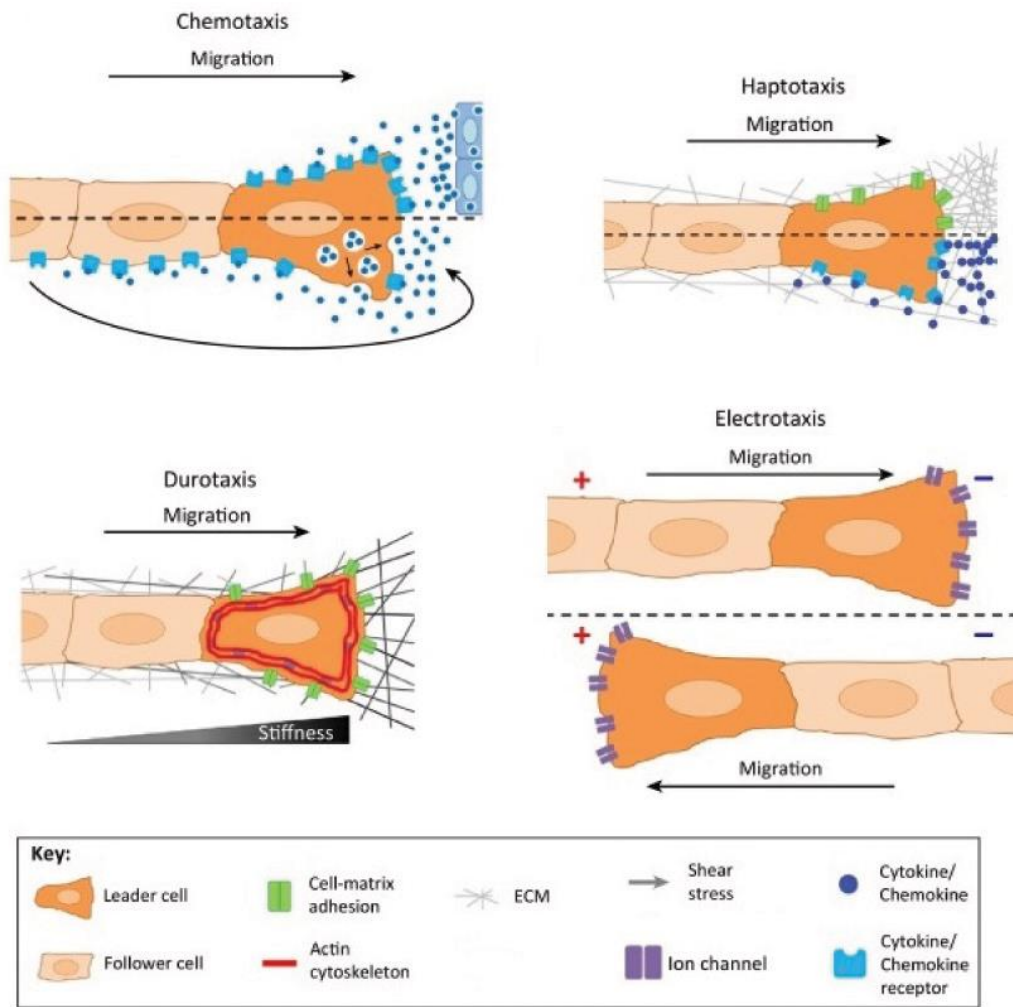


Figure I.10. Cell guidance modes during migration (Adapted from Haeger *et al.*, 2015)

3.2.1. Chemotaxis

The phenomenon of chemotaxis was first described in the 19th century when scientists first studied the mechanisms underlying the attraction of neutrophils to sites of infection (Harris, 1954). Since then, the notion of cell guidance was found to be relevant in many physiological processes such as development, homeostasis and wound healing, as well as pathological conditions such as cancer. Chemotaxis induces cell guidance via soluble chemical stimuli such as chemokines, cytokines, as well as altered pH and oxygen gradients (Haas and Gilmour, 2006; Jacob *et al.*, 1999; Lecaudey *et al.*, 2008; Lewis *et al.*, 2016; Valentin *et al.*, 2007). Receptor binding and activation by chemotactic molecules induces local formation of cell-matrix protrusions, hence polarization and motility towards the zone with the highest chemoattractant

availability (Insall, 2010). Chemotaxis is an essential guidance mechanism during development for the directional migration of the zebrafish lateral line (Dona et al., 2013; Haas and Gilmour, 2006; Valentin et al., 2007) and for the collective migration of the border cells in-between nurse cells in the *Drosophila* egg (Cai et al., 2014; Cai et al., 2016; McDonald et al., 2006) During cancer progression, sarcoma cells invade under the influence of hypoxic O₂ gradients, from the necrotic core in the direction of increasing O₂ tension (Lewis et al., 2016). Chemotaxis has also been suggested as an explanation for the “seed and soil” hypothesis (see section 5.3). For example, prostate cancer cell metastasis to the bone was suggested to be mediated by the chemotactic effect of osteonectin (Jacob et al., 1999).

Importantly, chemotaxis is not exclusively an effect of the extracellular milieu as cell collectives can establish a self-generated gradient along the migrating group (Dona et al., 2013; Tweedy et al., 2016). For example, leader cells can locally secrete migration enhancing cytokines and establish a positive feedback loop (Kriebel et al., 2008). Alternatively, cells at the rear can bind and internalize chemokines to create a gradient along the length axis of the group: during formation of the zebrafish lateral line, following cells at the rear of the group overexpress the scavenger chemokine receptor type 7 (CXCR7) which sequesters the stromal derived factor-1 (SDF-1), thus creating a front-rear SDF-1 gradient (Dona et al., 2013; Valentin et al., 2007).

3.2.2. Haptotaxis

Haptotactic movement was first described 100 years after the discovery of chemotaxis (Carter, 1967) and experimentally demonstrated 20 years later when cancer cells were found to move along a gradient of serum spreading factor established within a matrix (Basara et al., 1985). While chemotaxis depends on a ligand-receptor interaction, haptotaxis requires cells to mechanically sense matrix-bound ligands through integrin-mediated focal adhesions (Debruyne et al., 2002). Because of this ligand immobilization, haptotaxis therefore provides more temporally and spatially sustained signals compared to chemotaxis. Ligand gradients can result from different levels of sequestered ECM proteins. FN for example can be both secreted and assembled into the ECM (see section 4.1.2) and it was recently suggested that cancer cells haptotact towards ECM-bound FN secreted by endothelial cells lining the blood vessels (Oudin et al., 2016). Alternatively, matrix-bound chemoattractants can mediate haptotaxis. This is the

case of bile acids which are enriched in tumor microenvironments and stimulate haptotaxis of colon cancer cells through activation of Rac and Rho-GTPases (Debruyne et al., 2002).

Of note, cell movement may also orient towards decreasing ligand density, a mechanism which is termed “repulsion” (Fagotto et al., 2013; Sugiyama et al., 2013; Theveneau et al., 2013). In the case of chemorepulsion, ligand-receptor binding induces pro-migratory protrusions to form at the pole of the cell, opposed to receptor engagement (Tessier-Lavigne, 1994). Repulsive matrix-bound ligands act through Rac inhibition, which leads to disassembly of focal adhesions, collapse of cellular protrusions and cell reorientation in the opposite direction (Theveneau et al., 2013). In addition, Rho-dependent contractility accumulates at cell boundaries, preventing stable cell junctions and leading to tissue separation (Fagotto et al., 2013).

3.2.3. Durotaxis

Durotaxis refers to the directional response of cells according to a stiffness gradient of the substrate. Gradient orientation can be both positive (with cells moving towards high stiffness) and negative (with cells moving towards low stiffness). Durotaxis was first described in fibroblasts that migrated towards regions of high rigidity when placed on a matrix of varying stiffness (Lo et al., 2000). Similarly, sarcoma cell sheets were shown to enhance their migratory capacity on stiff compared to soft substrates (Beaune et al., 2014), suggesting a differential stiffness sensing. Similarly to haptotaxis, durotactic movement also requires traction-generation through a FAK/phosphopaxillin/vinculin pathway (Fouchard et al., 2011; Lange and Fabry, 2013; Plotnikov et al., 2012) which should eventually lead to the maturation of focal adhesions into fibrillar adhesions, local matrix secretion and self-generated haptotaxis gradients. Thus, one type of gradient could lead to the generation of another and stimulate more directed migration.

3.2.4. Galvanotaxis

Galvanotaxis (or electrotaxis) is defined as the directional migration of cells relative to an electric field with orientation towards either the anode or the cathode (Cortese et al., 2014; Liu and Song, 2014). Although the notion is counter-intuitive, electrical fields are frequently established within the organism, especially during neuronal synapses and wound healing (Yao et al., 2009; Zhao, 2009; Zhao et al., 2006). The discovery that cells undergoing galvanotaxis orient and migrate in a specific direction relative to a direct-current electric field dates to the late nineteenth century when a study performed by Wilibald A. Nagel proved that spontaneous

electrical fields arise at the site of epidermal wounds as a result of electrochemical imbalance. Recent data show that these fields serve as an important role in the wound healing process by providing a galvanotactic cue that seems to act on the same downstream motility pathways as chemotaxis and general cell migration (Cohen et al., 2014; Cortese et al., 2014; Li et al., 2012; Zhao et al., 2006). However, although many data suggest that most cells are electrically sensitive and that galvanotaxis is implicated in many cell movements that occur throughout development, morphogenesis and regeneration, the mechanisms and scenarios during which cells sense electrical gradients remain to be further described.

Of note, most of the mentioned studies on the mechanisms of cell guidance were performed on collectively moving sheets and clusters. The experiments on the zebrafish lateral line suggest that a collective unit is required to establish self-generated gradients. It has also been recently shown that collective durotaxis was more efficient than single-cell durotaxis due to cell-cell junctions which promote a better integration of cell-matrix adhesions at the tissue level (Sunyer et al., 2016). But whether the integration of signals controlling collective guidance is always more efficient to that in single cells remains to be established.

Chapter 4: The tumor microenvironment

There is a fundamental difference between a normal physiological stroma, and a reactive stroma found in cancers or inflammatory diseases for example. A normal stroma is characterized by a small number of quiescent fibroblasts and a physiological ECM mostly composed of collagen I fibers and displaying little to no physiological alterations e.g. cleavage sites, high crosslinking or enrichment in glycoproteins such as FN and tenascin C (TNC). A reactive stroma contains an increased number of fibroblasts along with a high number of vessels and capillaries. Due to this enhancement in angiogenesis, immune cells patrolling the circulation are enriched within the tumor microenvironment, creating a site of inflammation. In addition, the stiffness of the ECM increases due to altered collagen deposition, crosslinking and remodeling (Hanahan and Weinberg, 2011; Joyce and Pollard, 2009; Kalluri and Zeisberg, 2006). Such altered stroma is mostly found in conditions requiring tissue remodeling such as wound healing and fibrosis (Gabbiani et al., 1971; Powell et al., 2005). Importantly, this state of activation is supposed to be only transient and restricted to the healing process. A chronic state of activation would lead to

tissue dysplasia and a strong predisposition for cancer (Itzkowitz and Yio, 2004; Tanaka et al., 2006).

It is accepted that genetic and epigenetic modifications of cancer cells are not sufficient to drive metastasis formation. During their metastatic journey, cancer cells constantly interact with their microenvironment and modify it. In return, the microenvironment plays an active role throughout the metastatic progression, stimulating tumor growth, survival, and invasion (Hanahan and Weinberg, 2011; Joyce and Pollard, 2009). Moreover, a “normal” microenvironment can also have the ability to revert cancer cells to a “normal” phenotype (Bissell and Hines, 2011) suggesting that the tumor microenvironment may not only be an enabler that merely plays a passive role in cancer progression, but rather a potential inducer of carcinogenesis and metastasis.

4.1. The extracellular matrix – structural composition and architecture

The ECM is the scaffold that provides biomechanical and biochemical support to cells. Fundamentally, all ECMs are composed of water, proteins and polysaccharides (Hynes and Naba, 2012). However, each ECM has a unique topology that is generated during development to fit the specific biological functions and needs of its respective tissue (Frantz et al., 2010; Mecham, 2012; Mouw et al., 2014; Rozario and DeSimone, 2010). Not only do the organizational properties of the ECM vary tremendously between tissues (bone vs lungs vs muscle), it is also very heterogeneous within one tissue, from one physiological state to another (normal vs cancer) and according to the biological process undergoing (tissue morphogenesis vs differentiation vs homeostasis) (Mecham, 2012; Rozario and DeSimone, 2010).

Although the ECM can be thought of as a static and stable scaffold maintaining tissue integrity and morphology, it is surprisingly dynamic, constantly remodeled, and influences fundamental cell biology behaviors. This cell-ECM crosstalk is due to both the biochemical and physical properties of the ECM (Lu et al., 2012):

- Biochemically, because of its richness in polysaccharides, the ECM is a highly charged structure that can bind many growth factors such as bone morphogenetic proteins, hedgehogs and WNTs (Hynes, 2009; Hynes and Naba, 2012). By regulating growth factor bioavailability and distribution, the ECM creates internal gradients within a tissue,

establishes complex adhesion surfaces and forms diffusion barriers between cellular layers (Hynes, 2009).

- The physical properties of the ECM refer to its rigidity, porosity, spatial arrangement and orientation (or topography). Because of its tensile and compressive strength and elasticity, the ECM mediates protection by a buffering action that maintains extracellular homeostasis and water retention. Interestingly, proteoglycans, being negatively charged, also contribute to the sequestration of water and cations (such as calcium) (Hynes and Naba, 2012). In addition, the biomechanical properties of the ECM influence cell behaviors by regulating migration and adhesion. Indeed, any change in ECM elasticity or stiffness is sensed by cells through focal adhesions (Discher et al., 2005). Components of focal adhesions then undergo conformational changes that eventually, on a larger scale, modify the cell's functionality. Moreover, changes in mechanical forces can also be converted into deregulation of signaling pathways and growth factors secretion (Alexander et al., 2008; Enderling et al., 2008; Levental et al., 2009; Paszek et al., 2005), indicating that the physical and biochemical properties of the ECM are tightly linked and act concomitantly to regulate cell behavior.

Interstitial ECMs, like the one comprising the intestinal stroma, are compliant structures primarily composed of 2 main classes of macromolecules secreted and organized by resident fibroblasts: fibrous proteins (such as collagens and elastin) and glycoproteins (such as fibronectin, tenascins and proteoglycans) (Hynes and Naba, 2012; Mecham, 2012). These macromolecules are structured as a relaxed meshwork of type I collagen, elastin and FN that are embedded in a hydrogel of proteoglycans (Hynes and Naba, 2012; Mouw et al., 2014).

4.1.1. Collagen

General overview and structure

In multicellular animals, collagen represents up to 30% of the protein mass. It is also the most abundant protein of the interstitial ECM and constitutes its main structural element (Ricard-Blum, 2011; Ricard-Blum and Ruggiero, 2005; Rozario and DeSimone, 2010). To date, 28 members have been uncovered in the collagen family. They all share a common structural feature which is a triple helix consisting of 3 polypeptide chains, or α chains (Figure I.11) (Ricard-Blum, 2011; Ricard-Blum and Ruggiero, 2005). Each α chain contains repeats of the triplet Gly-X-Y which confers to collagen its stable, rod-like, coiled-coil architecture. X and Y

are frequently proline and 4-hydroxyproline residues respectively, and the repetitive glycine residue stabilizes the triple helix (Bella et al., 1994; Brodsky and Persikov, 2005). Due to the variability of X and Y, collagen chains can associate into either homotrimers (collagen II and III), heterotrimers (collagen XI), or both (collagen I) (Figure I.11).

Collagens are divided into network forming collagens (e.g. collagen IV) and fibril forming collagens (e.g. collagen I, II, III) (Ricard-Blum, 2011). Fibrillar collagens being discovered first, and because of their relatively simple structure, are also known as classical collagens. Their common large continuous triple helical domain (COL1) is bordered by non-collagenous domains (NCs): N- and C-terminal extensions (or N- and C-propeptides) respectively (Hohenester and Engel, 2002). The rod-like COL1 domain has the capacity to bind cell surface receptors, other proteins, glycosaminoglycans (GAGs) and nucleic acids while the NC propeptides are cleaved during collagen biogenesis for it to be fully processed into mature and functional molecules (Bella et al., 1994; Brodsky and Persikov, 2005; Hohenester and Engel, 2002).

Biosynthesis and assembly

The bulk of interstitial collagen I is transcribed and secreted by fibroblasts. Collagen is initially synthesized as procollagen α chains comprised of a central triple helix flanked by N and C-telopeptides followed by amino- and carboxy-terminal propeptides (Bella et al., 1994; Brodsky and Persikov, 2005). These α chains undergo numerous translational and post-translational modifications that are stopped by the formation of a triple helix within the endoplasmic reticulum and subsequently packaged into secretory vesicles in the Golgi apparatus (Hulmes, 2002). The carboxy- and amino-terminal propeptides are then cleaved in the extracellular space, leading to the formation of mature collagen molecules that have the ability to self-assemble. Crosslinking takes place on the telopeptides through deamination of lysyl-, hydroxylysyl- and histidine residues. It is catalyzed by lysyl-oxidase (LOX) and occurs at the intra and intermolecular levels between same type and different type collagen molecules (Hulmes, 2002; Ricard-Blum, 2011). Collagen crosslinking stabilizes the supramolecular structure of collagen while conferring it elastic properties making it reversibly deformable and compliant (Gutsmann et al., 2004).

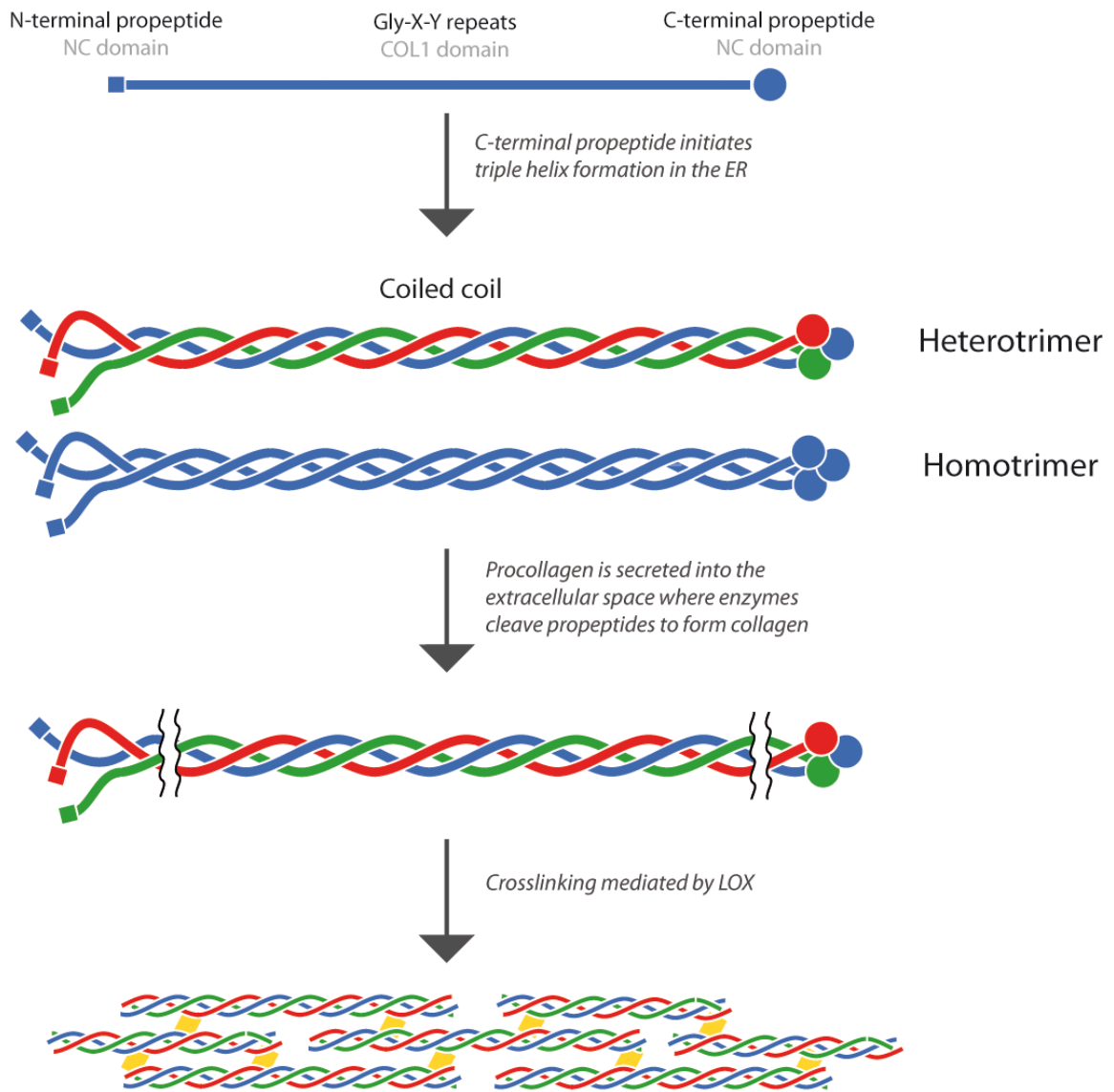


Figure I.11. Architecture, biosynthesis and assembly of collagen

Receptors

Cells adhere to collagen I-rich matrices mainly via integrins, more specifically via heterodimers containing a $\beta 1$ subunit combined with one of the 4 α -subunits: $\alpha 1$, $\alpha 2$, $\alpha 10$ or $\alpha 11$ (Heino, 2007; Humphries et al., 2006; Leitinger and Hohenester, 2007). Upon recognition of a GFOGER-like motif on collagen fibers, integrin heterodimers get activated, and through outside-in signaling trigger focal adhesion assembly (Emsley et al., 2000). In addition, proteolytic cleavage of collagen unmasks bioactive fragments which are ligands for further integrin heterodimers,

notably the FN receptors $\alpha 5\beta 1$ and $\alpha v\beta 3$ (Ricard-Blum and Ballut, 2011) suggesting that collagen degradation promotes FN fibrillogenesis (see section 3.1.2).

Collagen I is also a ligand of the dimeric discoidin receptors DDR1 and 2 which possess tyrosine kinase activity (Leitinger and Hohenester, 2007). DDRs have been suggested to affect the mechanical properties of collagen fibers (Coelho et al., 2017; Sivakumar and Agarwal, 2010). Indeed, a recent study has shown that fibroblasts induce collagen alignment through DDR1 and non-muscle myosin IIA-dependent high traction forces (Coelho et al., 2017). Interestingly, the DDR-myosin complex did not localize with focal adhesions indicating that DDR-mediated cell contractility was independent of integrin activity.

Finally, collagen receptors can also be cell-type specific. For example, the glycoprotein VI (GPVI) and the inhibitory leukocyte-associated immunoglobulin-like receptor (LAIR) mediate adhesion of platelets and leukocytes respectively to collagens (Heino, 2007; Ricard-Blum, 2011). The fact that immune and blood cells bind collagen in a different manner makes sense as these cell populations are more motile throughout the body, especially in the case of immune cells where a high affinity to the matrix would impair their capacity to rapidly patrol different environments.

4.1.2. Fibronectin

General overview and structure

FN is a major ECM glycoprotein that plays a central role in cell adhesion and migration during development, wound healing, angiogenesis and tumor progression (George et al., 1993; Hynes, 2009; Sakai et al., 2003; Van Obberghen-Schilling et al., 2011). The architecture of FN networks contribute directly to the structure and organization of the wider ECM, due to the presence of multiple binding sites within FN for other ECM components, such as collagens I and III (Shi et al., 2010; Velling et al., 2002). In addition to being part of the insoluble ECM, FN is also abundant in the plasma and other body fluids (Mosesson and Amrani, 1980). Based on its solubility, FN is divided into 2 major types: soluble plasma FN (pFN) synthesized predominantly in the liver by hepatocytes, and insoluble cellular FN (cFN) which is secreted locally within tissues and assembled into a fibrillary network. Both types present the same fundamental architecture with a dimer of 250KDa subunits linked covalently near their C-termini by a pair of disulfide bonds (Figure I.12) (Akiyama et al., 1981; Hynes, 1985). Each monomer consists of three types of repeating units, types I, II and III, and within these units are domains for binding

to a variety of extracellular and cell surface molecules including collagen, GAGs, integrins and FN itself (Akiyama et al., 1981; Pankov and Yamada, 2002). Although all FN molecules are the product of a single gene, the resulting mRNA can undergo alternative splicing, giving rise to as many as 20 FN variants in humans (French-Constant, 1995). Indeed, cFN is additionally spliced within the type III module, leading to the inclusion of EDA and EDB repeats (Figure I.12). cFN undergoes further cell-type-specific and specie-specific splicing, generating FNs with different cell-adhesive, ligand-binding, and solubility properties that provide a mechanism for cells to precisely alter the composition of the ECM in a developmental and tissue-specific manner (Akiyama et al., 1981; French-Constant, 1995).

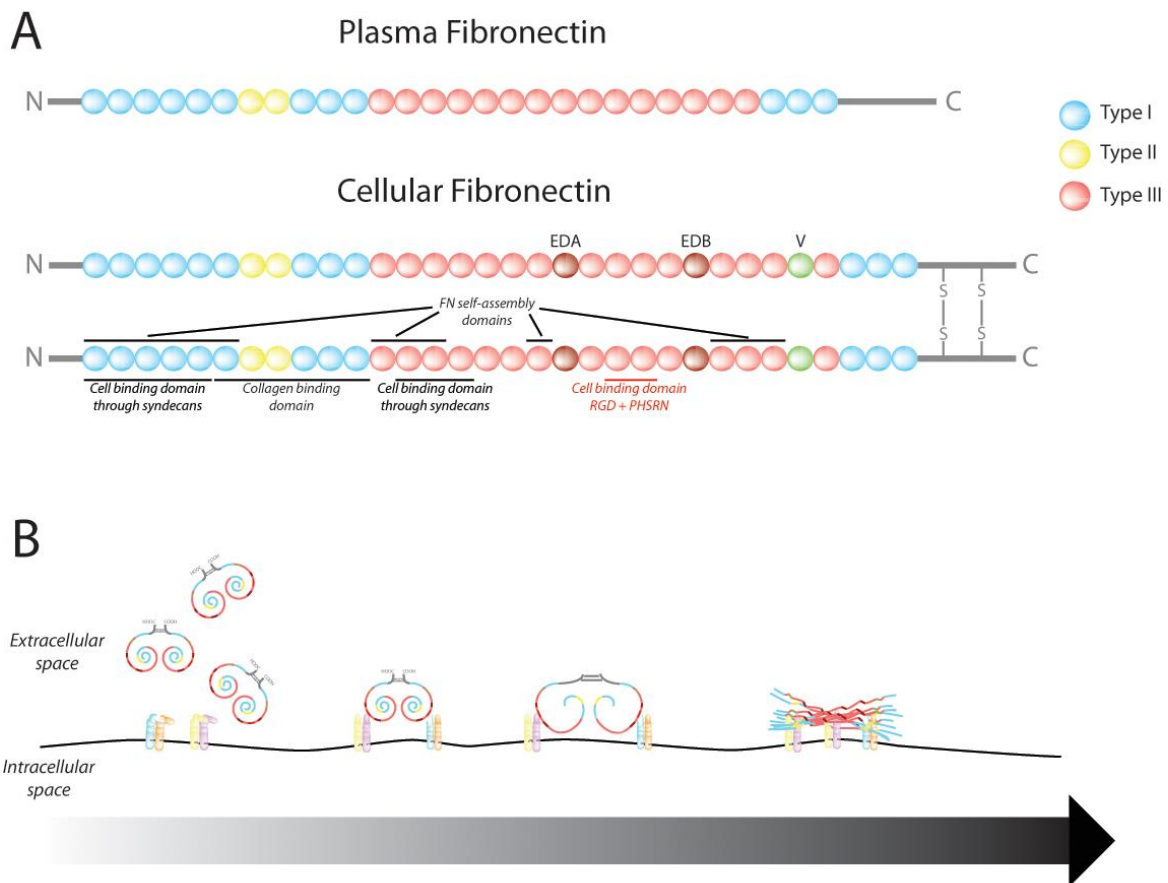


Figure I.12. Architecture and assembly of fibronectin
 A- Biochemical composition of cellular and plasma fibronectin
 B- Fibronectin matrix assembly

FN matrix assembly

FN matrix assembly is a cell-mediated process in which soluble FN is converted into a fibrillary network (Figure I.12) (Pankov and Yamada, 2002; Wolanska and Morgan, 2015). FN is initially

secreted by cells as a compact and soluble dimer where intramolecular ionic interactions within the type III modules maintain the molecule folded and prevent spontaneous formation of fibrils. While, some interaction sites are exposed and available for binding, others are cryptic and become accessible only after conformational changes and activation of the FN molecule (Erickson, 2016; Pankov and Yamada, 2002; Wolanska and Morgan, 2015). FN activation is induced by interactions with cell surface receptors, usually integrins, which recognize the central cell-binding domain (CCBD) that comprises the RGD and synergy sites within the type III module (Wierzbicka-Patynowski and Schwarzbauer, 2003; Wolanska and Morgan, 2015). Through outside-in activation, integrin binding induces reorganization of the actin cytoskeleton, leading to cell-mediated application of tensile forces through focal adhesions and later fibrillar adhesions (Erickson, 2016). The compact FN dimer then undergoes expansion, exposing cryptic “self-association” sites that participate in FN-FN interactions (Pankov and Yamada, 2002; Wierzbicka-Patynowski and Schwarzbauer, 2003; Wolanska and Morgan, 2015). FN molecules also associate to each other via non-covalent interactions in the N-terminus part (Schwarzbauer, 1991; Sottile and Mosher, 1997). These interactions enable soluble FN fibrils to branch and convert into a dense and stable insoluble network. Interestingly, the necessity of the FN compact dimers to unfold and expand prior to their assembly has particular significance for circulating plasma FN as it provides a mechanism to prevent the formation of insoluble fibrils in the bloodstream.

Receptors

To date, 4 integrin heterodimers have been reported to initiate FN assembly *in vitro*: $\alpha 5\beta 1$, $\alpha v\beta 3$, $\alpha 4\beta 1$ and $\alpha IIb\beta 3$, with $\alpha 5\beta 1$ being the major receptor mediating FN fibrillogenesis (Leiss et al., 2008; Sechler et al., 2000). Indeed, in addition to the RGD domain, $\alpha 5\beta 1$ is the only integrin heterodimer capable of recognizing the synergy site PHSRN, and therefore has 2 docking sites on the FN dimer (Aota et al., 1994; Rossier et al., 2012). Moreover, interactions between FN and $\alpha 5\beta 1$ integrin contribute to full activation of Rho and subsequent contractility and fibrillar adhesion maturation, all of which are necessary for optimal FN assembly (Danen et al., 2002). However, $\alpha 4\beta 1$ integrin was shown to interact with FN independently of RGD through binding of the CS1 site near the C-terminus region (Sechler et al., 2000). Another RGD-independent mechanism acts through $\alpha v\beta 3$ integrin which recognizes an *iso*DGR sequence located on the N-terminus of FN (Takahashi et al., 2007), though the extent to which the *iso*DGR site contributes

to normal FN fibrillogenesis is still unclear. Thus, it seems that integrin $\alpha 5\beta 1$ might be dispensable for FN matrix assembly. In fact, when forcing the expression of active RhoA in integrin $\beta 1$ depleted cells, FN fibrillogenesis was maintained by integrin $\beta 3$ (Danen et al., 2002). It was later shown that $\beta 1$ was required to establish focal adhesions (probably due to its involvement in adhesion to many types of matrices), while the expression of $\alpha v\beta 3$ correlated with focal adhesion to fibrillar adhesion transition. These experiments suggest that while $\alpha 5\beta 1$ is necessary for sensing of FN, increasing intracellular tension and fibrillar adhesion reinforcement, $\alpha v\beta 3$ mediates the initial focal adhesion to fibrillar adhesion transition. Therefore, in a scenario where cell contractility is $\alpha 5\beta 1$ -independent (in FN depleted matrices), FN-matrix assembly would be initiated by $\alpha v\beta 3$ but this hypothesis has never been tested.

Another class of candidates mediating FN matrix assembly are syndecans. Syndecans are transmembrane heparin sulfate proteoglycans which bind various ECM glycoproteins, notably FN through its types I and III modules (Morgan et al., 2007; Wolanska and Morgan, 2015). Although syndecans have been shown to directly influence FN fibrillogenesis (Klass et al., 2000; Stepp et al., 2010), they also modulate focal adhesion dynamics and subsequent matrix assembly by coordinating $\alpha 5\beta 1$ and $\alpha v\beta 3$ integrin trafficking (Morgan et al., 2013). More specifically syndecan-4 phosphorylation by the tyrosine kinase Src leads to concomitant inhibition of $\alpha 5\beta 1$ trafficking and localization of $\alpha v\beta 3$ to the cell surface, resulting in adhesion stabilization (Morgan et al., 2013). This phenotype makes sense as the continuous activity of Src correlates with focal adhesion to fibrillar adhesion transition (see sections 2.1.2 & 2.2.2). It is also in line with the previously described dynamics of $\beta 1$ and $\beta 3$ integrins where the expression of $\alpha v\beta 3$ correlates with the establishment of stable fibrillar adhesions (Schiller et al., 2013).

Finally, ECM degradation has been shown to trigger FN assembly as cleavage of collagen fibers sometimes exposes bioactive fragments which are ligands for $\alpha 5\beta 1$ and $\alpha v\beta 3$ integrins (Ricard-Blum and Ballut, 2011). However, another study shows that MT1-MMP has the capacity to cleave FN-rich matrices therefore negatively regulating FN fibrillogenesis (Takino et al., 2011). This implies that matrix proteolysis promotes FN matrix assembly if not under the action of MT1-MMP. In fact, the urokinase-type plasminogen activator receptor uPAR promotes the degradation of ECM molecules (Smith and Marshall, 2010) but also binds integrin $\alpha 5\beta 1$ and induces its activation and subsequent FN fibrillogenesis (Wei et al., 2005).

4.1.3. Alterations in tumors

During cancer progression, the biomechanical and biochemical properties of the ECM are deregulated (Bonnans et al., 2014; Lu et al., 2011): some ECM proteins like collagens and FN get enriched and others which are normally absent in the stroma, like laminin, appear. Collagen fibers become more crosslinked, stiffened and aligned, as the expression of ECM remodeling enzymes such as LOX is aberrant. As already described, these alterations enhance the formation of cell-matrix adhesions such as focal adhesions and invadopodia, and therefore boost the motility, contractility, and invasive phenotype of cancer cells (Alexander et al., 2008; Enderling et al., 2008; Levental et al., 2009; Paszek et al., 2005). ECM remodeling in tumors is mainly mediated by cancer-associated fibroblasts and this notion will be extensively discussed in section 5.2.2.

Chapter 5: Cancer-associated fibroblasts in tumor development

Fibroblasts are a population of cells characterized by their elongated spindle-like shape, their similarities to mesenchymal and smooth muscle cells and, in the context of a wound, their role in tissue contraction (Gabbiani et al., 1971; Hirschel et al., 1971; Majno et al., 1971). There have been many attempts to further define this cell population. However, to date, there is still no specific marker of fibroblasts. Experimentally, fibroblasts are defined based on their shape, the absence of markers of other cell types, as well as the expression of a combination of smooth muscle and mesenchymal cells' markers such as α -smooth muscle actin (α SMA), the platelet derived growth factor receptor β (PDGFR β), vimentin and desmin.

Fibroblasts are the main generators of ECMs, scaffolds that other cells are anchored to (see section 4.1). They are at their most active state during embryonic development when all matrices in the human body are being created (Powell et al., 2005). In adult normal tissues, they are quiescent residents of the stroma. Because of their non-proliferative nature, normal fibroblasts have never been successfully isolated and kept in a 'non-activated' form. To study fibroblast's functions it is possible to either immortalize normal adult fibroblasts or use embryonic fibroblasts that retain a proliferative capacity, albeit these two populations do not always recapitulate normal fibroblasts' functions.

In tissue inflammation, fibrosis, and during wound healing, fibroblasts get ‘activated’ (Gabbiani et al., 1971; Powell et al., 2005). In those conditions, they are often called myofibroblasts because of their increased capacity to contract and remodel the matrix which is necessary to heal the wounded tissue (Majno et al., 1971). Once the wound is healed, they either revert back to a normal state or undergo apoptosis as activated fibroblasts are not present in significant amounts in normal adult tissues. The presence of activated fibroblasts in adult tissues suggests the presence of a disease. At the tumor site, activated fibroblasts are known as cancer-associated fibroblasts (CAFs) (Kalluri and Zeisberg, 2006). CAFs were initially thought to be a consequence of tumor formation but later it has been shown that they actively contribute to tumor growth, invasion and metastasis (Bissell and Hines, 2011). Therefore, targeting CAFs seems to be a good clinical strategy to fight cancer (Hirata et al., 2015).

5.1. Their origin(s)

As promising as the concept sounds, targeting CAFs in clinics remains a complicated task as the lack of a specific fibroblast marker makes it difficult to discriminate what cell(s) population(s) give rise to CAFs. The most accepted hypothesis predicts that CAFs emerge from resident normal fibroblasts that are activated by cancer cells and the neighboring stroma (Albregues et al., 2015; Avgustinova et al., 2016; Calvo et al., 2013; Kojima et al., 2010; LeBleu et al., 2013). However, several studies have proposed alternative origins of CAFs: they can be the progeny of other resident cells of the stroma such as endothelial cells through endothelial to mesenchymal transition (EndMT) (LeBleu et al., 2013; Zeisberg et al., 2007), from pericytes (Hosaka et al., 2016; Ross et al., 1974), or from adipose derived stem cells (ASCs) (Jotzu et al., 2010). CAFs could also originate from the tumor itself through EMT (LeBleu et al., 2013; Radisky et al., 2007; Rowe et al., 2009; Schulte et al., 2012). Finally, some studies have shown that CAFs do not necessarily emerge from the cancer site itself as mesenchymal stem cells that are recruited from the bone marrow to the tumor acquire a CAF-like phenotype and promote invasion and proliferation of cancer cells (Karnoub et al., 2007; Lu et al., 2013; Mishra et al., 2008; Quante et al., 2011; Shinagawa et al., 2013; Talele et al., 2015). The fact that they could have multiple origins highlights the complex heterogeneity of CAFs and predicts that this one cell population could in fact play many roles in cancer progression. Indeed, the influence of CAFs on tumor invasion is still debated in the field (Kalluri, 2016): it has been shown that depleting CAFs from the stroma induces tumor invasion (Ozdemir et al., 2014; Rhim et al., 2014), but most studies

agree that an enrichment in CAFs stimulates cancer cell invasion (Calvo et al., 2013; De Wever et al., 2004; Gaggioli et al., 2007; Goetz et al., 2011; Orimo et al., 2005). There is also a disagreement concerning the mechanism by which CAFs act: do they enhance the invasive capacity of cancer cells through diffusible molecules (De Wever et al., 2004; Orimo et al., 2005)? Is their physical presence required to contract and align the matrix, facilitating cancer cell invasion (Calvo et al., 2013; Gaggioli et al., 2007; Goetz et al., 2011)? Or do they directly interact with cancer cells and lead their invasion into the matrix (Labernadie et al., 2017)?

5.2. At the primary site

5.2.1. Direct crosstalk between CAFs and cancer cells

The transforming growth factor- β (TGF- β) signaling pathway is a major player in cancer development and is known to regulate tumor growth through multiple cellular mechanisms such as apoptosis, proliferation, angiogenesis, migration and invasion (Bierie and Moses, 2006; Siegel and Massague, 2003). Aberrant expression of the TGF- β receptors (T β R) and their ligands is not specific of cancer cells, as both overexpression (Calon et al., 2012; Tsushima et al., 2001) and silencing (Achyut et al., 2013; Bhowmick et al., 2004; Franco et al., 2011; Oyanagi et al., 2014) of the TGF- β signaling pathway in fibroblasts is important for tumor progression. TGF- β remains the most commonly used growth factor to activate fibroblasts in culture as it activates many downstream pathways leading to growth factor secretion and matrix remodeling (Desmouliere et al., 1993; Ronnov-Jessen and Petersen, 1993). However, it is still a debate whether loss of the T β R or its overexpression leads to a more aggressive tumor profile.

Conditional loss of the TGF- β type II receptor (T β RII) in fibroblasts increases cell proliferation of both fibroblasts and neighboring epithelial cells, and results in preneoplastic lesions that could eventually progress to invasive carcinomas (Bhowmick et al., 2004). Upon silencing the T β RII, fibroblasts secrete upregulated amounts of HGF as a result of suppression of cell cycle regulators p21 and p27, and induction of transcription regulator c-Myc (Bhowmick et al., 2004; Oyanagi et al., 2014). Therefore, it seems that during cancer progression, CAFs can acquire conditional loss of TGF- β receptor II, which favors an increase of tumorigenesis (Figure I.13)

Loss of the T β R does not abolish the secretion of the TGF- β ligand, allowing a paracrine effect on neighboring CAFs that do not have the same deletion of T β R (Franco et al., 2011). In fact, the most optimal scenario for cancer progression is where CAFs are present in a heterogeneous

manner; tumor cells could benefit from the growth factors secreted by CAFs that lack the T β R, and the activated state of CAFs that can respond to TGF- β activation. Of note, in some cancers, the stroma is the only direct beneficiary of TGF- β as cancer cells display mutational deactivation of the TGF- β receptor (Calon et al., 2012). In other words, although they can secrete TGF- β , cancer cells cannot directly benefit from it, but only indirectly from the activated stroma (Figure I.13).

TGF- β is a solid predictor of cancer recurrence and metastasis (Calon et al., 2012; Tsushima et al., 2001). It upregulates genes coding for gp130 binding cytokines, more specifically IL11. IL11 activates the phosphorylation of Stat3 in cancer cells, and this interaction renders cancer cells resistant to apoptosis and favors metastasis (Calon et al., 2012). TGF- β also stimulates expression of SDF-1 in CAFs (Kojima et al., 2010), which is not only necessary for cancer cell proliferation and invasion, but also for recruitment of endothelial progenitor cells and angiogenesis (Izumi et al., 2016; Kojima et al., 2010; Orimo et al., 2005). A positive feedback loop is also established as SDF-1 has an autocrine effect on CAFs that leads to the secretion of TGF- β and the maintenance of CAFs' activated phenotype (Figure I.13) (Kojima et al., 2010).

In conclusion, inactivation of the TGF- β receptor pathway in fibroblasts can induce the secretion of growth factors and promote tumor growth by activating cancer cell proliferation. Its activation is also crucial for the acquisition of a 'CAF-like phenotype' and for promoting cancer cell invasion and survival, especially during organ colonization at the metastatic sites.

Another important growth factor enriched in the tumor microenvironment is the platelet derived growth factor (PDGF). PDGF is mainly secreted by endothelial cells in order to recruit pericytes and stabilize blood vessels (Lindblom et al., 2003). In cancer, PDGF is secreted by both tumor cells and other components of the tumor microenvironment (Heldin and Westermark, 1999). Stromal cells, more particularly α SMA-positive mesenchymal cells (Bhardwaj et al., 1996), express PDGFR. PDGFR belongs to the family of tyrosine kinase receptors and exists in 2 isoforms α and β . PDGFR β is expressed in higher levels during tissue inflammation, wound healing, in fibrosis, and in the tumor stroma (Alvarez et al., 2006; Heldin and Westermark, 1999). Upon activation, PDGFR dimerizes and activates multiple downstream pathways such as the phosphatidylinositol 3-kinase (PI3K) pathway, which leads to increased actomyosin activity, and the Ras pathway that induces cell proliferation (Cully et al., 2006; Schubert et al., 2007).

Besides acting as mitogen, PDGF exerts chemotactic effects on mesenchymal cells and increase their velocity and persistence (Martin et al., 2014; Osornio-Vargas et al., 1996). More specifically, PDGF serves as a cue to recruit fibroblasts to the tumor site (Cadamuro et al., 2013; Dong et al., 2004) where they are consequently activated to remodel the surrounding matrix (Kinnman et al., 2000; Pinzani et al., 1994; Yi et al., 1996). This appears to happen at early stages of cancer progression since cells expressing PDGFR β are found in the stroma adjacent to *in situ* carcinomas (Bhardwaj et al., 1996). Finally, as found in clinical trials, PDGFR inhibitors successfully improved patient outcome. Blockade of PDGFR signaling in the stroma of mice bearing cervical tumors using the receptor tyrosine kinase inhibitor imatinib cancelled FGF secretion by fibroblasts (Pietras et al., 2008). This treatment impaired tumor angiogenesis and slowed the progression and growth of both non-invasive and invasive lesions. Similarly, in a colon cancer model, imatinib therapy impaired the recruitment of MSCs to the site of the tumor, which ultimately led to the inhibition of cancer growth and metastasis (Shinagawa et al., 2013)

Growth factors like TGF- β and PDGF can be either freely secreted in the tumor microenvironment or delivered via exosomes. Exosomes are cargo-carrying multi-vesicular bodies released in the extracellular milieu (Simons and Raposo, 2009; They et al., 2006). They have both autocrine and paracrine effects on the microenvironment they are released in. Although most studies focus on cancer cell-secreted exosomes, recent study highlighted the role of CAF-secreted exosomes (Fullar et al., 2012; Luga et al., 2012). CAFs' exosomes specifically carry Wnt11, a ligand that is internalized by cancer cells through its receptor Fzd6, a component of the planar cell polarity (PCP) signaling pathway (Luga et al., 2012). Cancer cells' motility and metastatic potential is consequently stimulated (Figure I.13).

The tissue inhibitors of metalloproteinases (*Timps*) are also involved in acquisition of a "CAF phenotype" and in exosome-mediated cancer cell invasion. *Timps* play a role in controlling the activity of MMPs by inhibiting their catalytic activity (Fullar et al., 2012). Exosomes of *Timp*-less mouse dermal CAFs are rich in a metalloproteinase ADAM10 that stimulates cancer cell migration and conserve cancer's stemness through activation of RhoA and Notch signaling cascade, respectively (Shimoda et al., 2014). Even though *Timp*-less fibroblasts are more contractile and secrete exosomes rich in ECM proteins, the role of *Timp*-less CAFs in matrix remodeling has never been addressed (Figure I.13).

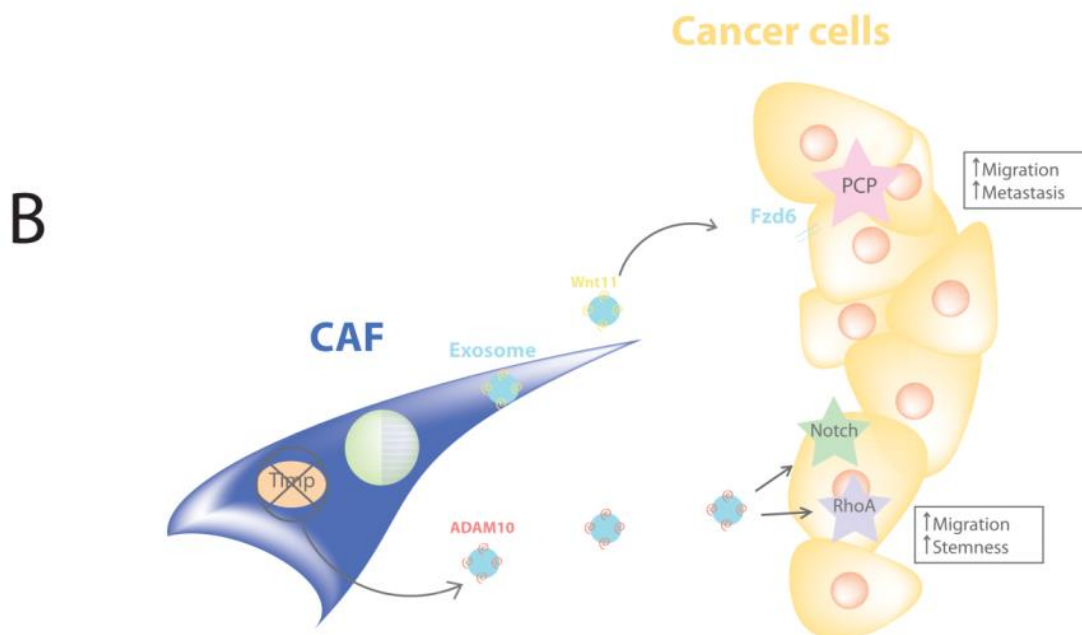
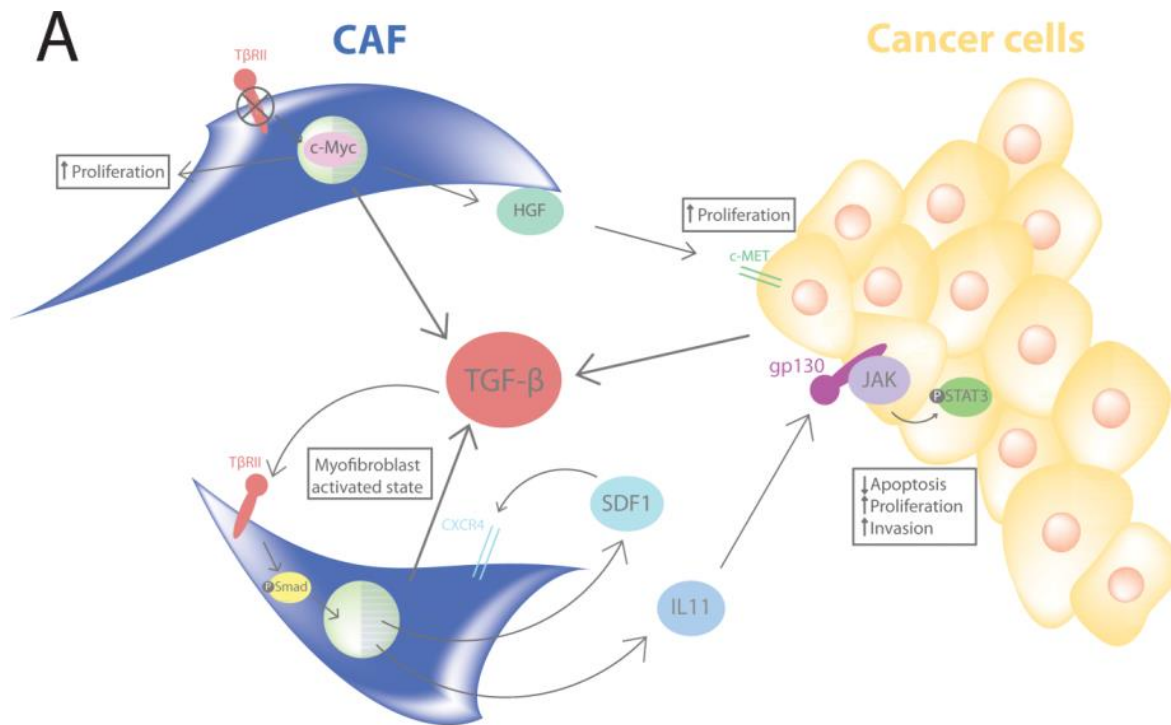


Figure I.13. A. The TGF-β pathway in CAF activation and cancer cell invasion
 B. CAFs' exosomes in cancer cell invasion
 (Attieh and Vignjevic, 2016)

Finally, one recent study suggests an even more direct and cooperative cancer cell-CAF crosstalk, where both cell populations establish direct heterotypic E-cadherin/N-cadherin adhesions (Labernadie et al., 2017). These adhesions being mechanically active, CAFs are thus able to repolarize away from cancer cells and physically pull collective streams of cancer cells out of the tumor mass and lead tumor invasion and dissemination.

5.2.2. The ECM as a mediator of the crosstalk

In addition to a direct secretome crosstalk, CAFs and cancer cells also communicate through the matrix they are embedded in. Because fibroblasts generate and organize the ECM in normal tissues and in development, CAFs are the cells of the tumor microenvironment that have the biggest hand on remodeling the ECM during cancer progression, making it more permissive for cancer invasion (Calvo et al., 2013; Gaggioli et al., 2007; Goetz et al., 2011; Sanz-Moreno et al., 2011). CAF's capacity to remodel the ECM has a direct consequence on treatment failure in patients (Venning et al., 2015). For example, a drug used in clinics to specifically target the mutated proto-oncogene BRAF in cancer cells, activates CAFs, increasing their capacity to contract and stiffen the ECM. The remodeled matrix provides a safe niche for cancer cell survival and proliferation leading to patient's relapse and cancer recurrence (Hirata et al., 2015).

Proteolysis

In CAFs, invadopodia formation is dependent on actin-binding protein, palladin (Goicoechea et al., 2014). If palladin is silenced, small GTPase Cdc42 is not activated and invadopodia formation is impaired. Normal fibroblasts are not able to form invadopodia, suggesting that these structures are a hallmark of activated fibroblasts. However, whether palladin is overexpressed in CAFs compared to normal fibroblasts has not been addressed so far.

Loss of transcription factor Snail1 in CAFs reduces their capacity to form clusters of membrane bound MT1-MMP in invadopodia via the PI3K/AKT and ERK1/2 pathways (Lu et al., 2013; Rowe et al., 2009). Of note, Snail1 was shown to be activated by the platelet derived growth factors PDGF-BB and PDGF-DD (Lu et al., 2013; Qin et al., 2015; Rowe et al., 2009). While MT1-MMP null mouse embryonic fibroblasts are not able to trigger tumor invasion, depletion of soluble MMPs, such as MMP9 and MMP2, has minimal to no effect on cancer cell invasion (Zhang et al., 2006). However, MMP2 and 9 might play another, fibroblast specific role. Fibroblast-secreted MMP2 could contribute to the activation of MT1-MMP (Taniwaki et al.,

2007), and MMP9 through binding to lysyl hydroxylase 3 (LH3) receptor is one of the inducers of TGF- β secretion and α -smooth muscle actin (α SMA) expression, inducing differentiation of fibroblasts into contractile myofibroblasts (Dayer and Stamenkovic, 2015). Therefore, both MMP2 and MMP9, even though not necessary for CAF's proteolytic activity, can be considered as markers of CAFs.

In addition to MMPs, it is speculated that the fibroblast activation protein (FAP) is also involved in CAF's proteolytic activity. FAP is a serine protease that can degrade both gelatin and collagen I (Park et al., 1999). FAP expression in human colon cancer samples is a marker of early stage in cancer development and is correlated with poor patient outcome (Henry et al., 2007). Although it has been reported that tumor cells can express FAP (Cheng et al., 2002; Monsky et al., 1994; Mueller et al., 1999; Wang et al., 2005), it is still considered a marker of mesenchymal cells, and activated fibroblasts in particular (Henry et al., 2007; Park et al., 1999; Scanlan et al., 1994). Fibroblasts expressing FAP generate a FN-rich ECM with parallel and aligned collagen fibers (Lee et al., 2011; Wang et al., 2005) which supports cancer cell invasion (Lee et al., 2011). FAP+ fibroblasts also show upregulation of α SMA, suggesting that, in addition to its proteolytic activity, FAP might indirectly switch on a contractile phenotype in CAFs (Lee et al., 2011).

It has been recently suggested that degradation and contraction of the matrix are two interdependent processes used by cancer cells during invasion as invadopodia could also generate traction forces on the matrix (Aung et al., 2014; Jerrell and Parekh, 2014). Whether this is true in CAFs remains unknown. It is tempting to hypothesize that all the tools that CAFs use to induce cancer cell invasion are somehow linked. Because they have multiple origins, it is assumed that CAFs are comprised of different cell populations expressing unique sets of markers. However, it is possible that by acquiring the 'activated fibroblast' state – through any of the hypothesized pathways – all other pathways get activated. Similarly, by inhibiting one of these pathways, a CAF might revert back to a normal state when all other pathways are subsequently silenced.

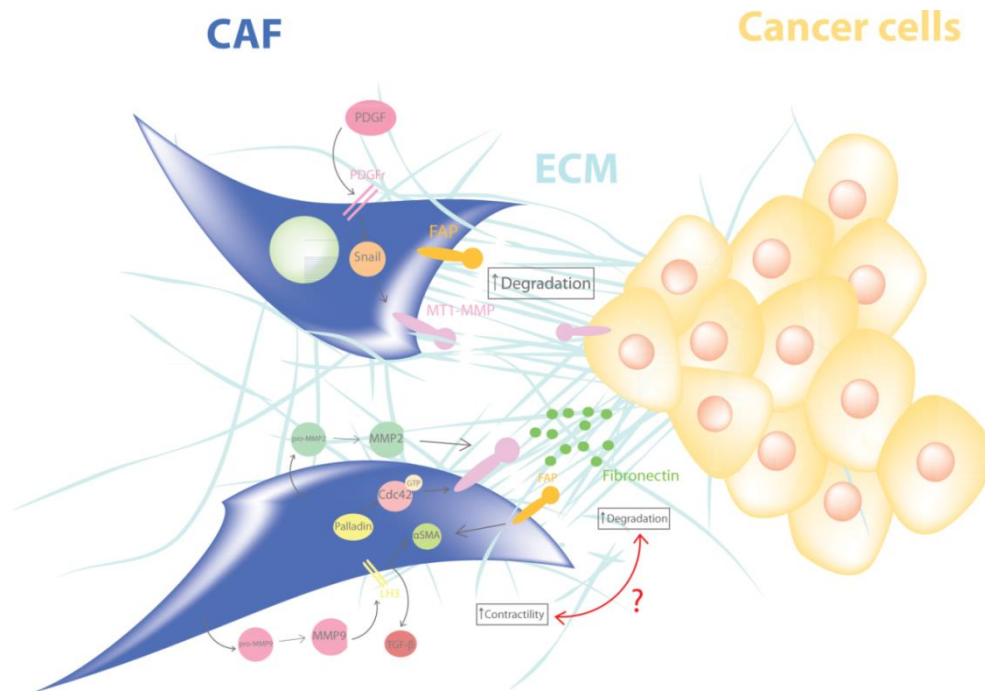


Figure I.14. CAF-mediated cancer cell invasion through ECM degradation (Attieh and Vignjevic, 2016)

Contractility

Although matrix degradation is relevant for tumor cell invasion, other mechanisms were shown to rescue cancer cell invasion when proteolysis is impeded (Wolf et al., 2003b; Wolf et al., 2013).

One of the most studied functions of CAFs is their increased ability to remodel the ECM by exerting mechanical forces on it. Thus, CAFs can either widen the pores in the ECM or align collagen fibers which will facilitate cancer cell invasion (Riching et al., 2014). Many studies argue that CAF's secretome is not sufficient to induce cancer cell invasion and that their effect on the matrix is the key player (Calvo et al., 2013; Gaggioli et al., 2007; Sanz-Moreno et al., 2011). For example, when CAFs are seeded in an organotypic matrix and left to remodel it before killing the fibroblasts, cancer cells invade these matrices to the same extent as when CAFs are physically present. Through the Rho-ROCK-myosin pathway, CAFs remodel and align collagen fibers generating tracks that cancer cells use to migrate along (Gaggioli et al., 2007). However, as Rho, ROCK and myosin are constitutive proteins in all cell populations, they cannot be considered as markers of CAFs. Therefore, their regulation, rather than their presence, is more likely different in activated fibroblasts compared to normal fibroblasts.

The Janus kinase 1 (JAK1), an intercellular non-receptor tyrosine kinase, could regulate actomyosin contractility in CAFs as it cooperates with ROCK to induce myosin light chain (MLC) phosphorylation (Sanz-Moreno et al., 2011). This signaling cascade is the result of the action of cytokines, such as oncostatin M, a member of the IL6 family (Sanz-Moreno et al., 2011) and TGF- β that triggers production of the leukemia inhibitory factor (LIF) leading to a constitutive CAF activated state (Albregues et al., 2015; Albregues et al., 2014). This suggests that CAF contractility is not cell autonomous as it relies on cues and growth factors provided by the tumor itself and its microenvironment.

Upstream of Rho-dependent CAF contractility is also caveolin 1 (Goetz et al., 2011), a component of membrane structures implicated in trafficking and upregulated in the tumor stroma (Goetz et al., 2008). By regulating the Rho inhibitor p190, caveolin 1 expression results in CAFs that generate stiffer and aligned matrices, which favors cancer cell invasion and metastasis (Goetz et al., 2011).

Finally, the transcription factor YAP could also regulate actomyosin contractility. While in normal fibroblasts YAP is localized in the cytoplasm and thus inactive, in CAFs it translocates to the nucleus and activates the transcription of a set of genes involved in matrix remodeling (Calvo et al., 2013). A positive feedback loop is then established between CAFs and the ECM, as stiffer matrix favors YAP translocation in the nucleus, maintaining CAF activated status (Calvo et al., 2013).

YAP translocation to the nucleus is also induced by α SMA (Talele et al., 2015). α SMA is an actin isoform specific for smooth muscle cells and myofibroblasts found in the wounds (Darby et al., 1990; Desmouliere et al., 1992a; Desmouliere et al., 1992b). Its expression directly correlates with tissue contractility and can be triggered by mechanical tension (Arora and McCulloch, 1994; Hinz et al., 2001b).

α SMA exists as monomeric actin at the perinuclear region and as filamentous actin in stress fibers, an actomyosin bundles involved in contractility, adhesion and migration (Arora and McCulloch, 1994; Hinz et al., 2001a; Hinz et al., 2002). Because α SMA is only effective if polymerized into stress fibers, α SMA expression *per se* could be irrelevant for a cell's ability to contract matrices. Therefore, if a cell expresses high levels of α SMA but is unable to assemble it

into stress fibers, it will remain non-contractile. This raises the question of how α SMA expression should be evaluated in fibroblast populations: maybe it is not the amount of α SMA that distinguishes activated fibroblasts from normal ones, but rather their ability to polymerize α SMA into stress fibers to acquire the contractile signature.

It has been suggested that α SMA mediates force generation in myofibroblasts via its NH₂-terminal peptide, absent in other forms of actin (Hinz et al., 2002). Nevertheless, it is still not clear how and why α SMA, as opposed to other forms of actin, favors cell contractility. Moreover, it is hard to distinguish if α SMA is a cause or a consequence of contractility. As suggested above, high levels of α SMA could be just a ‘passive’ companion of contractile fibroblasts. For example, TGF- β increases the levels of both α SMA and the active form of RhoA in a Snail1-dependent manner, so it could be that contractility is achieved in an α SMA-independent manner (Stanisavljevic et al., 2015). Indeed, some studies show that CAF-mediated remodeling of the matrix through actomyosin can be α SMA independent (Albregues et al., 2014).

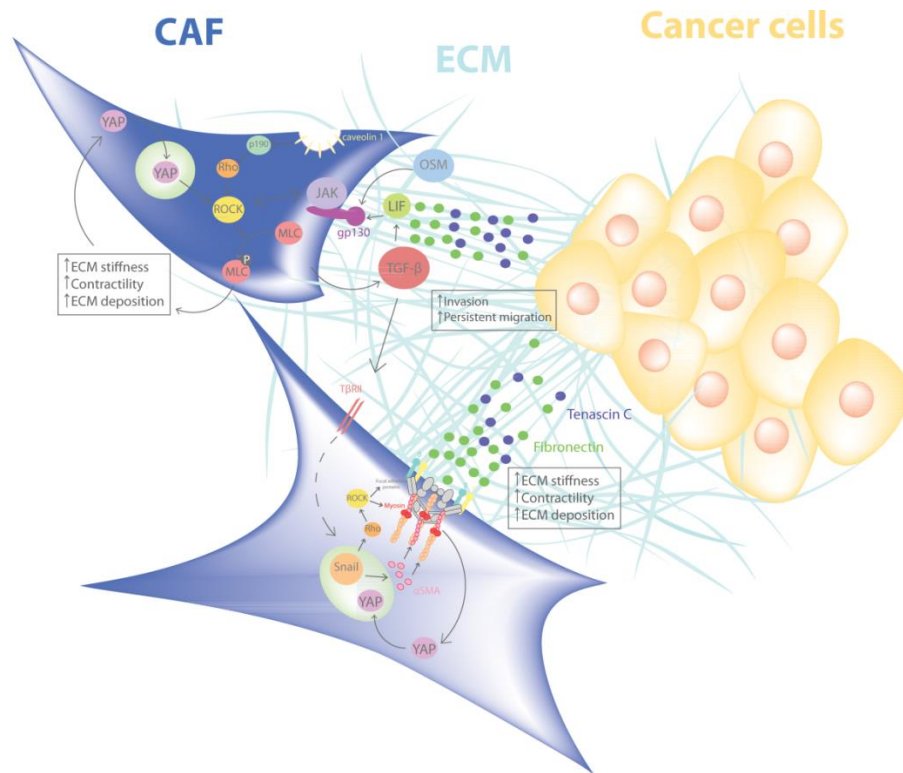


Figure I.15. CAF-mediated cancer cell invasion through ECM contraction and deposition (Attieh and Vignjevic, 2016)

Matrix deposition

One of the consequences of Rho pathway activation is the formation of stable fibrillar adhesions at which ECM is deposited and assembled (see section 2.1.2) (Plotnikov et al., 2012; Zaidel-Bar et al., 2007b). The more contractile the cell is, the more ECM it will deposit and more invasion of cancer cells will be induced (Oudin et al., 2016a; Oudin et al., 2016b; Sung et al., 2015; Zaidel-Bar et al., 2007b). Cells, fibroblasts in particular, have the ability to sense mechanical stimuli in their environment and to modulate the ECM assembly accordingly (Chiquet et al., 1996; Halliday and Tomasek, 1995). However, it is not clear which cellular function, contractility or matrix deposition, is directly responsible for tumor invasion. For example, mechanical stretching of normal fibroblasts stimulates deposition of FN in a linearly aligned structure, similarly to CAFs. These fibronectin patterns induce more persistent migration of cancer cells (Ao et al., 2015a). Cancer cells even perform haptotactic movements towards high concentrations of fibronectin (Oudin et al., 2016b; Sung et al., 2015). Thus, by depositing fibronectin, CAFs could increase cancer cell invasion, although there is no study showing that fibronectin is the major player in CAF-mediated cancer cell invasion.

CAF-secreted growth factors such as HGF are not sufficient to induce migration of cancer cells; they need additional cues, such as TNC (De Wever et al., 2004). TNC also induces proliferation of cancer cells. For example, TNC has the ability to abrogate cancer cell adhesion to FN-rich matrices by blocking syndecan-4. As a consequence, interactions between fibronectin and $\alpha 5\beta 1$ integrin are hindered and tumor proliferation is increased (Huang et al., 2001). It is interesting that tumor ECMs are enriched in both FN and TNC, as cancer cells need to migrate to reach the circulation, but also to proliferate and survive. Therefore, it is likely that aggressive tumors harbor a balanced expression of TNC and FN, leading to big primary tumors and a higher number of metastases.

Syndecan-4 is overexpressed in fibroblasts upon tissue injury. As a consequence of fibronectin enrichment, syndecan-4 mediates adhesion and spreading of fibroblasts, and eventually leads to the activation of RhoA and formation of stress fibers (Midwood et al., 2004; Morgan et al., 2007). Consequently, YAP translocates in the nucleus and activates transcription of actomyosin related genes (Kim and Gumbiner, 2015). This suggests a positive feedback loop between fibronectin-rich matrices and contractile fibroblasts.

Enrichment in ECM proteins can in certain cases inhibit cancer cell invasion. For example, decreased expression of decorin is associated with more invasive tumors, a higher risk of cancer recurrence and an increased amount of CAFs. TGF- β and the fibroblast growth factor (FGF) lead to the inhibition of decorin expression in CAFs and a more permissive ECM (Van Bockstal et al., 2014).

Matrix stiffening

Similarly to the influence of fibronectin on CAF contractility, stiff matrices can also stimulate fibroblasts to generate mechanical forces (Barker et al., 2013). A stiff matrix is a signature of aggressive tumors and it is characterized by crosslinked collagen fibers. CAFs can crosslink collagen fibers using Lysyl hydroxylase 2 (PLOD2/LH2), an enzyme not expressed in normal fibroblasts (Pankova et al., 2016). This enzyme generates aldehyde-derived collagen cross-links which increase the stiffness of the matrix, as well as cancer cell invasion.

More commonly, collagen crosslinking is mediated by the amine-oxidase LOX, a copper-dependent enzyme (see section 4.1.1). The LOX family is made of five isoforms: LOX and LOX-like (LOXL) paralogues 1-4 (Barker et al., 2012; Cox et al., 2016). LOX also promotes tumor invasion and metastasis, and its expression is increased under hypoxia and in fibrosis, both commonly observed in cancer (Cox et al., 2013; Cox et al., 2015; Erler et al., 2006; Levental et al., 2009). As both cancer cells and CAFs have the capacity to secrete LOX, it is still debated whether the tumor is stiffening the ECM at early stages, thus promoting the switch of fibroblasts into CAFs, or if CAFs secrete LOX to make the ECM more permissive in preparation for cancer cell invasion. Secretion of LOXL2 by tumor cells induces the expression of α SMA in CAFs as well as CAF-mediated collagen contraction through activation of the FAK-integrin axis (Barker et al., 2013). LOXL2 also influences CAF proteolytic activity as it regulates the expression and activity of MMP9 and *Timp1* (Barker et al., 2011; Barry-Hamilton et al., 2010).

As opposed to LOXL2, LOX expression is only found in the tumor stroma, whether at invasive or early *in situ* stages (Peyrol et al., 1997), supporting the possibility that ECM modifications happen before the onset of invasion. LOX is more likely to be downstream of TGF- β and α -SMA as targeting LOX in a fibrotic tissue does not abrogate CAF activated state (Cox et al., 2013). LOX can activate the Src kinase in cancer cells making them more proliferative and resistant to apoptosis (Cox et al., 2013). As discussed above, LOX also enhances cancer cell invasion by

it. Mainly, why do cancer cells, according to the tissue they rise from, choose to metastasize at specific secondary organs? For example, breast cancers mainly metastasize to lung, liver, bone and brain, intestinal cancers to liver and lungs and melanoma to liver, brain and skin while some sites, such as muscle, are rarely if ever sites of metastasis. Conversely, other tumors such as ovarian tumors are restricted to the peritoneal cavity.

In 1889, the English surgeon Stephen Paget emitted the “seed and soil” hypothesis to explain non-random patterns of metastasis. After analyzing more than 900 patient autopsies, he observed a pattern of metastasis according to the tumor of origin, indicating that the outcome of metastasis was not due to chance (Paget, 1889), and that certain tumor cells (the seed) have affinities for particular organs (the soil), meaning that metastases could only be achieved when the seed and soil were compatible (Fidler, 2003; Fidler et al., 2002). This hypothesis was challenged 40 years later when James Ewing proposed an alternative theory: in his opinion, metastasis was a random process determined by the anatomy of the vascular and lymphatic channels that drained the primary tumor (Ewing, 1928). For decades, Ewing’s theory prevailed until it was finally proven by Isaiah Fidler that although cancer cells spread evenly in the circulation, they only colonized specific organs (Fidler and Kripke, 1977; Hart and Fidler, 1980).

From these studies derived many others further exploring the metastatic soil and analyzing local tissue microenvironments both at the primary and secondary sites (Costa-Silva et al., 2015; Hoshino et al., 2015; Kaplan et al., 2005; Oskarsson et al., 2011). It was then suggested that the metastatic niche is conditioned prior to the arrival of cancer cells in order to facilitate their colonization and expansion (Kaplan et al., 2006). At the primary site, tumor cells secrete exosomes that preferentially fuse with resident cells of their predicted destination according to the nature of integrin dimers these exosomes contain (Costa-Silva et al., 2015; Hoshino et al., 2015). Exosome uptake would then cause an upregulation of TGF- β secretion, FN production and recruitment of bone-marrow derived macrophages. Interestingly, it had been shown 10 years prior to these studies that a pro-inflammatory metastatic site was favorable for cancer cell colonization: bone-marrow derived cells secrete MMP9 which in this study, is suggested to degrade the basement membrane, liberating the matrix sequestered vascular endothelial growth factor A (VEGFA) and promoting homing of VEGFR1 positive cells into the niche (Hiratsuka et al., 2002). Recruited bone-marrow derived hematopoietic progenitor cells then form cellular

clusters and their expression of VEGFR1 induces metastasis formation by providing a FN-rich permissive niche for incoming tumor cells (Kaplan et al., 2005). Circulating tumor cells also condition their niche of destination to support their own infiltration ability. Breast cancer cells were shown to overexpress TNC as they infiltrate the lungs (Oskarsson et al., 2011). TNC enhances the expression of stem cell signaling components and promotes the survival and outgrowth of pulmonary micrometastases. Eventually, the tumor stroma would take over as a source of TNC (O'Connell et al., 2011) highlighting the role of the tumor microenvironment in facilitating cancer invasion and metastasis.

Beyond their effect on the primary tumor site, CAFs were also shown to drive metastasis to secondary organs (Khamis et al., 2012). In addition to facilitating cancer cell invasion of the ECM and their reaching the circulation, CAFs pre-condition the metastatic niche (Jacob et al., 1999; Zhang et al., 2013) and select carcinoma clones that are primed for metastasis, both at the primary and secondary sites (Cornil et al., 1991; Zhang et al., 2013). It was first shown that dermal fibroblasts activate the growth of melanoma cell lines from metastatic lesions but not from early stage carcinomas (Cornil et al., 1991), highlighting the selective role of fibroblasts on aggressive cancer cells. As this study was performed using normal dermal fibroblasts, it is likely that normal fibroblasts are not primed to specifically act on metastatic cancer cells, but that aggressive cancer cells, as opposed to their non-invasive counterparts, activate normal fibroblasts to become CAFs and therefore enhance tumor invasion and metastasis. The focus later shifted to CAFs which, through high secretion of the chemokine ligand 12 (CXCL12) and the insulin-like growth factor 1 (IGF1), drive the selection of Src-hyperactive cancer cells and downstream activation of the Akt-PI3K pathway (Zhang et al., 2013). These genes being associated with metastasis and bone biology, CAFs therefore select clones that are primed for adaptation to the bone metastatic microenvironment. Mesenchymal stem cells (MSCs) of the bone premetastatic niche also contribute to conditioning the soil and the selection of the colonizing circulating tumor cells (Jacob et al., 1999). Through secretion of osteonectin, MSCs in the bones attract prostate and breast cancer cells and enhance their invasive capacity by increasing their MMP activity. In the non-bone metastasizing fibrosarcoma or melanoma cells, as well as in the non-invasive prostate epithelial cells, osteonectin does not exert any chemotactic effect or induce a change in MMP activity indicating that osteonectin is a specific inducer of collagenase activity in cancer cells that preferentially metastasize to the bone.

CAFs expressing the fibroblast-specific protein 1 (FSP1) were also shown to drive metastasis as FSP1 deficient mice showed a delayed tumor uptake and failed to develop any metastases (Grum-Schwensen et al., 2005). As co-injection of FSP1 positive CAFs with cancer cells in a FSP1 null background only partially rescues the dynamics of tumor development, this suggests that the role of CAFs goes beyond their conditioning of cancer cells at the primary site. Indeed, FSP1-expressing CAFs in the lungs produce VEGFA and TNC therefore promoting angiogenesis and providing protection for breast cancer cells against apoptosis (O'Connell et al., 2011). These data are in line with previously mentioned studies on the importance of VEGFA in conditioning the pre-metastatic niche (Hiratsuka et al., 2002; Kaplan et al., 2005). It is intriguing though that in a similar breast cancer model, cancer cells also overexpress TNC as they infiltrate the lungs (Oskarsson et al., 2011). This prompts to question why CAFs would enrich the soil in TNC when incoming cancer cells have the capacity to do it themselves. As these two studies were performed using different cancer cell lines, it is tempting to hypothesize that cancer cells, depending on their aggressiveness and EMT status, might not always be their own source of TNC and support a cell autonomous growth. They would then rely on CAFs to do it, but this idea has never been tested.

Finally, two studies have highlighted an even greater involvement of CAFs in the metastatic process as they were shown to escort cancer cells, from the primary site to secondary organs, facilitating their survival and proliferation (Ao et al., 2015b; Duda et al., 2010). When fluorescently labelled red lung cancer cells were implanted under the renal capsule of GFP mice, both red and green cells were detected in the bloodstream as single cells and heterotypic clumps, with the heterotypic fragments containing twice as many viable cancer cells (Duda et al., 2010). GFP cells overexpressed α SMA and FSP1 indicating that CAFs accompany cancer cells during the metastatic cascade and provide survival signals. Later on, a similar study was performed in humans: analysis of the peripheral blood of breast cancer patients revealed the presence of α SMA and FAP positive cells along with circulating tumor cells (Ao et al., 2015b). The presence of circulating CAFs (cCAFs) was greater in patients with metastatic disease compared to patients with localized breast cancer indicating that the presence of cCAFs is associated with clinical metastasis. These studies are very exciting as they push the “seed and soil” hypothesis one step further by suggesting that the seed (cancer cells) brings its own microenvironment in order to better establish itself in the soil.

CAFs' contribution to cancer development is even greater than described here. CAFs affect every single component of the tumor microenvironment: they modulate the action of immune cells and endothelial cells and therefore act on higher biological scales such as angiogenesis, hypoxia and inflammation.

In conclusion, CAFs are a very powerful component of the tumor microenvironment. As opposed to other cell populations of the tumor stroma, they have dual skills: one is to directly affect their neighbors through their secretome, the other is to have the power to create and modulate the matrix depending on the conditions they are in. As more clinical trials and therapies are being established to target CAFs, it is beforehand important to discriminate the normal fibroblasts from the activated ones for a better outcome.

II. Objectives and hypotheses

During metastasis, cancer cells breach the basement membrane, migrate through the stroma, enter the circulatory system and establish secondary tumors in previously unaffected organs. Understanding the individual steps of the metastatic cascade has been difficult because of its complex multifaceted nature.

The stroma underlying a tumor has been long-studied and established as a crucial actor in metastasis. Cancer-associated fibroblasts (CAFs) have been particularly examined and have been described as the leaders of cancer cell invasion as they act both directly by secreting pro-invasive stimuli and indirectly by remodeling the extracellular matrix (ECM). Furthermore, besides stimulating the migratory capacity of cancer cells, CAF-secreted molecules could also serve as a chemoattractant, providing a direction for migrating cells. Finally, as CAFs stimulate cancer cell invasion, they also accelerate the metastatic process. However, it is still not clear if CAFs contribute to metastasis solely by increasing invasion at the primary site, or if they also act on the secondary site, either by pre-conditioning the niche or by disseminating with cancer cells in the circulation.

During my PhD, I aimed to identify the involvement of CAFs in each step of the metastatic cascade by asking the following questions:

1. How do CAFs promote tumor progression at the primary site? Do they stimulate the invasive capacity of cancer cells or prepare the ECM?
2. Do CAFs have the capacity to guide cancer cells towards the blood vessels?
3. Do CAFs play a role beyond the primary tumor site and actively help cancer cells colonize secondary organs?

III. Results

1. How do CAFs assist cancer cell invasion at the primary site?

Introduction

During the progression of carcinoma, following breaching of the basement membrane, cancer cells reach the tumor stroma, encountering CAFs and the ECM. At this stage, the influence of CAFs on tumor invasion is still debated (Kalluri, 2016): it has been shown that depleting CAFs from the stroma induces tumor invasion (Ozdemir et al., 2014; Rhim et al., 2014), but most studies agree that an enrichment in CAFs stimulates cancer cell invasion (Calvo et al., 2013; De Wever et al., 2004; Gaggioli et al., 2007; Goetz et al., 2011; Orimo et al., 2005). There is also disagreement concerning the mechanism by which CAFs act: do they enhance the invasive capacity of cancer cells through diffusible molecules (De Wever et al., 2004; Orimo et al., 2005)? Or is their physical presence required to contract and align the matrix (Calvo et al., 2013; Gaggioli et al., 2007; Goetz et al., 2011; Sanz-Moreno et al., 2011), facilitating cancer cell invasion (Riching et al., 2014)?

Most new studies highlight the importance of contractility in CAFs in stimulating invasion. However, the ability of CAFs to remodel the matrix by other mechanisms (degradation, stiffening, deposition of new ECM) and the interdependence between those mechanisms have been poorly studied. For example, highly contractile cells are characterized by stable and long-lived fibrillar adhesions that deposit and assemble new ECMs (Zaidel-Bar et al., 2007b). Therefore, ECM deposition by CAFs is a direct consequence of their contractility. The tumor stroma is known to be enriched in matrix proteins like fibronectin (FN) and tenascin C that favor tumor progression (De Wever et al., 2004; Oudin et al., 2016a) but it is still not known which of the two functions, contractility or matrix deposition, is responsible for cancer cell invasion.

Here, we investigate how CAFs induce invasion of cancer cells through the ECM. Using a combination of pharmacological and genetic perturbations, we modulated the abilities of CAFs to contract, deposit and degrade the matrix. We found that FN assembly by CAFs downstream of $\beta 3$ integrin activation is critical to stimulate cancer cell invasion.

Results

The physical presence of CAFs in the matrix is required to induce cancer cell invasion

To investigate the role of CAFs in cancer invasion, we isolated CAFs and non-cancer-associated fibroblasts (NAFs) respectively from the tumor and the neighboring healthy tissue of the colon of patients, ending with a couple of NAFs and CAFs per patient. We characterized all cell populations using markers of activated fibroblasts (see section V.1.2; Table III.1.1).

Sample ID	Location	TNM classification	Tumor stage	Treatment
1	Colon	pT4a N2a	Stage IIIC	No
2	Colon	pT2 N1a	Stage IIIA	No
3	Colon	pT4b N1a	Stage IIIC	No

Table III.1.1. List of fibroblasts used in this study, isolated from CRC patients. Pairs of fibroblasts were isolated from untreated colon surgical resections; CAFs were isolated from the tumor and NAFs from the normal tissue. Tumor stage was given by pathologists (Columns 3 and 4)

In all patients, CAFs and NAFs expressed α SMA, FAP and PDGFR β indicating that even though they were isolated from a seemingly “healthy” tissue, NAFs exhibit features of activated fibroblasts (Fig. III.1).

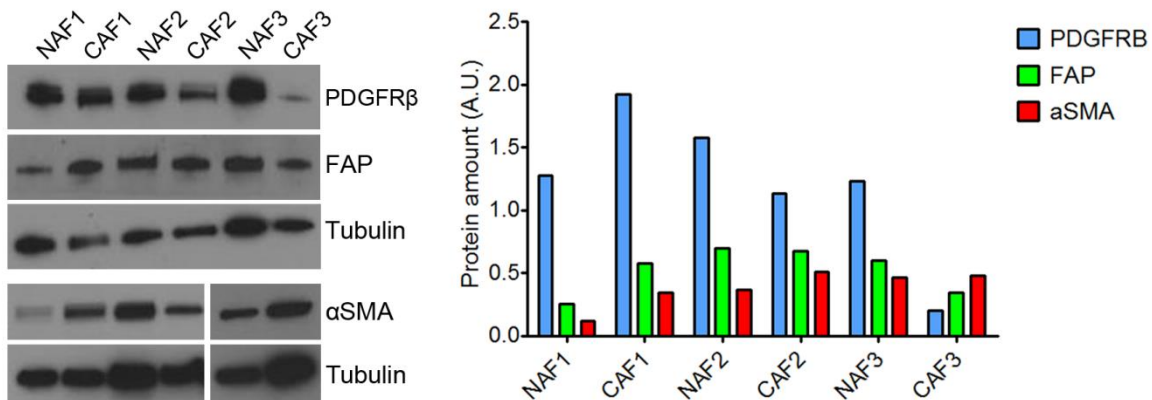


Figure III.1.1. Immunoblot analysis. Lysates prepared from NAFs and CAFs were probed against α SMA, FAP and PDGFR β antibodies. α -tubulin served as a loading control. Protein amount is calculated by normalizing α SMA (red), FAP (green) and PDGFR β (blue) amounts to Tubulin amount. Results are represented as column bars.

To assess the role of CAFs and NAFs in cancer cell invasion of the ECM, we embedded spheroids of CT26 cancer cells in a collagen I matrix either alone, or together with CAFs or NAFs (Fig. III.1.2A). This 3D model recapitulates the scenario of a tumor mass invading the stroma. The invasion capacity of cancer cells was quantified using custom analysis software 3 days post-embedding (see section V.1.3; Fig. III.1.2B).

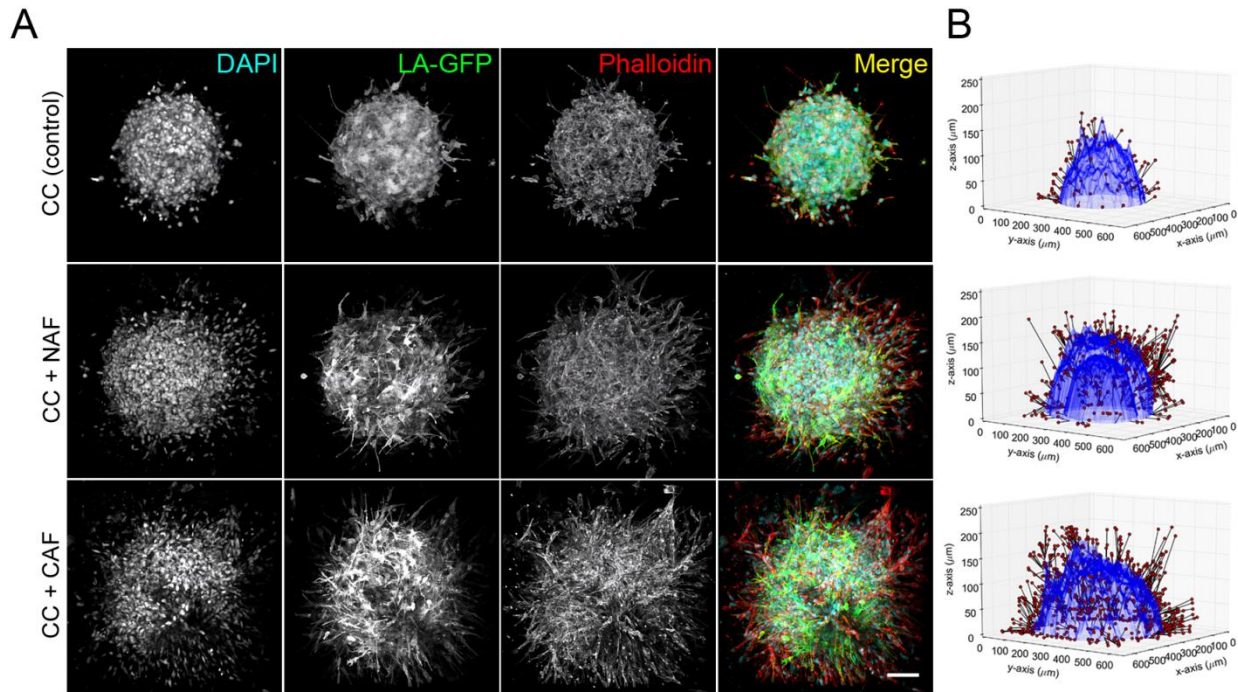


Figure III.1.2. (A) Maximum intensity projections of cancer cell spheroids in collagen I with or without fibroblasts, at day 3. CT26 cancer cells express LifeAct-GFP (green); F-actin (red) and DNA (cyan) were respectively stained with phalloidin-rhodamin and DAPI. Scale bar = 100µm. **(B)** 3D rendering of spheroids at day 3. Invasion is quantified using the invasion counter software. Red dots represent nuclei of invading cells (migrated out of the spheroid).

CT26 is an invasive cancer cell line (Geraldo et al., 2013), and in this assay, cells invaded the collagen matrix even when cultured alone (Fig. III.1.3). However, in the presence of fibroblasts, invasion of cancer cells was further enhanced, as previously shown for other non-invasive cancer cell lines (Fig. III.1.3) (Gaggioli et al., 2007; Goetz et al., 2011). Moreover, CAFs were more potent in increasing invasion compared to their paired NAFs (Fig. III.1.3).

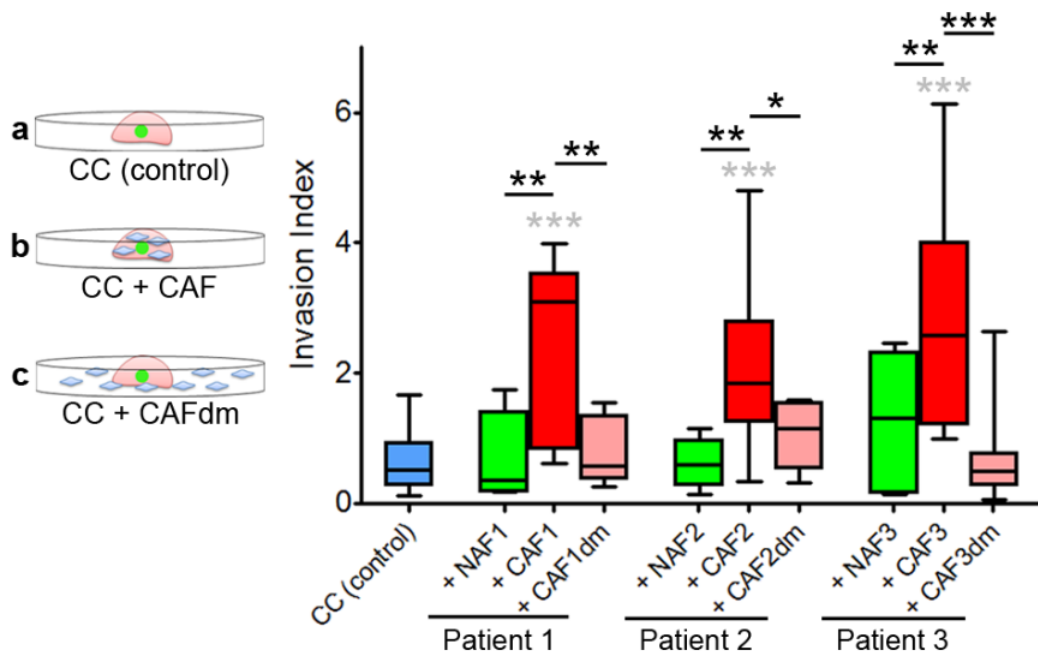


Figure III.1.3. Left: schematic representation of the experiment. Cancer cells were embedded in collagen gels (a). CAFs were either mixed with cancer cells in the collagen droplet (b) or they were plated around the collagen droplet (c). Right: quantification of cancer cell invasion alone (blue box), in the presence of NAFs (green box) or CAFs (red box) or in the presence of diffusible molecules (dm) secreted by CAFs (pink box) for 3 different patients. Invasion index is defined as the ratio between the number of invading nuclei and the area of the spheroid contour in arbitrary units (A.U.). Quantification results are expressed as box and whiskers (minimum to maximum) of at least N=3 separate experiments. p values are compared to cancer cells alone (in gray) and to cancer cells with CAFs (in black) using Newman-Keuls multiple comparison test (*p<0.05, **p<0.01, ***p<0.001).

In order to validate that this phenotype was not due to an increased attraction of CAFs compared to NAFs by the tumor, we quantified the mean number of fibroblasts as well as their distance from the spheroid in our assay. CAFs and NAFs were found in similar amounts around the spheroid (Fig. III.1.4A), and their distance from the contour was stable, between 50 and 120 μ m (Fig. III.1.4B). This suggests that the increased invasion index in the presence of CAFs compared to NAFs is most likely due to a more aggressive signature in CAFs.

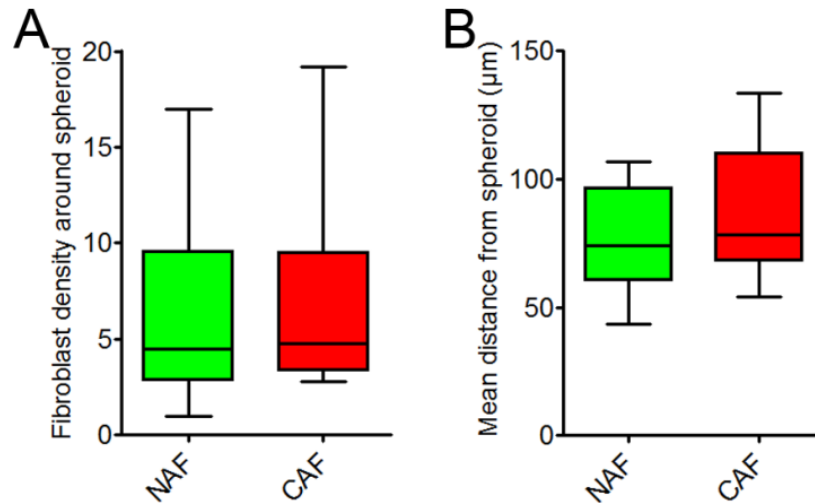


Figure III.1.4. (A) Quantification of the density of NAFs (green) and CAFs (red) around the spheroid. Fibroblast density is defined as the number of nuclei of non-GFP cells, normalized to the surface area of the spheroid contour in 3D in arbitrary units (A.U.). Quantification results are expressed as box and whiskers (minimum to maximum) and p value is calculated using Mann Whitney test for at least N=3 separate experiments. (B) Quantification of average distance of NAFs (green) and CAFs (red) from the spheroid. The mean distance from the spheroid is defined as the distance from the nuclei of non-LifeAct-GFP cells to the closest point along the cancer cell spheroid contour. Quantification results are expressed as box and whiskers (minimum to maximum) and p value is calculated using Mann Whitney test for at least N=3 separate experiments.

We next investigated whether CAFs have to be present in collagen gels to stimulate invasion of cancer cells, or if diffusible molecules (DM) secreted by CAFs were sufficient. We cultured CAFs in the distant presence of cancer cell spheroids (see schemes in Fig. III.1.3). In this condition, CAFs were not present in the matrix to remodel it but the secretome crosstalk of both cell types was maintained. In both conditions, cancer cells invaded collagen gels to a similar extent as in control conditions (Fig. III.1.3) indicating that the physical presence of CAFs in the matrix is necessary to increase cancer cell invasion.

These data show that CAFs induce more cancer cell invasion compared to their paired NAFs and that diffusible molecules of CAFs are not sufficient. Interestingly, the overall ability of fibroblasts to induce cancer cell invasion did not correlate with the expression levels of commonly used CAF markers (Fig. III.1.5), pointing to the absence of a good marker to evaluate the aggressiveness of CAFs.

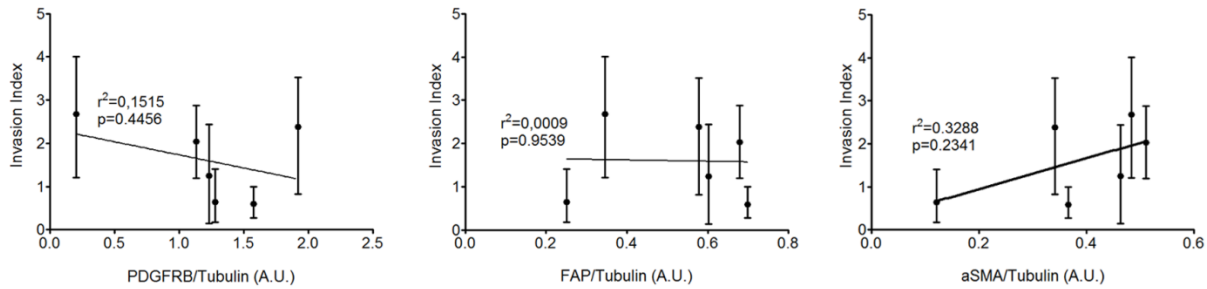


Figure III.1.5. Scatter dot graphs correlating the invasion index of cancer cells in the presence of NAFs and CAFs with the amount of α SMA, FAP and PDGFR β in fibroblasts. Error bars represent the quartile values. Quality of linear regression is represented by the values of p and r^2 .

Fibronectin deposition by CAFs induces cancer cell invasion

The necessity of CAFs to be physically present in the matrix to induce invasion points towards their role in matrix remodeling. Although NAFs were embedded into the ECM, they did not induce cancer cell invasion. These findings indicate that CAFs, and not NAFs, can remodel the matrix to induce invasion. Proteomic data analysis of two fibroblasts couples from colon cancer patients showed enrichment in FN in the secretome and proteome of CAFs compared to their paired NAFs (ProteomeXchange Consortium via the PRIDE partner repository with the dataset identifier PXD003670). In addition, FN is known to be enriched in the tumor microenvironment and is a pro-invasive ECM protein (Oudin et al., 2016a; Wolanska and Morgan, 2015). FN could thus be deposited by CAFs to promote cancer cell invasion. To test this hypothesis, we inhibited FN expression in CAFs using small interfering RNA (Fig.III.1.6A). Depletion of FN in CAFs from all patients abrogated their ability to stimulate invasion of cancer cells indicating that FN is necessary for CAFs to induce cancer cell invasion. (Fig. III.1.6B).

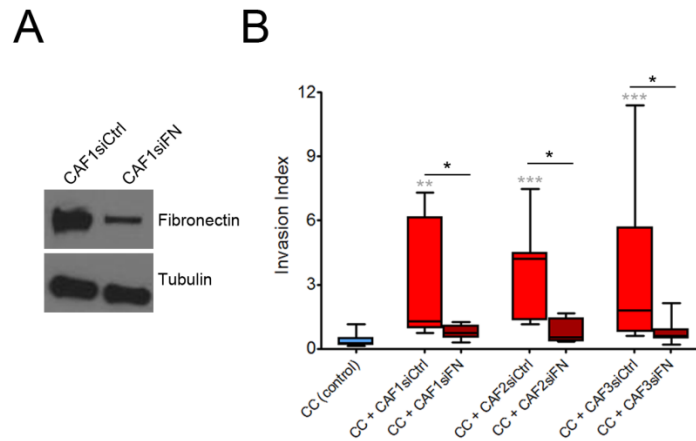


Figure III.1.6. (A) Immunoblot analysis. Lysates prepared from CAFs treated with siRNA scrambled control and CAFs treated with siRNA against fibronectin were probed with FN antibody. α -tubulin served as a loading control. (B) Quantification of cancer cell invasion alone or in the presence of CAFs from all patients, depleted or not for FN. Invasion index is defined as the ratio between the number of invading nuclei and the area of the spheroid contour. Results are expressed as box and whiskers (minimum to maximum) of at least N=3 separate experiments. p values are compared to cancer cells alone (in gray) and to cancer cells with CAFs (in black) using Newman-Keuls multiple comparison test (*p<0.05, **p<0.01, ***p<0.001).

This result was surprising as it has been shown that CAFs mainly stimulate cancer cell invasion by contracting and aligning the matrix (Calvo et al., 2013; Gaggioli et al., 2007; Goetz et al., 2011). Indeed, time-lapse imaging of cancer cell spheroids and CAFs in collagen revealed that CAFs were active in remodeling the matrix. CAFs aligned and pulled collagen fibers perpendicularly to the edge of the spheroids, facilitating migration of cancer cells (Fig. III.1.7), while in the absence of CAFs, collagen fibers were oriented parallel to the spheroid edge (Fig. III.1.7B) which is not favorable for cancer cell invasion (Kopanska et al., 2016). However, FN-depleted CAFs (CAFsiFN) retained the ability to align collagen fibers in the same fashion (Fig. III.1.7B). CAFsiFN also contracted and applied mechanical forces on the matrix similarly to control CAFs (Fig. III.1.8), indicating that depletion of FN in CAFs has no consequence on their ability to align the matrix. When inhibiting the contractility of CAFs using myosin II inhibitor blebbistatin, collagen alignment and contraction were abrogated, as well as downstream FN assembly, as previously shown (Fig. III.1.9A-B) (Zaidel-Bar et al., 2007b). In this condition, cancer cells did not invade the matrix, either alone or in the presence of CAFs (Fig. III.1.9C).

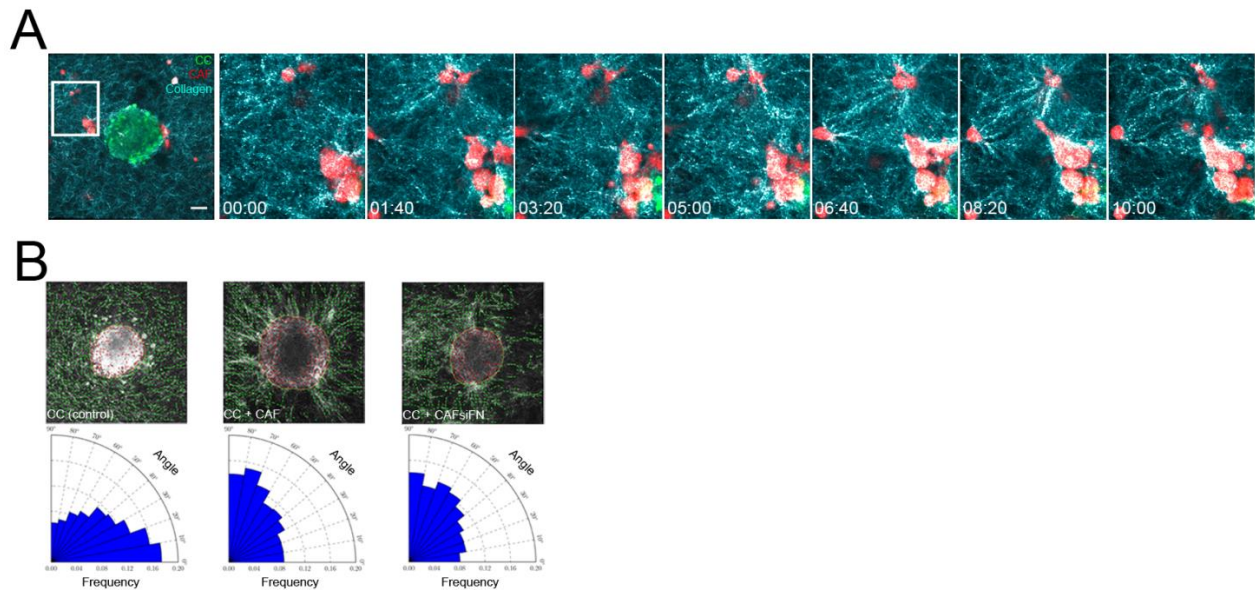


Figure III.1.7. (A) Time-lapse sequence of CT26 cancer cells and CAFs from patient 1 in collagen. CT26 cancer cells express LifeAct-GFP (green), CAFs are stained with a lyophilic carbocyanine dye (red) and collagen is acquired by reflection (blue). Time is in hours and minutes (HH:mm). (B) Up: overlaid images of collagen I matrices containing cancer cell spheroids alone or together with control or FN-depleted CAFs generated using the available software CurveAlign (UW-Madison; <http://loci.wisc.edu/software/curvealign>). Yellow line indicates the edge of the spheroid and green lines indicate fibers orientation with respect to the closest point on the spheroid edge. Down: roseplots representing the frequency of distribution of the absolute angles of collagen fibers within the range of 0 to 90° with respect to the closest point on the spheroid edge.

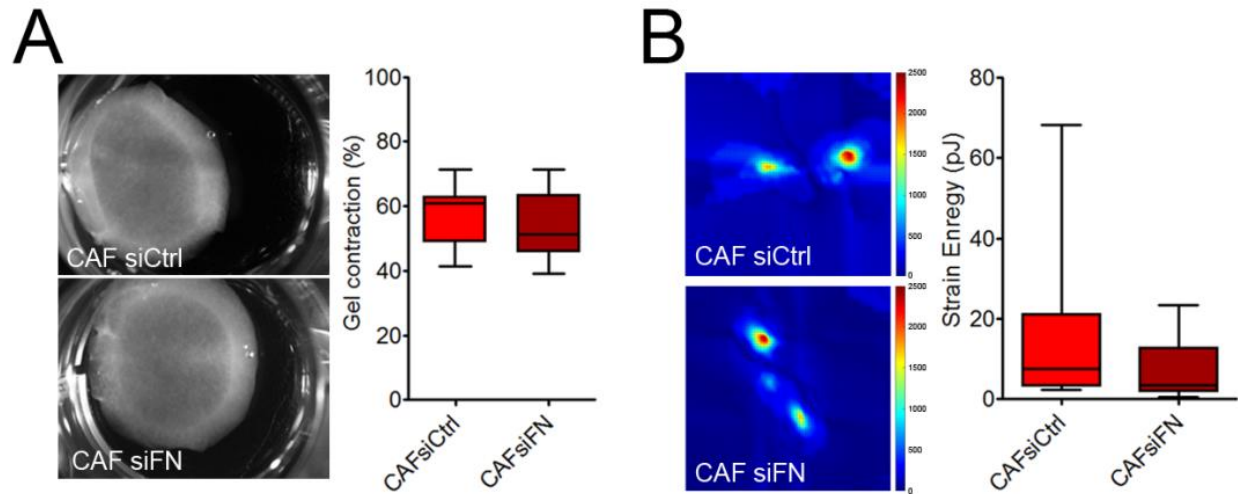


Figure III.1.8. (A) Left: control and FN-depleted CAFs cultured in collagen I gels 1 day post-embedding. Right: Percentage of gel contraction of control and FN-depleted CAFs from patient 1 calculated using the formula $100 \times (\text{gel area (T0)} - \text{gel area (T1)}) / \text{gel area (T0)}$. Quantification results are expressed as box and whiskers (minimum to maximum). p value is calculated using a paired t test for $n=3$ over $N=6$ separate experiments. (B) Left: traction force map of control and FN-depleted CAFs from patient 1 on collagen-coated polyacrylamide gels with Young's modulus of 5 kPa. Color code gives the magnitude of traction stress in Pa, which corresponds to forces of $\text{pN}/\mu\text{m}^2$. Right: corresponding average force (strain energy) exerted by CAFs over a 30min time-lapse. Quantification results are expressed as box and whiskers (minimum to maximum). p value is calculated using Mann Whitney test for $n=10$ cells over $N=2$ separate experiments.

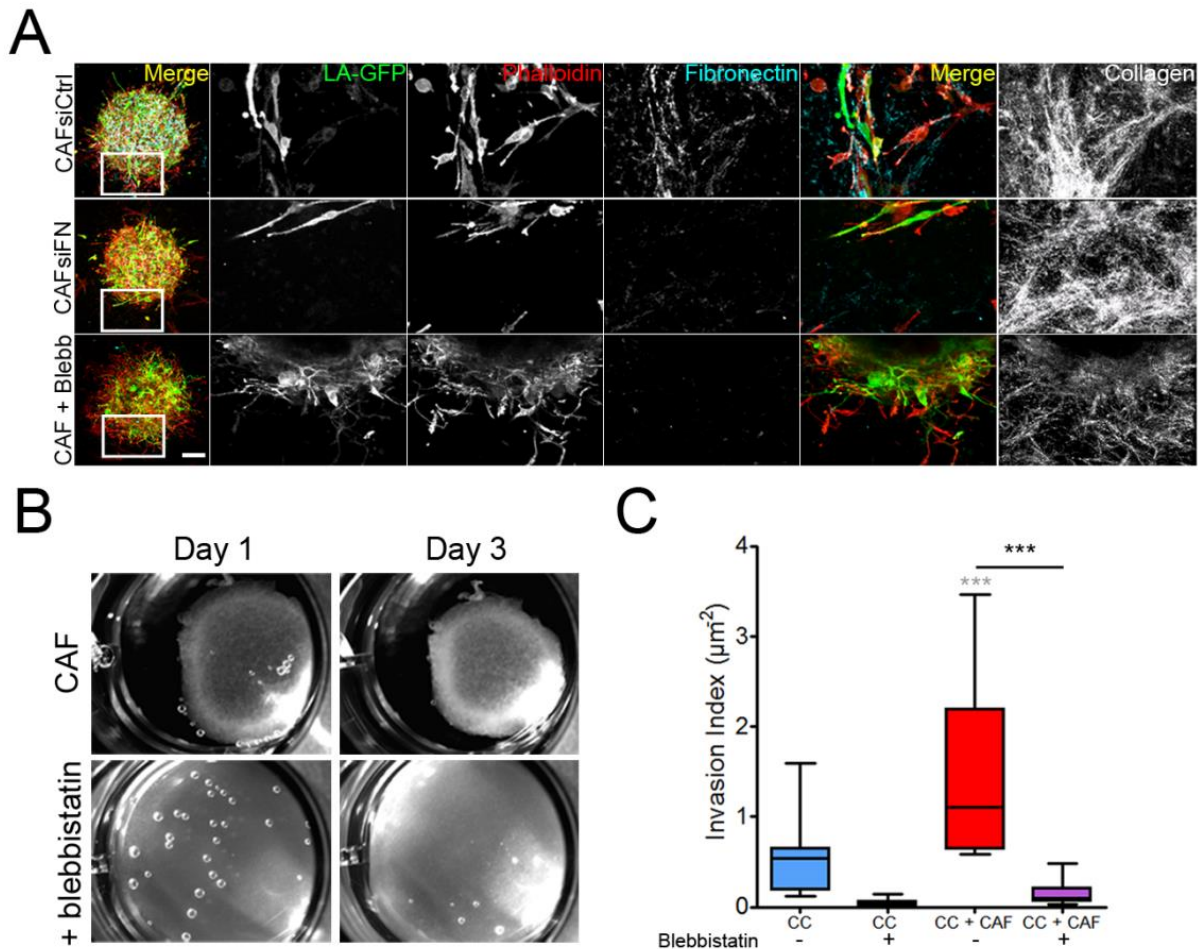


Figure III.1.9. (A) Maximum intensity projections of cancer cell spheroids in collagen I gels with CAFs treated with siRNA scrambled control (CAFSiCtrl), with siRNA targeting fibronectin (CAFSiFN) or with blebbistatin at day 3. Scale bar = 100 μm . Zoom-in region represented by the white square. CT26 cancer cells express LifeAct-GFP (green), F-actin is stained with phalloidin-rhodamin (red), fibronectin is immunostained (cyan) and collagen is acquired using reflection (white). Scale bar = 50 μm . (B) CAFs embedded in collagen plugs for 1 day and 3 days with or without blebbistatin treatment. (C) Quantification of cancer cell invasion in the presence of CAFs, with or without blebbistatin treatment. Invasion index is defined as the ratio between the number of invading nuclei and the area of the spheroid contour. All quantification results are expressed as box and whiskers (minimum to maximum) of at least N=3 separate experiments. p values are compared to cancer cells alone (in gray) and to cancer cells with CAFs (in black) using Newman-Keuls multiple comparison test (*p<0.05, **p<0.01, ***p<0.001).

Altogether, these results demonstrate that both contractility and FN are important for CAF-mediated cancer cell invasion. However, the overall ability of fibroblasts to induce cancer cell invasion did not significantly correlate with their capacity to contract collagen, especially in the case of couple 3 where NAFs and CAFs displayed similar collagen contraction (Fig. III.1.10). This suggests that mechanical forces are important for invasion as they will induce FN assembly. However, if not followed by FN deposition, mechanical forces by CAFs are not sufficient to promote invasion.

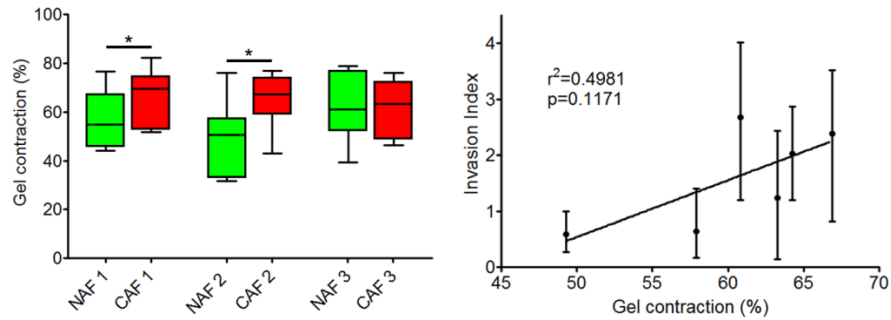


Figure III.1.10. Left: Percentage of gel contraction between all fibroblast couples calculated using the formula $100 \times (\text{gel area (T0)} - \text{gel area (T1)}) / \text{gel area (T0)}$. Quantification results are expressed as box and whiskers (minimum to maximum). p value is calculated using a paired t test for $n=3$ over $N=6$ separate experiments. Right: Scatter dot graphs correlating the invasion index of cancer cells in the presence of fibroblasts with the contractility of fibroblasts. Error bars represent the quartile values. Quality of linear regression is represented by the value of p and r^2 .

Finally, it has been suggested that invadopodia, actin rich structures responsible for matrix degradation, could also exert mechanical forces on the matrix and switch on a contractile phenotype (Aung et al., 2014). As contraction and degradation of the matrix could be interdependent, we also checked for the role of proteolysis in CAF-mediated cancer cell invasion. Inhibition of matrix proteolysis using broad spectrum MMP inhibitors GM6001 and BB94 abrogated the spontaneous invasion of cancer cells, as previously shown (Fig. III.1.11A) (Poincloux et al., 2009; Wolf et al., 2013). When treated with BB94, CAFs still contracted collagen plugs indicating that the ability of CAFs to contract the matrix was independent from their ability to degrade it (Fig. III.1.11B). Moreover, the presence of CAFs rescued cancer cell invasion which was not the case for CAFsiFN (Fig. III.1.11C). Together, these data show that cancer cell invasion is MMP-independent in the presence of CAFs if CAFs retain the ability to

assemble FN. These findings could provide an explanation to the failure of MMP inhibitors in clinics. As a major constituent of the tumor microenvironment, CAFs can provide an alternative escape mechanism for cancer cells by aligning collagen fibers and assembling FN that enables cancer cell invasion.

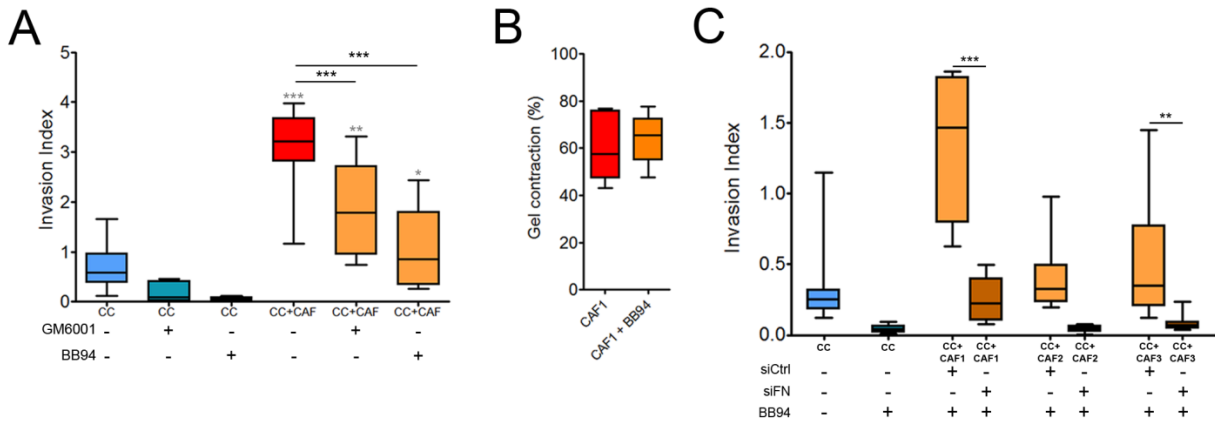


Figure III.1.11. (A) Quantification of cancer cell invasion alone or in the presence of CAFs from patient 1, without treatment, with GM6001 treatment or with BB94 treatment. Invasion index is defined as the ratio between the number of invading nuclei and the area of the spheroid contour. Results are expressed as box and whiskers (minimum to maximum) of at least N=3 separate experiments. p values are compared to cancer cells alone (in gray) and to cancer cells with CAFs (in black) using Newman-Keuls multiple comparison test (*p<0.05, **p<0.01, ***p<0.001). **(B)** Percentage of gel contraction between control CAFs and BB94 treated CAFs from patient 1 calculated using the formula $100 \times (\text{gel area (T0)} - \text{gel area (T1)}) / \text{gel area (T0)}$. Quantification results are expressed as box and whiskers (minimum to maximum). p value is calculated using a paired t test for n=3 over N=6 separate experiments. **(C)** Quantification of cancer cell invasion alone or in the presence of control or FN-depleted CAFs from all patients and treated with BB94. Invasion index is defined as the ratio between the number of invading nuclei and the area of the spheroid contour. Results are expressed as box and whiskers (minimum to maximum) of at least N=3 separate experiments. p values are compared to cancer cells alone (in gray) and to cancer cells with CAFs (in black) using Newman-Keuls multiple comparison test (*p<0.05, **p<0.01, ***p<0.001).

CAFs secrete and assemble more FN than NAFs

FN fibrillogenesis is a multistep process. Cells secrete FN as soluble dimers which then bind to integrin receptors, unfold and associate to each other to form a fibrillary matrix (see section I.4.1.2). It is possible that CAFs are more efficient in assembling FN than NAFs, and consequently induce more invasion of cancer cells. To address this, we compared the capacity of CAFs and NAFs to express, secrete and assemble FN (Fig. III.1.12).

The analysis of total cell lysates showed that CAFs from patients 1 and 2 produced higher amounts of FN compared to NAFs (Fig. III.1.12A). We also found larger amounts of secreted FN in CAFs compared to NAFs (Fig. III.1.12A). Similarly, CAFs assembled more FN fibrils compared to their paired NAFs (Fig. III.1.12B).

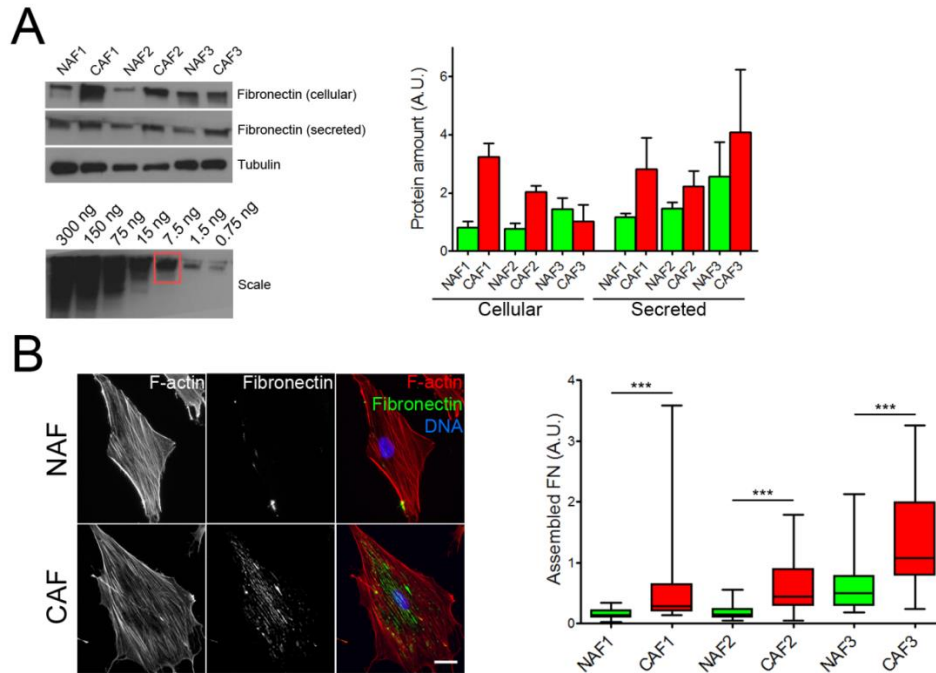


Figure III.1.12. (A) Immunoblot analysis. Conditioned media and lysates prepared from NAFs and CAFs were probed with FN antibody. α -tubulin served as a loading control. Protein amount is represented by normalizing to tubulin. Results are represented as column bars for N=3 separate experiments. For the FN scale: soluble FN loaded at a range of 300ng to 0.75ng. **(B)** Left: Immunostaining of FN (green) in NAFs and CAFs. F-actin is stained with phalloidin-rhodamin (red) and DNA was stained with DAPI (blue). Scale bar = 20 μ m. Right: Quantification of assembled FN. Amount of assembled fibronectin is defined as the amount of fluorescence in a cell (integrated density) normalized to the area of the cell and the background fluorescence. Data are represented as box and whiskers (minimum to maximum). p value is calculated using Mann Whitney test for n=20 cells over N=2 separate experiments.

When comparing the invasion induced by fibroblasts over their ability to express, secrete and assemble FN, we noticed a significant correlation between the amount of assembled FN and the invasion index (Fig. III.1.13). This result indicates that the ability of fibroblasts to induce cancer cell invasion directly correlates with the amount of FN they assemble in the matrix.

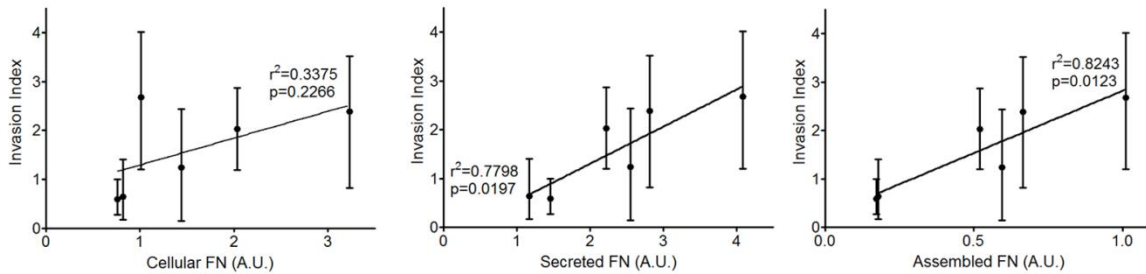


Figure III.1.13. Scatter dot graphs correlating the invasion index of cancer cells in the presence of fibroblasts with the amount of expressed (left), secreted (middle) and assembled FN (right) by fibroblasts. Error bars represent the quartile values. Quality of linear regression is represented by the values of p and r^2 .

To further address the role of secreted FN in cancer invasion, based on the estimation of the amount of FN secreted by CAFs, we added 250ng/mL of soluble FN to cancer cell spheroids (Fig. III.1.12A). We observed that supplementing collagen with soluble FN did not induce invasion (Fig. III.1.14). This was not surprising, as CAFs' secreted molecules did not promote cancer cell invasion (Fig. III.1.3).

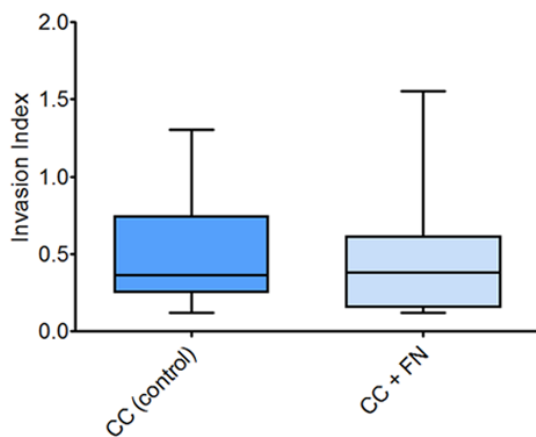


Figure III.1.14. Quantification of cancer cell invasion in a collagen matrix or in a collagen and fibronectin matrix. All quantification results are expressed as box and whiskers (minimum to maximum) for at least $N=3$ separate experiments. p value is calculated using Mann Whitney test.

Together, these results show that CAFs secrete and assemble FN more efficiently than NAFs and point towards the importance of FN assembly in CAF-mediated cancer cell invasion. As the invasion induced by all fibroblast populations significantly correlated with the amount of assembled FN, we uncover a signature of CAFs and a link between ECM remodeling by CAFs and cancer cell invasion.

CAF_s assemble FN via integrins $\alpha 5$ and $\beta 3$

As soluble FN did not stimulate cancer cell invasion, we addressed the role of assembled FN. FN is assembled via transmembrane proteins, integrins, more specifically mostly via integrins $\alpha 5\beta 1$ and $\alpha v\beta 3$ (see sections 2.2 and 4.1.2 of the introduction). We correlated the amounts of integrin isoforms $\alpha 5$, αv , $\beta 1$ and $\beta 3$ in CAFs, to their ability to induce invasion. Integrin $\beta 3$ expression showed the most significant correlation hinting towards the importance of $\beta 3$ integrin in CAF-mediated cancer cell invasion (Fig. III.1.15).

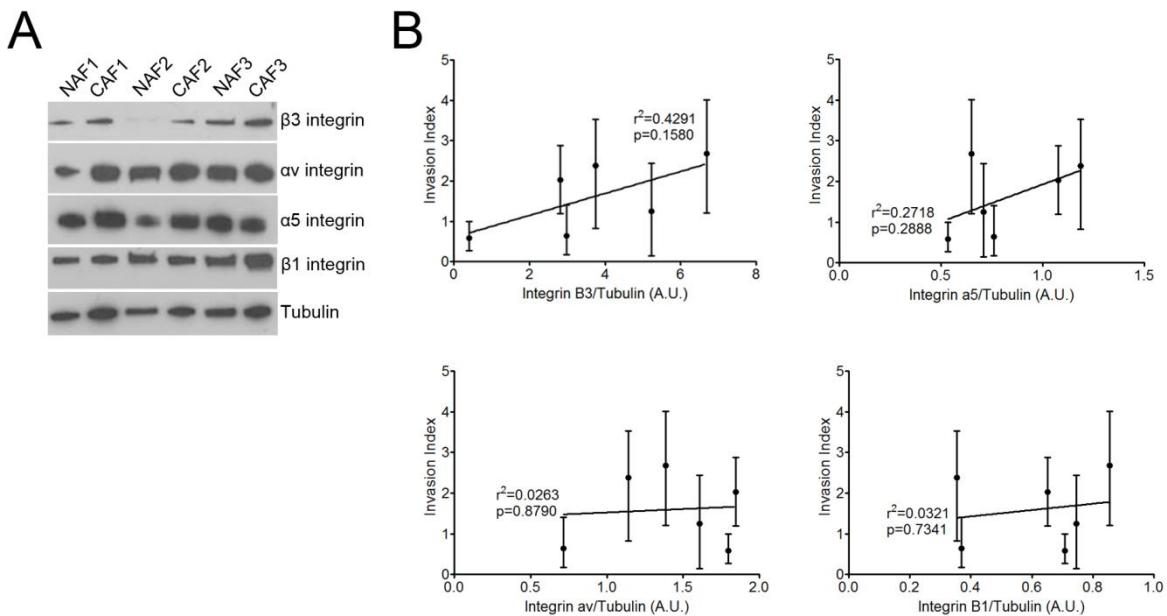


Figure III.1.15. (A) Immunoblot analysis. Lysates prepared from NAFs and CAFs were probed against integrins $\beta 3$, $\alpha 5$, αv and $\beta 1$ antibodies. α -tubulin served as a loading control. Protein amount is calculated by normalizing $\beta 3$ integrin, $\alpha 5$ integrin, αv integrin and $\beta 1$ integrin amounts to tubulin amount. Results are represented as column bars. (B) Scatter dot graphs correlating the invasion index of cancer cells in the presence of fibroblasts with the amounts of integrins $\beta 3$, $\alpha 5$, αv and $\beta 1$ in fibroblasts calculated by normalizing integrin amounts to tubulin amount. Error bars represent the quartile values. Quality of linear regression is represented by the value of p and r^2 .

We next depleted integrins $\beta 3$ or $\alpha 5$ in CAFs (Fig.III.1.16A). In this condition, CAFs were not able to assemble FN in the matrix but the amount of secreted FN by CAFs was unchanged (Fig.III.1.16B).

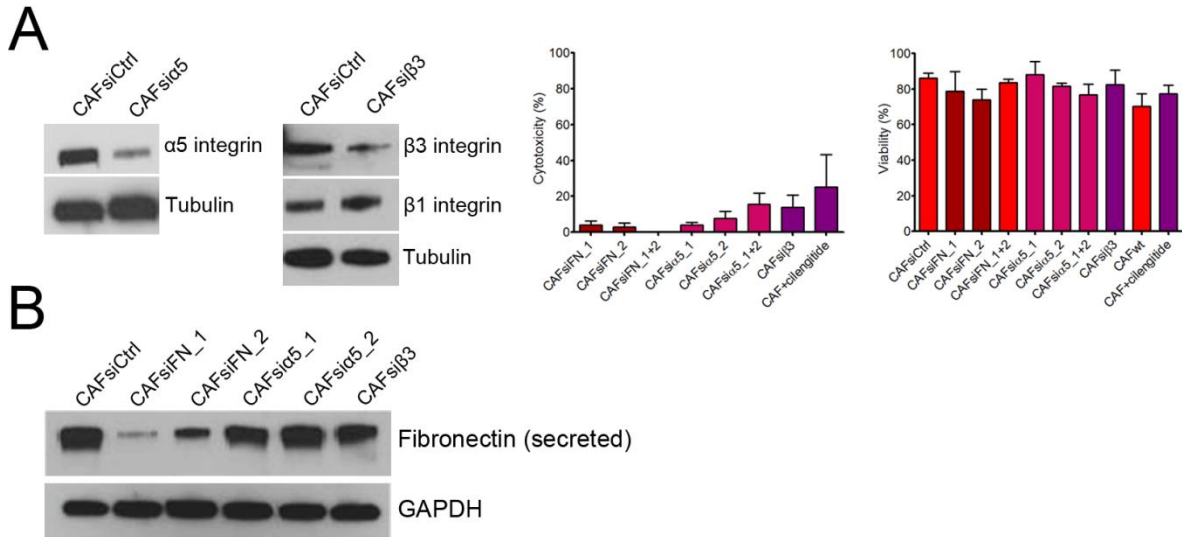


Figure III.1.16. (A) Left: Immunoblot analysis. Lysates prepared from CAFs treated with siRNA scrambled control and CAFs treated with siRNA against integrin $\alpha 5$ were probed with integrin $\alpha 5$ antibody. Lysates prepared from CAFs treated with siRNA scrambled control and CAFs treated with siRNA against integrin $\beta 3$ were probed with integrin $\beta 1$ and integrin $\beta 3$ antibodies. α -tubulin served as a loading control. Right: Cytotoxicity and viability of CAFs in the presence of RNAi against fibronectin, integrin $\alpha 5$, integrin $\beta 3$ and in the presence of cilengitide were evaluated. Results are represented as column bars. **(B)** Immunoblot analysis. Conditioned media and lysates prepared from CAFs treated with siRNA scrambled control and CAFs treated with siRNA against fibronectin, integrin $\alpha 5$ or integrin $\beta 3$ were probed with FN antibody. GAPDH served as a loading control.

In the presence of both CAFsi $\alpha 5$ and CAFsi $\beta 3$ invasion was significantly reduced, although a more striking phenotype was observed with $\beta 3$ -depleted CAFs (Fig.III.1.17A). This effect was confirmed using cilengitide, an inhibitor of $\beta 3$ integrin (Fig. III.1.17B). These results indicate that integrin $\beta 3$, and to a lesser extent integrin $\alpha 5$, are necessary for CAF-mediated cancer cell invasion. Because the fluorescence signal in these 3D assays is tricky to assess, we quantified the amount of assembled FN on 2D. Surprisingly, depletion of integrin $\alpha 5$ did not result in reduction of FN assembly by CAFs 1 day post-plating (Fig.III.1.18), while the ability to assemble FN was reduced in $\beta 3$ integrin-depleted CAFs. However, in a confluent monolayer when CAFs were

given longer time to assemble FN fibers (Fig. III.1.18), FN fibrillogenesis by CAFsi α 5 was reduced, but to a lesser extent than by CAFs treated with cilengitide (Fig. III.1.17). This suggests an earlier requirement of integrin β 3 compared to α 5 in FN fibrillogenesis.

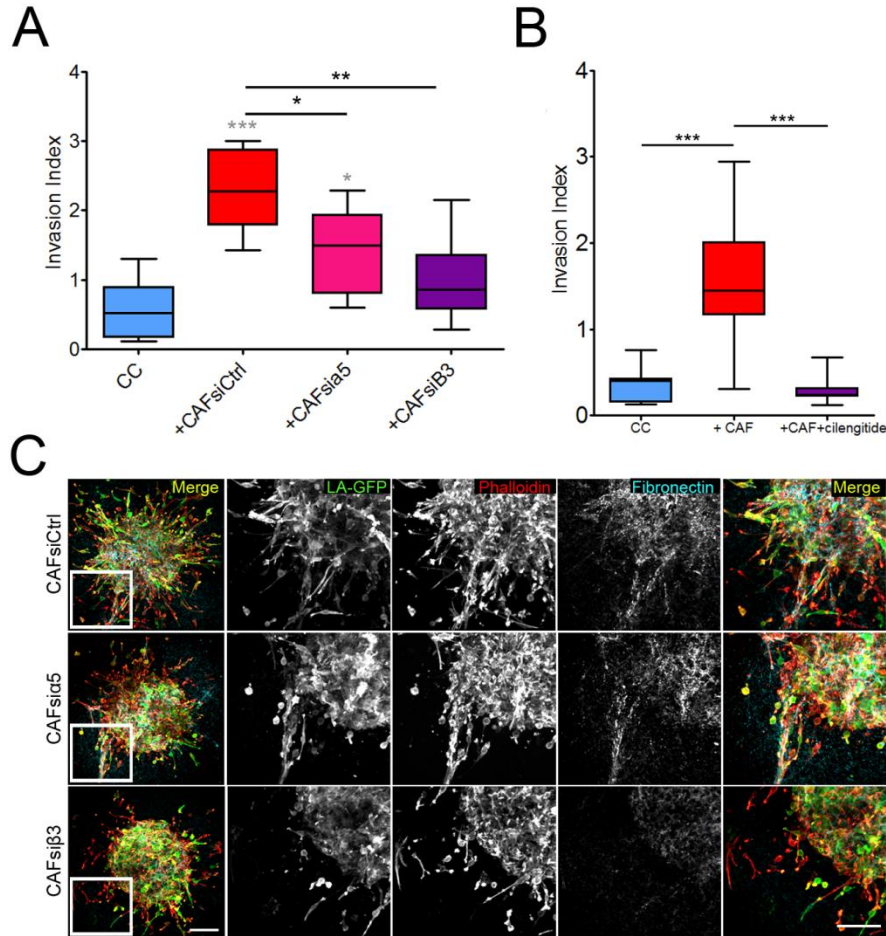


Figure III.1.17. (A) Quantification of cancer cell invasion alone or in the presence of control CAFs, α 5 depleted CAFs and β 3 depleted CAFs from patient 3. (B) Quantification of cancer cell invasion in the presence of CAFs from patient 2, with or without cilengitide treatment. Invasion index is defined as the ratio between the number of invading nuclei and the area of the spheroid contour. All quantification results are expressed as box and whiskers (minimum to maximum) of at least N=3 separate experiments. p values are compared to cancer cells alone (in gray) and to cancer cells with CAFs (in black) using Newman-Keuls multiple comparison test (*p<0.05, **p<0.01, ***p<0.001). (C) Maximum intensity projections of cancer cell spheroids in collagen I gels with CAFs treated with siRNA scrambled control (CAFsiCtrl), with siRNA targeting integrin α 5 (CAFsi α 5) or integrin β 3 (CAFsi β 3) at day 3. Scale bar = 100 μ m. Zoom-in region represented by the white square. CT26 cancer cells express LifeAct-GFP (green), F-actin is stained with phalloidin-rhodamin (red), fibronectin is immunostained (cyan) and collagen is acquired using reflection (white). Scale bar = 50 μ m.

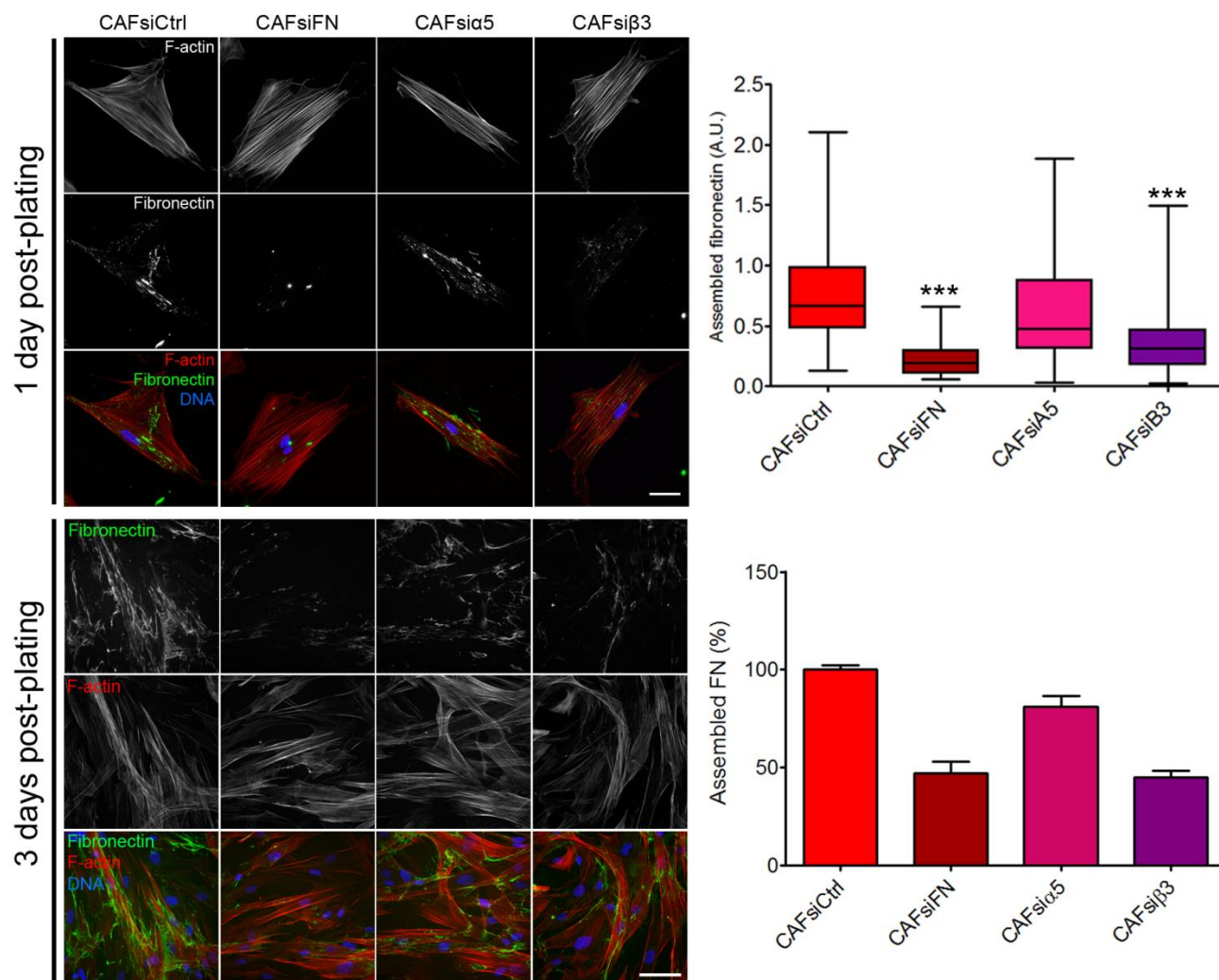


Figure III.1.18. Left: Immunostaining of FN (green) in control CAFs, FN depleted CAFs, α 5 depleted CAFs and β 3 depleted CAFs 1 or 3 days after plating cells. F-actin was stained with phalloidin-rhodamin (red) and DNA was stained with DAPI (blue). Scale bars = 40 μ m. Right up: Graph represents the amount of assembled fibronectin per cell defined as the amount of fluorescence in a cell (integrated density) normalized to the area of the cell and the background fluorescence. Quantification results are expressed as box and whiskers; minimum to maximum. Depleted CAFs were compared to control CAFs for n=20 cells over N=2 separate experiments. p value is calculated using Newman Keuls multiple comparison test. Right down: Graph represents the percentage of assembled fibronectin compared to control conditions defined as the amount of fluorescence in a monolayer (integrated density) normalized to the amount of F-actin and the background fluorescence. Quantification results are expressed as column bars with mean +/- SEM. Depleted CAFs were compared to control CAFs for n=10 frames over N=2 separate experiments.

Integrins $\alpha 5$ and $\beta 3$ are required at different stages of FN fibrillogenesis

As our results indicate that both integrin $\beta 3$, and to a lesser extent $\alpha 5$, are required for FN fibrillogenesis; we next wondered about their localization in CAFs and with respect to FN fibers. While integrin $\alpha 5$ was found in the center of the cells, in fibrillar adhesions localizing with FN fibers, $\alpha \nu \beta 3$ was more peripheral, present in nascent and mature focal adhesions and localizing with FN puncta (Fig. III.1.19). The localization of $\alpha \nu \beta 3$ at the cell periphery pointed towards its requirement during initial cell-matrix interactions. Indeed, 2h after plating cells, integrin $\alpha \nu \beta 3$ was localized at the cell periphery while integrin $\alpha 5$ was not detected (Fig. III.1.20A). Moreover, inhibition of $\alpha 5$ integrin in CAFs did not affect $\alpha \nu \beta 3$ localization to focal adhesions, while blocking of $\beta 3$ prevented $\alpha 5$ accumulation at the cell center (Fig. III.1.20B). We next investigated if blocking of $\alpha \nu \beta 3$ could impair CAFs' ability to contract the matrix or align collagen fibers. CAFs $\beta 3$ or CAFs treated with cilengitide retained the capacity to contract collagen plugs (Fig. III.1.21).

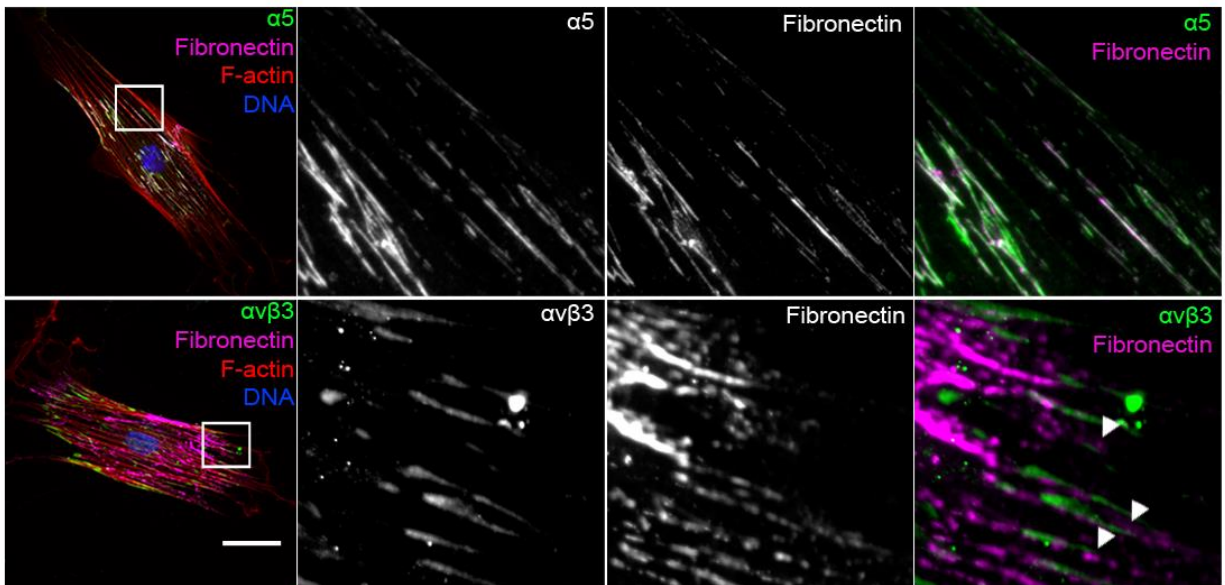


Figure III.1.19. Immunostaining of CAFs for integrins $\alpha 5$ or $\alpha \nu \beta 3$ (green) and fibronectin (magenta). F-actin was stained with phalloidin-rhodamin (red) and DNA was stained with DAPI (blue). Scale bar = 40 μ m. Zoom-in region represented by the white square.

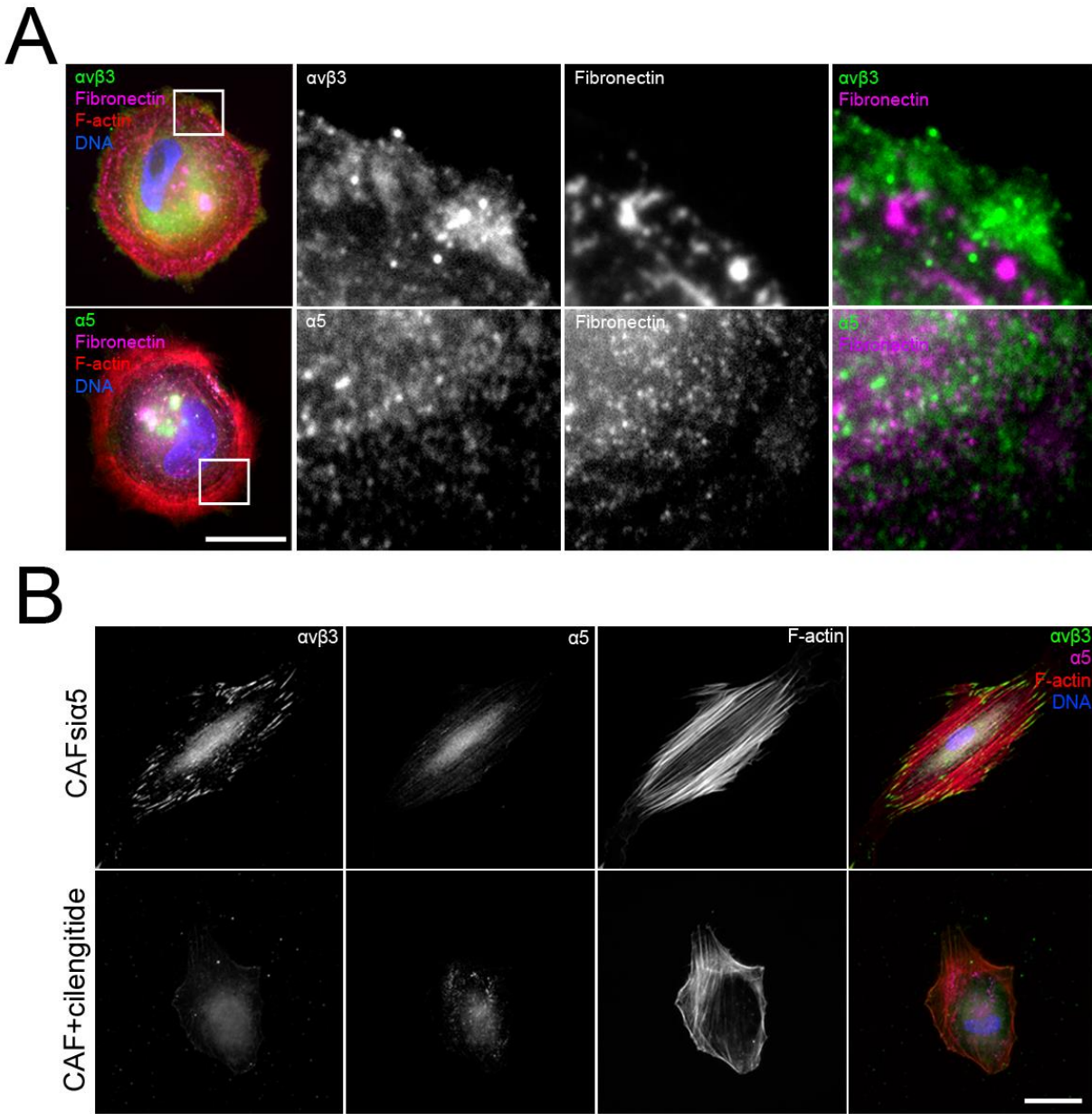


Figure III.1.20. (A) Immunostaining of CAFs 2 hours post-plating for integrins $\alpha 5$ or $\alpha 5\beta 3$ (green) and fibronectin (magenta). F-actin was stained with phalloidin-rhodamin (red) and DNA was stained with DAPI (blue). Scale bar = $20\mu\text{m}$. Zoom-in region represented by the white square. (B) Immunostaining of integrins $\alpha 5$ (magenta) and $\alpha 5\beta 3$ (green) in $\alpha 5$ depleted CAFs and CAFs treated with cilengitide. F-actin was stained with phalloidin-rhodamin (red) and DNA was stained with DAPI (blue). Scale bar = $40\mu\text{m}$.

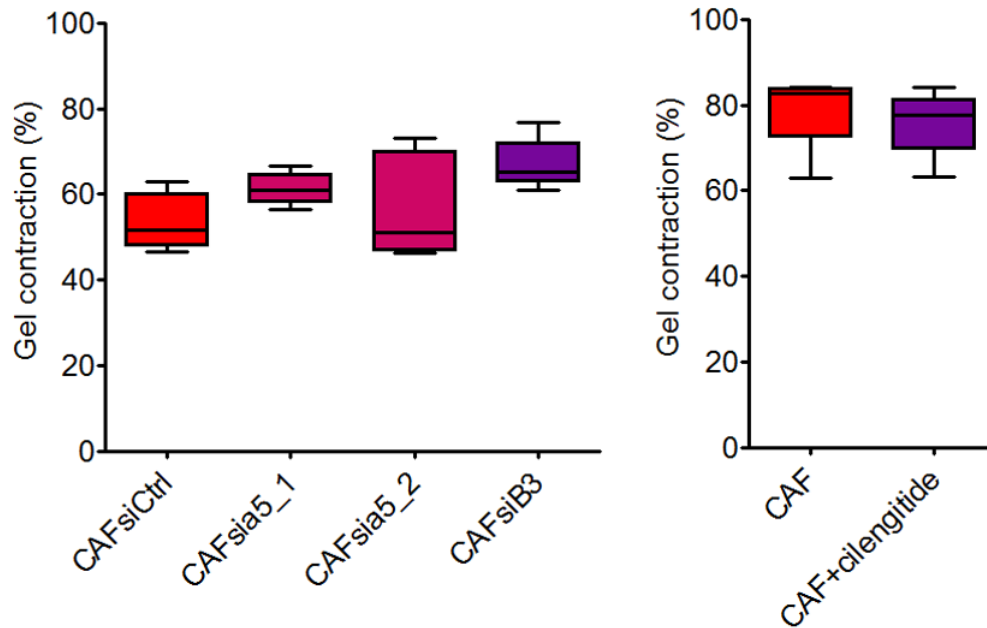


Figure III.1.21. Left: Percentage of gel contraction of control, integrin $\alpha 5$ and integrin $\beta 3$ -depleted CAFs from patient 1. Right: Percentage of gel contraction of CAFs with or without cilengitide treatment from patient 3. Gel contraction was calculated using the formula $100 \times (\text{gel area (T0)} - \text{gel area (T1)}) / \text{gel area (T0)}$. Quantification results are expressed as box and whiskers (minimum to maximum). p value is calculated using a paired t test for $n=3$ over $N=3$ separate experiments.

Conclusion

Altogether, our results show that CAFs, and not NAFs, induce cancer cell invasion of the ECM. While the secretome of CAFs was not sufficient for this process, CAFs' remodeling of the matrix was necessary. We uncover a new mechanism by which matrix alignment and contractility is not sufficient for the initial steps of tumor invasion and has to be followed by FN deposition, more specifically FN matrix assembly. As the amount of assembled FN by fibroblast populations correlates with the level of cancer cell invasion, this study reveals a new signature for cancer-associated fibroblasts. Finally, our results suggest that the activation of integrin $\alpha v \beta 3$ is necessary for the initial steps of FN fibrillogenesis and recruitment of $\alpha 5 \beta 1$ that further mediates the assembly FN fibers. These results will be extensively discussed in section IV of my thesis.

2. Can cancer cells find the blood vessels alone or do they need a guide?

Introduction

Cell guidance during development and wound healing is well established (Haeger et al., 2015). In the context of inflammatory niches and tumor microenvironments, immune cells have been suggested to be recruited through the establishment of a gradient of chemokines. However, whether cancer cells invade the ECM and reach the blood vessels by migrating along a gradient of extracellular cues is still not established. It is hypothesized that cancer cells reach the circulation by following chemoattractants released from the closest blood vessel. However, because CAFs align the matrix in addition to secreting cytokines, they could be the main attractants of cancer cells in the tumor microenvironment. Thus, it is possible that cancer cells preferentially migrate towards CAFs which in turn lead them to the circulation. This model is supported by data showing CAFs at the leading front of cancer cell invasion (Gaggioli et al., 2007; Labernadie et al., 2017).

In the following chapter, using a 2D chemotaxis chamber, I addressed the hypothesis that CAFs could attract cancer cells and also respond to cytokines secreted by endothelial cells. I tested the effect of CAF conditioned media (CM^{CAF}) and of endothelial cell conditioned media (CM^{HUVEC}) on directional cancer cell and CAF migration respectively.

Method optimization

In order to study cell migration under guidance cues, we used Dunn's chemotaxis chamber which consists of a bridge situated between 2 concentric compartments. By supplementing media with the chemoattractant in one of the chambers, gradients are formed between two compartments on the bridge which is too small to permit flow of fluid, but sufficiently large to allow diffusion of the chemoattractant. Migrating cells on the bridge were tracked overtime by wide-field microscope (Fig. III.2.1) (for details on the mounting and imaging of the chamber, see section V.1.11).

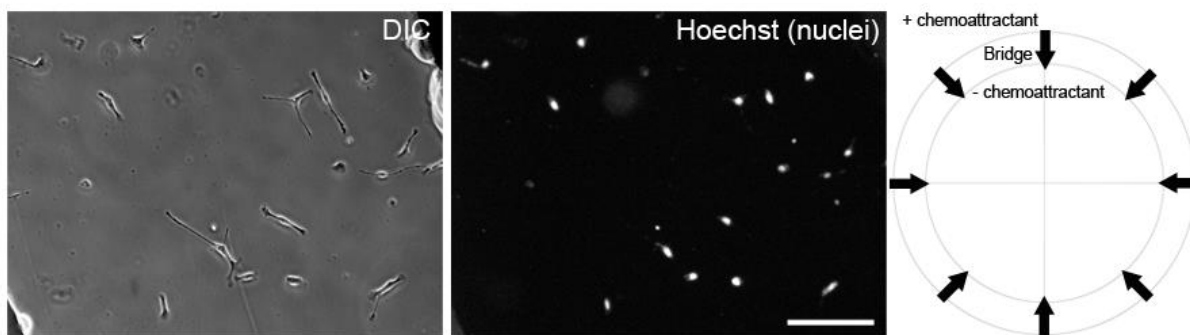


Figure III.2.1. From left to right: differential interference contrast (DIC) of cells migrating over the bridge; nuclear Hoechst staining. Scale bar =100 μ m. Right: Schematic representation of the bridge of Dunn's chemotaxis chamber.

To establish the optimal timeframe to study chemotactic migration of cancer cells, we first characterized the gradient of chemoattractant (its steepness and stability over time) by supplementing the chemoattractant-containing media with fluorescein. As shown in fig. III.2.2A, the gradient was lasting for approximately 12h, exhibiting a decrease of 1.17% per hour. To track cells, we labeled nuclei with Hoechst dye 30min before loading the chamber and collaborated with Dr. Paolo Maiuri, who developed a software that allows: 1. Automatic tracking of all cells on the bridge using the position of their nuclei over time (Fig. III.2.1; III.2.2B). 2. Alignment of the starting points of all tracks into the same xy coordinates that positions the gradient of all images from right to left and allows a direct comparison of migration of many cells (Fig.III.2.2B). 3. The analysis of the behavior of cells during their chemotactic migration. For a detailed description of used parameters, see the supplementary annex at the end of this section.

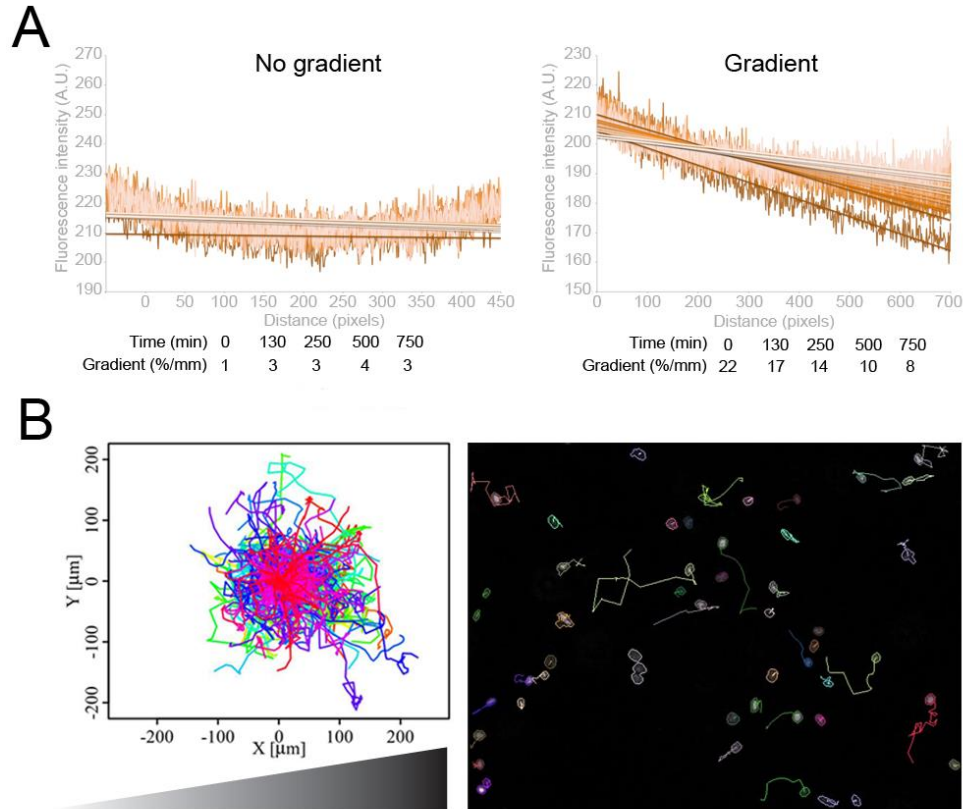


Figure III.2.2. (A) Intensity of the fluorescence signal as a function of distance from the compartment containing chemoattractant and fluorescein over the bridge. Evolution of the gradient over time represented as orange lines with decreasing shades (light orange for $t=10\text{min}$ to dark orange for $t=730\text{min}$). Left: Fluorescein is added in both chambers. Right: Fluorescein is added in one of the chambers. (B) Left: Experimental cell trajectories over time. Right: Mono-dimensional single cell trajectories in time.

Do cancer cells migrate along chemotaxis gradients?

In order to test the capacity of cancer cells to migrate towards specific diffusible cues, we first used varying concentrations of serum (ranging from 2.5 to 20%), as a chemoattractant (Fig.III.2.3). Supplementing the media with 2.5% of serum was the most potent in inducing directional migration of cancer cells, with 42% of cells migrating along the gradient. This condition was subsequently used as a positive control. These results indicate that cancer cells have the capacity to sense diffusible molecules and migrate along gradients in Dunn's 2D chamber.

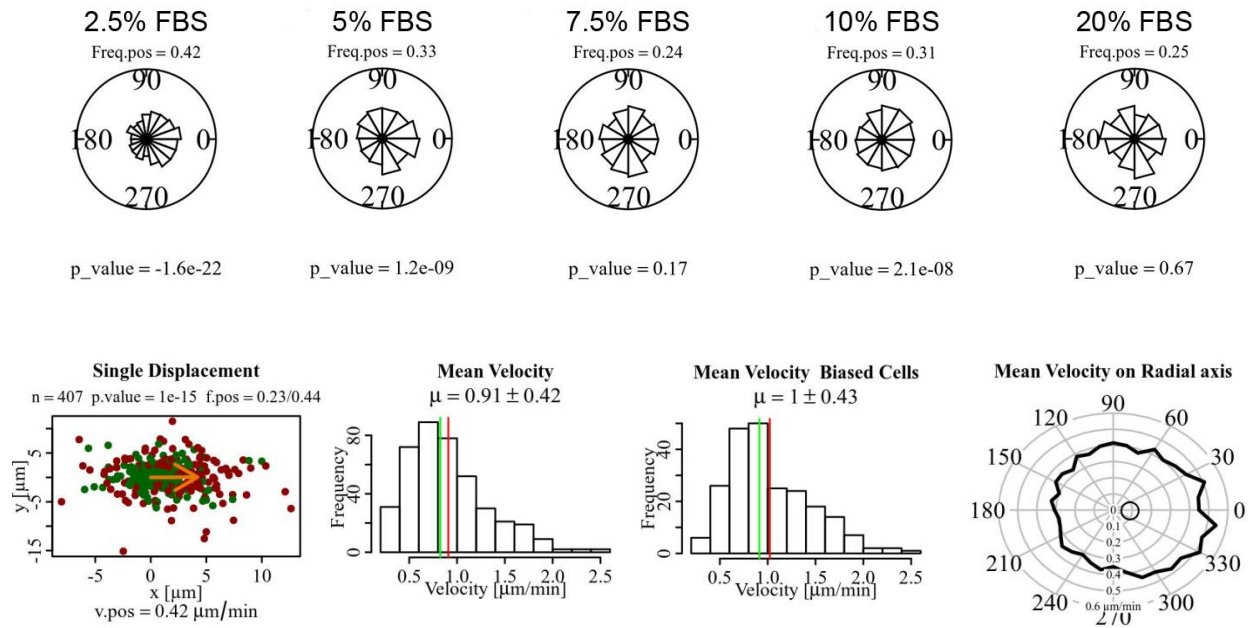


Figure III.2.3. Up: Roseplots representing a general bias or the % of cells that are in the radius of the gradient. Gradient is coming from the right.
Down: Detailed quantification of the chamber with 2.5% of serum in the outer chamber. Single displacement graph representing each step of the cell compared to the previous one, where each dot is the mean of each single displacement of each cell. Green dots represent cells moving randomly; red dots represent cells moving persistently.
Histograms representing the distribution of instantaneous speeds of all cells and directional cells.
Circular histogram representing the distribution of cell speeds according to source of chemoattractant (position 0).

Results

Do cancer cells migrate towards CAF secreted growth factors?

In order to test if CAFs could chemoattract cancer cells, we placed cancer cells in a gradient of CAFs' conditioned medium (serum free DMEM, CM^{CAF}). In these conditions, cancer cells migrated randomly (Fig.III.2.4A) suggesting that CAFs either cannot attract cancer cells, or that the concentration of growth factors was not optimal. To test the latter hypothesis, we concentrated CM^{CAF} 20 times using a 10KDa cutoff. This increased the chemotactic response of cancer cells, with 42% of cells migrating along the gradient (Fig.III.2.4B). However, only 21% of these cells were persistent and overall cells were slower than in control conditions (Fig.III.2.4B), probably due to the inability of CAFs to produce all growth factors/cytokines present in the serum that stimulate the migration of cancer cells. These results indicate that the CM^{CAF} is a potential chemoattractant of cancer cells, and that the main growth factors responsible for cancer cell guidance are at a molecular weight >10 KDa.

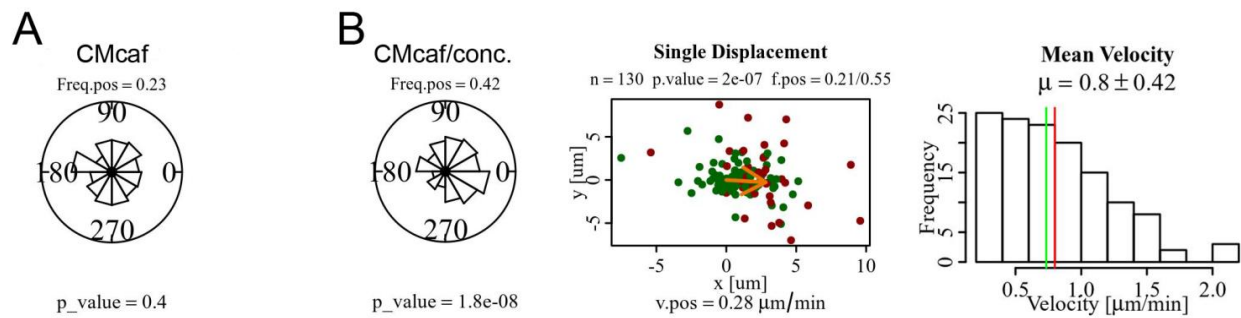


Figure III.2.4. (A) Roseplot representing a general bias or the % of cells that are in the radius of a gradient of CAF conditioned-media.
(B) Left: Roseplot representing a general bias or the % of cells that are in the radius of concentrated CAF conditioned-media. Middle: Single displacement graph representing the trajectory persistence of cells in the presence of concentrated CAF conditioned-media. Right: Histogram representing the distribution of instantaneous speeds of all cells and extracted from the corresponding experimental tracks.

Cancer cells migrate along a gradient of secreted fibronectin

Proteomic data analysis of two fibroblasts couples from colon cancer patients show enrichment in FN in the secretome and proteome of CAFs compared to their paired NAFs (ProteomeXchange Consortium via the PRIDE partner repository with the dataset identifier PXD003670). In addition, the FN fractionation assay (Section III.1) indicates that CAFs secrete

and assemble more FN than NAFs. Therefore, we evaluated if cancer cells migrate along a gradient of secreted FN.

Medium supplemented with 20µg/mL of soluble FN induced directional and persistent migration of cancer cells (Fig.III.2.4), indicating that soluble FN is a potential CAF-secreted chemoattractant for cancer cells. However, whether cancer cells respond to FN as a soluble growth factor or whether they assemble it at the cell front and self-generate a haptotactic gradient still needs to be evaluated.

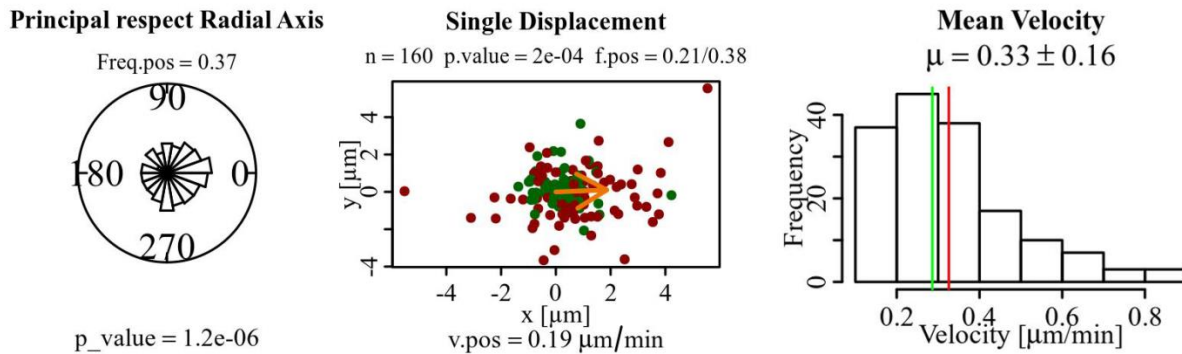
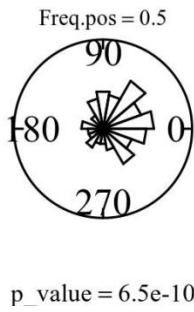


Figure III.2.5. Left: Roseplot representing a general bias or the % of cells that are in the radius of a gradient of fibronectin. Middle: Single displacement graph representing the trajectory persistence of cells in the presence of fibronectin. Right: Histogram representing the distribution of instantaneous speeds of all cells and extracted from the corresponding tracks.

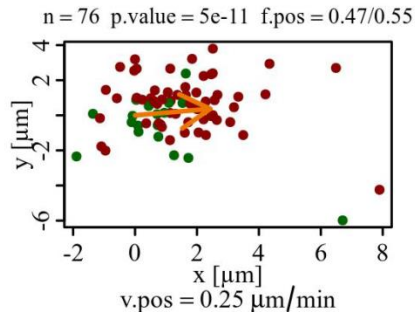
Fibroblasts migrate along a gradient of endothelial cell conditioned media

To assess if CAFs can chemotact towards the blood vessels, we tested the response of fibroblasts to the conditioned media of endothelial cells (CM^{HUVEC}). Because primary CAFs did not migrate in the chamber in the timeframe imposed, we used the NIH3T3 fibroblast cell line. Similarly to CT26, NIH3T3 migrated along a gradient of 2.5%FBS (data not shown). In the presence of CM^{HUVEC}, fibroblasts' migration was directional and highly persistent (Fig.III.2.6) indicating that endothelial cells (and possibly blood vessels in general) can chemoattract fibroblasts.

Principal respect Radial Axis



Single Displacement



Mean Velocity

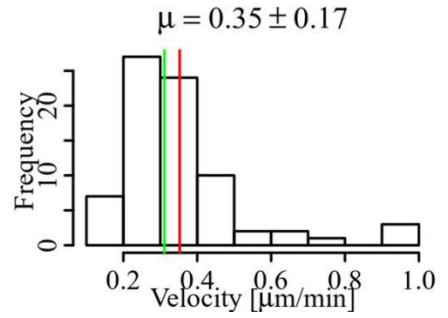


Figure III.2.6. Left: Roseplot representing a general bias or the % of cells that are in the radius of a gradient of endothelial cell conditioned media. Middle: Single displacement graph representing the trajectory persistence of cells in the presence of endothelial cell conditioned media. Right: Histogram representing the distribution of instantaneous speeds of all cells and extracted from the corresponding experimental tracks.

Conclusion and perspectives

Cell guidance in the context of cancer invasion is a concept that remains poorly studied. The idea that cancer cells reach the circulation by following external cues has been hypothesized but never really demonstrated. In this study, we use an *in vitro* chemotaxis chamber to test the migration of cancer cells along gradients of growth factors secreted by fibroblasts. Our results show that cancer cells respond to CAF-secreted cytokines above a molecular weight of 10KDa. Based on a SILAC analysis performed by another student in the lab and the results of the section III.1, FN was a prime candidate as a potential chemoattractant secreted by fibroblasts. Indeed, cancer cell migrated along a FN gradient in our model, even in the absence of serum. Finally, similarly to cancer cells, CAFs also migrated along gradients of endothelial cell conditioned media.

Based on these results, we suggest a working model in which cancer cells invading the stroma migrate towards CAFs which in turn escort them to the circulation.

However, as cancer cells come from mice and CAFs from human, this represents a major flaw in the system as a vast majority of cytokines (e.g. HGF) undergo specie-specific post-translational modifications. Further experiments are still needed in order to validate this model. Mainly, do normal fibroblasts also have the capacity to attract cancer cells, and because they are less efficient than CAFs in aligning the matrix, can they compete with other cells of the tumor microenvironment? Can FN-depleted CAFs also attract cancer cells? If cancer cells are subjected to CM^{CAF} on one side and CM^{HUVEC} on the other, will CAFs be more efficient in attracting cancer cells? Finally, are all these results reproducible in 3D? Recently, in collaboration with N. Bremond (ESPCI), we have developed a 3D collagen microfluidic chamber in which stable gradients of chemokines could be maintained several days. Importantly, this device allows culturing of cancer cells spheroids together with CAFs. By establishing a gradient of endothelial cell-conditioned media, we will be able to test the hypothesis that cancer cells reach the circulation faster when in the presence of CAFs.

ANNEX

Detailed explanation of the data

Single displacement

Represents each step of the cell compared to the previous one, where each dot is the mean of each single displacement of each cell

Green dots: cells moving randomly

Red dots: cells responding to the gradient all along the track compared to the bias

Orange arrow: mean direction of red dots

Trajectory lifetime

Represents the timescale of each track

Path length

Represents the distance of each track

Effective path length

Circles each trajectory and represents the diameter of each disk

Principal axes ratio

Represents the directionality of each track by dividing the overall length of track in y to its length in x. The smaller the value of x/y (ρ), the more directional the movement

Path persistence

Represents the persistence of each track by establishing the ratio of the Eff. Path length/Path length. The closest the ratio is to 1, the more persistent the movement

Mean turning angle

Represents the average of all single turning angles over time

Mean cumulative velocity on time

Represents the instantaneous speed of cells at certain time points

Mean velocity

Represents the distribution of the average speed of each track

Cumulative velocity

Represents the distribution of the instantaneous speeds of all tracks

Interpretation of the mean velocity and the cumulative velocity

If cells are very heterogeneous, they can be very fast at first and again at the end. In this case, the mean velocity histogram will display 2 separate pics.

If cells are alternating overtime, the mean velocity histogram will only show one pic but the cumulative velocity histogram will show 2 separate pics.

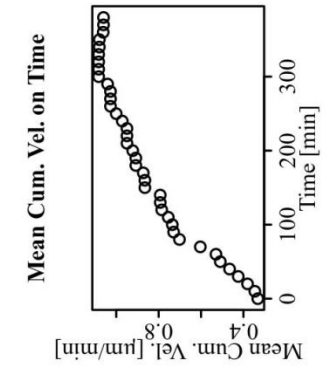
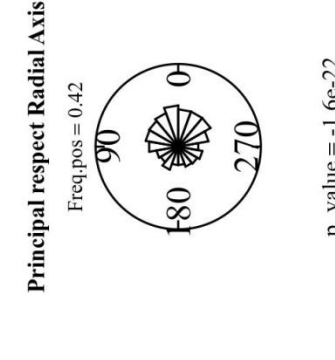
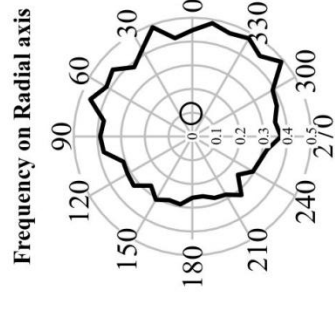
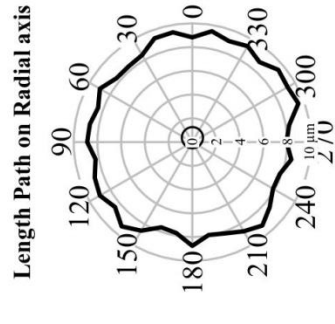
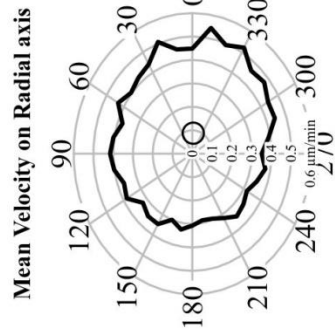
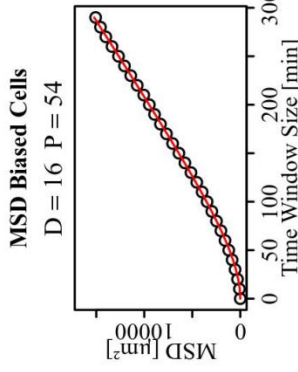
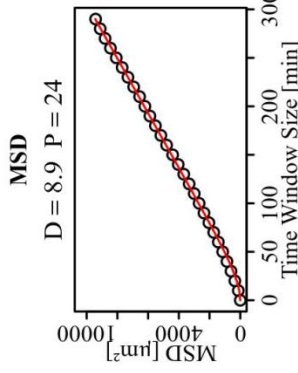
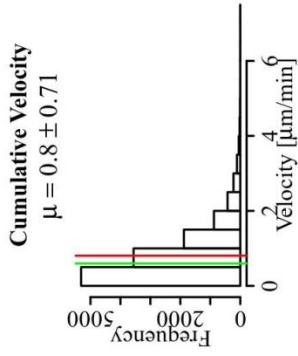
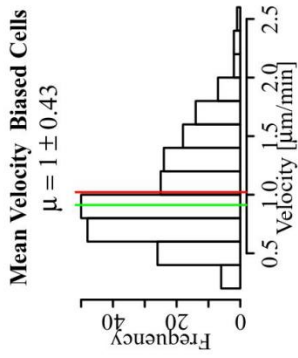
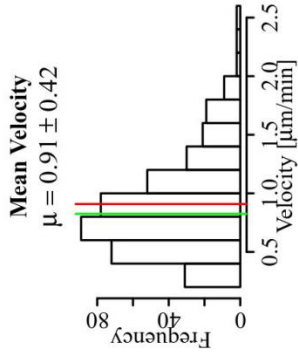
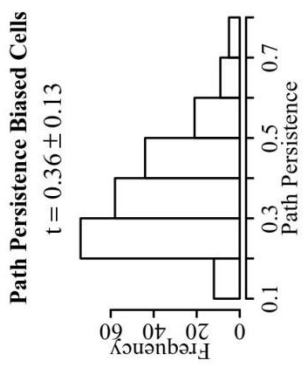
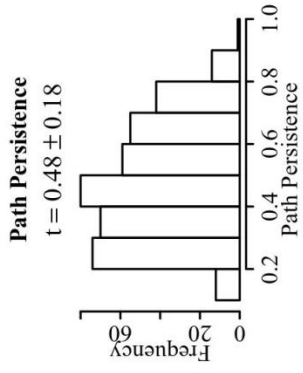
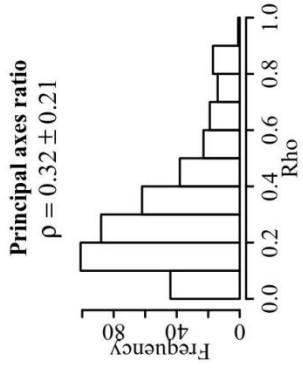
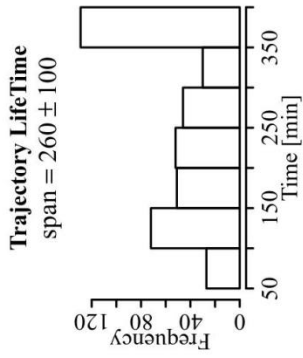
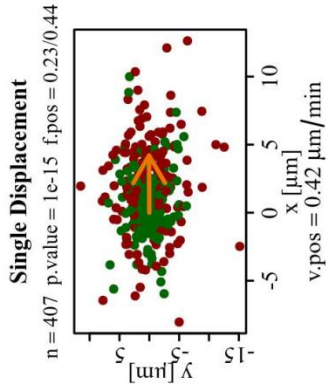
Mean square displacement (MSD)

Represents the type of movement (diffuse vs confined vs directional) where D is the coefficient of mobility ($\mu\text{m}^2/\text{min}$) and represents how fast the cells are, and P is the time during which cells are migrating persistently on average.

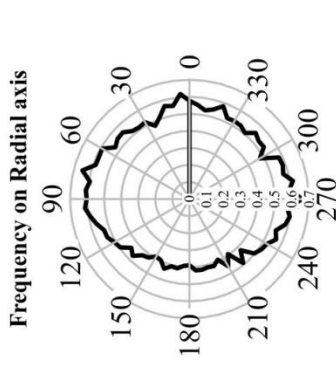
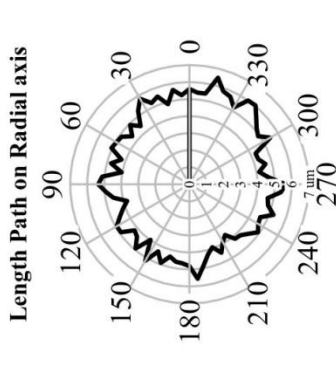
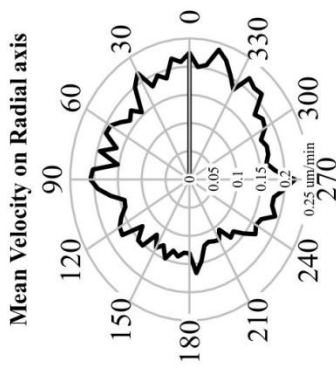
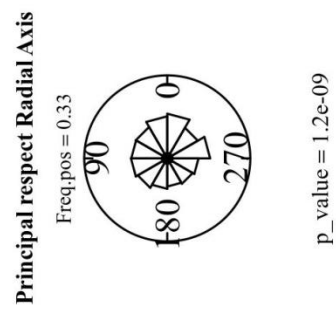
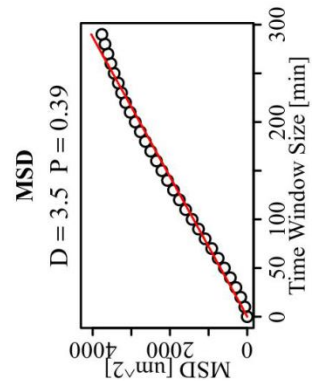
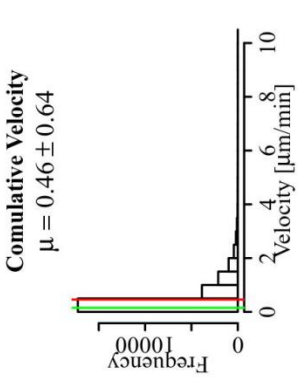
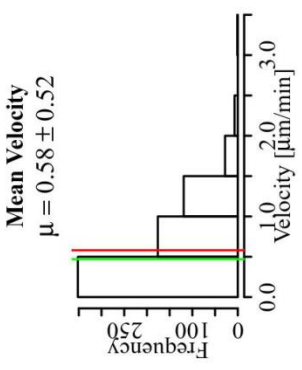
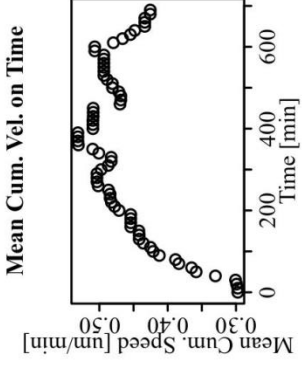
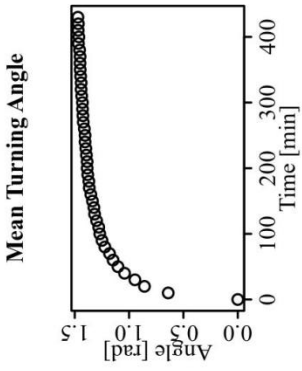
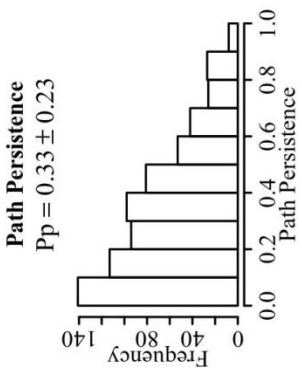
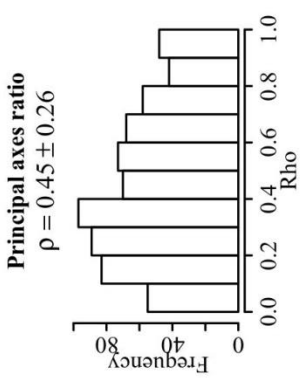
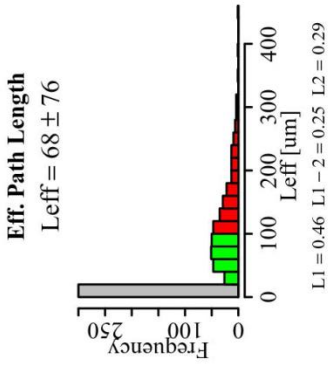
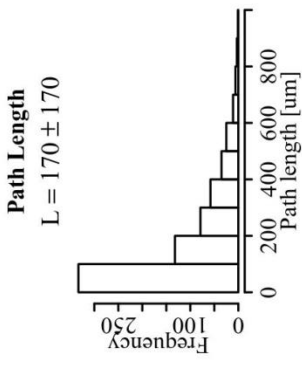
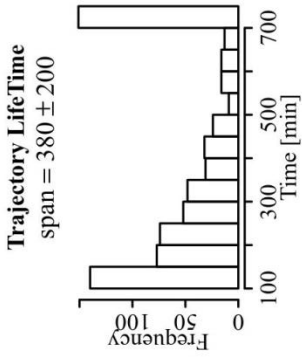
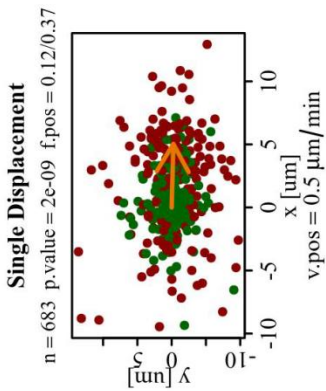
Principal respect radial axis

Represents a general bias or the % of cells that are in the radius of the gradient

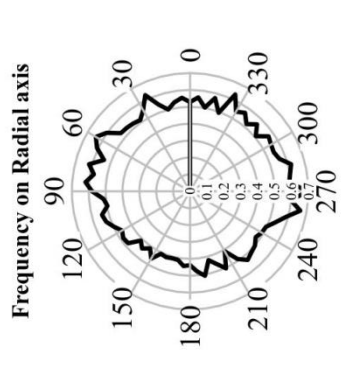
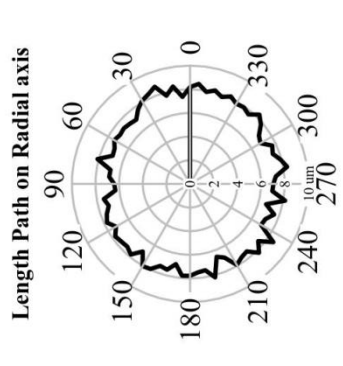
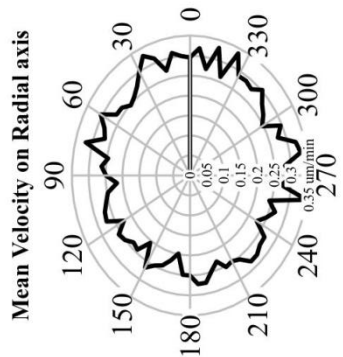
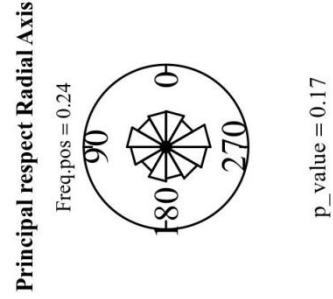
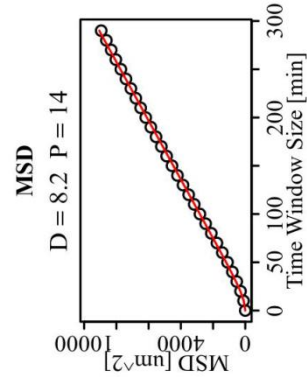
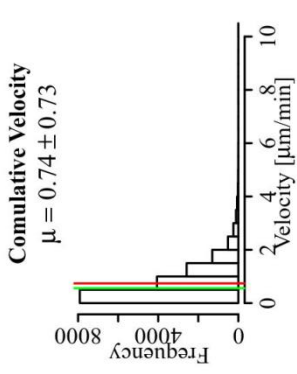
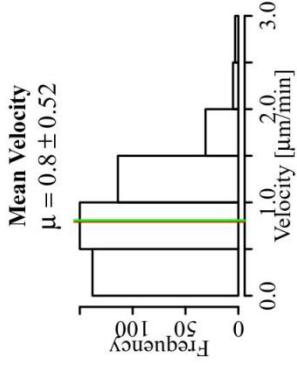
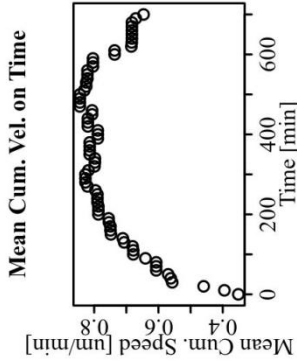
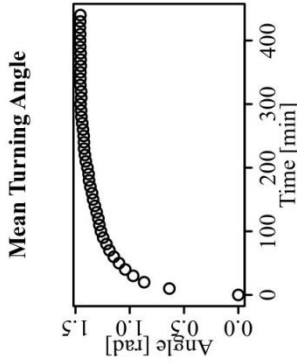
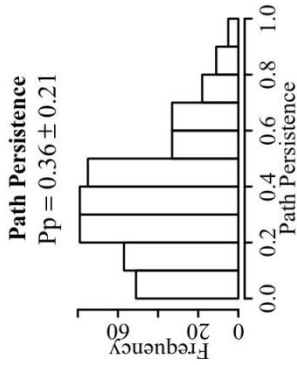
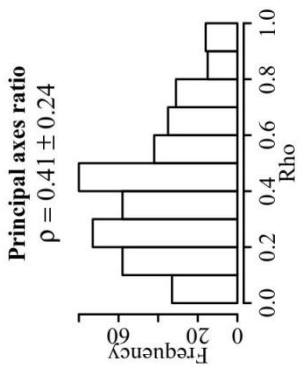
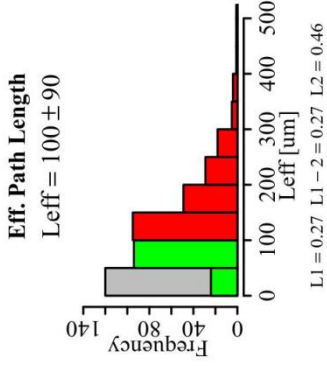
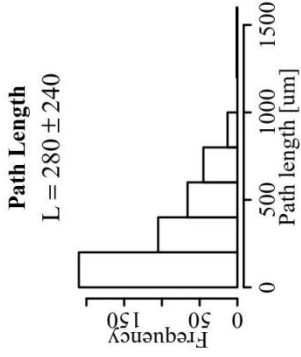
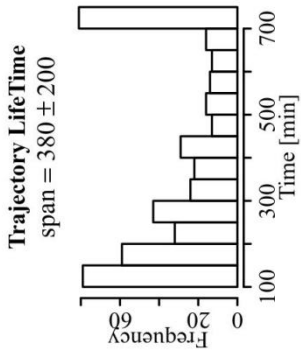
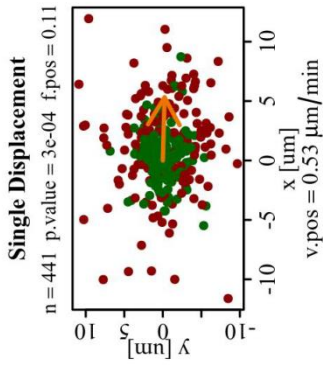
2.5% FBS



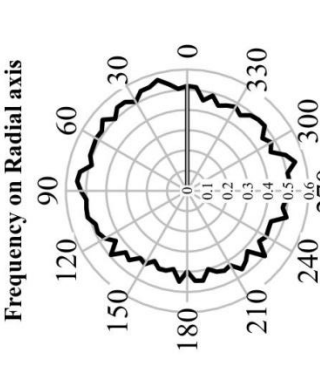
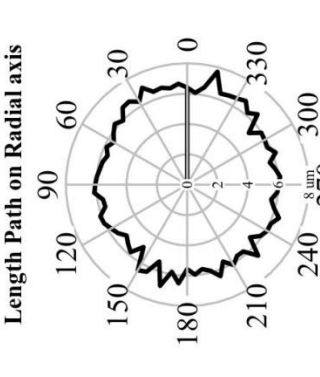
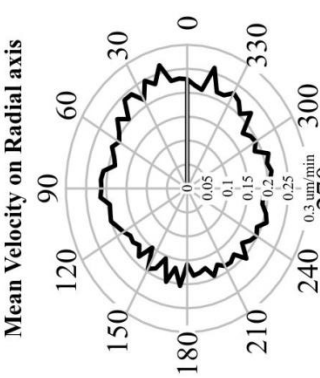
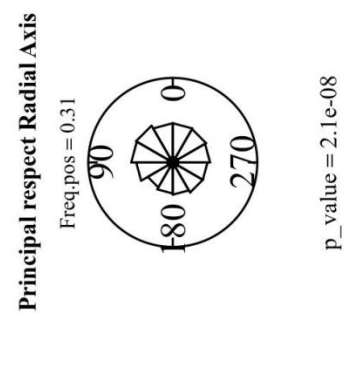
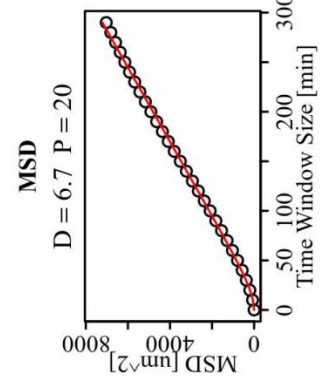
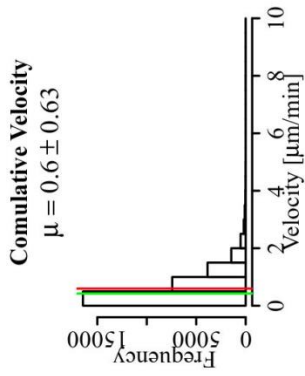
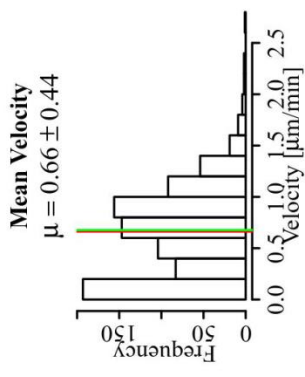
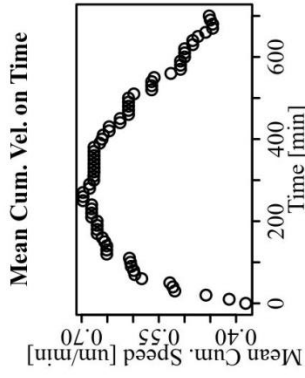
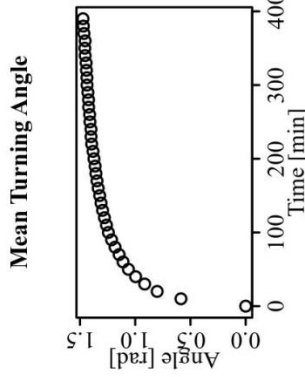
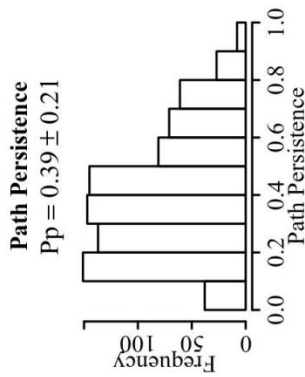
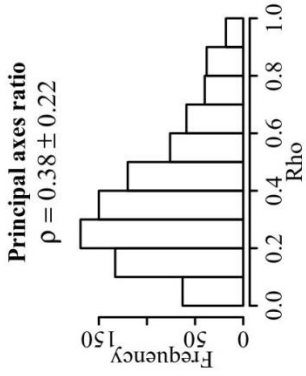
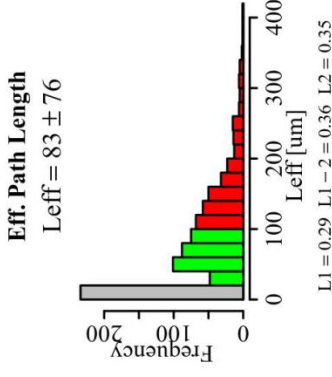
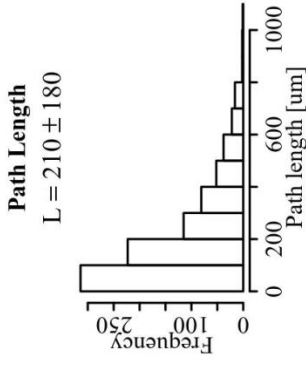
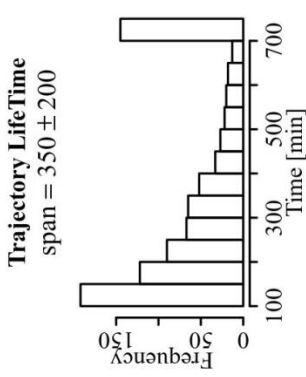
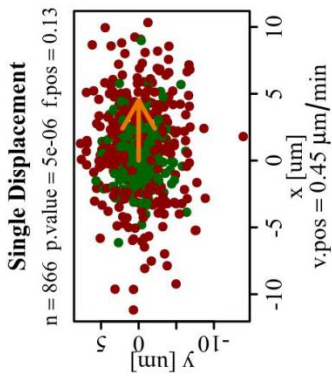
5% FBS



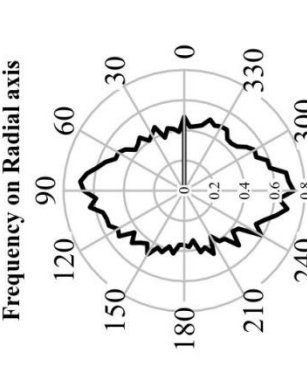
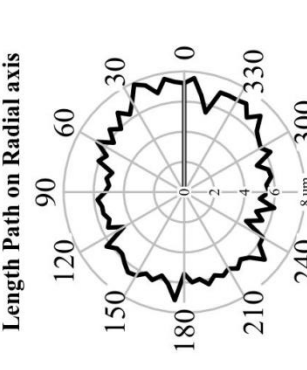
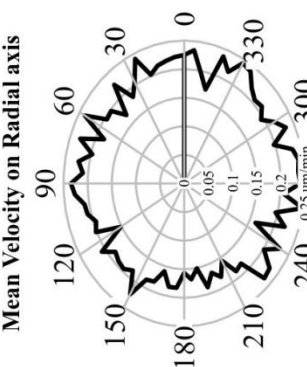
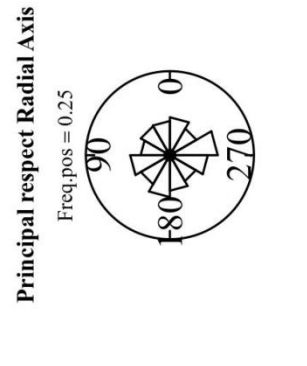
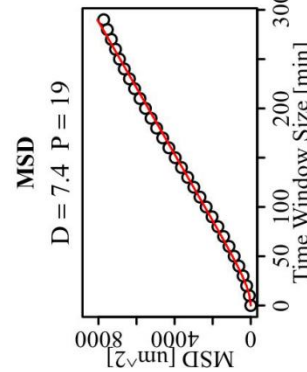
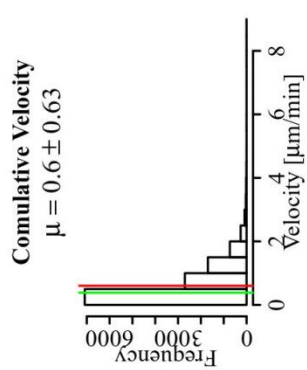
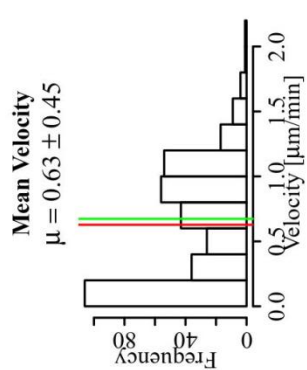
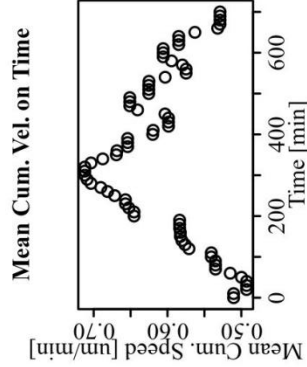
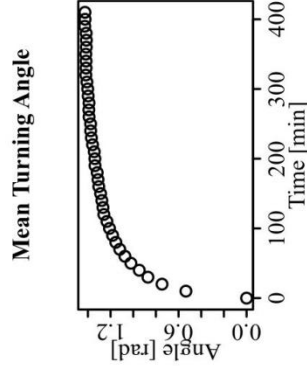
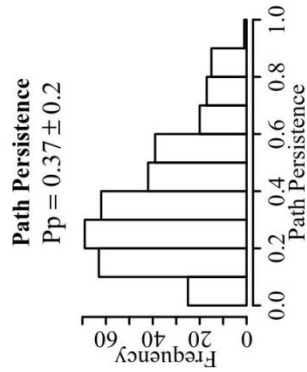
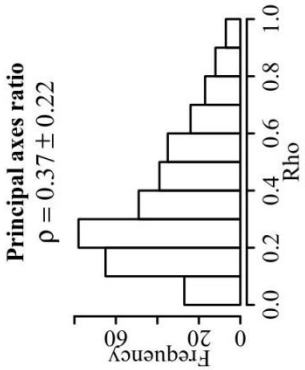
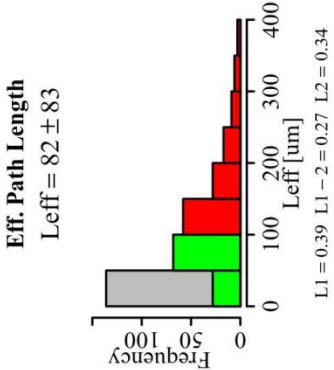
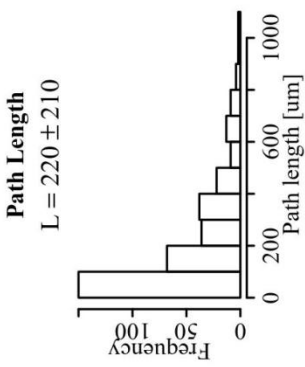
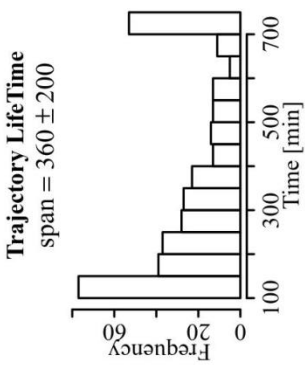
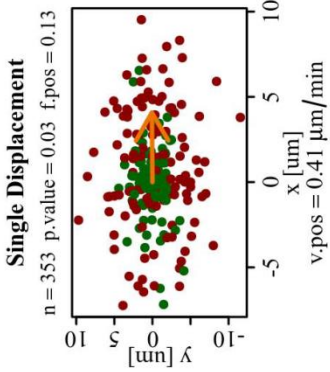
7.5% FBS



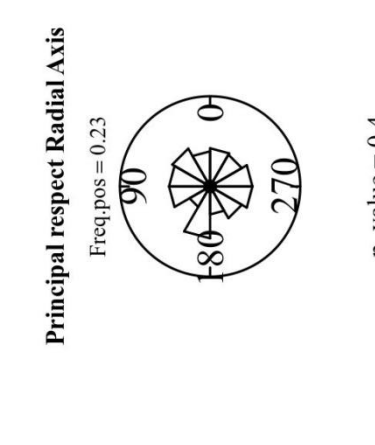
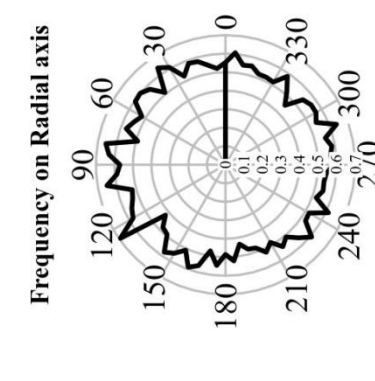
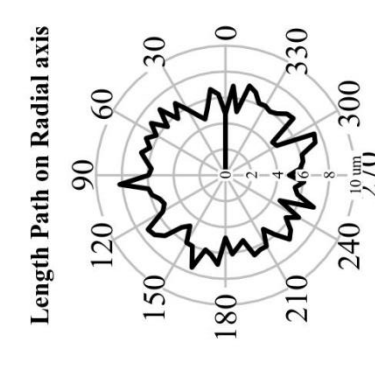
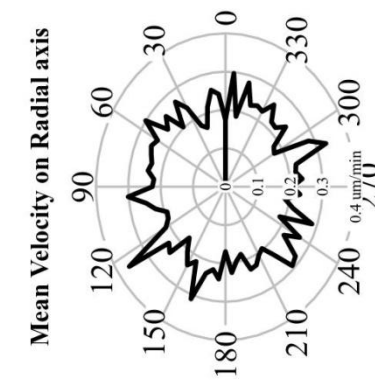
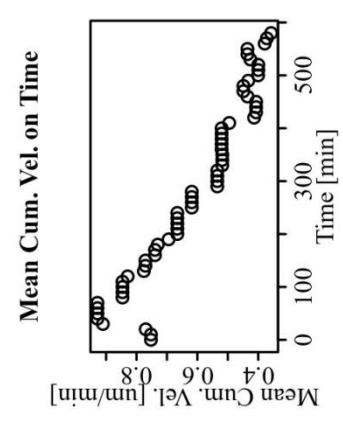
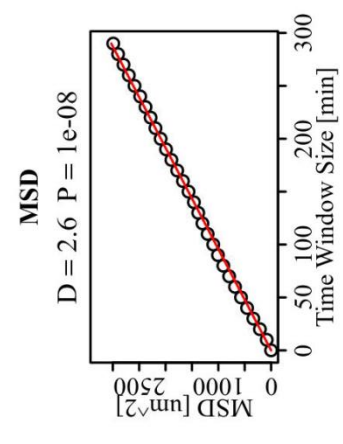
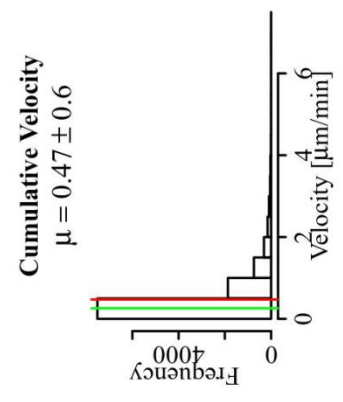
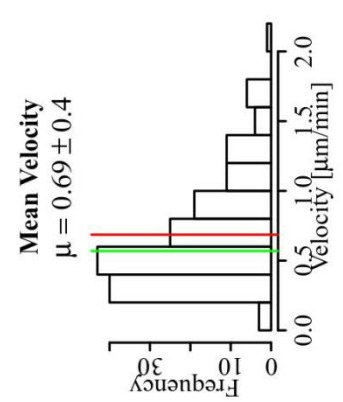
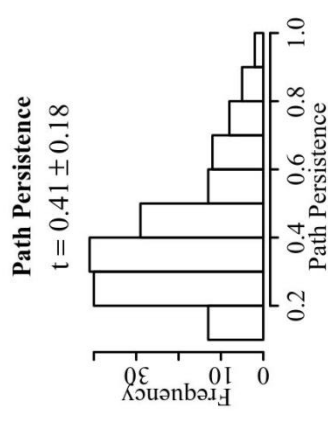
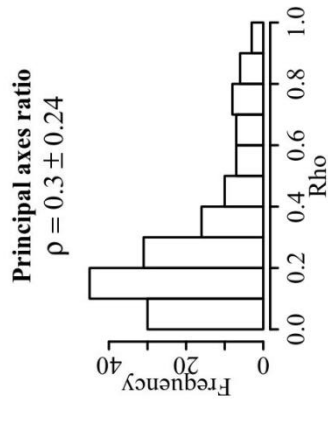
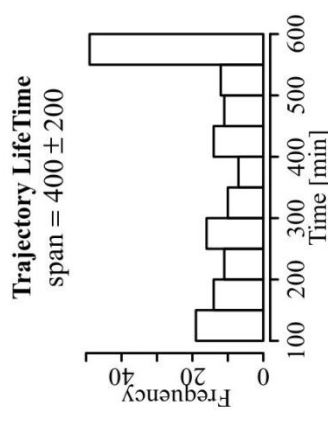
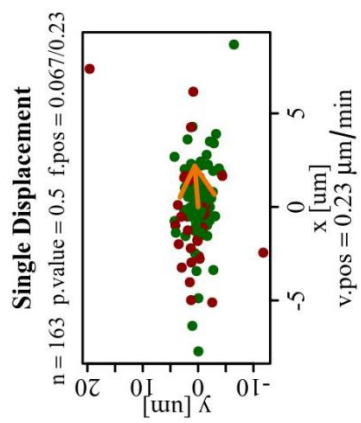
10% FBS



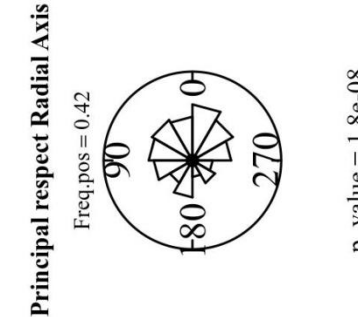
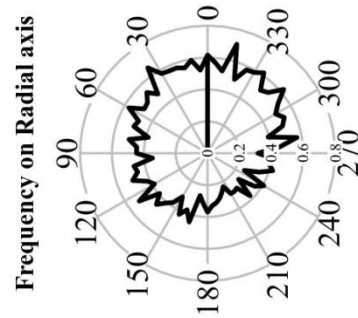
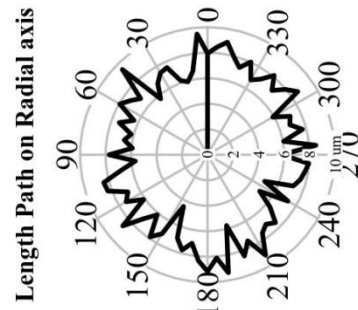
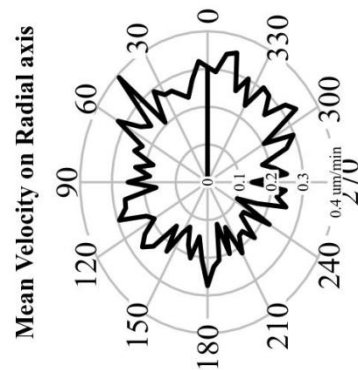
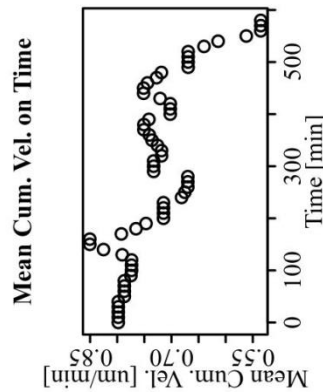
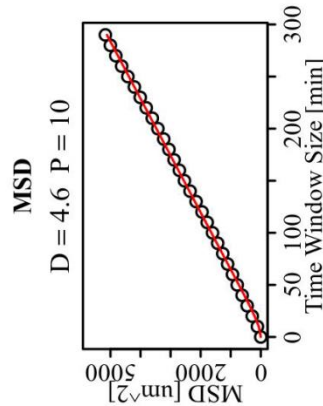
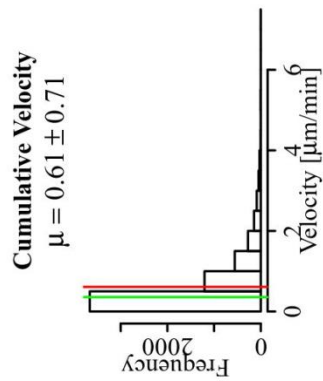
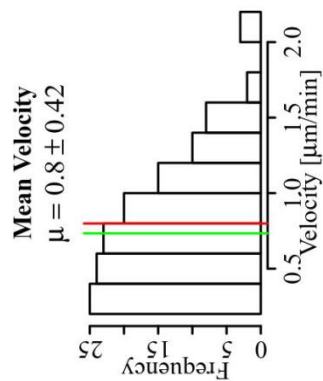
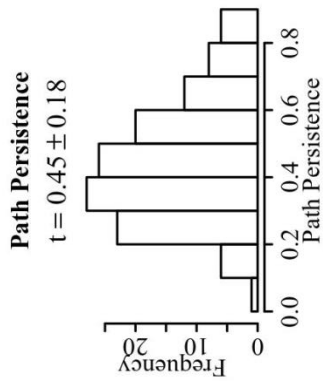
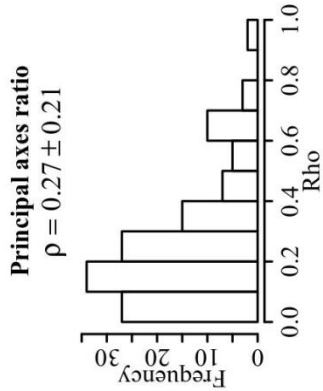
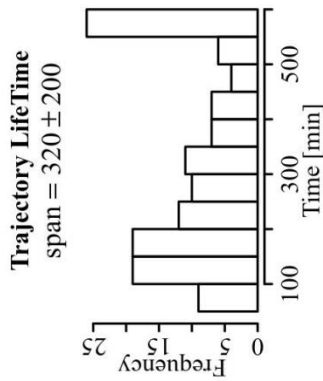
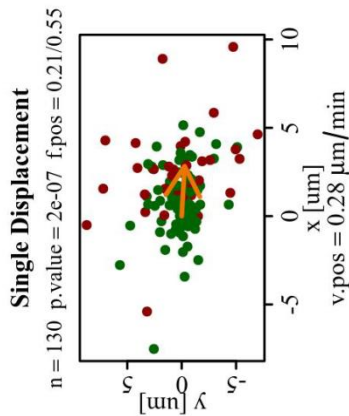
20% FBS



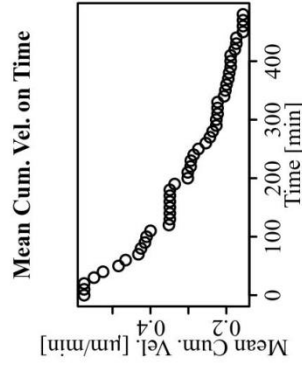
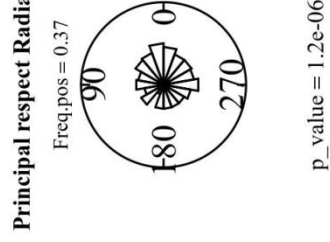
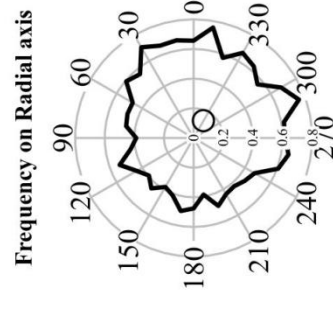
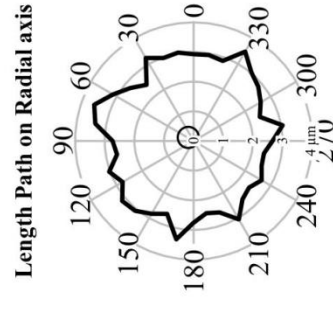
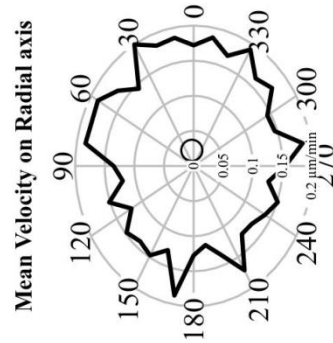
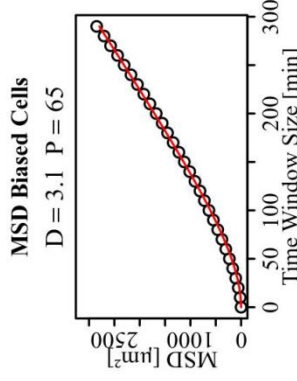
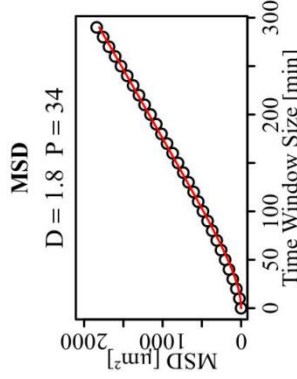
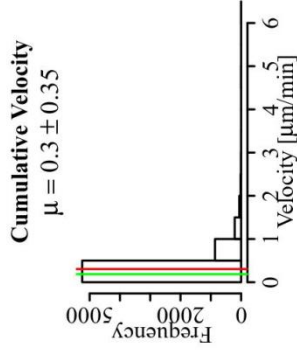
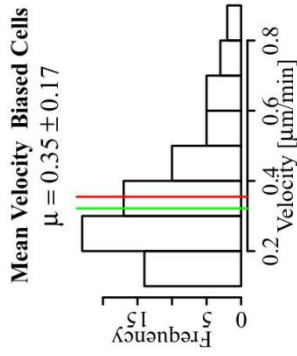
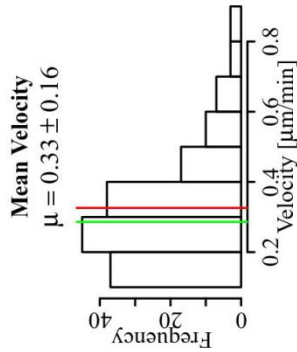
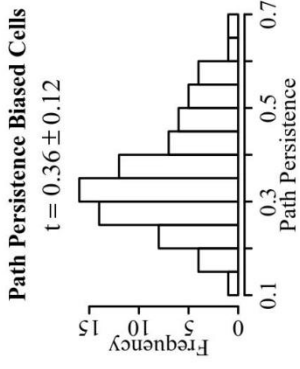
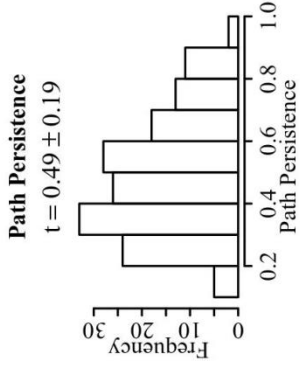
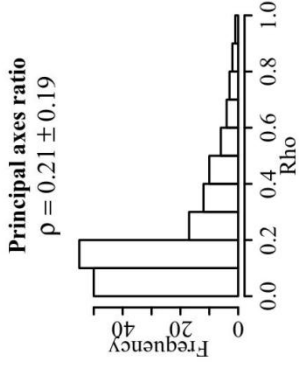
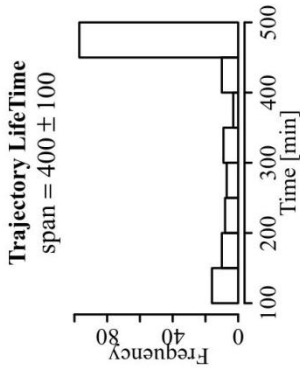
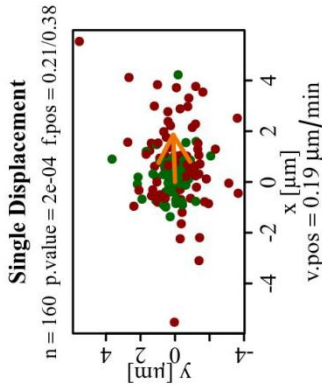
CMcaf



CMcaf/conc.

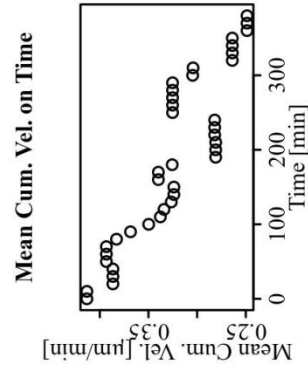
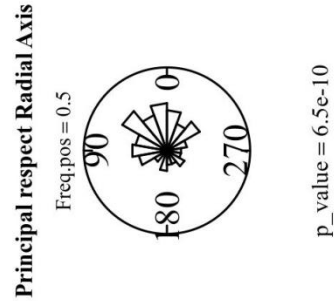
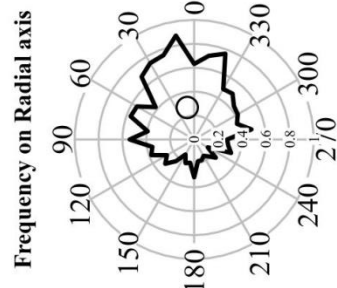
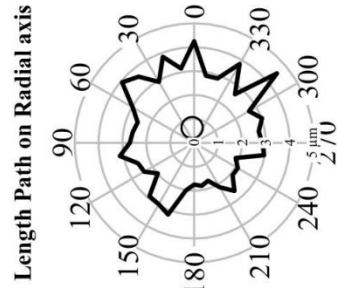
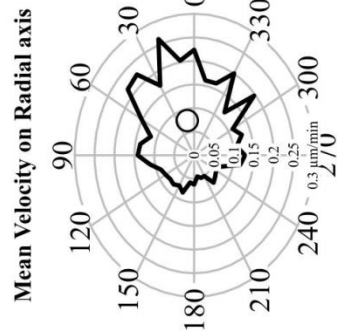
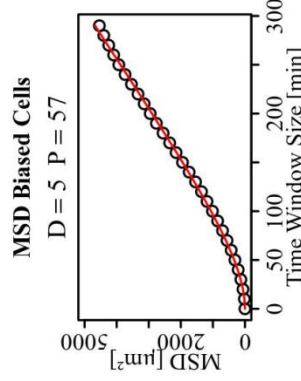
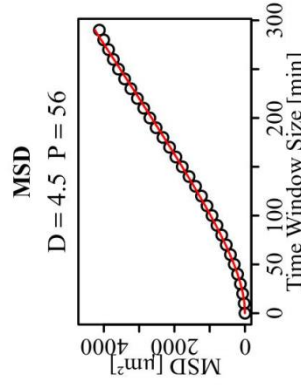
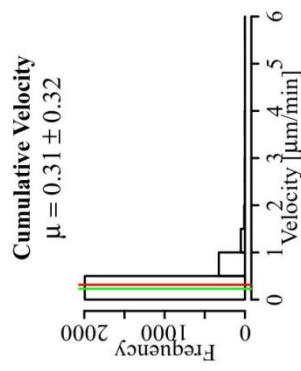
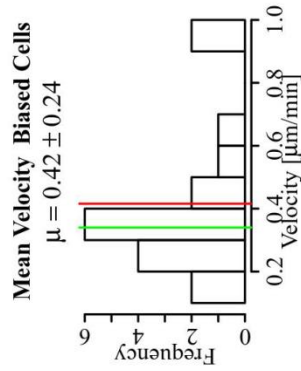
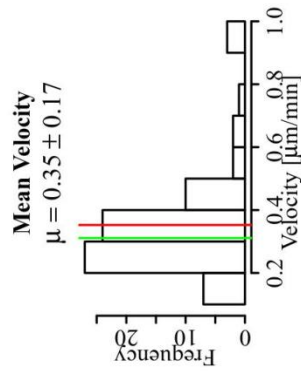
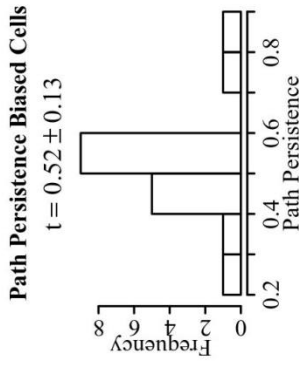
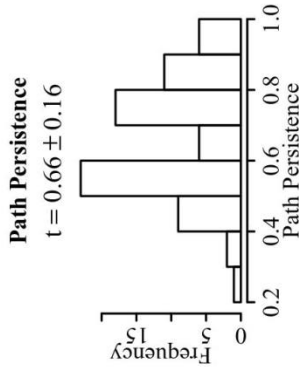
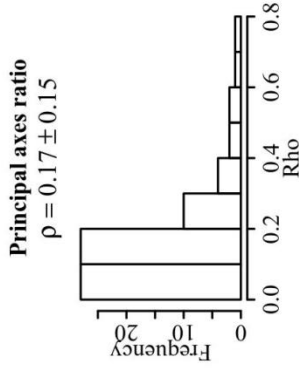
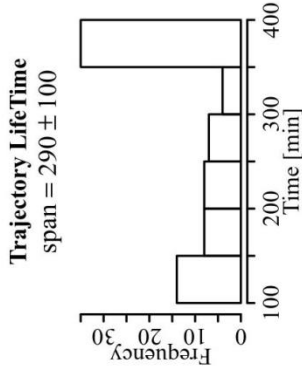
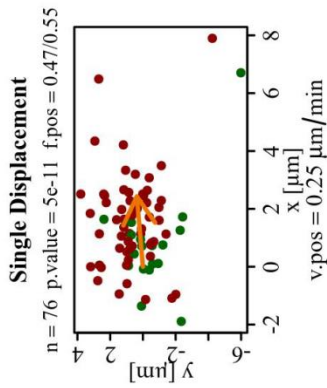


Fibronectin



$p_value = 1.2e-06$

CMhuvec



3. What role do CAFs play in metastasis formation?

Introduction

Metastasis is the last step of tumor progression and occurs when circulating tumor cells anchor, survive and proliferate in secondary organs. The idea that cancer cells do not patrol the circulation alone and are accompanied by the stroma of the primary tumor has recently been suggested (see section 5.3) (Ao et al., 2015b; Duda et al., 2010).

As CAFs have been shown to establish direct heterotypic contacts with cancer cells at the primary site (Labernadie et al., 2017), and in light of the previous section showing that endothelial cells are able to chemoattract fibroblasts, it is tempting to hypothesize that CAFs travel along with cancer cells during metastasis.

In the following section, we tested this hypothesis using an orthotopic mouse model. By implanting cancer cells either alone or together with CAFs in the colon wall of mice, we generated colorectal tumors, followed their growth, and tested their ability to metastasize to the liver and to bring along their microenvironment.

Method establishment

In order to establish a colon cancer model, we optimized an orthotopic injection of cancer cells in the colon wall of mice using an endoscope. This method, although challenging, presents many advantages: implanting cancer cells into the colon wall will provide them the right microenvironment to grow, invade and metastasize. Moreover, the use of human cells allows us to track the origin of cells if they metastasize, specifically we will be able to discriminate if CAFs in the secondary organ are coming from the primary tumor. However, this also imposes the use of immunocompromised mice meaning that our model does not fully take into account the impact of the immune system in tumor progression.

As CT26 cancer cells are very aggressive, we resorted to the use of HT29 or HCT116 human colon cancer cells, which are less invasive. This choice was made in order to allow time for the cells to give rise to tumors that will not grow too fast and kill the mouse by intestinal occlusion before invasion and metastasis has time to occur. By varying the number and ratio of cancer cells and fibroblasts, we first determined the optimal number of cells (see section 3.2 of materials and methods) and the optimal timeframe for mice to develop metastases (Figure III.3.1).



Figure III.3.1. Left: Tumor growth was followed weekly by colonoscopy starting 2 weeks post-injection and all mice were sacrificed at week 6. Right: In some cases, macrometastases were found in the livers.

Using the endoscope, we followed tumor development weekly. Tumors usually appeared two weeks post-injection (Figure III.3.1). For most of the mice, tumors obstructed more than 50% of the colon lumen at week 6 and this time point was subsequently chosen to sacrifice all mice (Figure III.3.1). While HCT116 cancer cells metastasized to the liver, none of the mice injected with HT29 showed apparent metastases (Figure III.3.1). This result indicates that the tested cell lines could be used to answer two questions: do fibroblasts increase metastases formation of already metastatic cancer cells? Can fibroblasts induce metastases of non-invasive cancer cells? The latter question will be addressed in the following section.

Results

How do fibroblasts affect tumor development at the primary site?

For this part of the study, CAFs and NAFs were isolated and characterized as described in section III.1 from two different patients. While couple 5 showed the expected overexpression of α SMA and FAP in CAFs compared to NAFs, this was not the case for couple 4 where CAFs and NAFs expressed similar amounts of both markers (Figure III.3.2). Furthermore, NAF4 contracted collagen gels more than CAF4 (Figure III.3.2), indicating that in this particular couple, NAFs might be more pro-invasive than CAFs.

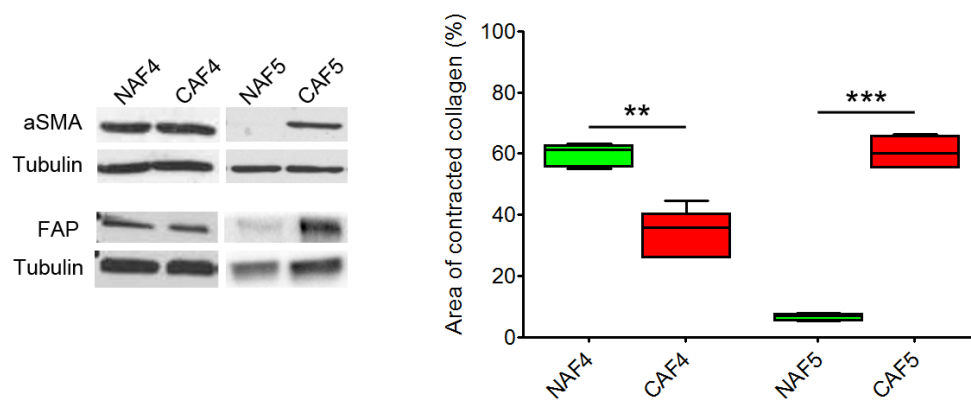


Figure III.3.2. Left: Immunoblot analysis. Lysates prepared from NAFs and CAFs were probed against integrin α SMA and FAP antibodies. α -tubulin served as a loading control. Right: Percentage of gel contraction of NAFs and CAFs from patients 4 and 5 calculated using the formula $100 \times (\text{gel area (T0)} - \text{gel area (T1)}) / \text{gel area (T0)}$. Quantification results are expressed as box and whiskers (minimum to maximum). p value is calculated using a paired t test for $n=3$ over $N=6$ separate experiments.

Orthotopic injection of HT29 cancer cells alone or together with fibroblasts from couples 4 or 5 showed that mice from all conditions developed tumors at a similar frequency (Figure III.3.3.). When mice were sacrificed, the measured size and the aggressiveness of primary tumors were assessed. Although tumors deriving from the co-injection of cancer cells and fibroblasts were slightly bigger than the ones arising from cancer cells, those differences were not significant (Figure III.3.3.). This result suggests that fibroblasts do not impact tumor growth *in vivo* at the primary site. In addition, histological examination revealed that all tumors, even those made without injected fibroblasts, were invasive. Tumors were enriched in stroma and cancer cells infiltrated the mucosa, the muscle layer and the serosa of the colon (Figure III.3.4.). This

suggests that cancer cells have the capacity to create their own activated microenvironment as shown by the enrichment in stroma in histological sections.

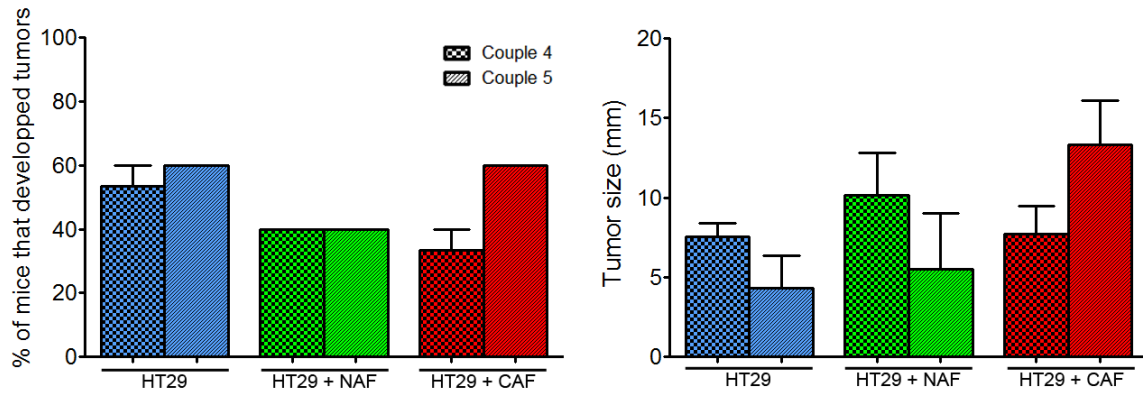


Figure III.3.3. Left: Histogram representing the % of mice that developed tumors when injected with HT29 cancer cells alone or together with NAFs or CAFs from patients 4 and 5. Right: Histogram representing the tumor size developed by mice injected HT29 cancer cells alone or together with NAFs or CAFs from patients 4 and 5.

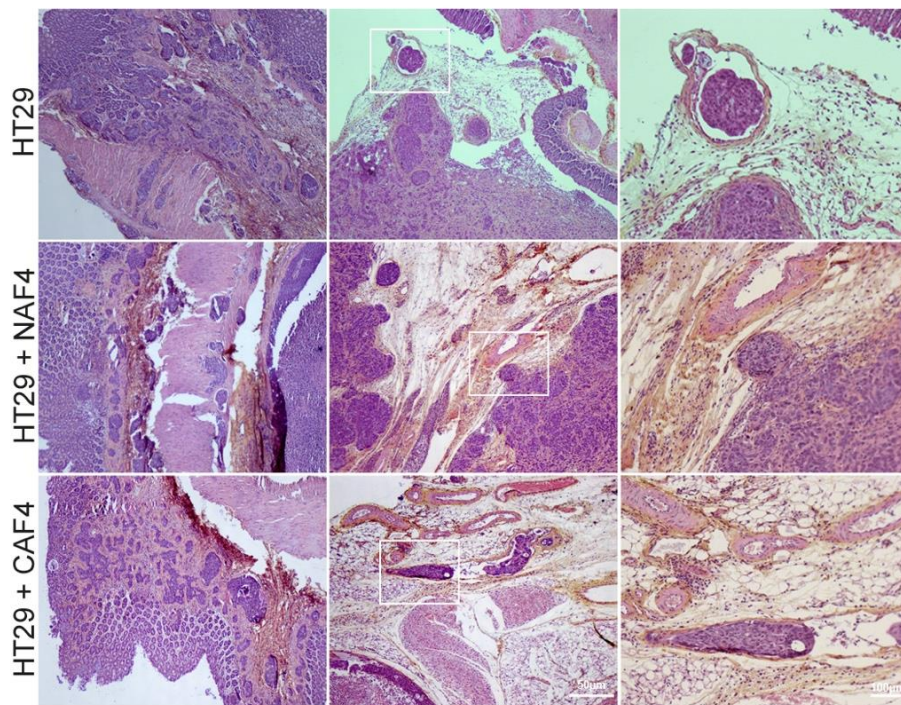


Figure III.3.4. Representative images of tumor sections stained for hematoxylin and eosin from mice injected with HT29 cancer cells alone or together with NAFs or CAFs from patient 4. Left: mucosa and muscle layer. Middle: serosa. Scale bar = 100µm. Right: High magnification of serosa. Scale bar = 50µm

Can fibroblasts induce metastases of non-invasive cancer cells?

Although fibroblasts had no apparent impact on primary tumor development, we evaluated the capacity of cancer cells to metastasize with or without fibroblasts. As already described, HT29 do not form liver macro metastases 6 weeks post-injection. However, q-RT-PCR analyses of livers revealed the presence of human RNA in all groups of mice, indicating that in all cases, cancer cells were able to infiltrate the blood vessels and anchor in secondary organs, although at a slightly higher rate in the presence of NAF4 (Figure III.3.5). However, macro metastases was only detected in mice co-injected with NAF4 and cancer cells (Figure III.3.5) indicating that only in the presence of fibroblasts cancer cells were able to proliferate and colonize secondary organs. Immunofluorescence staining of liver slices showed the presence of vimentin positive cells along with human cancer cells (Figure III.3.5), which suggests that fibroblasts might be accompanying cancer cells to secondary organs, helping them survive and proliferate.

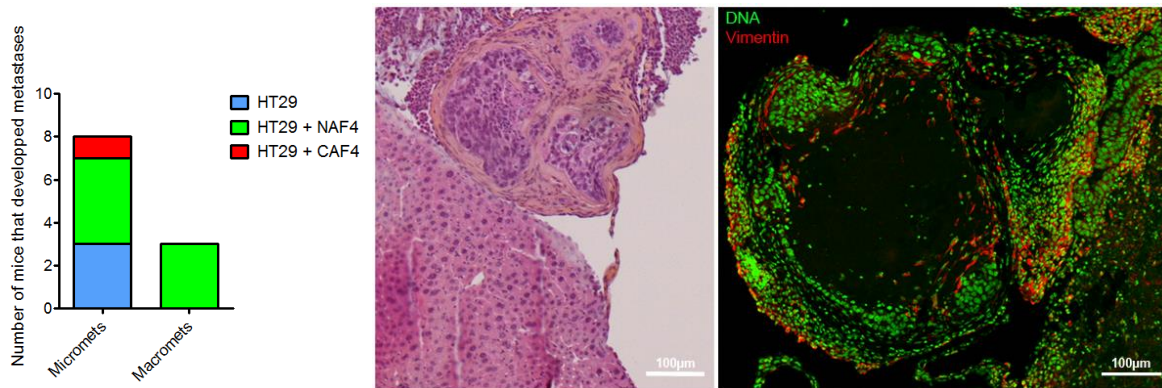


Figure III.3.5. Left: Histogram representing the number of mice that developed either macro or micrometastases when injected with cancer cells alone or together with NAFs or CAFs from patient 4. Right: Representative images of liver sections harboring metastases stained for hematoxylin and eosin (middle) or co-stained with DAPI (green) and vimentin (red). Scale bar = 100µm.

Conclusion and perspectives

The “seed and soil” hypothesis suggests that metastasis is not a random process, and that according to the nature of the seed, cancer cells preferentially anchor at a defined soil. The idea that cancer cells bring along their microenvironment to secondary niches has been recently suggested (Ao et al., 2015b; Duda et al., 2010) (ref).

In this study, we show that HT29 cancer cells are able to reach the liver independently of the presence of fibroblasts at the primary site. However, only when co-injected with activated fibroblasts, cancer cells have the capacity to proliferate in the liver and form macro metastases. As histological sections of these livers reveal the presence of vimentin positive cells in close proximity with cancer cells, this suggests that fibroblasts could possibly travel alongside cancer cells and help their survival and proliferation in the secondary niche.

Additional experiments still need to be done in order to test this possibility. Specifically, we will test if the vimentin positive cells detected in metastatic livers are of human or mouse origin. Preliminary q-RT-PCR analyses using a promoter for the human Acta2 gene (coding for α SMA) were negative. However, it is possible that the method is not sensitive enough to detect a low number of cells. To overcome this, we can stain histological sections with a human specific antibody and correlate its presence in CAFs. Alternatively, we will repeat injections using fluorescently labeled fibroblasts that will allow easier tracking. In addition, it would be interesting to extract the blood of the mice and investigate the presence of circulating tumor cells possibly accompanied by CAFs. Finally, to test if CAFs are indeed necessary at the secondary site to help cancer cells survive, we could inject fibroblasts in the liver and cancer cells in the colon wall. In this scenario, HT29 that reach the liver should have no problem establishing macro metastasis.

IV. Discussion

Metastasis is a process that is achieved by the capacity of cancer cells to navigate, survive and find their way through different environments, from the tumor of origin, to secondary organs. During, each step, cancer cells work together with stromal cells and this crosstalk can be favorable for the accomplishment of metastasis. CAFs are an enriched cell population of the tumor microenvironment. They are the only cells capable of influencing tumor invasion using 3 mechanisms: direct contact (Labernadie et al., 2017), secretome crosstalk (De Wever et al., 2004; Orimo et al., 2005), and ECM remodeling (Calvo et al., 2013; Gaggioli et al., 2007).

However, CAFs remain a big question mark in the field of cancer, because of the absence of a marker to identify them and their unknown origin. Indeed, the term “CAF” is generically used for any spindle-shaped cell of the tumor microenvironment that expresses the mesenchymal marker vimentin and is enriched in α SMA, FAP and/or PDGFR β , all markers of smooth muscle and mesenchymal cells. Because of that, it is difficult to study their functions in mice and thus impossible to specifically target CAFs *in vivo* and it is. Therefore, most studies have resorted to *in vitro* co-cultures of CAFs and cancer cells in order to evaluate their effect on each other. More recently, with the advances made in the field of imaging, 3D cultures of CAFs, cancer cells and the ECM are also very commonly used.

My PhD aims to further understand this complex 3-way crosstalk in the context of colorectal carcinoma. In this perspective, we used a 3D model consisting of embedding cancer cell spheroids together with CAFs in a collagen I matrix, a scenario that closely mimics the *in vivo* invasion of the stroma, following breaching of the basement membrane. At this step, cancer cells are believed to have undergone epithelial-to-mesenchymal transition (EMT) (Thiery, 2002) where E-cadherin is down-regulated at the expense of N-cadherin expression. In agreement with this notion, we have chosen to use invasive mouse CT26 cancer cells in our model. CAFs were isolated from the colon of patients of varying carcinoma stages. To date, normal adult fibroblasts have never been isolated and kept in their primary non-immortalized state. Many studies have used immortalized fibroblasts or mouse embryonic fibroblasts (MEFs) which, at the stage of development, are highly proliferative. However, normal fibroblasts in a developed colon have

low proliferation status (Otranto et al., 2012; Tomasek et al., 2002), thus immortalized fibroblasts or MEFs are poor mimics of normal fibroblasts. In this project, as a control, we isolated non-cancer-associated fibroblasts (NAFs) from the seemingly healthy, “normal” tissue surrounding the tumor. Moreover, all fibroblast populations were used as non-transformed and cultured at 30KPa stiff dishes in order to avoid mechanical activation. However, as NAFs were proliferative even after many passages in culture, they also cannot be referred to as “normal” fibroblasts. NAFs did also induce a slight increase in cancer cell invasion, although not to the same extent as CAFs. Finally, our WB analysis shows that NAFs express all markers of activated fibroblasts, sometimes more than CAFs, pointing again to their activated state. Yet, as the expression of α SMA, FAP and PDGFR β did not correlate with the amount CAF-mediated cancer cell invasion, one could argue that these proteins should not be referred to as CAF markers, but rather fibroblast markers. In any case, it is interesting that a tissue described as healthy and cancer-free by pathologists still harbored a stroma enriched in activated fibroblasts. These data suggest that by widening the margins of the surgical resection, patient relapse could be avoided. It would be interesting to correlate incidence of relapse with the status of NAFs post-surgery and thus use the state of fibroblasts as a predictive marker.

Our next question was to compare the effect of CAFs’ secretome to their presence in the matrix on cancer cell invasion. It has already been shown that CAFs’ contractility is necessary to generate tracks in the matrix that would drive collective invasion of tumor cells (Calvo et al., 2013; Gaggioli et al., 2007). However, these studies were performed on cancer cells that had retained an epithelial phenotype and could not invade in an autonomous manner. According to this, prediction would be that once cancer cells undergo EMT and become independently invasive, they would not need CAFs to remodel the matrix. A secretome crosstalk between two cell populations could be sufficient to boost cancer cell invasion. However, we found that diffusible molecules secreted by CAFs were not sufficient to significantly increase invasion of CT26 cancer cells. Instead, the presence of CAFs within the matrix was necessary. A recent study has shown that CAFs and cancer cells establish direct heterotypic contacts which are necessary for cancer invasion of the stroma (Labernadie et al., 2017). However, in our study, both cell populations express the same Cadherins, making the establishment of heterotypic contacts impossible. However, our time-lapse analysis showed that CAFs remodel the matrix,

suggesting that the ECM plays a mediator role between CAFs and cancer cells, as already shown in the E. Sahai's lab (Calvo et al., 2013; Gaggioli et al., 2007).

Still, these results are surprising as the contractility of CAF and NAF populations failed to closely correlate with the level of invasion induced by these fibroblast populations. Thus, it seems that contractility of the matrix is not the only factor that drives cancer cell invasion. Indeed, depletion of FN in all CAF populations also abrogated their capacity to promote cancer cell invasion. The link between contractility and FN matrix assembly had already been described (Zaidel-Bar et al., 2007b); together with our SILAC analysis showing overexpression of FN in the secretome and proteome of CAFs compared to their paired NAFs, our data show that fibroblast-secreted FN is a key protein that stimulate cancer cell invasion. FN assembly by CAFs and NAFs correlated with their capacity to induce cancer cell invasion, thus highlighting FN matrix assembly as a new hallmark of CAFs. This result is in agreement with a new study where the analysis of FN expression in tumors from 435 head and neck cancer patients revealed an inverse correlation between high levels of FN and patient prognosis (Gopal et al., 2017). One question our study fails to explain though is the drastic reduction of cancer cell invasion in the presence of FN-depleted CAFs, even though the experiments are performed in the presence of serum which contains high levels of soluble FN. Moreover, supplementing the media with additional soluble FN also fails to stimulate invasion. However, there is a fundamental difference between plasma FN present in the serum and cellular FN (see section 4.1.2 of introduction). Gopal et al., also suggest that only cellular FN can induce cancer cell migration on CAF-derived matrices, suggesting that the EDA and/or EDB repeats specific of cellular FN might be key factors for FN matrix assembly and in FN-driven cancer cell motility. Alternative hypothesis would be that secreted but not-assembled FN is not sufficient to induce invasion. Indeed, although integrin depleted CAFs failed to assemble FN in the matrix, they could still secrete FN to similar levels as control CAFs. One explanation could be that secreted FN diffuses in the extracellular milieu while assembled FN is more spatially concentrated. Thus, it could be that cancer cells can respond only to a high local concentration of FN. We tested this hypothesis by saturating collagen with high concentrations of FN. In these conditions, cancer cell invasion was significantly enhanced independently of the presence of CAFs and cellular FN, a phenotype that was not recapitulated when the same amounts of TNC or laminin were used (Fig. IV.1).

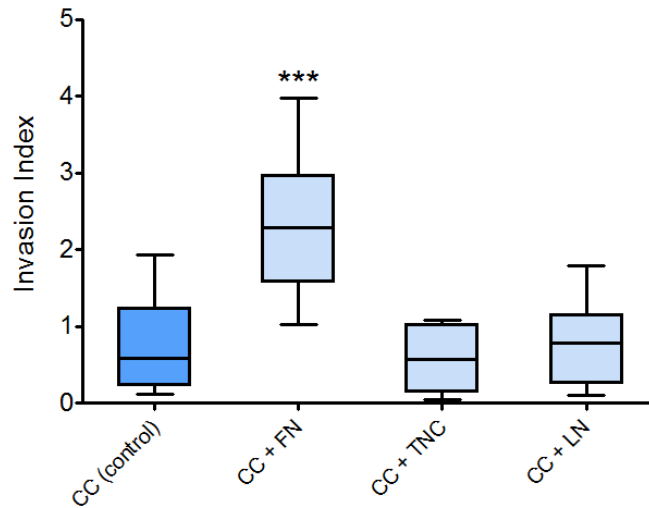


Figure IV.1 Quantification of cancer cell invasion alone or in the presence of collagen pre-mixed with FN, TNC or laminin. Invasion index is defined as the ratio between the number of invading nuclei and the area of the spheroid contour. Quantification results are expressed as box and whiskers (minimum to maximum) of at least N=3 separate experiments. p values are compared to cancer cells alone (in gray) and to cancer cells with CAFs (in black) using Newman-Keuls multiple comparison test (*p<0.05, **p<0.01, ***p<0.001).

It is therefore tempting to hypothesize that tumor invasion of the stroma, at its initial steps, depends on local FN matrix assembly, a process mainly mediated by CAFs due of their high contractility. As the tumor progresses, soluble FN in the extracellular milieu could get gradually concentrated to a point where assembled FN, and even cellular FN would not be necessary anymore. This could, for example, be a way for cancer cells to find their way to the circulation, as the blood vessels which are a reservoir of plasma FN, become more and more leaky in a tumor. Indeed, chemotaxis experiments using Dunn's chamber indicate that highly concentrated plasma FN is sufficient to drive directed cancer cell migration.

Matrix remodeling also encompasses degradation, a process that has already been described in the context of tumor invasion and that is mainly dependent on the membrane-bound matrix metalloprotease MT1-MMP (Castro-Castro et al., 2016; Hotary et al., 2006; Hotary et al., 2003; Poincloux et al., 2009; Wolf et al., 2013). When plated on a native basement membrane, cancer cell invasion was shown to be exclusively dependent on MT1-MMP (Hotary et al., 2006). However, the presence of CAFs in the stroma could widen the pores of the basement membrane

and allow cancer cells to pass through in a degradation independent manner (Glentis et al., *in revision*). In the context of stromal invasion where the ECM is made of wider and more deformable pores, it had been initially shown that MT1-MMP was also the main protease required for cancer cell invasion (Hotary et al., 2003). This idea was challenged later on when a study in the lab of P. Friedl showed that cancer cell invasion could also be degradation and MT1-MMP independent due to the capacity of cells to squeeze through matrix pores (Wolf et al., 2003a). It was finally demonstrated that the nature and polymerizing conditions of collagen define the invasion mode of cancer cells (Wolf et al., 2013). Briefly, it is only in non-crosslinked collagen gels or in crosslinked gels below a concentration of 1.7mg/mL that cancer cells could invade independently of MMPs. However, when crosslinked rat-tail collagen was used at 2mg/mL, cancer cells relied on MT1-MMP to invade, similarly to our data. Nevertheless, whether CAFs can drive MMP-independent cancer cell invasion of the ECM has never been shown. Indeed, our data show that in the presence of broad MMP inhibitors, CAFs can still drive cancer cell invasion even though the autonomous invasion of cancer cells is inhibited. One could argue however that MMPs are not the only proteins involved in matrix degradation. Studies have shown that the urokinase plasminogen activator receptor-associated protein (uPAR) could be also involved in matrix cleavage (Wolf and Friedl, 2011). It would be thus interesting to confirm our phenotype in CAFs by blocking the action of these other proteases as well as the membrane-bound protease FAP. Our data indicate that cancer cells can bypass necessity for matrix degradation in the presence of CAFs, probably because of the capacity of fibroblasts to contract the ECM, align collagen fibers and generate “highways” that cancer cells could migrate on. Thus, it seems that degradation and contractility and subsequent matrix assembly are two independent processes in CAFs, as opposed to what has been suggested in cancer cells (Aung et al., 2014). This idea is reinforced by the fact that the co-inhibition of MMPs and FN in CAFs shows a cumulative effect and completely blocks invasion. These data are in agreement with studies showing that cancer cells cannot autonomously invade the ECM (in the conditions at which we polymerize collagen) in the presence of MMP inhibitors and this invasion cannot be rescued by CAFs depleted of FN. It does seem surprising though that the alignment of collagen fibers by FN-depleted CAFs would not be sufficient for cancer cells to migrate as it has been shown that aligned collagen fibers favor cell migration (Riching et al., 2014). However, it is likely that at long-term, CAFs stimulate tumor invasion exclusively by mechanical remodeling. It

is also possible that at longer time points, contractility of FN-depleted CAFs is impaired as the positive feedback loop in which CAFs pull on FN matrices is compromised (Ao et al., 2015a). From a clinical point of view, it would be interesting to target MMPs together with FN assembly, the latter being done by using cilengitide for example. Interestingly, these two drugs have failed in clinics, but coupled together, could slow down tumor development and improve patient's survival. As a continuation of this project, it would be interesting to test this hypothesis using transgenic mice. For example, using the transgenic mice in our lab which consist of conditionally activating the Notch1 receptor and deleting p53 in the digestive epithelium (NICD/p53(-/-)), we could induce tumor formation by tamoxifen injection. The appearance of a tumor could then be detected by using a fluorescent probe for *in vivo* targeting of tumors that typically exhibit elevated glucose uptake; at which point we could start treating mice with cilengitide and MMP inhibitors, either alone or together. In addition, using our orthotopic mouse model, we could track the dissemination of cancer cells and CAFs in the circulation and their eventual metastasis in the presence of drugs targeting MMPs and $\alpha v\beta 3$ either alone or together.

As FN assembly appeared to be the main path used by CAFs to stimulate tumor invasion of the ECM, the next question was to understand how CAFs assemble FN. The main receptors involved in this process are integrins, cell-matrix adhesion proteins (see sections 2.2 and 4.1.2 of the introduction). The involvement of both $\alpha 5\beta 1$ and $\alpha v\beta 3$ integrins in FN matrix assembly has been reported in many studies (Danen et al., 2002; Pankov et al., 2000; Rossier et al., 2012; Schiller et al., 2013). It is not clear though what differentiates the functions of $\alpha 5\beta 1$ and αv class integrins. Our results indicate that silencing $\beta 3$ integrin or blocking the activity of $\alpha v\beta 3$ significantly reduces FN matrix assembly by CAFs, immediately after plating cells or in an established cell monolayer. $\alpha 5$ depletion, however, only impairs sustained assembly of fibers. These results indicate that integrin $\alpha v\beta 3$ initiates the process of FN assembly before $\alpha 5\beta 1$. This observation is reinforced by the cellular localization of both integrins: while $\alpha v\beta 3$ accumulated at the site of peripheral focal adhesions, $\alpha 5$ was located in the cell center in fibrillar adhesions that form later on during cell spreading (Rossier et al., 2012) (see section 2.1.2 of the introduction). However, FN did not localize at the site of nascent adhesions, even very early on during cell spreading. This result challenges the involvement of $\alpha v\beta 3$ in FN matrix assembly and raise a possibility that $\alpha v\beta 3$ is indirectly involved in FN assembly. As already discussed, cells need to contract the matrix in order to assemble FN (Zaidel-Bar et al., 2007b), but blocking of $\alpha v\beta 3$ in CAFs did not

abrogate their capacity to contract collagen plugs. Alternatively, $\alpha\text{v}\beta\text{3}$ could be involved in mediating the signal, from contractility, to FN assembly of the matrix. In other words, $\alpha\text{v}\beta\text{3}$ could act as a sensor at the cell periphery and signal to the cell center to trigger FN assembly. This hypothesis is supported by a study performed on vascular smooth muscle cells using a device which consists of culturing cells with beads coated with an ECM protein or an antibody directed against an integrin receptor, and exposing those beads to a magnetic field (Wang et al., 1993). The response to these mechanical stimuli is assessed by the activity of the mitogen ERK 1/2^{MAPK} (Goldschmidt et al., 2001). When beads were coated with β3 integrin-receptor antibody, a significant increase in phosphorylated ERK was observed, which was not the case when the experiment was performed with α2 or β1 antibody-coated beads. Similarly, Wilson et al showed that blockade of integrin β3 , and not β1 , abrogated DNA synthesis induced by mechanical strain in vascular smooth muscle cells (Wilson et al., 1995). These results indicate that β3 , but not β1 integrin, function as the principal mechanosensor in vascular smooth muscle cells. It has also been shown that in cells plated on RGD rich substrates, $\alpha\text{v}\beta\text{3}$ localizes at focal contacts and is responsible for force dependent focal adhesion maturation (Changede et al., 2015; Roca-Cusachs et al., 2013a; von Wichert et al., 2003). A study in the lab of M. Sheetz shows that α -actinin and talin compete in binding of the cytoplasmic tail of β3 integrin, but cooperate in binding to integrin β1 (Roca-Cusachs et al., 2013a). While talin localized with α -actinin and β3 at the site of nascent focal adhesions, replacement of talin with α -actinin is necessary for adhesion maturation and mechanosensing. Integrin β1 however is only detected later, at the site of fibrillar adhesions (Roca-Cusachs et al., 2013a). These studies are in line with our experiments where blocking of integrin $\alpha\text{v}\beta\text{3}$ impaired α5 localization to the cell center and fibrillar adhesion formation. Interestingly, although depletion of α -actinin prevented adhesion maturation, force generation in initial adhesions was enhanced indicating that the contractile capacity of cells was not impaired, but rather their capacity to assimilate and respond to mechanical stimuli (Roca-Cusachs et al., 2013a).

One conflicting issue in our model is the choice of the matrix. Collagen is not an RGD substrate and should not trigger $\alpha\text{v}\beta\text{3}$ localization to the cell periphery. However, in our assay, cells are constantly exposed to RGD motifs because of the presence of serum, or alternatively, of cellular FN secreted by the cells themselves. Adding fluorescently-labelled soluble FN on collagen

reveals that FN can stick to collagen fibers, indicating that our ECM is enriched in RGD peptides (Fig. IV.2).

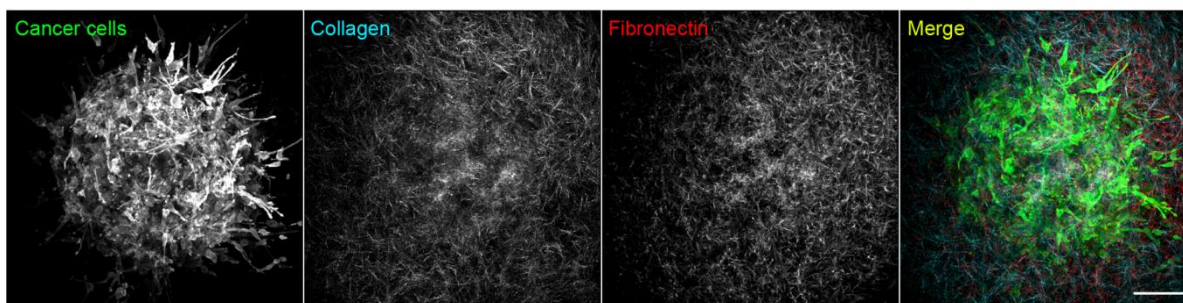


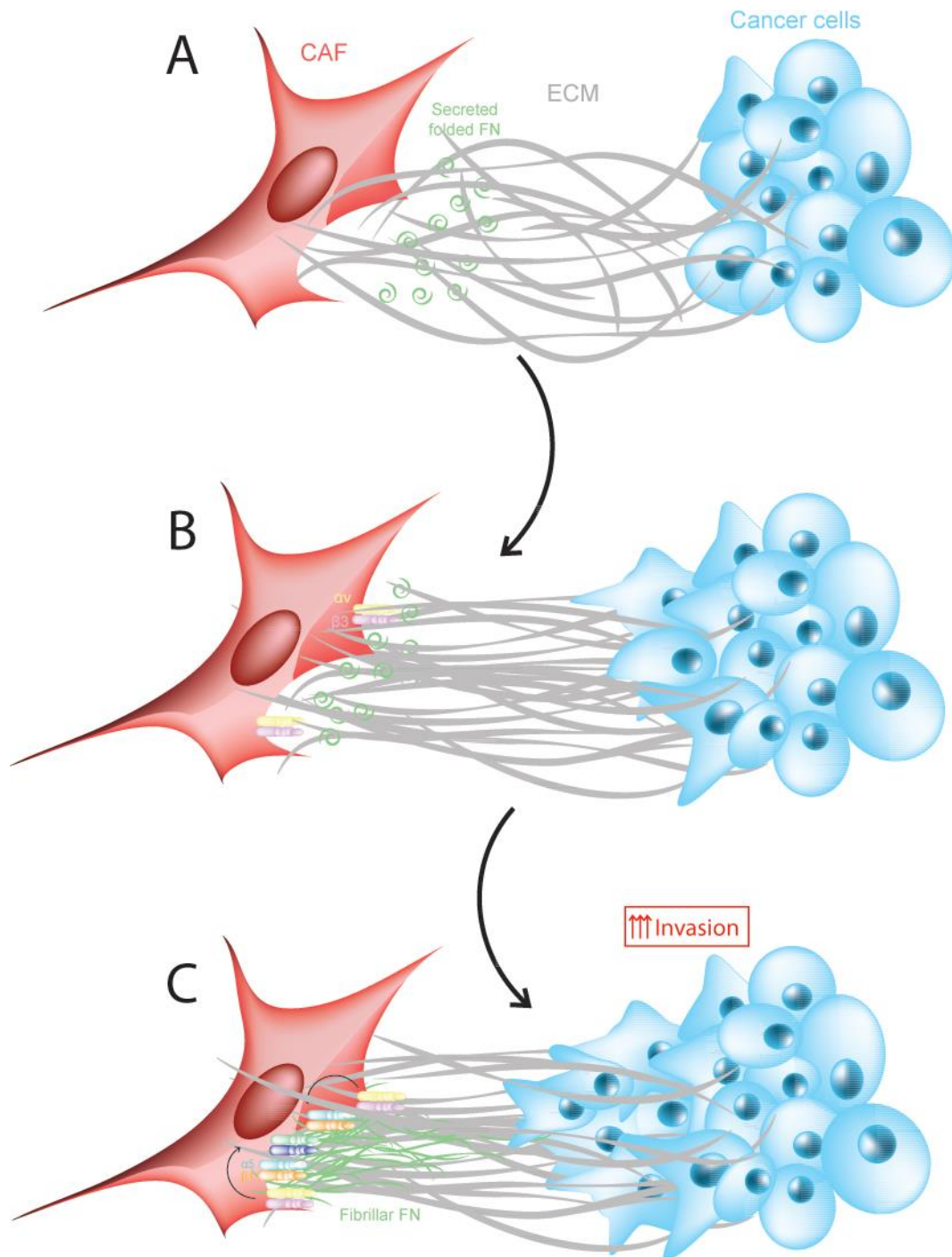
Figure IV.2. Maximum intensity projections of cancer cell spheroids in collagen I supplemented with soluble fluorescently-labelled FN. CT26 cancer cells express LifeAct-GFP (green), collagen is acquired using reflection (cyan) and FN is labelled with rhodamin (red). Scale bar = 100 μ m.

Thus, it could be that through a positive feedback loop, CAFs secrete their own FN and trigger re-localization and activation of $\alpha\beta$ 3 heterodimers at the cell periphery. Another study has also shown that $\alpha\beta$ 3 can localize to the cell's edge upon stimulation by growth factors such as FGF (Kiosses et al., 2001). In the context of a tumor where FN and growth factors are constantly released from CAFs, blood vessels or cancer cells themselves, the nature of the matrix would not really matter as it is constantly enriched in RGD peptides. Matrix contractility, however, is an important requirement as focal adhesions need to form in order for $\alpha\beta$ 3 heterodimers to gather at these sites. Indeed, studies have shown that β 3 integrins specifically accumulate at areas of high traction force and are stationary within focal adhesions while β 1 integrins are more mobile (Rossier et al., 2012; Schiller et al., 2013). Inhibition of myosin with blebbistatin disassembles β 3 clusters without affecting levels and localization of β 1 integrin (Schiller et al., 2013). This agrees with our experiments as treatment of CAFs with blebbistatin abrogates FN assembly. Another issue addressed in our study is the assembly of FN independently of integrin α 5 β 1. Indeed, depletion of α 5 β 1 becomes critical only at later stages of FN assembly. One hypothesis is that other integrin heterodimers, such as α 4 β 1 or α IIb β 3 could sustain initial FN assembly in the absence of α 5 β 1. A triple depletion of α 5, α 4 and β 3 would therefore be necessary to validate this hypothesis.

Another interesting perspective of our study is the effect of cilengitide on CAF-mediated cancer cell invasion. Clinically, the use of cilengitide showed no improvement in overall patients' survival in clinical trials (Lombardi et al., 2017). However, as previously discussed, it might be that cilengitide alone is not sufficient to inhibit tumor development as it only targets $\beta 3$ and $\beta 5$ expressing cells. Notably, a transcriptomic analysis in our lab on CT26 cancer cells revealed that they do not express integrin $\beta 3$, meaning that these cells would be resistant to cilengitide. A recent study has also shown heterogeneity in $\alpha v\beta 3$ expression in non-small cell lung and small cell lung cancer cells (Kang et al., 2017). Conversely, some drugs only have an effect on cancer cells but have been clinically unsuccessful most likely due to their inability to target the tumor microenvironment. For example, PLX4720 is a drug that specifically targets the mutated proto-oncogene BRAF in melanoma cells. However, it also activates CAFs, increasing their capacity to contract and stiffen the ECM providing a safe niche for cancer cells promoting their survival and proliferation (Hirata et al., 2015). In this scenario, targeting both CAFs and cancer cells could be an interesting strategy. Again, these hypotheses could be tested in an orthotopic mouse model for melanoma, by subcutaneously injecting cancer cells either alone or with CAFs.

In conclusion, our study shows that diffusible molecules secreted by CAFs are not sufficient to induce cancer cell invasion. Instead, CAFs' remodeling of the matrix is the key player. We propose a model where contractility of CAFs is necessary for downstream integrin activation and FN assembly. As the ability of all fibroblast populations to assemble FN directly correlates with their ability to induce cancer cell invasion, we demonstrate that ECM deposition, more specifically FN deposition, is the key component for CAF-mediated cancer cell invasion. Finally, we propose that downstream of contractility, integrin $\beta 3$ acts as a mechano-sensor that stimulates formation of $\alpha 5\beta 1$ enriched fibrillar adhesions where FN matrix assembly is maintained.

Working model



CAFs present in the collagen I-rich tumor stroma secrete FN (A). Contractile forces exerted by CAFs align the ECM and activate $\alpha 5 \beta 3$ at the sites of focal adhesions (B). $\alpha 5 \beta 3$ activation leads to the formation of fibrillar adhesions and FN fibrillogenesis (C).

V. Material and methods

1. Cell Biology

1.1. Cell lines

Mouse intestinal cancer cells CT26, human intestinal cancer cells HT29 and mouse embryonic fibroblasts NIH3T3 were obtained from American Type Culture Collection (ATCC). Cells were cultured in Dulbecco's Modified Eagle Medium (DMEM) (Life Technologies) supplemented with 10% FBS (Invitrogen) and 5% CO₂. CT26 cancer cells were infected with a lentiviral GFP plasmid following standard procedures. HT29 cancer cells were transfected with a GFP plasmid following standard procedures.

1.2. Isolation and culture of primary fibroblasts

Human primary fibroblasts were isolated from fresh colon tumors (CAFs) and adjacent non-carcinoma tissue (NAFs) samples from patients treated at Lariboisière Hospital, Paris, with written consent of the patients and approval of the local ethics committee. Samples were treated as previously described (Amatangelo et al., 2005): briefly, tissues were collected after surgical resection in Roswell Park Memorial Institute buffer (RPMI) and washed in Phosphate Buffered Saline (PBS) supplemented with 10% Antibiotic-Antimycotic (AA) (Gibco). 100mm² tissue culture plates were scratched using a scalpel and tissue pieces of approximately 1 to 2mm² were cut and placed on the junctions (Figure V.1). Following isolation, the tumor pieces were kept in 10mL of DMEM supplemented with 10% FBS (Life Technologies) and 10% AA. 24h later, the medium was changed and AA concentration was reduced to 5%. From this point, medium was changed every 2 days, reducing AA concentration by half every time, until AA concentration reached 1%. Fibroblasts typically started going out of the tissue after 2 to 3 weeks. When having reached confluency, fibroblasts were trypsinized and plated on a 30KPa 30 mm² soft plates (Excellness), previously coated with 5µg/mL of rat tail collagen I (Corning) in DMEM polymerized at 37°C for at least 24h. Soft plates were used to avoid activation of fibroblasts by matrix rigidity. Unless stated otherwise, all fibroblasts were cultured on soft plates and kept in their primary non-transformed state until passage 10.

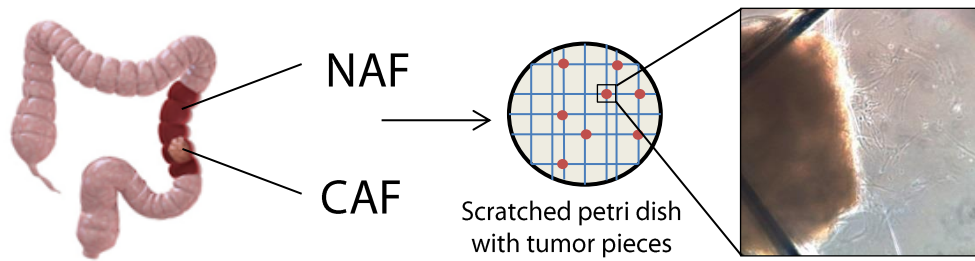


Figure V.1. Isolation of CAFs and NAFs from human colons

1.3. Invasion assay

Spheroid preparation

Agarose (Invitrogen) was dissolved in water to a concentration of 0.01g/mL and boiled. 150 μ L of the solution were added to wells of a 48 well-plate and agarose was left to polymerize for at least 10min at RT. A solution of 1×10^4 cells/mL of CT26 cancer cells was made, and 75 to 100 μ L of the solution was added to the wells. The wells were subsequently filled with DMEM supplemented with 10% FBS and spheroids were left to form for 3 to 4 days.

Plates preparation

30mm² tissue culture plates were specifically fashioned for the invasion assay: 3 holes of around 3mm in diameter were drilled in a plate and widened around the edges using a scalpel. The bottom of the dish was covered with Epoxy (Loctite) and 20x20mm square coverslips were glued to the dish overnight at RT. 1 day prior to the experiment, the dishes were silanized with 3-aminopropyl-trimethoxysilane (Sigma-Aldrich). The dishes were washed extensively with water and treated for 30 min with 0.5% glutaraldehyde followed by a final wash. This treatment was made to avoid collagen detachment from the plastic wholes due to the high contractility exerted by CAFs.

Embedding in collagen

2mg/mL rat tail collagen I (Corning) was prepared in DMEM, 10X PBS and 1M NaOH, to a pH=7. The solution was kept on ice in order to avoid collagen polymerization. Spheroids were embedded in 15 μ L collagen drops containing 5×10^3 fibroblasts, positioned in the hole of the culture plate. After filling all 3 holes, the plate was flipped every 30s for 5min, in order for the cells to stay in the middle of the collagen drop (preventing sedimentation of spheroids to the

glass or to collagen/air interface). Collagen was left to polymerize for an additional 15min at room temperature (RT) before 3mL of DMEM supplemented with 5% FBS and 1% AA were added. Cancer cells were left to invade for 3 days before fixing and staining.

For evaluation of cancer cell invasion in the presence of CAF's diffusible molecules (CAFdm), 15×10^3 CAFs were plated around the 3 collagen droplets, on the plastic dish.

1.4. Collagen contraction assay

1.5×10^5 fibroblasts were suspended in 1.5mL of 2 mg/mL rat tail collagen I (Corning) and added to a 24 well plate in triplicates (500 μ L/well). After 30 min of incubation at RT, collagen plugs were detached from the walls of the well with a scalpel and DMEM supplemented with 10% FBS was added. Images of the collagen plugs were acquired at time 0 (T0) and after 24h (T1) using a M165FC microscope (Leica). To obtain the gel contraction value, the relative area of the gel was measured using ImageJ software at T0 and T1, and the percentage of contraction was calculated using the formula $100 \times (\text{gel area (T0)} - \text{gel area (T1)}) / \text{gel area (T0)}$.

1.5. 3D Immunofluorescence

Spheroids embedded in collagen were fixed using 4% paraformaldehyde (PFA) in PBS for 30min at RT and washed with PBS. Anti-fibronectin antibody was added in 500 μ L of PBS at a dilution and dishes were left under agitation at RT for 2 days. Spheroids were then washed with PBS and permeabilized with 0.1% Triton X-100 in PBS for 30min at RT. DNA and F-actin were stained using DAPI and Phalloidin respectively (Life Technologies). Collagen was imaged using either reflectance.

For integrin staining, CAFs were embedded in collagen drops for 3 days in identical culture conditions. Cells were fixed using 4% paraformaldehyde (PFA) in PBS for 30min at RT and washed with PBS. Anti-fibronectin antibody was added in 500 μ L of PBS and dishes were left under agitation at RT for 2 days. Spheroids were then washed with PBS and permeabilized with 0.1% Triton X-100 in PBS for 30min at RT. Anti-integrin antibodies were added in 500 μ L of PBS and dishes were left under agitation at RT for an additional 2 days. Appropriate secondary antibodies were added in 500 μ L of PBS along with Phalloidin. Collagen was imaged using second harmonic generation (SHG).

1.6. 2D Immunofluorescence

For quantification of fibronectin assembly in CAFs and NAFs, fibroblasts were plated on glass coverslips in CT26 conditioned media as previously described. For the remaining of 2D staining, fibroblasts were plated on glass coverslips in DMEM supplemented with 10%FBS. For staining of early FN assembly and integrin localization, cells were fixed 24h post-plating. For staining of mature FN fibers on confluent monolayers, cells were fixed 3 days post-plating. Fibroblasts were plated on glass coverslips in CT26 conditioned media (details in paragraph II.2 of materials and methods). One day after plating, cells were fixed using 4% PFA in PBS for 20min at RT and washed with PBS. Anti-fibronectin antibody was added for 1h at RT. Cells were then washed and permeabilized with 0.1% Triton X-100 in PBS for 5min at RT. DNA and F-actin were stained using DAPI and Phalloidin respectively. Coverslips were mounted on slides in AquaPolymount (Polysciences) and imaged using an upright wide-field microscope (Leica DM6000) with a 63x/1.32NA oil immersion objective. The images were processed and quantified with ImageJ (NIH): the amount of assembled fibronectin per cell is calculated by normalizing the amount of fluorescence in a cell (integrated density) to the area of the cell and the background fluorescence.

1.7. Traction force microscopy

Traction force microscopy experiments were conducted as previously described (Elkhatib et al., 2014). Glass bottom dishes (World Precision Instrument, Inc) were plasma treated for 1 min and silanized with 3-aminopropyl-trimethoxysilane (Sigma-Aldrich, St.Louis, MO). The dishes were washed extensively with water and the glass surface was treated for 30 min with 0.5% glutaraldehyde followed by a final wash. Acrylamide 40% (46.88 μ L) and 2% bis-acrylamide (7.5 μ L) (Bio-Rad Laboratories, Richmond, CA) were mixed in PBS solution to a final volume of 250 μ L to achieve a Young's modulus of 5 kPa. The elasticity was determined by macroscopic force extension measurements. For traction force measurements, FluoSphere bead solution (0.2 μ m, 505-515 nm; Invitrogen) was added at 2.5% volume. Polymerization was initiated by addition of 2.5 μ L freshly prepared ammonium persulfate (10% w/v solution) and 0.5 μ L of N,N,N,N-tetramethylethylenediamine (TEMED). Immediately after initiation, 9 μ L PAA solution was pipetted onto the glass-bottom dish and an 18mm coverslip was quickly placed onto the gel droplet and gently pressed down. After 15 min the gel was immersed in PBS for 10 min, and then the top coverslips were gently removed under PBS. The gels were washed 3 times in PBS

for 10 min. Then, the gel's surface was activated to allow for laminin coating by applying a solution containing 50mM Hepes pH7.5, 10mg/ml of 1-Ethyl-3-[3-dimethylaminopropyl] carbodimide hydrochloride (EDC) (Thermos Scientific) and 1mg/ml of Sulfo-SANPAH (Pierce) for 30 min at RT. After the incubation, the cross-linker Sulfo-Sanpah is photo-activated by UV light for 10 min. After several washes with PBS, the gels were coated with 20 μ g/ml of laminin for 1h at RT. Before seeding cells, the gels were incubated in cell culture media for a minimum of 2 h at 37°C. The cells were plated at least 12h before imaging to allow for proper spreading. For time-lapse imaging, we used an inverted wide confocal spinning disk microscope (Roper/Nikon, 40x oil immersion objective, NA 1.3). A fluorescent image of beads and a phase contrast image of the cells were recorded every 3 min during 30min. At the end of the measurement, cells were detached by adding 10% Triton (Euromedex), and a reference image without cells was recorded. To ensure good quality imaging of fluorescent beads, we performed Z stacks of 30 images with a distance of 1 μ m and automatically chose the best focus (MetaMorph software). We used a previously described correlation algorithm developed by Timo Betz to extract the bead displacement fields. Traction forces were determined using the Fourier transform traction force algorithm as introduced by Butler et al. To quantify the applied tension of a whole cell, we measured the strain energy, which corresponds to the energy the cells expend to deform the substrate which is proportional to the average tension applied by a cell.

1.8. Imaging 3D samples

For time-lapse experiments, CAFs were stained with a lyophilic carbocyanine dye (Vybrant DiI-Cell labeling Solutions, ThermoFisher) according to the manufacture recommendation. Cells were embedded in collagen as described above. The dish was incubated at 5% CO₂, 37°C in the on-stage incubator (Okolab). For fixed and live 3D samples, images were acquired with an inverted AOBS two-photon laser scanning confocal microscope SP8 (Leica) coupled to femtosecond laser Chameleon Vision II (Coherent Inc) using 25x/1.0NA water-immersion objective. The microscope is equipped with three non-descanned HyD detectors: NDD1 (500–550 nm), NDD2 (\geq 590nm) and NDD3 (450 nm). Fluorescence channels were recorded simultaneously using the excitation wavelength 980nm. Collagen was visualized by confocal reflectance microscopy, using light at a wavelength of 488 nm and a standard photomultiplier tube (PMT) detector, at a low gain (500V). Images were recorded every 10 min up to 72h. 3D

stacks were obtained at a step size of 2 μm intervals. The images were processed with Leica Application Suite (LAS), ImageJ (NIH) and Imaris (Bitplane).

1.9. Invasion counter software

Quantification of cell invasion from spheroids was performed using a custom semi-automated image analysis program written in Python using the following packages: numpy, scipy, matplotlib, scikit-image and PyQt4. Image stacks of nuclei are first loaded into a custom GUI, and the spheroid contour is determined using adjustable Gaussian filtering, thresholding and 3D morphological operations. The nuclei of invading cells are then automatically detected using adjustable Gaussian filtering, thresholding and size exclusion. Centroid positions are determined by taking a weighted mean of the intensity for each nucleus. The positions of invading cancer cell nuclei are then manually verified and modified as necessary. Based on the LifeAct-GFP signal (expressed in cancer cells only), the nuclei of cancer cells are discriminated from the nuclei of fibroblasts. The invasion index, defined as the number of invading cancer cells normalized to the surface area of the spheroid contour in 3D, is then determined. This normalization is necessary to control for the slight variability in spheroid size. Due to the high optical density of the spheroids, only the bottom half of the spheroid is visible.

To quantify the distance of fibroblasts from the spheroid, the distance from the nuclei of non-LifeAct-GFP cells to the closest point along the cancer cell spheroid contour was determined. Fibroblast density was defined as the number of nuclei of non-GFP cells, normalized to the surface area of the spheroid contour in 3D.

1.10. Fiber alignment measurements

Fibers alignment and their angles with respect to the spheroid edge were measured using the available software CurveAlign (UW-Madison; <http://loci.wisc.edu/software/curvealign>). The angles of collagen fibers compared to the spheroid edge were determined for a slice of 10 series per sample.

1.11. Dunn's chemotaxis chamber

Cell plating

Square coverslips (20x20mm) were coated with 20 $\mu\text{g}/\text{mL}$ of laminin in PBS for 1h at RT, washed and blocked with a 0.1% BSA solution for 30min. After a second round of washing, the coverslips were placed in 6-well plate (1 coverslip/well) and 2mL of growth media containing

1x10⁴ cells/mL were added (CT26 or NIH3T3 depending on the experiment). Cells were then left to properly adhere overnight.

Mounting of the chamber

At least 2h prior to the mounting, the cells were starved. Hoechst dye was added at a final concentration of 0.2µg/mL in order to visualize the cells' nuclei during imaging. Dunn (-) and (+) media were warmed at 37°C and Dunn (+) medium was supplemented with fluorescein in order to follow gradient diffusion overtime. After proper sterilization in a 100% ethanol bath, the chambers were left to dry under the hood before undergoing several rounds of washing with DMEM to remove any residual traces of ethanol. 150µL of Dunn (-) medium was then added over the chamber until both wells were filled. The coverslip was then inverted over the two wells in the center of the chamber, and then positioned slightly off center so that a small gap remains in the outer well (Fig.). Excess medium was then absorbed with a Whatman paper from sides 1, 2 and 3 until the medium of the outer chamber starts to be drained, and warm wax (Vaseline:paraffin:beeswax – 1:1:1) was applied using a paint brush, leaving side 4 with the outer well gap unwaxed. A piece of whatman paper was placed on a small corner of the torn edge, just inside the outer well gap, in order to absorb the medium from the outer well. Approximately 100µL of Dunn (+) medium was then added into the outer well through the gap until it was full, and the last side was then sealed shut with wax. Once the wax had set, the coverslip surface was washed with distilled water and dried with a Whatman paper.

Growth medium	DMEM + 10% FBS
Starve medium	DMEM
Dunn (-) medium	DMEM
Dunn (+) media	<ul style="list-style-type: none"> • DMEM + 2.5% FBS • Conditioned media of CAFs (obtained by incubating CAFs for 24h in 10ml of starving medium) • 20µg/mL of fibronectin in DMEM • Conditioned media of HUVECs (obtained by incubating HUVECs in 10mL of starving medium)

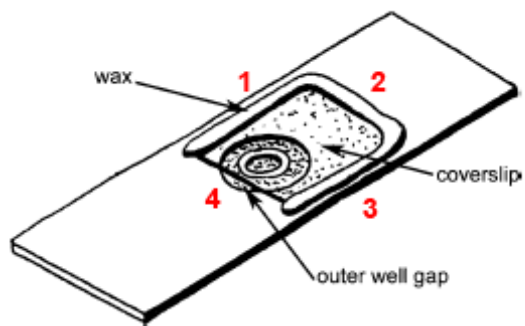


Figure V.2. Part-assembled chamber

Once the coverslip is in place, the chamber is sealed on 3 sides with wax. The 4th side remains unsealed and the medium is removed from the outer well and replaced with medium supplemented with chemoattractant using the outer well gap. (Adapted from a figure provided by Dr. Graham Dunn)

Imaging of the chamber

The stage of the microscope was pre-heated to 37°C so that filming could begin immediately after the chambers were assembled. The chambers were placed on the stage coverslip down and incubated at 5% CO₂. Images were acquired with an inverted Ti-E widefield microscope (Nikon) using a 10x/0.3NA dry objective. Images were recorded every 10 min up to 12h.

Cell tracking and analysis

Cell tracking and analysis was performed by Dr. Paolo Maiuri as already described (Maiuri et al., 2015).

1.12. Statistical analyses

All experiments were performed in triplicates in 2-6 independent experiments. All statistical analysis and graphic representations were performed using Prism software. For invasion assays and contractility assays, data are represented as box and whiskers (minimum to maximum). To show protein amounts and percentages, data are represented as column bars (mean +/- SEM). Statistical significance was determined with one-way analysis of variance (ANOVA). Newman-Keuls test was applied for multi-comparisons of different conditions. Mann-Whitney t-test was applied for paired comparisons.

2. Molecular biology and biochemistry

2.1. Immunoblotting

Protein lysates were obtained from fibroblasts seeded on soft plates at passage 3. Protein lysates were processed following standard procedures. Briefly, cells were washed with PBS, lysed in RIPA buffer (1% triton, 50mM Tris pH7.5, 1mM EDTA, 150mM NaCl) supplemented with protease and phosphatase inhibitors cocktails (Sigma), and boiled in Laemmli buffer for 5min. The samples were separated in SDS-PAGE gradient gels (4-15%), transferred to a nitrocellulose membrane using the BioRad system and blocked in 5% non-fat dried milk dissolved in PBS supplemented with 0.1% Tween for 30min at RT. The membranes were incubated with primary antibodies overnight at 4°C followed by incubation with peroxidase-conjugated secondary antibodies for 1h at RT. Antibody description and working dilutions can be found in Table V.1. Immunoreactive bands were detected using an ECL-plus kit (Roche). Quantifications were done using ImageJ (NIH) by normalizing protein amount to α -tubulin amount (loading control).

2.2. Quantification of fibronectin secretion and expression

CT26 cancer cells were incubated in 10mL of serum-deprived DMEM at a density of 1×10^6 cells for 24h. Media was collected, passed through 0.2 μ m filter to eliminate cell debris, and added on soft plates containing 15×10^4 fibroblasts for 3 days. Media was collected, filtered again and a 300 μ L sample was processed following western-blot standard procedures. Remaining cells were trypsinized and processed following western-blot standard procedures. 30 μ L of all samples (cell lysates and conditioned media) were finally loaded into a polyacrylamide SDS-PAGE gel (our Laemmli sample buffer being 2X concentrated, this volume corresponds to 15 μ L of proteins). To generate FN scale, increasing concentrations (ranging from 0.75ng to 300ng) of purified human FN were loaded on the gel.

For quantification of FN secretion by integrin and FN depleted CAFs, CAFs were plated in a well of a 6-well plate and subjected to transfection as previously described for 3 days. CAFs were then extensively washed with serum deprived DMEM, incubated in 1mL of serum deprived DMEM and re-transfected with another round of siRNA to maintain protein depletion. Media was collected, filtered and processed for western-blot as already described.

2.3. Inhibitors, matrices and siRNA

Blebbistatin (Sigma), BB94 (AbCam) and cilengitide (Selleckchem) were used at 15 μ M, 5 μ M and 1 μ M respectively. They were mixed with the media and added to the invasion assay after collagen polymerization. GM6001 was used at 20 μ M and mixed with both the collagen before its polymerization and added to the media as previously described (Wolf et al., 2013).

Fibronectin (corning), tenascin C (Abcam) and laminin (Invitrogen) were all pre-mixed with collagen at a final concentration of 20 μ g/mL. Fluorescently labelled fibronectin (Cytoskeleton Inc.) was added soluble at the same concentration.

For protein depletion using siRNA, CAFs were cultured in standard conditions and transfected using HiPerFect (Qiagen 301704). 6×10^4 CAFs were plated in a well of a 6-well plate and transfected with 100nM of siRNA. siRNA was purchased from Qiagen and sequences are listed in Table V.2.

2.4. Cytotoxicity and viability tests

1×10^4 CAFs were plated in triplicate in a 96-well plate in DMEM supplemented with 10%FBS and treated with siRNA for 3 days as previously described. For testing cilengitide effects, CAFs were plated in the same conditions for 3 days without siRNA treatment. CAFs were then washed and treated with either another round of siRNA or 1 μ M of cilengitide for 24h. 100 μ L of conditioned media of each condition was harvested for cytotoxicity tests using the Cytotoxicity Detection Kit LDH (Cat. No. 11 644 793 001) according to the manufacturer's recommendations. Remaining cells were used for viability tests using cell proliferation reagent WST-1 (Cat. No. 11 644 793 001) following the manufacturer's recommendations.

2.5. Statistical analysis

All statistical analysis and graphic representations were performed using Prism software. To show protein amounts data are represented as column bars (mean +/- SEM).

3. Animal experiments

3.1. Animal care

All mice were obtained from Janvier and were maintained in a specific pathogen-free environment. All experiments were carried out with the approval of the local ethical authorities.

3.2. Orthotopic injections

HT29 cancer cells were trypsinized and counted. 2×10^6 cells were suspended in 0.5 mL of PBS, alone, or with either NAFs or CAFs. 0.5 mL of Matrigel 10 mg/mL (Corning; growth factor depleted) was then added to the cell suspension. 6 week-old female Nude mice were divided into 3 groups and injected with: (1) 1×10^5 cancer cells alone (2) 1×10^5 cancer cells with 3×10^4 NAFs (cancer cells-to-fibroblasts ratio 3:1) (3) 1×10^5 cancer cells with 3×10^4 CAFs (cancer cells-to-fibroblasts ratio 3:1). Mice were anesthetized using gas anesthesia – 1-2% (vol/vol) of isoflurane. Cells were loaded into an 8 inch-long, 30 gauge and 45 degree bevel hypodermic needle. The needle was inserted through a lock screwed on the working channel of the endoscope (Karl Storz) to avoid air leakage. The endoscope was then inserted into the mouse colon through the anus. Following inflation of the colon with air, the needle was brought through the working channel to the scope's front. The implantation of cells was performed by two people: one person navigating the endoscope and one person operating the injection maneuver. The injection was performed by gentle sub-mucosal penetration with the open side of the bevel heading up in a flat angle. A volume of 50 μ L of PBS/Matrigel containing cells was injected into the colonic sub-mucosa. Mice were labeled by ear punching. Once a week, mice were anesthetized following the same procedure and colon was explored for tumors using the video endoscopic system (Karl Storz) which consists of a miniature endoscope, xenon light source, a triple chip camera and an air pump to achieve regulated inflation of the mouse colon. Growth of the primary tumor was digitally recorded. Unless the mice were exhibiting signs of non-fitness (weight loss, rigid abdomen, ascites...) they were kept alive until week 6 post-injection and sacrificed by cervical dislocation. Colon, liver and lymph node were harvested.

3.3. RNA extraction from liver

Harvested liver was immediately snap frozen in liquid nitrogen in order to avoid RNA degradation. Livers were stored at -80°C until tissue processing. Homogenization of the tissue was done by mortar and pestle in a liquid nitrogen bath in order to avoid tissue defreeze. Briefly,

tissue was transferred to the pestle and grinded until a layer of very fine dust was left. Using a RNase free spatula, the dust was homogenized and part of it was transferred to a solution of RNABLE (eurobio – approximately 2mL of solution for 100mg of tissue). The mixture was vortexed and left for 5min at RT. Chloroform was added at a ratio of 1/10 to the tissue-RNABLE mixture, vortexed for 30s and left at 4°C for 5min before centrifugation for 15min at a speed of 12000g to allow formation of 2 phases: an inferior blue phase (phenolic) containing DNA and proteins, and a superior transparent phase (aqueous) containing RNA. The aqueous phase was transferred to a new tube, diluted twice with isopropanol and left at RT for 5-10min. The tubes were then centrifuged for 5min at 12000g. Following centrifugation, RNA precipitates forming a white pellet. After discarding the supernatant, the RNA pellet was washed with 1mL of a 75% ethanol solution, vortexed and centrifuged again at 7500g for 5min. The supernatant was discarded again and the pellet was left to dry for 5-10min before suspending it in a 100µL of RNase free water. The quality of the RNA samples was determined by electrophoresis on agarose gels and staining with ethidium bromide, and the 18S and 28S RNA bands were visualized under UV light. The concentration of extracted RNA was determined using a NanoVue (BioRad).

3.4. Detection of human micrometastatic lesions

Real-time PCR allows distinguishing human from mouse gene expression in xenograft models. The presence of human cells within a host organ is quantified by mean of the transcript of human genes highly and exclusively represented in the human genome (Alu sequences). Results are expressed as n-fold differences in human Alu expression relative to the TBP genes (primers for TBP were selected to amplify both the mouse and the human TBP genes).

3.5. Preparation of paraffin-embedded tissues and staining

Tissues were fixed for 2h in 4% PFA in PBS, washed in PBS and embedded in paraffin. 5µm-thick sections were cut, placed on slides and processed for immunostaining as follow: a series of baths were performed as follow in order to dissolve paraffin: two xylene baths, 5min each; two EtOH 100% baths 2min each; EtOH 90% 2min; EtOH 85% 2min; EtOH 70% 2min; EtOH 50% 2min; H₂O 5min; PBS 5min.

- For immunofluorescence, antigen retrieval was performed for 20min in boiling antigen unmasking solution (Vector Laboratories). Sections were blocked with 5% FBS in PBS,

incubated with primary antibodies in the blocking solution for 2h at RT or overnight at 4°C, and followed by incubation with secondary antibodies for 1h at RT. Sections were mounted in AquaPolymount (Polysciences).

- For immunohistochemistry, slides were incubated in hematoxylin for 3min, rinsed with water, destained with a 70% EtOH solution containing 3% of HCl and rinsed with water again before being incubated in eosin for 30s, washed 3 times in 95% EtOH then 100% EtOH and then incubated in Xylene overnight to get a good clearing of any water. Sections were mounted the next day using Permount (xylene based solution; Fisher Scientific).

Table V.1: List of antibodies

Antibody	Company	Cat. No	Clonal	Dilution		
				2D IF	3D IF	WB
α SMA	Sigma Aldrich	A2547	monoclonal	x	x	1/1000
FAP	R&D systems	AF3715	polyclonal	x	x	1/500
PDGFR β	Cell Signaling	28E1	monoclonal	x	x	1/1000
α -tubulin	Sigma Aldrich	T9026	monoclonal	x	x	1/5000
GAPDH	Sigma Aldrich	G9545	polyclonal	x	x	1/10000
Fibronectin (Rabbit)	Sigma Aldrich	F3648	polyclonal	1/500	1/300	1/5000
Fibronectin (Mouse)	AbCam	Ab6328	monoclonal	1/100	x	x
Integrin α 5	AbCam	ab150361	monoclonal	1/100	1/50	1/1000
Integrin α v	AbCam	ab179475	monoclonal	x	x	1/2500
Integrin β 1	Santa Cruz	sc-53711	monoclonal	x	x	1/1000
Integrin β 3	EMD Millipore	AB2984	polyclonal	x	x	1/500
Integrin α v β 3	AbCam	Ab190147	monoclonal	1/100	1/50	x

Table V.2: List of sequences

siRNAs	Company	Cat. No	Sequence	Species
Fibronectin oligo1	Qiagen	SI0266400 4	CCCGGTTGTTATGACAATGG A	human
Fibronectin oligo2	Qiagen	SI0266399 7	CCGGTTGTTATGACAATGGA A	human
Integrin α 5 oligo1	Qiagen	SI0003420 2	CCCATTTGAATTTGACAGCAA A	human
Integrin α 5 oligo2	Qiagen	SI0265484 1	AATCCTTAATGGCTCAGACA T	human
Integrin β 3 oligo1	Qiagen	SI0000458 5	CCGCTTCAATGAGGAAGTG AA	human
Integrin β 3 oligo2	Qiagen	SI0000459 9	CTCTCCTGATGTTAGCACTT AA	human
Integrin β 3 oligo3	Qiagen	SI0000460 6	CAAGCTGAACCTAATAGCC AT	human

VI. References

2003. Goodbye, flat biology? *Nature*. 424:861.
- Abercrombie, M. 1961. The bases of the locomotory behaviour of fibroblasts. *Exp Cell Res. Suppl* 8:188-198.
- Abercrombie, M., J.E. Heaysman, and S.M. Pegrum. 1971. The locomotion of fibroblasts in culture. IV. Electron microscopy of the leading lamella. *Exp Cell Res.* 67:359-367.
- Aceto, N., A. Bardia, D.T. Miyamoto, M.C. Donaldson, B.S. Wittner, J.A. Spencer, M. Yu, A. Pely, A. Engstrom, H. Zhu, B.W. Brannigan, R. Kapur, S.L. Stott, T. Shioda, S. Ramaswamy, D.T. Ting, C.P. Lin, M. Toner, D.A. Haber, and S. Maheswaran. 2014. Circulating tumor cell clusters are oligoclonal precursors of breast cancer metastasis. *Cell*. 158:1110-1122.
- Achyut, B.R., D.A. Bader, A.I. Robles, D. Wangsa, C.C. Harris, T. Ried, and L. Yang. 2013. Inflammation-mediated genetic and epigenetic alterations drive cancer development in the neighboring epithelium upon stromal abrogation of TGF-beta signaling. *PLoS Genet.* 9:e1003251.
- Adair, B.D., J.P. Xiong, C. Maddock, S.L. Goodman, M.A. Arnaout, and M. Yeager. 2005. Three-dimensional EM structure of the ectodomain of integrin α V β 3 in a complex with fibronectin. *J Cell Biol.* 168:1109-1118.
- Akiyama, S.K., K.M. Yamada, and M. Hayashi. 1981. The structure of fibronectin and its role in cellular adhesion. *J Supramol Struct Cell Biochem.* 16:345-348.
- Albiges-Rizo, C., O. Destaing, B. Fourcade, E. Planus, and M.R. Block. 2009. Actin machinery and mechanosensitivity in invadopodia, podosomes and focal adhesions. *J Cell Sci.* 122:3037-3049.
- Albregues, J., T. Bertero, E. Grasset, S. Bonan, M. Maiel, I. Bourget, C. Philippe, C. Herraiz Serrano, S. Benamar, O. Croce, V. Sanz-Moreno, G. Meneguzzi, C.C. Feral, G. Cristofari, and C. Gaggioli. 2015. Epigenetic switch drives the conversion of fibroblasts into proinvasive cancer-associated fibroblasts. *Nat Commun.* 6:10204.
- Albregues, J., I. Bourget, C. Pons, V. Butet, P. Hofman, S. Tartare-Deckert, C.C. Feral, G. Meneguzzi, and C. Gaggioli. 2014. LIF mediates proinvasive activation of stromal fibroblasts in cancer. *Cell Rep.* 7:1664-1678.
- Alexander, N.R., K.M. Branch, A. Parekh, E.S. Clark, I.C. Iwueke, S.A. Guelcher, and A.M. Weaver. 2008. Extracellular matrix rigidity promotes invadopodia activity. *Curr Biol.* 18:1295-1299.
- Alvarez, R.H., H.M. Kantarjian, and J.E. Cortes. 2006. Biology of platelet-derived growth factor and its involvement in disease. *Mayo Clin Proc.* 81:1241-1257.
- Amatangelo, M.D., D.E. Bassi, A.J. Klein-Szanto, and E. Cukierman. 2005. Stroma-derived three-dimensional matrices are necessary and sufficient to promote desmoplastic differentiation of normal fibroblasts. *Am J Pathol.* 167:475-488.
- Anthis, N.J., J.R. Haling, C.L. Oxley, M. Memo, K.L. Wegener, C.J. Lim, M.H. Ginsberg, and I.D. Campbell. 2009. Beta integrin tyrosine phosphorylation is a conserved mechanism for regulating talin-induced integrin activation. *J Biol Chem.* 284:36700-36710.

- Ao, M., B.M. Brewer, L. Yang, O.E. Franco Coronel, S.W. Hayward, D.J. Webb, and D. Li. 2015a. Stretching fibroblasts remodels fibronectin and alters cancer cell migration. *Sci Rep.* 5:8334.
- Ao, Z., S.H. Shah, L.M. Machlin, R. Parajuli, P.C. Miller, S. Rawal, A.J. Williams, R.J. Cote, M.E. Lippman, R.H. Datar, and D. El-Ashry. 2015b. Identification of Cancer-Associated Fibroblasts in Circulating Blood from Patients with Metastatic Breast Cancer. *Cancer Res.* 75:4681-4687.
- Aota, S., M. Nomizu, and K.M. Yamada. 1994. The short amino acid sequence Pro-His-Ser-Arg-Asn in human fibronectin enhances cell-adhesive function. *J Biol Chem.* 269:24756-24761.
- Arnold, M., E.A. Cavalcanti-Adam, R. Glass, J. Blummel, W. Eck, M. Kantlehner, H. Kessler, and J.P. Spatz. 2004. Activation of integrin function by nanopatterned adhesive interfaces. *Chemphyschem.* 5:383-388.
- Arora, P.D., and C.A. McCulloch. 1994. Dependence of collagen remodelling on alpha-smooth muscle actin expression by fibroblasts. *J Cell Physiol.* 159:161-175.
- Artym, V.V., Y. Zhang, F. Seillier-Moiseiwitsch, K.M. Yamada, and S.C. Mueller. 2006. Dynamic interactions of cortactin and membrane type 1 matrix metalloproteinase at invadopodia: defining the stages of invadopodia formation and function. *Cancer Res.* 66:3034-3043.
- Aung, A., Y.N. Seo, S. Lu, Y. Wang, C. Jamora, J.C. del Alamo, and S. Varghese. 2014. 3D traction stresses activate protease-dependent invasion of cancer cells. *Biophys J.* 107:2528-2537.
- Avgustinova, A., M. Iravani, D. Robertson, A. Fearn, Q. Gao, P. Klingbeil, A.M. Hanby, V. Speirs, E. Sahai, F. Calvo, and C.M. Isacke. 2016. Tumour cell-derived Wnt7a recruits and activates fibroblasts to promote tumour aggressiveness. *Nat Commun.* 7:10305.
- Barbazan, J., L. Alonso-Alconada, L. Muinelo-Romay, M. Vieito, A. Abalo, M. Alonso-Nocelo, S. Candamio, E. Gallardo, B. Fernandez, I. Abdulkader, M. de Los Angeles Casares, A. Gomez-Tato, R. Lopez-Lopez, and M. Abal. 2012. Molecular characterization of circulating tumor cells in human metastatic colorectal cancer. *PLoS One.* 7:e40476.
- Barker, H.E., D. Bird, G. Lang, and J.T. Erler. 2013. Tumor-secreted LOXL2 activates fibroblasts through FAK signaling. *Mol Cancer Res.* 11:1425-1436.
- Barker, H.E., J. Chang, T.R. Cox, G. Lang, D. Bird, M. Nicolau, H.R. Evans, A. Gartland, and J.T. Erler. 2011. LOXL2-mediated matrix remodeling in metastasis and mammary gland involution. *Cancer Res.* 71:1561-1572.
- Barker, H.E., T.R. Cox, and J.T. Erler. 2012. The rationale for targeting the LOX family in cancer. *Nat Rev Cancer.* 12:540-552.
- Barker, N. 2014. Adult intestinal stem cells: critical drivers of epithelial homeostasis and regeneration. *Nat Rev Mol Cell Biol.* 15:19-33.
- Barry-Hamilton, V., R. Spangler, D. Marshall, S. McCauley, H.M. Rodriguez, M. Oyasu, A. Mikels, M. Vaysberg, H. Ghermazien, C. Wai, C.A. Garcia, A.C. Velayo, B. Jorgensen, D. Biermann, D. Tsai, J. Green, S. Zaffryar-Eilot, A. Holzer, S. Ogg, D. Thai, G. Neufeld, P. Van Vlasselaer, and V. Smith. 2010. Allosteric inhibition of lysyl oxidase-like-2 impedes the development of a pathologic microenvironment. *Nat Med.* 16:1009-1017.
- Basara, M.L., J.B. McCarthy, D.W. Barnes, and L.T. Furcht. 1985. Stimulation of haptotaxis and migration of tumor cells by serum spreading factor. *Cancer Res.* 45:2487-2494.

- Beaune, G., T.V. Stirbat, N. Khalifat, O. Cochet-Escartin, S. Garcia, V.V. Gurchenkov, M.P. Murrell, S. Dufour, D. Cuvelier, and F. Brochard-Wyart. 2014. How cells flow in the spreading of cellular aggregates. *Proc Natl Acad Sci U S A*. 111:8055-8060.
- Bella, J., M. Eaton, B. Brodsky, and H.M. Berman. 1994. Crystal and molecular structure of a collagen-like peptide at 1.9 Å resolution. *Science*. 266:75-81.
- Bhardwaj, B., J. Klassen, N. Cossette, E. Sterns, A. Tuck, R. Deeley, S. Sengupta, and B. Elliott. 1996. Localization of platelet-derived growth factor beta receptor expression in the periepithelial stroma of human breast carcinoma. *Clin Cancer Res*. 2:773-782.
- Bhowmick, N.A., A. Chytil, D. Plieth, A.E. Gorska, N. Dumont, S. Shappell, M.K. Washington, E.G. Neilson, and H.L. Moses. 2004. TGF-beta signaling in fibroblasts modulates the oncogenic potential of adjacent epithelia. *Science*. 303:848-851.
- Bierie, B., and H.L. Moses. 2006. Tumour microenvironment: TGFbeta: the molecular Jekyll and Hyde of cancer. *Nat Rev Cancer*. 6:506-520.
- Bissell, M.J., and W.C. Hines. 2011. Why don't we get more cancer? A proposed role of the microenvironment in restraining cancer progression. *Nat Med*. 17:320-329.
- Bonnans, C., J. Chou, and Z. Werb. 2014. Remodelling the extracellular matrix in development and disease. *Nat Rev Mol Cell Biol*. 15:786-801.
- Bosman, F.T., A. de Bruine, C. Flohil, A. van der Wurff, J. ten Kate, and W.W. Dinjens. 1993. Epithelial-stromal interactions in colon cancer. *Int J Dev Biol*. 37:203-211.
- Bouvard, D., J. Pouwels, N. De Franceschi, and J. Ivaska. 2013. Integrin inactivators: balancing cellular functions in vitro and in vivo. *Nat Rev Mol Cell Biol*. 14:430-442.
- Bouvard, D., L. Vignoud, S. Dupe-Manet, N. Abed, H.N. Fournier, C. Vincent-Monegat, S.F. Retta, R. Fassler, and M.R. Block. 2003. Disruption of focal adhesions by integrin cytoplasmic domain-associated protein-1 alpha. *J Biol Chem*. 278:6567-6574.
- Bowden, E.T., M. Barth, D. Thomas, R.I. Glazer, and S.C. Mueller. 1999. An invasion-related complex of cortactin, paxillin and PKCmu associates with invadopodia at sites of extracellular matrix degradation. *Oncogene*. 18:4440-4449.
- Brodsky, B., and A.V. Persikov. 2005. Molecular structure of the collagen triple helix. *Adv Protein Chem*. 70:301-339.
- Buccione, R., J.D. Orth, and M.A. McNiven. 2004. Foot and mouth: podosomes, invadopodia and circular dorsal ruffles. *Nat Rev Mol Cell Biol*. 5:647-657.
- Cadamuro, M., G. Nardo, S. Indraccolo, L. Dall'olmo, L. Sambado, L. Moserle, I. Franceschet, M. Colledan, M. Massani, T. Stecca, N. Bassi, S. Morton, C. Spirli, R. Fiorotto, L. Fabris, and M. Strazzabosco. 2013. Platelet-derived growth factor-D and Rho GTPases regulate recruitment of cancer-associated fibroblasts in cholangiocarcinoma. *Hepatology*. 58:1042-1053.
- Cai, D., S.C. Chen, M. Prasad, L. He, X. Wang, V. Choesmel-Cadamuro, J.K. Sawyer, G. Danuser, and D.J. Montell. 2014. Mechanical feedback through E-cadherin promotes direction sensing during collective cell migration. *Cell*. 157:1146-1159.
- Cai, D., W. Dai, M. Prasad, J. Luo, N.S. Gov, and D.J. Montell. 2016. Modeling and analysis of collective cell migration in an in vivo three-dimensional environment. *Proc Natl Acad Sci U S A*. 113:E2134-2141.
- Calderwood, D.A., I.D. Campbell, and D.R. Critchley. 2013. Talins and kindlins: partners in integrin-mediated adhesion. *Nat Rev Mol Cell Biol*. 14:503-517.
- Calderwood, D.A., Y. Fujioka, J.M. de Pereda, B. Garcia-Alvarez, T. Nakamoto, B. Margolis, C.J. McGlade, R.C. Liddington, and M.H. Ginsberg. 2003. Integrin beta cytoplasmic

- domain interactions with phosphotyrosine-binding domains: a structural prototype for diversity in integrin signaling. *Proc Natl Acad Sci U S A.* 100:2272-2277.
- Calderwood, D.A., A. Huttenlocher, W.B. Kiosses, D.M. Rose, D.G. Woodside, M.A. Schwartz, and M.H. Ginsberg. 2001. Increased filamin binding to beta-integrin cytoplasmic domains inhibits cell migration. *Nat Cell Biol.* 3:1060-1068.
- Calderwood, D.A., B. Yan, J.M. de Pereda, B.G. Alvarez, Y. Fujioka, R.C. Liddington, and M.H. Ginsberg. 2002. The phosphotyrosine binding-like domain of talin activates integrins. *J Biol Chem.* 277:21749-21758.
- Calderwood, D.A., R. Zent, R. Grant, D.J. Rees, R.O. Hynes, and M.H. Ginsberg. 1999. The Talin head domain binds to integrin beta subunit cytoplasmic tails and regulates integrin activation. *J Biol Chem.* 274:28071-28074.
- Calon, A., E. Espinet, S. Palomo-Ponce, D.V. Tauriello, M. Iglesias, M.V. Cespedes, M. Sevillano, C. Nadal, P. Jung, X.H. Zhang, D. Byrom, A. Riera, D. Rossell, R. Mangués, J. Massague, E. Sancho, and E. Batlle. 2012. Dependency of colorectal cancer on a TGF-beta-driven program in stromal cells for metastasis initiation. *Cancer Cell.* 22:571-584.
- Calvo, F., N. Ege, A. Grande-Garcia, S. Hooper, R.P. Jenkins, S.I. Chaudhry, K. Harrington, P. Williamson, E. Moendarbary, G. Charras, and E. Sahai. 2013. Mechanotransduction and YAP-dependent matrix remodelling is required for the generation and maintenance of cancer-associated fibroblasts. *Nat Cell Biol.* 15:637-646.
- Carter, S.B. 1967. Haptotaxis and the mechanism of cell motility. *Nature.* 213:256-260.
- Case, L.B., and C.M. Waterman. 2015. Integration of actin dynamics and cell adhesion by a three-dimensional, mechanosensitive molecular clutch. *Nat Cell Biol.* 17:955-963.
- Castro-Castro, A., V. Marchesin, P. Monteiro, C. Lodillinsky, C. Rosse, and P. Chavrier. 2016. Cellular and Molecular Mechanisms of MT1-MMP-Dependent Cancer Cell Invasion. *Annu Rev Cell Dev Biol.* 32:555-576.
- Chang, D.D., C. Wong, H. Smith, and J. Liu. 1997. ICAP-1, a novel beta1 integrin cytoplasmic domain-associated protein, binds to a conserved and functionally important NPXY sequence motif of beta1 integrin. *J Cell Biol.* 138:1149-1157.
- Changede, R., X. Xu, F. Margadant, and M.P. Sheetz. 2015. Nascent Integrin Adhesions Form on All Matrix Rigidities after Integrin Activation. *Dev Cell.* 35:614-621.
- Chen, J., D. Pee, R. Ayyagari, B. Graubard, C. Schairer, C. Byrne, J. Benichou, and M.H. Gail. 2006. Projecting absolute invasive breast cancer risk in white women with a model that includes mammographic density. *J Natl Cancer Inst.* 98:1215-1226.
- Chen, S., and E.H. Huang. 2014. The colon cancer stem cell microenvironment holds keys to future cancer therapy. *J Gastrointest Surg.* 18:1040-1048.
- Chen, W.T. 1989. Proteolytic activity of specialized surface protrusions formed at rosette contact sites of transformed cells. *J Exp Zool.* 251:167-185.
- Cheng, J.D., R.L. Dunbrack, Jr., M. Valianou, A. Rogatko, R.K. Alpaugh, and L.M. Weiner. 2002. Promotion of tumor growth by murine fibroblast activation protein, a serine protease, in an animal model. *Cancer Res.* 62:4767-4772.
- Cheung, K.J., E. Gabrielson, Z. Werb, and A.J. Ewald. 2013. Collective invasion in breast cancer requires a conserved basal epithelial program. *Cell.* 155:1639-1651.
- Chiquet, M., M. Matthisson, M. Koch, M. Tannheimer, and R. Chiquet-Ehrismann. 1996. Regulation of extracellular matrix synthesis by mechanical stress. *Biochem Cell Biol.* 74:737-744.

- Choi, C.K., M. Vicente-Manzanares, J. Zareno, L.A. Whitmore, A. Mogilner, and A.R. Horwitz. 2008. Actin and alpha-actinin orchestrate the assembly and maturation of nascent adhesions in a myosin II motor-independent manner. *Nat Cell Biol.* 10:1039-1050.
- Chrzanowska-Wodnicka, M., and K. Burridge. 1994. Tyrosine phosphorylation is involved in reorganization of the actin cytoskeleton in response to serum or LPA stimulation. *J Cell Sci.* 107 (Pt 12):3643-3654.
- Clark, A.G., and D.M. Vignjevic. 2015. Modes of cancer cell invasion and the role of the microenvironment. *Curr Opin Cell Biol.* 36:13-22.
- Clark, E.S., and A.M. Weaver. 2008. A new role for cortactin in invadopodia: regulation of protease secretion. *Eur J Cell Biol.* 87:581-590.
- Clark, E.S., A.S. Whigham, W.G. Yarbrough, and A.M. Weaver. 2007. Cortactin is an essential regulator of matrix metalloproteinase secretion and extracellular matrix degradation in invadopodia. *Cancer Res.* 67:4227-4235.
- Clevers, H. 2013. The intestinal crypt, a prototype stem cell compartment. *Cell.* 154:274-284.
- Coelho, N.M., P.D. Arora, S. van Putten, S. Boo, P. Petrovic, A.X. Lin, B. Hinz, and C.A. McCulloch. 2017. Discoidin Domain Receptor 1 Mediates Myosin-Dependent Collagen Contraction. *Cell Rep.* 18:1774-1790.
- Cohen, D.J., W.J. Nelson, and M.M. Maharbiz. 2014. Galvanotactic control of collective cell migration in epithelial monolayers. *Nat Mater.* 13:409-417.
- Cornil, I., D. Theodorescu, S. Man, M. Herlyn, J. Jambrosic, and R.S. Kerbel. 1991. Fibroblast cell interactions with human melanoma cells affect tumor cell growth as a function of tumor progression. *Proc Natl Acad Sci U S A.* 88:6028-6032.
- Cortese, B., I.E. Palama, S. D'Amone, and G. Gigli. 2014. Influence of electrotaxis on cell behaviour. *Integr Biol (Camb).* 6:817-830.
- Cory, G.O., and P.J. Cullen. 2007. Membrane curvature: the power of bananas, zeppelins and boomerangs. *Curr Biol.* 17:R455-457.
- Costa-Silva, B., N.M. Aiello, A.J. Ocean, S. Singh, H. Zhang, B.K. Thakur, A. Becker, A. Hoshino, M.T. Mark, H. Molina, J. Xiang, T. Zhang, T.M. Theilen, G. Garcia-Santos, C. Williams, Y. Ararso, Y. Huang, G. Rodrigues, T.L. Shen, K.J. Labori, I.M. Lothe, E.H. Kure, J. Hernandez, A. Doussot, S.H. Ebbesen, P.M. Grandgenett, M.A. Hollingsworth, M. Jain, K. Mallya, S.K. Batra, W.R. Jarnagin, R.E. Schwartz, I. Matei, H. Peinado, B.Z. Stanger, J. Bromberg, and D. Lyden. 2015. Pancreatic cancer exosomes initiate pre-metastatic niche formation in the liver. *Nat Cell Biol.* 17:816-826.
- Courtneidge, S.A., E.F. Azucena, I. Pass, D.F. Seals, and L. Tesfay. 2005. The SRC substrate Tks5, podosomes (invadopodia), and cancer cell invasion. *Cold Spring Harb Symp Quant Biol.* 70:167-171.
- Coussens, L.M., B. Fingleton, and L.M. Matrisian. 2002. Matrix metalloproteinase inhibitors and cancer: trials and tribulations. *Science.* 295:2387-2392.
- Cox, T.R., D. Bird, A.M. Baker, H.E. Barker, M.W. Ho, G. Lang, and J.T. Erler. 2013. LOX-mediated collagen crosslinking is responsible for fibrosis-enhanced metastasis. *Cancer Res.* 73:1721-1732.
- Cox, T.R., A. Gartland, and J.T. Erler. 2016. Lysyl Oxidase, a Targetable Secreted Molecule Involved in Cancer Metastasis. *Cancer Res.* 76:188-192.
- Cox, T.R., R.M. Rumney, E.M. Schoof, L. Perryman, A.M. Hoye, A. Agrawal, D. Bird, N.A. Latif, H. Forrest, H.R. Evans, I.D. Huggins, G. Lang, R. Linding, A. Gartland, and J.T.

- Erler. 2015. The hypoxic cancer secretome induces pre-metastatic bone lesions through lysyl oxidase. *Nature*. 522:106-110.
- Critchley, D.R. 2000. Focal adhesions - the cytoskeletal connection. *Curr Opin Cell Biol*. 12:133-139.
- Cukierman, E., R. Pankov, D.R. Stevens, and K.M. Yamada. 2001. Taking cell-matrix adhesions to the third dimension. *Science*. 294:1708-1712.
- Cully, M., H. You, A.J. Levine, and T.W. Mak. 2006. Beyond PTEN mutations: the PI3K pathway as an integrator of multiple inputs during tumorigenesis. *Nat Rev Cancer*. 6:184-192.
- Curtis, A.S. 1964. The Mechanism of Adhesion of Cells to Glass. A Study by Interference Reflection Microscopy. *J Cell Biol*. 20:199-215.
- Danen, E.H., P. Sonneveld, C. Brakebusch, R. Fassler, and A. Sonnenberg. 2002. The fibronectin-binding integrins alpha5beta1 and alphavbeta3 differentially modulate RhoA-GTP loading, organization of cell matrix adhesions, and fibronectin fibrillogenesis. *J Cell Biol*. 159:1071-1086.
- Darby, I., O. Skalli, and G. Gabbiani. 1990. Alpha-smooth muscle actin is transiently expressed by myofibroblasts during experimental wound healing. *Lab Invest*. 63:21-29.
- Dayer, C., and I. Stamenkovic. 2015. Recruitment of Matrix Metalloproteinase-9 (MMP-9) to the Fibroblast Cell Surface by Lysyl Hydroxylase 3 (LH3) Triggers Transforming Growth Factor-beta (TGF-beta) Activation and Fibroblast Differentiation. *J Biol Chem*. 290:13763-13778.
- De Wever, O., Q.D. Nguyen, L. Van Hoorde, M. Bracke, E. Bruyneel, C. Gespach, and M. Mareel. 2004. Tenascin-C and SF/HGF produced by myofibroblasts in vitro provide convergent pro-invasive signals to human colon cancer cells through RhoA and Rac. *FASEB J*. 18:1016-1018.
- Debruyne, P.R., E.A. Bruyneel, I.M. Karaguni, X. Li, G. Flatau, O. Muller, A. Zimmer, C. Gespach, and M.M. Mareel. 2002. Bile acids stimulate invasion and haptotaxis in human colorectal cancer cells through activation of multiple oncogenic signaling pathways. *Oncogene*. 21:6740-6750.
- DeMali, K.A., C.A. Barlow, and K. Burridge. 2002. Recruitment of the Arp2/3 complex to vinculin: coupling membrane protrusion to matrix adhesion. *J Cell Biol*. 159:881-891.
- Desmouliere, A., A. Geinoz, F. Gabbiani, and G. Gabbiani. 1993. Transforming growth factor-beta 1 induces alpha-smooth muscle actin expression in granulation tissue myofibroblasts and in quiescent and growing cultured fibroblasts. *J Cell Biol*. 122:103-111.
- Desmouliere, A., L. Rubbia-Brandt, A. Abdiu, T. Walz, A. Macieira-Coelho, and G. Gabbiani. 1992a. Alpha-smooth muscle actin is expressed in a subpopulation of cultured and cloned fibroblasts and is modulated by gamma-interferon. *Exp Cell Res*. 201:64-73.
- Desmouliere, A., L. Rubbia-Brandt, G. Grau, and G. Gabbiani. 1992b. Heparin induces alpha-smooth muscle actin expression in cultured fibroblasts and in granulation tissue myofibroblasts. *Lab Invest*. 67:716-726.
- Destaing, O., M.R. Block, E. Planus, and C. Albiges-Rizo. 2011. Invadosome regulation by adhesion signaling. *Curr Opin Cell Biol*. 23:597-606.
- Destaing, O., E. Planus, D. Bouvard, C. Oddou, C. Badowski, V. Bossy, A. Raducanu, B. Fourcade, C. Albiges-Rizo, and M.R. Block. 2010. beta1A integrin is a master regulator of invadosome organization and function. *Mol Biol Cell*. 21:4108-4119.

- Destaing, O., F. Saltel, J.C. Geminard, P. Jurdic, and F. Bard. 2003. Podosomes display actin turnover and dynamic self-organization in osteoclasts expressing actin-green fluorescent protein. *Mol Biol Cell*. 14:407-416.
- Discher, D.E., P. Janmey, and Y.L. Wang. 2005. Tissue cells feel and respond to the stiffness of their substrate. *Science*. 310:1139-1143.
- Dona, E., J.D. Barry, G. Valentin, C. Quirin, A. Khmelinskii, A. Kunze, S. Durdu, L.R. Newton, A. Fernandez-Minan, W. Huber, M. Knop, and D. Gilmour. 2013. Directional tissue migration through a self-generated chemokine gradient. *Nature*. 503:285-289.
- Dong, J., J. Grunstein, M. Tejada, F. Peale, G. Frantz, W.C. Liang, W. Bai, L. Yu, J. Kowalski, X. Liang, G. Fuh, H.P. Gerber, and N. Ferrara. 2004. VEGF-null cells require PDGFR alpha signaling-mediated stromal fibroblast recruitment for tumorigenesis. *EMBO J*. 23:2800-2810.
- Du, X.P., E.F. Plow, A.L. Frelinger, 3rd, T.E. O'Toole, J.C. Loftus, and M.H. Ginsberg. 1991. Ligands "activate" integrin alpha IIb beta 3 (platelet GPIIb-IIIa). *Cell*. 65:409-416.
- Duda, D.G., A.M. Duyverman, M. Kohno, M. Snuderl, E.J. Steller, D. Fukumura, and R.K. Jain. 2010. Malignant cells facilitate lung metastasis by bringing their own soil. *Proc Natl Acad Sci U S A*. 107:21677-21682.
- Ebisuno, Y., K. Katagiri, T. Katakai, Y. Ueda, T. Nemoto, H. Inada, J. Nabekura, T. Okada, R. Kannagi, T. Tanaka, M. Miyasaka, N. Hogg, and T. Kinashi. 2010. Rap1 controls lymphocyte adhesion cascade and interstitial migration within lymph nodes in RAPL-dependent and -independent manners. *Blood*. 115:804-814.
- Edwards, D.R., and G. Murphy. 1998. Cancer. Proteases--invasion and more. *Nature*. 394:527-528.
- Egeblad, M., and Z. Werb. 2002. New functions for the matrix metalloproteinases in cancer progression. *Nat Rev Cancer*. 2:161-174.
- Eisenhoffer, G.T., P.D. Loftus, M. Yoshigi, H. Otsuna, C.B. Chien, P.A. Morcos, and J. Rosenblatt. 2012. Crowding induces live cell extrusion to maintain homeostatic cell numbers in epithelia. *Nature*. 484:546-549.
- Elkhatib, N., M.B. Neu, C. Zensen, K.M. Schmoller, D. Louvard, A.R. Bausch, T. Betz, and D.M. Vignjevic. 2014. Fascin plays a role in stress fiber organization and focal adhesion disassembly. *Curr Biol*. 24:1492-1499.
- Emsley, J., C.G. Knight, R.W. Farndale, M.J. Barnes, and R.C. Liddington. 2000. Structural basis of collagen recognition by integrin alpha2beta1. *Cell*. 101:47-56.
- Enderling, H., N.R. Alexander, E.S. Clark, K.M. Branch, L. Estrada, C. Croke, J. Jourquin, N. Lobdell, M.H. Zaman, S.A. Guelcher, A.R. Anderson, and A.M. Weaver. 2008. Dependence of invadopodia function on collagen fiber spacing and cross-linking: computational modeling and experimental evidence. *Biophys J*. 95:2203-2218.
- Erickson, H.P. 2016. Protein unfolding under isometric tension-what force can integrins generate, and can it unfold FNIII domains? *Curr Opin Struct Biol*. 42:98-105.
- Erler, J.T., K.L. Bennewith, M. Nicolau, N. Dornhofer, C. Kong, Q.T. Le, J.T. Chi, S.S. Jeffrey, and A.J. Giaccia. 2006. Lysyl oxidase is essential for hypoxia-induced metastasis. *Nature*. 440:1222-1226.
- Ezratty, E.J., C. Bertaux, E.E. Marcantonio, and G.G. Gundersen. 2009. Clathrin mediates integrin endocytosis for focal adhesion disassembly in migrating cells. *J Cell Biol*. 187:733-747.

- Ezzoukhry, Z., E. Henriot, L. Piquet, K. Boye, P. Bioulac-Sage, C. Balabaud, G. Couchy, J. Zucman-Rossi, V. Moreau, and F. Saltel. 2016. TGF-beta1 promotes linear invadosome formation in hepatocellular carcinoma cells, through DDR1 up-regulation and collagen I cross-linking. *Eur J Cell Biol.* 95:503-512.
- Fackler, O.T., and R. Grosse. 2008. Cell motility through plasma membrane blebbing. *J Cell Biol.* 181:879-884.
- Fagotto, F., N. Rohani, A.S. Touret, and R. Li. 2013. A molecular base for cell sorting at embryonic boundaries: contact inhibition of cadherin adhesion by ephrin/ Eph-dependent contractility. *Dev Cell.* 27:72-87.
- Ferlay, J., H.R. Shin, F. Bray, D. Forman, C. Mathers, and D.M. Parkin. 2010. Estimates of worldwide burden of cancer in 2008: GLOBOCAN 2008. *Int J Cancer.* 127:2893-2917.
- French-Constant, C. 1995. Alternative splicing of fibronectin--many different proteins but few different functions. *Exp Cell Res.* 221:261-271.
- Fidler, I.J. 1970. Metastasis: quantitative analysis of distribution and fate of tumor emboli labeled with ¹²⁵I-5-iodo-2'-deoxyuridine. *J Natl Cancer Inst.* 45:773-782.
- Fidler, I.J. 2003. The pathogenesis of cancer metastasis: the 'seed and soil' hypothesis revisited. *Nat Rev Cancer.* 3:453-458.
- Fidler, I.J., and M.L. Kripke. 1977. Metastasis results from preexisting variant cells within a malignant tumor. *Science.* 197:893-895.
- Fidler, I.J., S. Yano, R.D. Zhang, T. Fujimaki, and C.D. Bucana. 2002. The seed and soil hypothesis: vascularisation and brain metastases. *Lancet Oncol.* 3:53-57.
- Fogelgren, B., N. Polgar, K.M. Szauter, Z. Ujfaludi, R. Laczko, K.S. Fong, and K. Csiszar. 2005. Cellular fibronectin binds to lysyl oxidase with high affinity and is critical for its proteolytic activation. *J Biol Chem.* 280:24690-24697.
- Fouchard, J., D. Mitrossilis, and A. Asnacios. 2011. Acto-myosin based response to stiffness and rigidity sensing. *Cell Adh Migr.* 5:16-19.
- Fraley, S.I., Y. Feng, R. Krishnamurthy, D.H. Kim, A. Celedon, G.D. Longmore, and D. Wirtz. 2010. A distinctive role for focal adhesion proteins in three-dimensional cell motility. *Nat Cell Biol.* 12:598-604.
- Franco, O.E., M. Jiang, D.W. Strand, J. Peacock, S. Fernandez, R.S. Jackson, 2nd, M.P. Revelo, N.A. Bhowmick, and S.W. Hayward. 2011. Altered TGF-beta signaling in a subpopulation of human stromal cells promotes prostatic carcinogenesis. *Cancer Res.* 71:1272-1281.
- Frantz, C., K.M. Stewart, and V.M. Weaver. 2010. The extracellular matrix at a glance. *J Cell Sci.* 123:4195-4200.
- Friedl, P. 2004. Preshaping and plasticity: shifting mechanisms of cell migration. *Curr Opin Cell Biol.* 16:14-23.
- Friedl, P., and S. Alexander. 2011. Cancer invasion and the microenvironment: plasticity and reciprocity. *Cell.* 147:992-1009.
- Friedl, P., F. Entschladen, C. Conrad, B. Niggemann, and K.S. Zanker. 1998. CD4+ T lymphocytes migrating in three-dimensional collagen lattices lack focal adhesions and utilize beta1 integrin-independent strategies for polarization, interaction with collagen fibers and locomotion. *Eur J Immunol.* 28:2331-2343.
- Friedl, P., and D. Gilmour. 2009. Collective cell migration in morphogenesis, regeneration and cancer. *Nat Rev Mol Cell Biol.* 10:445-457.

- Friedl, P., J. Locker, E. Sahai, and J.E. Segall. 2012. Classifying collective cancer cell invasion. *Nat Cell Biol.* 14:777-783.
- Friedl, P., and K. Wolf. 2009. Proteolytic interstitial cell migration: a five-step process. *Cancer Metastasis Rev.* 28:129-135.
- Friedl, P., and K. Wolf. 2010. Plasticity of cell migration: a multiscale tuning model. *J Cell Biol.* 188:11-19.
- Fullar, A., I. Kovalszky, M. Bitsche, A. Romani, V.H. Scharfetter, G.M. Sprinzl, H. Riechelmann, and J. Dudas. 2012. Tumor cell and carcinoma-associated fibroblast interaction regulates matrix metalloproteinases and their inhibitors in oral squamous cell carcinoma. *Exp Cell Res.* 318:1517-1527.
- Gabbiani, G., G.B. Ryan, and G. Majne. 1971. Presence of modified fibroblasts in granulation tissue and their possible role in wound contraction. *Experientia.* 27:549-550.
- Gaggioli, C., S. Hooper, C. Hidalgo-Carcedo, R. Grosse, J.F. Marshall, K. Harrington, and E. Sahai. 2007. Fibroblast-led collective invasion of carcinoma cells with differing roles for RhoGTPases in leading and following cells. *Nat Cell Biol.* 9:1392-1400.
- Gawecka, J.E., S.S. Young-Robbins, F.J. Sulzmaier, M.J. Caliva, M.M. Heikkila, M.L. Matter, and J.W. Ramos. 2012. RSK2 protein suppresses integrin activation and fibronectin matrix assembly and promotes cell migration. *J Biol Chem.* 287:43424-43437.
- Geiger, B., A. Bershadsky, R. Pankov, and K.M. Yamada. 2001. Transmembrane crosstalk between the extracellular matrix--cytoskeleton crosstalk. *Nat Rev Mol Cell Biol.* 2:793-805.
- Geiger, B., J.P. Spatz, and A.D. Bershadsky. 2009. Environmental sensing through focal adhesions. *Nat Rev Mol Cell Biol.* 10:21-33.
- Geiger, B., and K.M. Yamada. 2011. Molecular architecture and function of matrix adhesions. *Cold Spring Harb Perspect Biol.* 3.
- George, E.L., E.N. Georges-Labouesse, R.S. Patel-King, H. Rayburn, and R.O. Hynes. 1993. Defects in mesoderm, neural tube and vascular development in mouse embryos lacking fibronectin. *Development.* 119:1079-1091.
- Geraldo, S., A. Simon, N. Elkhatib, D. Louvard, L. Fetler, and D.M. Vignjevic. 2012. Do cancer cells have distinct adhesions in 3D collagen matrices and in vivo? *Eur J Cell Biol.* 91:930-937.
- Geraldo, S., A. Simon, and D.M. Vignjevic. 2013. Revealing the cytoskeletal organization of invasive cancer cells in 3D. *J Vis Exp:*e50763.
- Glentis, A., V. Gurchenkov, and D. Matic Vignjevic. 2014. Assembly, heterogeneity, and breaching of the basement membranes. *Cell Adh Migr.* 8:236-245.
- Gligorijevic, B., A. Bergman, and J. Condeelis. 2014. Multiparametric classification links tumor microenvironments with tumor cell phenotype. *PLoS Biol.* 12:e1001995.
- Gligorijevic, B., J. Wyckoff, H. Yamaguchi, Y. Wang, E.T. Roussos, and J. Condeelis. 2012. N-WASP-mediated invadopodium formation is involved in intravasation and lung metastasis of mammary tumors. *J Cell Sci.* 125:724-734.
- Goetz, J.G., P. Lajoie, S.M. Wiseman, and I.R. Nabi. 2008. Caveolin-1 in tumor progression: the good, the bad and the ugly. *Cancer Metastasis Rev.* 27:715-735.
- Goetz, J.G., S. Minguet, I. Navarro-Lerida, J.J. Lazcano, R. Samaniego, E. Calvo, M. Tello, T. Osteso-Ibanez, T. Pellinen, A. Echarri, A. Cerezo, A.J. Klein-Szanto, R. Garcia, P.J. Keely, P. Sanchez-Mateos, E. Cukierman, and M.A. Del Pozo. 2011. Biomechanical

- remodeling of the microenvironment by stromal caveolin-1 favors tumor invasion and metastasis. *Cell*. 146:148-163.
- Goicoechea, S.M., R. Garcia-Mata, J. Staub, A. Valdivia, L. Sharek, C.G. McCulloch, R.F. Hwang, R. Urrutia, J.J. Yeh, H.J. Kim, and C.A. Otey. 2014. Palladin promotes invasion of pancreatic cancer cells by enhancing invadopodia formation in cancer-associated fibroblasts. *Oncogene*. 33:1265-1273.
- Goldschmidt, M.E., K.J. McLeod, and W.R. Taylor. 2001. Integrin-mediated mechanotransduction in vascular smooth muscle cells: frequency and force response characteristics. *Circ Res*. 88:674-680.
- Gopal, S., L. Veracini, D. Grall, C. Butori, S. Schaub, S. Audebert, L. Camoin, E. Baudelet, A. Radwanska, S. Beghelli-de la Forest Divonne, S.M. Violette, P.H. Weinreb, S. Rekima, M. Ilie, A. Sudaka, P. Hofman, and E. Van Obberghen-Schilling. 2017. Fibronectin-guided migration of carcinoma collectives. *Nat Commun*. 8:14105.
- Grum-Schwensen, B., J. Klingelhofer, C.H. Berg, C. El-Naaman, M. Grigorian, E. Lukanidin, and N. Ambartsumian. 2005. Suppression of tumor development and metastasis formation in mice lacking the S100A4(mts1) gene. *Cancer Res*. 65:3772-3780.
- Gutsmann, T., G.E. Fantner, J.H. Kindt, M. Venturoni, S. Danielsen, and P.K. Hansma. 2004. Force spectroscopy of collagen fibers to investigate their mechanical properties and structural organization. *Biophys J*. 86:3186-3193.
- Haas, P., and D. Gilmour. 2006. Chemokine signaling mediates self-organizing tissue migration in the zebrafish lateral line. *Dev Cell*. 10:673-680.
- Haeger, A., K. Wolf, M.M. Zegers, and P. Friedl. 2015. Collective cell migration: guidance principles and hierarchies. *Trends Cell Biol*. 25:556-566.
- Hakkinen, K.M., J.S. Harunaga, A.D. Doyle, and K.M. Yamada. 2011. Direct comparisons of the morphology, migration, cell adhesions, and actin cytoskeleton of fibroblasts in four different three-dimensional extracellular matrices. *Tissue Eng Part A*. 17:713-724.
- Halliday, N.L., and J.J. Tomasek. 1995. Mechanical properties of the extracellular matrix influence fibronectin fibril assembly in vitro. *Exp Cell Res*. 217:109-117.
- Hanada, M., K. Tanaka, Y. Matsumoto, F. Nakatani, R. Sakimura, T. Matsunobu, X. Li, T. Okada, T. Nakamura, M. Takasaki, and Y. Iwamoto. 2005. Focal adhesion kinase is activated in invading fibrosarcoma cells and regulates metastasis. *Clin Exp Metastasis*. 22:485-494.
- Hanahan, D., and R.A. Weinberg. 2011. Hallmarks of cancer: the next generation. *Cell*. 144:646-674.
- Harada, N., Y. Tamai, T. Ishikawa, B. Sauer, K. Takaku, M. Oshima, and M.M. Taketo. 1999. Intestinal polyposis in mice with a dominant stable mutation of the beta-catenin gene. *EMBO J*. 18:5931-5942.
- Harburger, D.S., M. Bouaouina, and D.A. Calderwood. 2009. Kindlin-1 and -2 directly bind the C-terminal region of beta integrin cytoplasmic tails and exert integrin-specific activation effects. *J Biol Chem*. 284:11485-11497.
- Harris, H. 1954. Role of chemotaxis in inflammation. *Physiol Rev*. 34:529-562.
- Hart, I.R., and D. Easty. 1991. Tumor cell progression and differentiation in metastasis. *Semin Cancer Biol*. 2:87-95.
- Hart, I.R., and I.J. Fidler. 1980. Role of organ selectivity in the determination of metastatic patterns of B16 melanoma. *Cancer Res*. 40:2281-2287.
- Harunaga, J.S., and K.M. Yamada. 2011. Cell-matrix adhesions in 3D. *Matrix Biol*. 30:363-368.

- Head, J.A., D. Jiang, M. Li, L.J. Zorn, E.M. Schaefer, J.T. Parsons, and S.A. Weed. 2003. Cortactin tyrosine phosphorylation requires Rac1 activity and association with the cortical actin cytoskeleton. *Mol Biol Cell*. 14:3216-3229.
- Heath, J.P., and G.A. Dunn. 1978. Cell to substratum contacts of chick fibroblasts and their relation to the microfilament system. A correlated interference-reflexion and high-voltage electron-microscope study. *J Cell Sci*. 29:197-212.
- Heino, J. 2007. The collagen family members as cell adhesion proteins. *Bioessays*. 29:1001-1010.
- Heldin, C.H., and B. Westermark. 1999. Mechanism of action and in vivo role of platelet-derived growth factor. *Physiol Rev*. 79:1283-1316.
- Henry, L.R., H.O. Lee, J.S. Lee, A. Klein-Szanto, P. Watts, E.A. Ross, W.T. Chen, and J.D. Cheng. 2007. Clinical implications of fibroblast activation protein in patients with colon cancer. *Clin Cancer Res*. 13:1736-1741.
- Hinz, B., G. Celetta, J.J. Tomasek, G. Gabbiani, and C. Chaponnier. 2001a. Alpha-smooth muscle actin expression upregulates fibroblast contractile activity. *Mol Biol Cell*. 12:2730-2741.
- Hinz, B., G. Gabbiani, and C. Chaponnier. 2002. The NH2-terminal peptide of alpha-smooth muscle actin inhibits force generation by the myofibroblast in vitro and in vivo. *J Cell Biol*. 157:657-663.
- Hinz, B., D. Mastrangelo, C.E. Iselin, C. Chaponnier, and G. Gabbiani. 2001b. Mechanical tension controls granulation tissue contractile activity and myofibroblast differentiation. *Am J Pathol*. 159:1009-1020.
- Hirata, E., M.R. Girotti, A. Viros, S. Hooper, B. Spencer-Dene, M. Matsuda, J. Larkin, R. Marais, and E. Sahai. 2015. Intravital imaging reveals how BRAF inhibition generates drug-tolerant microenvironments with high integrin beta1/FAK signaling. *Cancer Cell*. 27:574-588.
- Hiratsuka, S., K. Nakamura, S. Iwai, M. Murakami, T. Itoh, H. Kijima, J.M. Shipley, R.M. Senior, and M. Shibuya. 2002. MMP9 induction by vascular endothelial growth factor receptor-1 is involved in lung-specific metastasis. *Cancer Cell*. 2:289-300.
- Hirschel, B.J., G. Gabbiani, G.B. Ryan, and G. Majno. 1971. Fibroblasts of granulation tissue: immunofluorescent staining with antismooth muscle serum. *Proc Soc Exp Biol Med*. 138:466-469.
- Ho, H.Y., R. Rohatgi, A.M. Lebensohn, M. Le, J. Li, S.P. Gygi, and M.W. Kirschner. 2004. Toca-1 mediates Cdc42-dependent actin nucleation by activating the N-WASP-WIP complex. *Cell*. 118:203-216.
- Hohenester, E., and J. Engel. 2002. Domain structure and organisation in extracellular matrix proteins. *Matrix Biol*. 21:115-128.
- Horton, E.R., J.D. Humphries, J. James, M.C. Jones, J.A. Askari, and M.J. Humphries. 2016. The integrin adhesome network at a glance. *J Cell Sci*. 129:4159-4163.
- Hosaka, K., Y. Yang, T. Seki, C. Fischer, O. Dubey, E. Fredlund, J. Hartman, P. Religa, H. Morikawa, Y. Ishii, M. Sasahara, O. Larsson, G. Cossu, R. Cao, S. Lim, and Y. Cao. 2016. Pericyte-fibroblast transition promotes tumor growth and metastasis. *Proc Natl Acad Sci U S A*. 113:E5618-5627.
- Hoshino, A., B. Costa-Silva, T.L. Shen, G. Rodrigues, A. Hashimoto, M. Tesic Mark, H. Molina, S. Kohsaka, A. Di Giannatale, S. Ceder, S. Singh, C. Williams, N. Soplop, K. Uryu, L. Pharmed, T. King, L. Bojmar, A.E. Davies, Y. Ararso, T. Zhang, H. Zhang, J. Hernandez,

- J.M. Weiss, V.D. Dumont-Cole, K. Kramer, L.H. Wexler, A. Narendran, G.K. Schwartz, J.H. Healey, P. Sandstrom, K.J. Labori, E.H. Kure, P.M. Grandgenett, M.A. Hollingsworth, M. de Sousa, S. Kaur, M. Jain, K. Mallya, S.K. Batra, W.R. Jarnagin, M.S. Brady, O. Fodstad, V. Muller, K. Pantel, A.J. Minn, M.J. Bissell, B.A. Garcia, Y. Kang, V.K. Rajasekhar, C.M. Ghajar, I. Matei, H. Peinado, J. Bromberg, and D. Lyden. 2015. Tumour exosome integrins determine organotropic metastasis. *Nature*. 527:329-335.
- Hotary, K., X.Y. Li, E. Allen, S.L. Stevens, and S.J. Weiss. 2006. A cancer cell metalloprotease triad regulates the basement membrane transmigration program. *Genes Dev*. 20:2673-2686.
- Hotary, K.B., E.D. Allen, P.C. Brooks, N.S. Datta, M.W. Long, and S.J. Weiss. 2003. Membrane type I matrix metalloproteinase usurps tumor growth control imposed by the three-dimensional extracellular matrix. *Cell*. 114:33-45.
- Huang, W., R. Chiquet-Ehrismann, J.V. Moyano, A. Garcia-Pardo, and G. Orend. 2001. Interference of tenascin-C with syndecan-4 binding to fibronectin blocks cell adhesion and stimulates tumor cell proliferation. *Cancer Res*. 61:8586-8594.
- Hughes, P.E., F. Diaz-Gonzalez, L. Leong, C. Wu, J.A. McDonald, S.J. Shattil, and M.H. Ginsberg. 1996. Breaking the integrin hinge. A defined structural constraint regulates integrin signaling. *J Biol Chem*. 271:6571-6574.
- Hulmes, D.J. 2002. Building collagen molecules, fibrils, and suprafibrillar structures. *J Struct Biol*. 137:2-10.
- Humphries, J.D., A. Byron, and M.J. Humphries. 2006. Integrin ligands at a glance. *J Cell Sci*. 119:3901-3903.
- Hynes, R. 1985. Molecular biology of fibronectin. *Annu Rev Cell Biol*. 1:67-90.
- Hynes, R.O. 2002. Integrins: bidirectional, allosteric signaling machines. *Cell*. 110:673-687.
- Hynes, R.O. 2009. The extracellular matrix: not just pretty fibrils. *Science*. 326:1216-1219.
- Hynes, R.O., and A. Naba. 2012. Overview of the matrisome--an inventory of extracellular matrix constituents and functions. *Cold Spring Harb Perspect Biol*. 4:a004903.
- Insall, R.H. 2010. Understanding eukaryotic chemotaxis: a pseudopod-centred view. *Nat Rev Mol Cell Biol*. 11:453-458.
- Itzkowitz, S.H., and X. Yio. 2004. Inflammation and cancer IV. Colorectal cancer in inflammatory bowel disease: the role of inflammation. *Am J Physiol Gastrointest Liver Physiol*. 287:G7-17.
- Izumi, D., T. Ishimoto, K. Miyake, H. Sugihara, K. Eto, H. Sawayama, T. Yasuda, Y. Kiyozumi, T. Kaida, J. Kurashige, Y. Imamura, Y. Hiyoshi, M. Iwatsuki, S. Iwagami, Y. Baba, Y. Sakamoto, Y. Miyamoto, N. Yoshida, M. Watanabe, H. Takamori, N. Araki, P. Tan, and H. Baba. 2016. CXCL12/CXCR4 activation by cancer-associated fibroblasts promotes integrin beta1 clustering and invasiveness in gastric cancer. *Int J Cancer*. 138:1207-1219.
- Izzard, C.S., and L.R. Lochner. 1976. Cell-to-substrate contacts in living fibroblasts: an interference reflexion study with an evaluation of the technique. *J Cell Sci*. 21:129-159.
- Jacob, K., M. Webber, D. Benayahu, and H.K. Kleinman. 1999. Osteonectin promotes prostate cancer cell migration and invasion: a possible mechanism for metastasis to bone. *Cancer Res*. 59:4453-4457.
- Jerrell, R.J., and A. Parekh. 2014. Cellular traction stresses mediate extracellular matrix degradation by invadopodia. *Acta Biomater*. 10:1886-1896.

- Jodele, S., L. Blavier, J.M. Yoon, and Y.A. DeClerck. 2006. Modifying the soil to affect the seed: role of stromal-derived matrix metalloproteinases in cancer progression. *Cancer Metastasis Rev.* 25:35-43.
- Jotzu, C., E. Alt, G. Welte, J. Li, B.T. Hennessy, E. Devarajan, S. Krishnappa, S. Pinilla, L. Droll, and Y.H. Song. 2010. Adipose tissue-derived stem cells differentiate into carcinoma-associated fibroblast-like cells under the influence of tumor-derived factors. *Anal Cell Pathol (Amst).* 33:61-79.
- Joyce, J.A., and J.W. Pollard. 2009. Microenvironmental regulation of metastasis. *Nat Rev Cancer.* 9:239-252.
- Juin, A., J. Di Martino, B. Leitinger, E. Henriët, A.S. Gary, L. Paysan, J. Bomo, G. Baffet, C. Gauthier-Rouvière, J. Rosenbaum, V. Moreau, and F. Saltel. 2014. Discoidin domain receptor 1 controls linear invadosome formation via a Cdc42-Tuba pathway. *J Cell Biol.* 207:517-533.
- Kalluri, R. 2016. The biology and function of fibroblasts in cancer. *Nat Rev Cancer.* 16:582-598.
- Kalluri, R., and M. Zeisberg. 2006. Fibroblasts in cancer. *Nat Rev Cancer.* 6:392-401.
- Kanchanawong, P., G. Shtengel, A.M. Pasapera, E.B. Ramko, M.W. Davidson, H.F. Hess, and C.M. Waterman. 2010. Nanoscale architecture of integrin-based cell adhesions. *Nature.* 468:580-584.
- Kang, F., Z. Wang, G. Li, S. Wang, D. Liu, M. Zhang, M. Zhao, W. Yang, and J. Wang. 2017. Inter-heterogeneity and intra-heterogeneity of alpha v beta 3 in non-small cell lung cancer and small cell lung cancer patients as revealed by 68Ga-RGD2 PET imaging. *Eur J Nucl Med Mol Imaging.*
- Kaplan, R.N., S. Rafii, and D. Lyden. 2006. Preparing the "soil": the premetastatic niche. *Cancer Res.* 66:11089-11093.
- Kaplan, R.N., R.D. Riba, S. Zacharoulis, A.H. Bramley, L. Vincent, C. Costa, D.D. MacDonald, D.K. Jin, K. Shido, S.A. Kerns, Z. Zhu, D. Hicklin, Y. Wu, J.L. Port, N. Altorki, E.R. Port, D. Ruggero, S.V. Shmelkov, K.K. Jensen, S. Rafii, and D. Lyden. 2005. VEGFR1-positive haematopoietic bone marrow progenitors initiate the pre-metastatic niche. *Nature.* 438:820-827.
- Karnoub, A.E., A.B. Dash, A.P. Vo, A. Sullivan, M.W. Brooks, G.W. Bell, A.L. Richardson, K. Polyak, R. Tubo, and R.A. Weinberg. 2007. Mesenchymal stem cells within tumour stroma promote breast cancer metastasis. *Nature.* 449:557-563.
- Katagiri, K., A. Maeda, M. Shimonaka, and T. Kinashi. 2003. RAPL, a Rap1-binding molecule that mediates Rap1-induced adhesion through spatial regulation of LFA-1. *Nat Immunol.* 4:741-748.
- Katz, M., I. Amit, A. Citri, T. Shay, S. Carvalho, S. Lavi, F. Milanezi, L. Lyass, N. Amariglio, J. Jacob-Hirsch, N. Ben-Chetrit, G. Tarcic, M. Lindzen, R. Avraham, Y.C. Liao, P. Trusk, A. Lyass, G. Rechavi, N.L. Spector, S.H. Lo, F. Schmitt, S.S. Bacus, and Y. Yarden. 2007. A reciprocal tensin-3-cten switch mediates EGF-driven mammary cell migration. *Nat Cell Biol.* 9:961-969.
- Kedrin, D., B. Gligorićević, J. Wyckoff, V.V. Verkhusha, J. Condeelis, J.E. Segall, and J. van Rheenen. 2008. Intravital imaging of metastatic behavior through a mammary imaging window. *Nat Methods.* 5:1019-1021.
- Khamis, Z.I., Z.J. Sahab, and Q.X. Sang. 2012. Active roles of tumor stroma in breast cancer metastasis. *Int J Breast Cancer.* 2012:574025.

- Kiema, T., Y. Lad, P. Jiang, C.L. Oxley, M. Baldassarre, K.L. Wegener, I.D. Campbell, J. Ylanne, and D.A. Calderwood. 2006. The molecular basis of filamin binding to integrins and competition with talin. *Mol Cell*. 21:337-347.
- Kim, M., C.V. Carman, and T.A. Springer. 2003. Bidirectional transmembrane signaling by cytoplasmic domain separation in integrins. *Science*. 301:1720-1725.
- Kim, N.G., and B.M. Gumbiner. 2015. Adhesion to fibronectin regulates Hippo signaling via the FAK-Src-PI3K pathway. *J Cell Biol*. 210:503-515.
- King, S.J., and M. Parsons. 2011. Imaging cells within 3D cell-derived matrix. *Methods Mol Biol*. 769:53-64.
- Kinley, A.W., S.A. Weed, A.M. Weaver, A.V. Karginov, E. Bissonette, J.A. Cooper, and J.T. Parsons. 2003. Cortactin interacts with WIP in regulating Arp2/3 activation and membrane protrusion. *Curr Biol*. 13:384-393.
- Kinnman, N., R. Hultcrantz, V. Barbu, C. Rey, D. Wendum, R. Poupon, and C. Housset. 2000. PDGF-mediated chemoattraction of hepatic stellate cells by bile duct segments in cholestatic liver injury. *Lab Invest*. 80:697-707.
- Kiosses, W.B., S.J. Shattil, N. Pampori, and M.A. Schwartz. 2001. Rac recruits high-affinity integrin α v β 3 to lamellipodia in endothelial cell migration. *Nat Cell Biol*. 3:316-320.
- Klass, C.M., J.R. Couchman, and A. Woods. 2000. Control of extracellular matrix assembly by syndecan-2 proteoglycan. *J Cell Sci*. 113 (Pt 3):493-506.
- Kojima, Y., A. Acar, E.N. Eaton, K.T. Mellody, C. Scheel, I. Ben-Porath, T.T. Onder, Z.C. Wang, A.L. Richardson, R.A. Weinberg, and A. Orimo. 2010. Autocrine TGF-beta and stromal cell-derived factor-1 (SDF-1) signaling drives the evolution of tumor-promoting mammary stromal myofibroblasts. *Proc Natl Acad Sci U S A*. 107:20009-20014.
- Kopanska, K.S., Y. Alcheikh, R. Staneva, D. Vignjevic, and T. Betz. 2016. Tensile Forces Originating from Cancer Spheroids Facilitate Tumor Invasion. *PLoS One*. 11:e0156442.
- Kriebel, P.W., V.A. Barr, E.C. Rericha, G. Zhang, and C.A. Parent. 2008. Collective cell migration requires vesicular trafficking for chemoattractant delivery at the trailing edge. *J Cell Biol*. 183:949-961.
- Kubow, K.E., and A.R. Horwitz. 2011. Reducing background fluorescence reveals adhesions in 3D matrices. *Nat Cell Biol*. 13:3-5; author reply 5-7.
- Labernadie, A., T. Kato, A. Brugues, X. Serra-Picamal, S. Derzsi, E. Arwert, A. Weston, V. Gonzalez-Tarrago, A. Elosegui-Artola, L. Albertazzi, J. Alcaraz, P. Roca-Cusachs, E. Sahai, and X. Trepat. 2017. A mechanically active heterotypic E-cadherin/N-cadherin adhesion enables fibroblasts to drive cancer cell invasion. *Nat Cell Biol*. 19:224-237.
- Ladoux, B., R.M. Mege, and X. Trepat. 2016. Front-Rear Polarization by Mechanical Cues: From Single Cells to Tissues. *Trends Cell Biol*. 26:420-433.
- Lafuente, E.M., A.A. van Puijenbroek, M. Krause, C.V. Carman, G.J. Freeman, A. Berezovskaya, E. Constantine, T.A. Springer, F.B. Gertler, and V.A. Boussiotis. 2004. RIAM, an Ena/VASP and Profilin ligand, interacts with Rap1-GTP and mediates Rap1-induced adhesion. *Dev Cell*. 7:585-595.
- Lammermann, T., B.L. Bader, S.J. Monkley, T. Worbs, R. Wedlich-Soldner, K. Hirsch, M. Keller, R. Forster, D.R. Critchley, R. Fassler, and M. Sixt. 2008. Rapid leukocyte migration by integrin-independent flowing and squeezing. *Nature*. 453:51-55.
- Lange, J.R., and B. Fabry. 2013. Cell and tissue mechanics in cell migration. *Exp Cell Res*. 319:2418-2423.

- LeBleu, V.S., B. Macdonald, and R. Kalluri. 2007. Structure and function of basement membranes. *Exp Biol Med (Maywood)*. 232:1121-1129.
- LeBleu, V.S., G. Taduri, J. O'Connell, Y. Teng, V.G. Cooke, C. Woda, H. Sugimoto, and R. Kalluri. 2013. Origin and function of myofibroblasts in kidney fibrosis. *Nat Med*. 19:1047-1053.
- Lecaudey, V., G. Cakan-Akdogan, W.H. Norton, and D. Gilmour. 2008. Dynamic Fgf signaling couples morphogenesis and migration in the zebrafish lateral line primordium. *Development*. 135:2695-2705.
- Lee, H.O., S.R. Mullins, J. Franco-Barraza, M. Valianou, E. Cukierman, and J.D. Cheng. 2011. FAP-overexpressing fibroblasts produce an extracellular matrix that enhances invasive velocity and directionality of pancreatic cancer cells. *BMC Cancer*. 11:245.
- Leiss, M., K. Beckmann, A. Giros, M. Costell, and R. Fassler. 2008. The role of integrin binding sites in fibronectin matrix assembly in vivo. *Curr Opin Cell Biol*. 20:502-507.
- Leitinger, B., and E. Hohenester. 2007. Mammalian collagen receptors. *Matrix Biol*. 26:146-155.
- Levental, K.R., H. Yu, L. Kass, J.N. Lakins, M. Egeblad, J.T. Erler, S.F. Fong, K. Csiszar, A. Giaccia, W. Weninger, M. Yamauchi, D.L. Gasser, and V.M. Weaver. 2009. Matrix crosslinking forces tumor progression by enhancing integrin signaling. *Cell*. 139:891-906.
- Lewis, D.M., K.M. Park, V. Tang, Y. Xu, K. Pak, T.S. Eisinger-Mathason, M.C. Simon, and S. Gerecht. 2016. Intratumoral oxygen gradients mediate sarcoma cell invasion. *Proc Natl Acad Sci U S A*. 113:9292-9297.
- Li, L., R. Hartley, B. Reiss, Y. Sun, J. Pu, D. Wu, F. Lin, T. Hoang, S. Yamada, J. Jiang, and M. Zhao. 2012. E-cadherin plays an essential role in collective directional migration of large epithelial sheets. *Cell Mol Life Sci*. 69:2779-2789.
- Li, W., D.G. Metcalf, R. Gorelik, R. Li, N. Mitra, V. Nanda, P.B. Law, J.D. Lear, W.F. Degrado, and J.S. Bennett. 2005. A push-pull mechanism for regulating integrin function. *Proc Natl Acad Sci U S A*. 102:1424-1429.
- Lilja, J., T. Zacharchenko, M. Georgiadou, G. Jacquemet, N. Franceschi, E. Peuhu, H. Hamidi, J. Pouwels, V. Martens, F.H. Nia, M. Beifuss, T. Boeckers, H.J. Kreienkamp, I.L. Barsukov, and J. Ivaska. 2017. SHANK proteins limit integrin activation by directly interacting with Rap1 and R-Ras. *Nat Cell Biol*. 19:292-305.
- Lindblom, P., H. Gerhardt, S. Liebner, A. Abramsson, M. Enge, M. Hellstrom, G. Backstrom, S. Fredriksson, U. Landegren, H.C. Nystrom, G. Bergstrom, E. Dejana, A. Ostman, P. Lindahl, and C. Betsholtz. 2003. Endothelial PDGF-B retention is required for proper investment of pericytes in the microvessel wall. *Genes Dev*. 17:1835-1840.
- Linder, S. 2007. The matrix corroded: podosomes and invadopodia in extracellular matrix degradation. *Trends Cell Biol*. 17:107-117.
- Linder, S., D. Nelson, M. Weiss, and M. Aepfelbacher. 1999. Wiskott-Aldrich syndrome protein regulates podosomes in primary human macrophages. *Proc Natl Acad Sci U S A*. 96:9648-9653.
- Liu, Q., and B. Song. 2014. Electric field regulated signaling pathways. *Int J Biochem Cell Biol*. 55:264-268.
- Liu, S., D.A. Calderwood, and M.H. Ginsberg. 2000. Integrin cytoplasmic domain-binding proteins. *J Cell Sci*. 113 (Pt 20):3563-3571.

- Lizarraga, F., R. Poincloux, M. Romao, G. Montagnac, G. Le Dez, I. Bonne, G. Rigai, G. Raposo, and P. Chavrier. 2009. Diaphanous-related formins are required for invadopodia formation and invasion of breast tumor cells. *Cancer Res.* 69:2792-2800.
- Lo, C.M., H.B. Wang, M. Dembo, and Y.L. Wang. 2000. Cell movement is guided by the rigidity of the substrate. *Biophys J.* 79:144-152.
- Lombardi, G., A. Pambuku, L. Bellu, M. Farina, A. Della Puppa, L. Denaro, and V. Zagonel. 2017. Effectiveness of antiangiogenic drugs in glioblastoma patients: A systematic review and meta-analysis of randomized clinical trials. *Crit Rev Oncol Hematol.* 111:94-102.
- Lu, C., X. Sun, L. Sun, J. Sun, Y. Lu, X. Yu, L. Zhou, and X. Gao. 2013. Snail mediates PDGF-BB-induced invasion of rat bone marrow mesenchymal stem cells in 3D collagen and chick chorioallantoic membrane. *J Cell Physiol.* 228:1827-1833.
- Lu, P., K. Takai, V.M. Weaver, and Z. Werb. 2011. Extracellular matrix degradation and remodeling in development and disease. *Cold Spring Harb Perspect Biol.* 3.
- Lu, P., V.M. Weaver, and Z. Werb. 2012. The extracellular matrix: a dynamic niche in cancer progression. *J Cell Biol.* 196:395-406.
- Luga, V., L. Zhang, A.M. Vitoria-Petit, A.A. Ogunjimi, M.R. Inanlou, E. Chiu, M. Buchanan, A.N. Hosein, M. Basik, and J.L. Wrana. 2012. Exosomes mediate stromal mobilization of autocrine Wnt-PCP signaling in breast cancer cell migration. *Cell.* 151:1542-1556.
- Luo, B.H., C.V. Carman, J. Takagi, and T.A. Springer. 2005. Disrupting integrin transmembrane domain heterodimerization increases ligand binding affinity, not valency or clustering. *Proc Natl Acad Sci U S A.* 102:3679-3684.
- Luo, B.H., T.A. Springer, and J. Takagi. 2004. A specific interface between integrin transmembrane helices and affinity for ligand. *PLoS Biol.* 2:e153.
- Ma, Y.Q., J. Qin, C. Wu, and E.F. Plow. 2008. Kindlin-2 (Mig-2): a co-activator of beta3 integrins. *J Cell Biol.* 181:439-446.
- Maiuri, P., J.F. Rupprecht, S. Wieser, V. Rupprecht, O. Benichou, N. Carpi, M. Coppey, S. De Beco, N. Gov, C.P. Heisenberg, C. Lage Crespo, F. Lautenschlaeger, M. Le Berre, A.M. Lennon-Dumenil, M. Raab, H.R. Thiam, M. Piel, M. Sixt, and R. Voituriez. 2015. Actin flows mediate a universal coupling between cell speed and cell persistence. *Cell.* 161:374-386.
- Majno, G., G. Gabbiani, B.J. Hirschel, G.B. Ryan, and P.R. Statkov. 1971. Contraction of granulation tissue in vitro: similarity to smooth muscle. *Science.* 173:548-550.
- Markowitz, S.D., and M.M. Bertagnolli. 2009. Molecular origins of cancer: Molecular basis of colorectal cancer. *N Engl J Med.* 361:2449-2460.
- Martin, K., M. Vilela, N.L. Jeon, G. Danuser, and O. Pertz. 2014. A growth factor-induced, spatially organizing cytoskeletal module enables rapid and persistent fibroblast migration. *Dev Cell.* 30:701-716.
- McDonald, J.A., E.M. Pinheiro, L. Kadlec, T. Schupbach, and D.J. Montell. 2006. Multiple EGFR ligands participate in guiding migrating border cells. *Dev Biol.* 296:94-103.
- Mecham, R.P. 2012. Overview of extracellular matrix. *Curr Protoc Cell Biol.* Chapter 10:Unit 10 11.
- Medema, J.P., and L. Vermeulen. 2011. Microenvironmental regulation of stem cells in intestinal homeostasis and cancer. *Nature.* 474:318-326.

- Midwood, K.S., L.V. Valenick, H.C. Hsia, and J.E. Schwarzbauer. 2004. Coregulation of fibronectin signaling and matrix contraction by tenascin-C and syndecan-4. *Mol Biol Cell*. 15:5670-5677.
- Mishra, P.J., R. Humeniuk, D.J. Medina, G. Alexe, J.P. Mesirov, S. Ganesan, J.W. Glod, and D. Banerjee. 2008. Carcinoma-associated fibroblast-like differentiation of human mesenchymal stem cells. *Cancer Res*. 68:4331-4339.
- Miyamoto, S., H. Teramoto, O.A. Coso, J.S. Gutkind, P.D. Burbelo, S.K. Akiyama, and K.M. Yamada. 1995. Integrin function: molecular hierarchies of cytoskeletal and signaling molecules. *J Cell Biol*. 131:791-805.
- Monsky, W.L., C.Y. Lin, A. Aoyama, T. Kelly, S.K. Akiyama, S.C. Mueller, and W.T. Chen. 1994. A potential marker protease of invasiveness, seprase, is localized on invadopodia of human malignant melanoma cells. *Cancer Res*. 54:5702-5710.
- Montanez, E., S. Ussar, M. Schifferer, M. Bosl, R. Zent, M. Moser, and R. Fassler. 2008. Kindlin-2 controls bidirectional signaling of integrins. *Genes Dev*. 22:1325-1330.
- Monteiro, P., C. Rosse, A. Castro-Castro, M. Ironelle, E. Lagoutte, P. Paul-Gilloteaux, C. Desnos, E. Formstecher, F. Darchen, D. Perrais, A. Gautreau, M. Hertzog, and P. Chavrier. 2013. Endosomal WASH and exocyst complexes control exocytosis of MT1-MMP at invadopodia. *J Cell Biol*. 203:1063-1079.
- Morgan, M.R., H. Hamidi, M.D. Bass, S. Warwood, C. Ballestrem, and M.J. Humphries. 2013. Syndecan-4 phosphorylation is a control point for integrin recycling. *Dev Cell*. 24:472-485.
- Morgan, M.R., M.J. Humphries, and M.D. Bass. 2007. Synergistic control of cell adhesion by integrins and syndecans. *Nat Rev Mol Cell Biol*. 8:957-969.
- Morrissey, M.A., and D.R. Sherwood. 2015. An active role for basement membrane assembly and modification in tissue sculpting. *J Cell Sci*. 128:1661-1668.
- Moser, M., B. Nieswandt, S. Ussar, M. Pozgajova, and R. Fassler. 2008. Kindlin-3 is essential for integrin activation and platelet aggregation. *Nat Med*. 14:325-330.
- Mosesson, M.W., and D.L. Amrani. 1980. The structure and biologic activities of plasma fibronectin. *Blood*. 56:145-158.
- Mouw, J.K., G. Ou, and V.M. Weaver. 2014. Extracellular matrix assembly: a multiscale deconstruction. *Nat Rev Mol Cell Biol*. 15:771-785.
- Mueller, S.C., G. Gherzi, S.K. Akiyama, Q.X. Sang, L. Howard, M. Pineiro-Sanchez, H. Nakahara, Y. Yeh, and W.T. Chen. 1999. A novel protease-docking function of integrin at invadopodia. *J Biol Chem*. 274:24947-24952.
- Naik, U.P., P.M. Patel, and L.V. Parise. 1997. Identification of a novel calcium-binding protein that interacts with the integrin alphaIIb cytoplasmic domain. *J Biol Chem*. 272:4651-4654.
- Nevo, J., A. Mai, S. Tuomi, T. Pellinen, O.T. Pentikainen, P. Heikkila, J. Lundin, H. Joensuu, P. Bono, and J. Ivaska. 2010. Mammary-derived growth inhibitor (MDGI) interacts with integrin alpha-subunits and suppresses integrin activity and invasion. *Oncogene*. 29:6452-6463.
- Nevo, J., E. Mattila, T. Pellinen, D.L. Yamamoto, H. Sara, K. Iljin, O. Kallioniemi, P. Bono, P. Heikkila, H. Joensuu, A. Warri, and J. Ivaska. 2009. Mammary-derived growth inhibitor alters traffic of EGFR and induces a novel form of cetuximab resistance. *Clin Cancer Res*. 15:6570-6581.

- Ng, T., D. Shima, A. Squire, P.I. Bastiaens, S. Gschmeissner, M.J. Humphries, and P.J. Parker. 1999. PKC α regulates beta1 integrin-dependent cell motility through association and control of integrin traffic. *EMBO J.* 18:3909-3923.
- Nguyen-Ngoc, K.V., K.J. Cheung, A. Brenot, E.R. Shamir, R.S. Gray, W.C. Hines, P. Yaswen, Z. Werb, and A.J. Ewald. 2012. ECM microenvironment regulates collective migration and local dissemination in normal and malignant mammary epithelium. *Proc Natl Acad Sci U S A.* 109:E2595-2604.
- Nobes, C.D., and A. Hall. 1995. Rho, rac, and cdc42 GTPases regulate the assembly of multimolecular focal complexes associated with actin stress fibers, lamellipodia, and filopodia. *Cell.* 81:53-62.
- O'Connell, J.T., H. Sugimoto, V.G. Cooke, B.A. MacDonald, A.I. Mehta, V.S. LeBleu, R. Dewar, R.M. Rocha, R.R. Brentani, M.B. Resnick, E.G. Neilson, M. Zeisberg, and R. Kalluri. 2011. VEGF-A and Tenascin-C produced by S100A4+ stromal cells are important for metastatic colonization. *Proc Natl Acad Sci U S A.* 108:16002-16007.
- Orimo, A., P.B. Gupta, D.C. Sgroi, F. Arenzana-Seisdedos, T. Delaunay, R. Naeem, V.J. Carey, A.L. Richardson, and R.A. Weinberg. 2005. Stromal fibroblasts present in invasive human breast carcinomas promote tumor growth and angiogenesis through elevated SDF-1/CXCL12 secretion. *Cell.* 121:335-348.
- Oskarsson, T., S. Acharyya, X.H. Zhang, S. Vanharanta, S.F. Tavazoie, P.G. Morris, R.J. Downey, K. Manova-Todorova, E. Brogi, and J. Massague. 2011. Breast cancer cells produce tenascin C as a metastatic niche component to colonize the lungs. *Nat Med.* 17:867-874.
- Osornio-Vargas, A.R., P.M. Lindroos, P.G. Coin, A. Badgett, N.A. Hernandez-Rodriguez, and J.C. Bonner. 1996. Maximal PDGF-induced lung fibroblast chemotaxis requires PDGF receptor-alpha. *Am J Physiol.* 271:L93-99.
- Otranto, M., V. Sarrazy, F. Bonte, B. Hinz, G. Gabbiani, and A. Desmouliere. 2012. The role of the myofibroblast in tumor stroma remodeling. *Cell Adh Migr.* 6:203-219.
- Oudin, M.J., O. Jonas, T. Kosciuk, L.C. Broye, B.C. Guido, J. Wyckoff, D. Riquelme, J.M. Lamar, S.B. Asokan, C. Whittaker, D. Ma, R. Langer, M.J. Cima, K.B. Wisinski, R.O. Hynes, D.A. Lauffenburger, P.J. Keely, J.E. Bear, and F.B. Gertler. 2016a. Tumor Cell-Driven Extracellular Matrix Remodeling Drives Haptotaxis during Metastatic Progression. *Cancer Discov.* 6:516-531.
- Oudin, M.J., O. Jonas, T. Kosciuk, L.C. Broye, B.C. Guido, J. Wyckoff, D. Riquelme, J.M. Lamar, S.B. Asokan, C. Whittaker, D. Ma, R. Langer, M.J. Cima, K.B. Wisinski, R.O. Hynes, D.A. Lauffenburger, P.J. Keely, J.E. Bear, and F.B. Gertler. 2016b. Tumor cell-driven extracellular matrix remodeling enables haptotaxis during metastatic progression. *Cancer Discov.*
- Overall, C.M., and O. Kleifeld. 2006. Tumour microenvironment - opinion: validating matrix metalloproteinases as drug targets and anti-targets for cancer therapy. *Nat Rev Cancer.* 6:227-239.
- Oxley, C.L., N.J. Anthis, E.D. Lowe, I. Vakonakis, I.D. Campbell, and K.L. Wegener. 2008. An integrin phosphorylation switch: the effect of beta3 integrin tail phosphorylation on Dok1 and talin binding. *J Biol Chem.* 283:5420-5426.
- Oyanagi, J., N. Kojima, H. Sato, S. Higashi, K. Kikuchi, K. Sakai, K. Matsumoto, and K. Miyazaki. 2014. Inhibition of transforming growth factor-beta signaling potentiates

- tumor cell invasion into collagen matrix induced by fibroblast-derived hepatocyte growth factor. *Exp Cell Res.* 326:267-279.
- Ozdemir, B.C., T. Pentcheva-Hoang, J.L. Carstens, X. Zheng, C.C. Wu, T.R. Simpson, H. Laklai, H. Sugimoto, C. Kahlert, S.V. Novitskiy, A. De Jesus-Acosta, P. Sharma, P. Heidari, U. Mahmood, L. Chin, H.L. Moses, V.M. Weaver, A. Maitra, J.P. Allison, V.S. LeBleu, and R. Kalluri. 2014. Depletion of carcinoma-associated fibroblasts and fibrosis induces immunosuppression and accelerates pancreas cancer with reduced survival. *Cancer Cell.* 25:719-734.
- Page-McCaw, A., A.J. Ewald, and Z. Werb. 2007. Matrix metalloproteinases and the regulation of tissue remodelling. *Nat Rev Mol Cell Biol.* 8:221-233.
- Pankov, R., E. Cukierman, B.Z. Katz, K. Matsumoto, D.C. Lin, S. Lin, C. Hahn, and K.M. Yamada. 2000. Integrin dynamics and matrix assembly: tensin-dependent translocation of alpha(5)beta(1) integrins promotes early fibronectin fibrillogenesis. *J Cell Biol.* 148:1075-1090.
- Pankov, R., and K.M. Yamada. 2002. Fibronectin at a glance. *J Cell Sci.* 115:3861-3863.
- Pankova, D., Y. Chen, M. Terajima, M.J. Schliekelman, B.N. Baird, M. Fahrenholtz, L. Sun, B.J. Gill, T.J. Vadakkan, M.P. Kim, Y.H. Ahn, J.D. Roybal, X. Liu, E.R. Parra Cuentas, J. Rodriguez, Wistuba, II, C.J. Creighton, D.L. Gibbons, J.M. Hicks, M.E. Dickinson, J.L. West, K.J. Grande-Allen, S.M. Hanash, M. Yamauchi, and J.M. Kurie. 2016. Cancer-Associated Fibroblasts Induce a Collagen Cross-link Switch in Tumor Stroma. *Mol Cancer Res.* 14:287-295.
- Park, J.E., M.C. Lenter, R.N. Zimmermann, P. Garin-Chesa, L.J. Old, and W.J. Rettig. 1999. Fibroblast activation protein, a dual specificity serine protease expressed in reactive human tumor stromal fibroblasts. *J Biol Chem.* 274:36505-36512.
- Parsons, M., M.D. Keppler, A. Kline, A. Messent, M.J. Humphries, R. Gilchrist, I.R. Hart, C. Quittau-Prevostel, W.E. Hughes, P.J. Parker, and T. Ng. 2002. Site-directed perturbation of protein kinase C- integrin interaction blocks carcinoma cell chemotaxis. *Mol Cell Biol.* 22:5897-5911.
- Partridge, A.W., S. Liu, S. Kim, J.U. Bowie, and M.H. Ginsberg. 2005. Transmembrane domain helix packing stabilizes integrin alphaIIb beta3 in the low affinity state. *J Biol Chem.* 280:7294-7300.
- Paszek, M.J., N. Zahir, K.R. Johnson, J.N. Lakin, G.I. Rozenberg, A. Gefen, C.A. Reinhart-King, S.S. Margulies, M. Dembo, D. Boettiger, D.A. Hammer, and V.M. Weaver. 2005. Tensional homeostasis and the malignant phenotype. *Cancer Cell.* 8:241-254.
- Pellinen, T., A. Arjonen, K. Vuoriluoto, K. Kallio, J.A. Fransen, and J. Ivaska. 2006. Small GTPase Rab21 regulates cell adhesion and controls endosomal traffic of beta1-integrins. *J Cell Biol.* 173:767-780.
- Peterson, F.C., Q. Deng, M. Zettl, K.E. Prehoda, W.A. Lim, M. Way, and B.F. Volkman. 2007. Multiple WASP-interacting protein recognition motifs are required for a functional interaction with N-WASP. *J Biol Chem.* 282:8446-8453.
- Petroll, W.M., L. Ma, and J.V. Jester. 2003. Direct correlation of collagen matrix deformation with focal adhesion dynamics in living corneal fibroblasts. *J Cell Sci.* 116:1481-1491.
- Petropoulos, C., C. Oddou, A. Emadali, E. Hiriart-Bryant, C. Boyault, E. Faurobert, S. Vande Pol, J.R. Kim-Kaneyama, A. Kraut, Y. Coute, M. Block, C. Albiges-Rizo, and O. Destaing. 2016. Roles of paxillin family members in adhesion and ECM degradation coupling at invadosomes. *J Cell Biol.* 213:585-599.

- Peuhu, E., R. Kaukonen, M. Lerche, M. Saari, C. Guzman, P. Rantakari, N. De Franceschi, A. Warri, M. Georgiadou, G. Jacquemet, E. Mattila, R. Virtakoivu, Y. Liu, Y. Attieh, K.A. Silva, T. Betz, J.P. Sundberg, M. Salmi, M.A. Deugnier, K.W. Eliceiri, and J. Ivaska. 2017. SHARPIN regulates collagen architecture and ductal outgrowth in the developing mouse mammary gland. *EMBO J.* 36:165-182.
- Peyrol, S., M. Raccurt, F. Gerard, C. Gleyzal, J.A. Grimaud, and P. Sommer. 1997. Lysyl oxidase gene expression in the stromal reaction to in situ and invasive ductal breast carcinoma. *Am J Pathol.* 150:497-507.
- Philippar, U., E.T. Roussos, M. Oser, H. Yamaguchi, H.D. Kim, S. Giampieri, Y. Wang, S. Goswami, J.B. Wyckoff, D.A. Lauffenburger, E. Sahai, J.S. Condeelis, and F.B. Gertler. 2008. A Mena invasion isoform potentiates EGF-induced carcinoma cell invasion and metastasis. *Dev Cell.* 15:813-828.
- Pietras, K., J. Pahler, G. Bergers, and D. Hanahan. 2008. Functions of paracrine PDGF signaling in the proangiogenic tumor stroma revealed by pharmacological targeting. *PLoS Med.* 5:e19.
- Pinzani, M., S. Milani, C. Grappone, F.L. Weber, Jr., P. Gentilini, and H.E. Abboud. 1994. Expression of platelet-derived growth factor in a model of acute liver injury. *Hepatology.* 19:701-707.
- Plotnikov, S.V., A.M. Pasapera, B. Sabass, and C.M. Waterman. 2012. Force fluctuations within focal adhesions mediate ECM-rigidity sensing to guide directed cell migration. *Cell.* 151:1513-1527.
- Plutoni, C., E. Bazellieres, M. Le Borgne-Rochet, F. Comunale, A. Brugues, M. Seveno, D. Planchon, S. Thuault, N. Morin, S. Bodin, X. Trepas, and C. Gauthier-Rouviere. 2016. P-cadherin promotes collective cell migration via a Cdc42-mediated increase in mechanical forces. *J Cell Biol.* 212:199-217.
- Poincloux, R., F. Lizarraga, and P. Chavrier. 2009. Matrix invasion by tumour cells: a focus on MT1-MMP trafficking to invadopodia. *J Cell Sci.* 122:3015-3024.
- Pollard, T.D., and G.G. Borisy. 2003. Cellular motility driven by assembly and disassembly of actin filaments. *Cell.* 112:453-465.
- Posner, J.B. 1977. Management of central nervous system metastases. *Semin Oncol.* 4:81-91.
- Pouwels, J., J. Nevo, T. Pellinen, J. Ylanne, and J. Ivaska. 2012. Negative regulators of integrin activity. *J Cell Sci.* 125:3271-3280.
- Powell, D.W., P.A. Adegboyega, J.F. Di Mari, and R.C. Mifflin. 2005. Epithelial cells and their neighbors I. Role of intestinal myofibroblasts in development, repair, and cancer. *Am J Physiol Gastrointest Liver Physiol.* 289:G2-7.
- Qin, Z., J. Feng, Y. Liu, L.L. Deng, and C. Lu. 2015. PDGF-D promotes dermal fibroblast invasion in 3-dimensional extracellular matrix via Snail-mediated MT1-MMP upregulation. *Tumour Biol.*
- Quante, M., S.P. Tu, H. Tomita, T. Gonda, S.S. Wang, S. Takashi, G.H. Baik, W. Shibata, B. Diprete, K.S. Betz, R. Friedman, A. Varro, B. Tycko, and T.C. Wang. 2011. Bone marrow-derived myofibroblasts contribute to the mesenchymal stem cell niche and promote tumor growth. *Cancer Cell.* 19:257-272.
- Radisky, D.C., P.A. Kenny, and M.J. Bissell. 2007. Fibrosis and cancer: do myofibroblasts come also from epithelial cells via EMT? *J Cell Biochem.* 101:830-839.
- Radtke, F., H. Clevers, and O. Riccio. 2006. From gut homeostasis to cancer. *Curr Mol Med.* 6:275-289.

- Rajfur, Z., P. Roy, C. Otey, L. Romer, and K. Jacobson. 2002. Dissecting the link between stress fibres and focal adhesions by CALI with EGFP fusion proteins. *Nat Cell Biol.* 4:286-293.
- Rantala, J.K., J. Pouwels, T. Pellinen, S. Veltel, P. Laasola, E. Mattila, C.S. Potter, T. Duffy, J.P. Sundberg, O. Kallioniemi, J.A. Askari, M.J. Humphries, M. Parsons, M. Salmi, and J. Ivaska. 2011. SHARPIN is an endogenous inhibitor of beta1-integrin activation. *Nat Cell Biol.* 13:1315-1324.
- Retta, S.F., S.T. Barry, D.R. Critchley, P. Defilippi, L. Silengo, and G. Tarone. 1996. Focal adhesion and stress fiber formation is regulated by tyrosine phosphatase activity. *Exp Cell Res.* 229:307-317.
- Rhim, A.D., P.E. Oberstein, D.H. Thomas, E.T. Mirek, C.F. Palermo, S.A. Sastra, E.N. Dekleva, T. Saunders, C.P. Becerra, I.W. Tattersall, C.B. Westphalen, J. Kitajewski, M.G. Fernandez-Barrena, M.E. Fernandez-Zapico, C. Iacobuzio-Donahue, K.P. Olive, and B.Z. Stanger. 2014. Stromal elements act to restrain, rather than support, pancreatic ductal adenocarcinoma. *Cancer Cell.* 25:735-747.
- Ricard-Blum, S. 2011. The collagen family. *Cold Spring Harb Perspect Biol.* 3:a004978.
- Ricard-Blum, S., and L. Ballut. 2011. Matricryptins derived from collagens and proteoglycans. *Front Biosci (Landmark Ed).* 16:674-697.
- Ricard-Blum, S., and F. Ruggiero. 2005. The collagen superfamily: from the extracellular matrix to the cell membrane. *Pathol Biol (Paris).* 53:430-442.
- Riching, K.M., B.L. Cox, M.R. Salick, C. Pehlke, A.S. Riching, S.M. Ponik, B.R. Bass, W.C. Crone, Y. Jiang, A.M. Weaver, K.W. Eliceiri, and P.J. Keely. 2014. 3D collagen alignment limits protrusions to enhance breast cancer cell persistence. *Biophys J.* 107:2546-2558.
- Ridley, A.J., M.A. Schwartz, K. Burridge, R.A. Firtel, M.H. Ginsberg, G. Borisy, J.T. Parsons, and A.R. Horwitz. 2003. Cell migration: integrating signals from front to back. *Science.* 302:1704-1709.
- Roca-Cusachs, P., A. del Rio, E. Puklin-Faucher, N.C. Gauthier, N. Biais, and M.P. Sheetz. 2013a. Integrin-dependent force transmission to the extracellular matrix by alpha-actinin triggers adhesion maturation. *Proc Natl Acad Sci U S A.* 110:E1361-1370.
- Roca-Cusachs, P., R. Sunyer, and X. Trepac. 2013b. Mechanical guidance of cell migration: lessons from chemotaxis. *Curr Opin Cell Biol.* 25:543-549.
- Ronnov-Jessen, L., and O.W. Petersen. 1993. Induction of alpha-smooth muscle actin by transforming growth factor-beta 1 in quiescent human breast gland fibroblasts. Implications for myofibroblast generation in breast neoplasia. *Lab Invest.* 68:696-707.
- Ross, J.B., D. Huh, L.B. Noble, and S.F. Tavazoie. 2015. Identification of molecular determinants of primary and metastatic tumour re-initiation in breast cancer. *Nat Cell Biol.* 17:651-664.
- Ross, R., J. Glomset, B. Kariya, and L. Harker. 1974. A platelet-dependent serum factor that stimulates the proliferation of arterial smooth muscle cells in vitro. *Proc Natl Acad Sci U S A.* 71:1207-1210.
- Rosse, C., C. Lodillinsky, L. Fuhrmann, M. Nourieh, P. Monteiro, M. Irondelle, E. Lagoutte, S. Vacher, F. Waharte, P. Paul-Gilloteaux, M. Romao, L. Sengmanivong, M. Linch, J. van Lint, G. Raposo, A. Vincent-Salomon, I. Bieche, P.J. Parker, and P. Chavrier. 2014. Control of MT1-MMP transport by atypical PKC during breast-cancer progression. *Proc Natl Acad Sci U S A.* 111:E1872-1879.

- Rossier, O., V. Oceau, J.B. Sibarita, C. Leduc, B. Tessier, D. Nair, V. Gatterdam, O. Destaing, C. Albiges-Rizo, R. Tampe, L. Cognet, D. Choquet, B. Lounis, and G. Giannone. 2012. Integrins beta1 and beta3 exhibit distinct dynamic nanoscale organizations inside focal adhesions. *Nat Cell Biol.* 14:1057-1067.
- Rowe, R.G., X.Y. Li, Y. Hu, T.L. Saunders, I. Virtanen, A. Garcia de Herreros, K.F. Becker, S. Ingvarsen, L.H. Engelholm, G.T. Bommer, E.R. Fearon, and S.J. Weiss. 2009. Mesenchymal cells reactivate Snail1 expression to drive three-dimensional invasion programs. *J Cell Biol.* 184:399-408.
- Rozario, T., and D.W. DeSimone. 2010. The extracellular matrix in development and morphogenesis: a dynamic view. *Dev Biol.* 341:126-140.
- Sabeh, F., R. Shimizu-Hirota, and S.J. Weiss. 2009. Protease-dependent versus -independent cancer cell invasion programs: three-dimensional amoeboid movement revisited. *J Cell Biol.* 185:11-19.
- Sahai, E. 2005. Mechanisms of cancer cell invasion. *Curr Opin Genet Dev.* 15:87-96.
- Sakai, T., M. Larsen, and K.M. Yamada. 2003. Fibronectin requirement in branching morphogenesis. *Nature.* 423:876-881.
- Sakurai-Yageta, M., C. Recchi, G. Le Dez, J.B. Sibarita, L. Daviet, J. Camonis, C. D'Souza-Schorey, and P. Chavrier. 2008. The interaction of IQGAP1 with the exocyst complex is required for tumor cell invasion downstream of Cdc42 and RhoA. *J Cell Biol.* 181:985-998.
- Salgia, R., J.L. Li, D.S. Ewaniuk, Y.B. Wang, M. Sattler, W.C. Chen, W. Richards, E. Pisick, G.I. Shapiro, B.J. Rollins, L.B. Chen, J.D. Griffin, and D.J. Sugarbaker. 1999. Expression of the focal adhesion protein paxillin in lung cancer and its relation to cell motility. *Oncogene.* 18:67-77.
- Sansom, O.J., K.R. Reed, A.J. Hayes, H. Ireland, H. Brinkmann, I.P. Newton, E. Battle, P. Simon-Assmann, H. Clevers, I.S. Nathke, A.R. Clarke, and D.J. Winton. 2004. Loss of Apc in vivo immediately perturbs Wnt signaling, differentiation, and migration. *Genes Dev.* 18:1385-1390.
- Sanz-Moreno, V., C. Gaggioli, M. Yeo, J. Albregues, F. Wallberg, A. Viros, S. Hooper, R. Mitter, C.C. Feral, M. Cook, J. Larkin, R. Marais, G. Meneguzzi, E. Sahai, and C.J. Marshall. 2011. ROCK and JAK1 signaling cooperate to control actomyosin contractility in tumor cells and stroma. *Cancer Cell.* 20:229-245.
- Sanz-Moreno, V., and C.J. Marshall. 2009. Rho-GTPase signaling drives melanoma cell plasticity. *Cell Cycle.* 8:1484-1487.
- Sawaya, R., B.L. Ligon, A.K. Bindal, R.K. Bindal, and K.R. Hess. 1996. Surgical treatment of metastatic brain tumors. *J Neurooncol.* 27:269-277.
- Scanlan, M.J., B.K. Raj, B. Calvo, P. Garin-Chesa, M.P. Sanz-Moncasi, J.H. Healey, L.J. Old, and W.J. Rettig. 1994. Molecular cloning of fibroblast activation protein alpha, a member of the serine protease family selectively expressed in stromal fibroblasts of epithelial cancers. *Proc Natl Acad Sci U S A.* 91:5657-5661.
- Schiller, H.B., M.R. Hermann, J. Polleux, T. Vignaud, S. Zanivan, C.C. Friedel, Z. Sun, A. Raducanu, K.E. Gottschalk, M. Thery, M. Mann, and R. Fassler. 2013. beta1- and alphaV-class integrins cooperate to regulate myosin II during rigidity sensing of fibronectin-based microenvironments. *Nat Cell Biol.* 15:625-636.

- Schoumacher, M., R.D. Goldman, D. Louvard, and D.M. Vignjevic. 2010. Actin, microtubules, and vimentin intermediate filaments cooperate for elongation of invadopodia. *J Cell Biol.* 189:541-556.
- Schubbert, S., K. Shannon, and G. Bollag. 2007. Hyperactive Ras in developmental disorders and cancer. *Nat Rev Cancer.* 7:295-308.
- Schulte, J., M. Weidig, P. Balzer, P. Richter, M. Franz, K. Junker, M. Gajda, K. Friedrich, H. Wunderlich, A. Ostman, I. Petersen, and A. Berndt. 2012. Expression of the E-cadherin repressors Snail, Slug and Zeb1 in urothelial carcinoma of the urinary bladder: relation to stromal fibroblast activation and invasive behaviour of carcinoma cells. *Histochem Cell Biol.* 138:847-860.
- Schwartz, M.A. 2010. Integrins and extracellular matrix in mechanotransduction. *Cold Spring Harb Perspect Biol.* 2:a005066.
- Schwarzbauer, J.E. 1991. Identification of the fibronectin sequences required for assembly of a fibrillar matrix. *J Cell Biol.* 113:1463-1473.
- Sechler, J.L., A.M. Cumiskey, D.M. Gazzola, and J.E. Schwarzbauer. 2000. A novel RGD-independent fibronectin assembly pathway initiated by alpha4beta1 integrin binding to the alternatively spliced V region. *J Cell Sci.* 113 (Pt 8):1491-1498.
- Serrels, B., A. Serrels, V.G. Brunton, M. Holt, G.W. McLean, C.H. Gray, G.E. Jones, and M.C. Frame. 2007. Focal adhesion kinase controls actin assembly via a FERM-mediated interaction with the Arp2/3 complex. *Nat Cell Biol.* 9:1046-1056.
- Shattil, S.J., C. Kim, and M.H. Ginsberg. 2010. The final steps of integrin activation: the end game. *Nat Rev Mol Cell Biol.* 11:288-300.
- Shi, F., J. Harman, K. Fujiwara, and J. Sottile. 2010. Collagen I matrix turnover is regulated by fibronectin polymerization. *Am J Physiol Cell Physiol.* 298:C1265-1275.
- Shimoda, M., S. Principe, H.W. Jackson, V. Luga, H. Fang, S.D. Molyneux, Y.W. Shao, A. Aiken, P.D. Waterhouse, C. Karamboulas, F.M. Hess, T. Ohtsuka, Y. Okada, L. Ailles, A. Ludwig, J.L. Wrana, T. Kislinger, and R. Khokha. 2014. Loss of the Timp gene family is sufficient for the acquisition of the CAF-like cell state. *Nat Cell Biol.* 16:889-901.
- Shinagawa, K., Y. Kitadai, M. Tanaka, T. Sumida, M. Onoyama, M. Ohnishi, E. Ohara, Y. Higashi, S. Tanaka, W. Yasui, and K. Chayama. 2013. Stroma-directed imatinib therapy impairs the tumor-promoting effect of bone marrow-derived mesenchymal stem cells in an orthotopic transplantation model of colon cancer. *Int J Cancer.* 132:813-823.
- Shyer, A.E., T. Tallinen, N.L. Nerurkar, Z. Wei, E.S. Gil, D.L. Kaplan, C.J. Tabin, and L. Mahadevan. 2013. Villification: how the gut gets its villi. *Science.* 342:212-218.
- Siegel, P.M., and J. Massague. 2003. Cytostatic and apoptotic actions of TGF-beta in homeostasis and cancer. *Nat Rev Cancer.* 3:807-821.
- Simons, B.D., and H. Clevers. 2011. Strategies for homeostatic stem cell self-renewal in adult tissues. *Cell.* 145:851-862.
- Simons, M., and G. Raposo. 2009. Exosomes--vesicular carriers for intercellular communication. *Curr Opin Cell Biol.* 21:575-581.
- Sivakumar, L., and G. Agarwal. 2010. The influence of discoidin domain receptor 2 on the persistence length of collagen type I fibers. *Biomaterials.* 31:4802-4808.
- Small, J.V., T. Stradal, E. Vignal, and K. Rottner. 2002. The lamellipodium: where motility begins. *Trends Cell Biol.* 12:112-120.
- Smith, H.W., and C.J. Marshall. 2010. Regulation of cell signalling by uPAR. *Nat Rev Mol Cell Biol.* 11:23-36.

- Sottile, J., and D.F. Mosher. 1997. N-terminal type I modules required for fibronectin binding to fibroblasts and to fibronectin's III1 module. *Biochem J.* 323 (Pt 1):51-60.
- Stanisavljevic, J., J. Loubat-Casanovas, M. Herrera, T. Luque, R. Pena, A. Lluch, J. Albanell, F. Bonilla, A. Rovira, C. Pena, D. Navajas, F. Rojo, A. Garcia de Herreros, and J. Baulida. 2015. Snail1-expressing fibroblasts in the tumor microenvironment display mechanical properties that support metastasis. *Cancer Res.* 75:284-295.
- Steffen, A., G. Le Dez, R. Poincloux, C. Recchi, P. Nassoy, K. Rottner, T. Galli, and P. Chavrier. 2008. MT1-MMP-dependent invasion is regulated by TI-VAMP/VAMP7. *Curr Biol.* 18:926-931.
- Stepp, M.A., W.P. Daley, A.M. Bernstein, S. Pal-Ghosh, G. Tadvalkar, A. Shashurin, S. Palsen, R.A. Jurjus, and M. Larsen. 2010. Syndecan-1 regulates cell migration and fibronectin fibril assembly. *Exp Cell Res.* 316:2322-2339.
- Sugiyama, N., E. Gucciardo, O. Tatti, M. Varjosalo, M. Hyytiainen, M. Gstaiger, and K. Lehti. 2013. EphA2 cleavage by MT1-MMP triggers single cancer cell invasion via homotypic cell repulsion. *J Cell Biol.* 201:467-484.
- Sun, Z., S.S. Guo, and R. Fassler. 2016. Integrin-mediated mechanotransduction. *J Cell Biol.* 215:445-456.
- Sung, B.H., T. Ketova, D. Hoshino, A. Zijlstra, and A.M. Weaver. 2015. Directional cell movement through tissues is controlled by exosome secretion. *Nat Commun.* 6:7164.
- Sunyer, R., V. Conte, J. Escribano, A. Elosegui-Artola, A. Labernadie, L. Valon, D. Navajas, J.M. Garcia-Aznar, J.J. Munoz, P. Roca-Cusachs, and X. Trepat. 2016. Collective cell durotaxis emerges from long-range intercellular force transmission. *Science.* 353:1157-1161.
- Tadokoro, S., S.J. Shattil, K. Eto, V. Tai, R.C. Liddington, J.M. de Pereda, M.H. Ginsberg, and D.A. Calderwood. 2003. Talin binding to integrin beta tails: a final common step in integrin activation. *Science.* 302:103-106.
- Takahashi, S., M. Leiss, M. Moser, T. Ohashi, T. Kitao, D. Heckmann, A. Pfeifer, H. Kessler, J. Takagi, H.P. Erickson, and R. Fassler. 2007. The RGD motif in fibronectin is essential for development but dispensable for fibril assembly. *J Cell Biol.* 178:167-178.
- Takano, K., K. Toyooka, and S. Suetsugu. 2008. EFC/F-BAR proteins and the N-WASP-WIP complex induce membrane curvature-dependent actin polymerization. *EMBO J.* 27:2817-2828.
- Takino, T., R. Nagao, R. Manabe, T. Domoto, K. Sekiguchi, and H. Sato. 2011. Membrane-type 1 matrix metalloproteinase regulates fibronectin assembly to promote cell motility. *FEBS Lett.* 585:3378-3384.
- Talele, N.P., J. Fradette, J.E. Davies, A. Kapus, and B. Hinz. 2015. Expression of alpha-Smooth Muscle Actin Determines the Fate of Mesenchymal Stromal Cells. *Stem Cell Reports.* 4:1016-1030.
- Tanaka, T., H. Kohno, R. Suzuki, K. Hata, S. Sugie, N. Niho, K. Sakano, M. Takahashi, and K. Wakabayashi. 2006. Dextran sodium sulfate strongly promotes colorectal carcinogenesis in Apc(Min/+) mice: inflammatory stimuli by dextran sodium sulfate results in development of multiple colonic neoplasms. *Int J Cancer.* 118:25-34.
- Taniwaki, K., H. Fukamachi, K. Komori, Y. Ohtake, T. Nonaka, T. Sakamoto, T. Shiomi, Y. Okada, T. Itoh, S. Itoharu, M. Seiki, and I. Yana. 2007. Stroma-derived matrix metalloproteinase (MMP)-2 promotes membrane type 1-MMP-dependent tumor growth in mice. *Cancer Res.* 67:4311-4319.

- Tatin, F., C. Varon, E. Genot, and V. Moreau. 2006. A signalling cascade involving PKC, Src and Cdc42 regulates podosome assembly in cultured endothelial cells in response to phorbol ester. *J Cell Sci.* 119:769-781.
- Teckchandani, A., N. Toida, J. Goodchild, C. Henderson, J. Watts, B. Wollscheid, and J.A. Cooper. 2009. Quantitative proteomics identifies a Dab2/integrin module regulating cell migration. *J Cell Biol.* 186:99-111.
- Tessier-Lavigne, M. 1994. Axon guidance by diffusible repellants and attractants. *Curr Opin Genet Dev.* 4:596-601.
- Tetu, B., J. Brisson, C.S. Wang, H. Lapointe, G. Beaudry, C. Blanchette, and D. Trudel. 2006. The influence of MMP-14, TIMP-2 and MMP-2 expression on breast cancer prognosis. *Breast Cancer Res.* 8:R28.
- Thery, C., S. Amigorena, G. Raposo, and A. Clayton. 2006. Isolation and characterization of exosomes from cell culture supernatants and biological fluids. *Curr Protoc Cell Biol.* Chapter 3:Unit 3 22.
- Theveneau, E., B. Steventon, E. Scarpa, S. Garcia, X. Trepast, A. Streit, and R. Mayor. 2013. Chase-and-run between adjacent cell populations promotes directional collective migration. *Nat Cell Biol.* 15:763-772.
- Thiery, J.P. 2002. Epithelial-mesenchymal transitions in tumour progression. *Nature Reviews Cancer.* 2:442-454.
- Tomasek, J.J., G. Gabbiani, B. Hinz, C. Chaponnier, and R.A. Brown. 2002. Myofibroblasts and mechano-regulation of connective tissue remodelling. *Nat Rev Mol Cell Biol.* 3:349-363.
- Tsushima, H., N. Ito, S. Tamura, Y. Matsuda, M. Inada, I. Yabuuchi, Y. Imai, R. Nagashima, H. Misawa, H. Takeda, Y. Matsuzawa, and S. Kawata. 2001. Circulating transforming growth factor beta 1 as a predictor of liver metastasis after resection in colorectal cancer. *Clin Cancer Res.* 7:1258-1262.
- Tweedy, L., D.A. Knecht, G.M. Mackay, and R.H. Insall. 2016. Self-Generated Chemoattractant Gradients: Attractant Depletion Extends the Range and Robustness of Chemotaxis. *PLoS Biol.* 14:e1002404.
- Valentin, G., P. Haas, and D. Gilmour. 2007. The chemokine SDF1a coordinates tissue migration through the spatially restricted activation of Cxcr7 and Cxcr4b. *Curr Biol.* 17:1026-1031.
- Van Bockstal, M., K. Lambein, M. Van Gele, E. De Vlieghere, R. Limame, G. Braems, R. Van den Broecke, V. Cocquyt, H. Denys, M. Bracke, L. Libbrecht, and O. De Wever. 2014. Differential regulation of extracellular matrix protein expression in carcinoma-associated fibroblasts by TGF-beta1 regulates cancer cell spreading but not adhesion. *Oncoscience.* 1:634-648.
- Van Obberghen-Schilling, E., R.P. Tucker, F. Saupe, I. Gasser, B. Cseh, and G. Orend. 2011. Fibronectin and tenascin-C: accomplices in vascular morphogenesis during development and tumor growth. *Int J Dev Biol.* 55:511-525.
- Velling, T., J. Risteli, K. Wennerberg, D.F. Mosher, and S. Johansson. 2002. Polymerization of type I and III collagens is dependent on fibronectin and enhanced by integrins alpha 11beta 1 and alpha 2beta 1. *J Biol Chem.* 277:37377-37381.
- Venning, F.A., L. Wullkopf, and J.T. Ertler. 2015. Targeting ECM Disrupts Cancer Progression. *Front Oncol.* 5:224.
- Vermeulen, L., E.M.F. De Sousa, M. van der Heijden, K. Cameron, J.H. de Jong, T. Borovski, J.B. Tuijnman, M. Todaro, C. Merz, H. Rodermond, M.R. Sprick, K. Kemper, D.J.

- Richel, G. Stassi, and J.P. Medema. 2010. Wnt activity defines colon cancer stem cells and is regulated by the microenvironment. *Nat Cell Biol.* 12:468-476.
- von Wichert, G., G. Jiang, A. Kostic, K. De Vos, J. Sap, and M.P. Sheetz. 2003. RPTP-alpha acts as a transducer of mechanical force on alpha5/beta3-integrin-cytoskeleton linkages. *J Cell Biol.* 161:143-153.
- Wang, F., V.M. Weaver, O.W. Petersen, C.A. Larabell, S. Dedhar, P. Briand, R. Lupu, and M.J. Bissell. 1998. Reciprocal interactions between beta1-integrin and epidermal growth factor receptor in three-dimensional basement membrane breast cultures: a different perspective in epithelial biology. *Proc Natl Acad Sci U S A.* 95:14821-14826.
- Wang, N., J.P. Butler, and D.E. Ingber. 1993. Mechanotransduction across the cell surface and through the cytoskeleton. *Science.* 260:1124-1127.
- Wang, X.M., D.M. Yu, G.W. McCaughan, and M.D. Gorrell. 2005. Fibroblast activation protein increases apoptosis, cell adhesion, and migration by the LX-2 human stellate cell line. *Hepatology.* 42:935-945.
- Weaver, A.M. 2006. Invadopodia: specialized cell structures for cancer invasion. *Clin Exp Metastasis.* 23:97-105.
- Weaver, A.M. 2008. Invadopodia. *Curr Biol.* 18:R362-364.
- Weaver, A.M., J.E. Heuser, A.V. Karginov, W.L. Lee, J.T. Parsons, and J.A. Cooper. 2002. Interaction of cortactin and N-WASp with Arp2/3 complex. *Curr Biol.* 12:1270-1278.
- Weaver, A.M., A.V. Karginov, A.W. Kinley, S.A. Weed, Y. Li, J.T. Parsons, and J.A. Cooper. 2001. Cortactin promotes and stabilizes Arp2/3-induced actin filament network formation. *Curr Biol.* 11:370-374.
- Weaver, V.M., O.W. Petersen, F. Wang, C.A. Larabell, P. Briand, C. Damsky, and M.J. Bissell. 1997. Reversion of the malignant phenotype of human breast cells in three-dimensional culture and in vivo by integrin blocking antibodies. *J Cell Biol.* 137:231-245.
- Wei, Y., R.P. Czekay, L. Robillard, M.C. Kugler, F. Zhang, K.K. Kim, J.P. Xiong, M.J. Humphries, and H.A. Chapman. 2005. Regulation of alpha5beta1 integrin conformation and function by urokinase receptor binding. *J Cell Biol.* 168:501-511.
- Wierzbicka-Patynowski, I., and J.E. Schwarzbauer. 2003. The ins and outs of fibronectin matrix assembly. *J Cell Sci.* 116:3269-3276.
- Wilson, E., K. Sudhir, and H.E. Ives. 1995. Mechanical strain of rat vascular smooth muscle cells is sensed by specific extracellular matrix/integrin interactions. *J Clin Invest.* 96:2364-2372.
- Winograd-Katz, S.E., R. Fassler, B. Geiger, and K.R. Legate. 2014. The integrin adhesome: from genes and proteins to human disease. *Nat Rev Mol Cell Biol.* 15:273-288.
- Wolanska, K.I., and M.R. Morgan. 2015. Fibronectin remodelling: cell-mediated regulation of the microenvironment. *Biochem Soc Trans.* 43:122-128.
- Wolf, K., S. Alexander, V. Schacht, L.M. Coussens, U.H. von Andrian, J. van Rheenen, E. Deryugina, and P. Friedl. 2009. Collagen-based cell migration models in vitro and in vivo. *Semin Cell Dev Biol.* 20:931-941.
- Wolf, K., and P. Friedl. 2011. Extracellular matrix determinants of proteolytic and non-proteolytic cell migration. *Trends Cell Biol.* 21:736-744.
- Wolf, K., I. Mazo, H. Leung, K. Engelke, U.H. von Andrian, E.I. Deryugina, A.Y. Strongin, E.B. Brocker, and P. Friedl. 2003a. Compensation mechanism in tumor cell migration: mesenchymal-amoeboid transition after blocking of pericellular proteolysis. *J Cell Biol.* 160:267-277.

- Wolf, K., R. Muller, S. Borgmann, E.B. Brocker, and P. Friedl. 2003b. Amoeboid shape change and contact guidance: T-lymphocyte crawling through fibrillar collagen is independent of matrix remodeling by MMPs and other proteases. *Blood*. 102:3262-3269.
- Wolf, K., M. Te Lindert, M. Krause, S. Alexander, J. Te Riet, A.L. Willis, R.M. Hoffman, C.G. Figdor, S.J. Weiss, and P. Friedl. 2013. Physical limits of cell migration: control by ECM space and nuclear deformation and tuning by proteolysis and traction force. *J Cell Biol*. 201:1069-1084.
- Woo, M.S., Y. Ohta, I. Rabinovitz, T.P. Stossel, and J. Blenis. 2004. Ribosomal S6 kinase (RSK) regulates phosphorylation of filamin A on an important regulatory site. *Mol Cell Biol*. 24:3025-3035.
- Wozniak, M.A., K. Modzelewska, L. Kwong, and P.J. Keely. 2004. Focal adhesion regulation of cell behavior. *Biochim Biophys Acta*. 1692:103-119.
- Yamada, K.M., and B. Geiger. 1997. Molecular interactions in cell adhesion complexes. *Curr Opin Cell Biol*. 9:76-85.
- Yana, I., and S.J. Weiss. 2000. Regulation of membrane type-1 matrix metalloproteinase activation by proprotein convertases. *Mol Biol Cell*. 11:2387-2401.
- Yao, L., C.D. McCaig, and M. Zhao. 2009. Electrical signals polarize neuronal organelles, direct neuron migration, and orient cell division. *Hippocampus*. 19:855-868.
- Yi, E.S., H. Lee, S. Yin, P. Piguette, I. Sarosi, S. Kaufmann, J. Tarpley, N.S. Wang, and T.R. Ulich. 1996. Platelet-derived growth factor causes pulmonary cell proliferation and collagen deposition in vivo. *Am J Pathol*. 149:539-548.
- Yu, Y.P., and J.H. Luo. 2006. Myopodin-mediated suppression of prostate cancer cell migration involves interaction with zyxin. *Cancer Res*. 66:7414-7419.
- Yuan, W., T.M. Leisner, A.W. McFadden, Z. Wang, M.K. Larson, S. Clark, C. Boudignon-Proudhon, S.C. Lam, and L.V. Parise. 2006. CIB1 is an endogenous inhibitor of agonist-induced integrin α IIb β 3 activation. *J Cell Biol*. 172:169-175.
- Zaidel-Bar, R., C. Ballestrem, Z. Kam, and B. Geiger. 2003. Early molecular events in the assembly of matrix adhesions at the leading edge of migrating cells. *J Cell Sci*. 116:4605-4613.
- Zaidel-Bar, R., M. Cohen, L. Addadi, and B. Geiger. 2004. Hierarchical assembly of cell-matrix adhesion complexes. *Biochem Soc Trans*. 32:416-420.
- Zaidel-Bar, R., and B. Geiger. 2010. The switchable integrin adhesome. *J Cell Sci*. 123:1385-1388.
- Zaidel-Bar, R., S. Itzkovitz, A. Ma'ayan, R. Iyengar, and B. Geiger. 2007a. Functional atlas of the integrin adhesome. *Nat Cell Biol*. 9:858-867.
- Zaidel-Bar, R., R. Milo, Z. Kam, and B. Geiger. 2007b. A paxillin tyrosine phosphorylation switch regulates the assembly and form of cell-matrix adhesions. *J Cell Sci*. 120:137-148.
- Zamir, E., and B. Geiger. 2001. Components of cell-matrix adhesions. *J Cell Sci*. 114:3577-3579.
- Zeisberg, E.M., S. Potenta, L. Xie, M. Zeisberg, and R. Kalluri. 2007. Discovery of endothelial to mesenchymal transition as a source for carcinoma-associated fibroblasts. *Cancer Res*. 67:10123-10128.
- Zhang, B., X. Cao, Y. Liu, W. Cao, F. Zhang, S. Zhang, H. Li, L. Ning, L. Fu, Y. Niu, R. Niu, B. Sun, and X. Hao. 2008. Tumor-derived matrix metalloproteinase-13 (MMP-13) correlates with poor prognoses of invasive breast cancer. *BMC Cancer*. 8:83.

- Zhang, W., L.M. Matrisian, K. Holmbeck, C.C. Vick, and E.L. Rosenthal. 2006. Fibroblast-derived MT1-MMP promotes tumor progression in vitro and in vivo. *BMC Cancer*. 6:52.
- Zhang, X.H., X. Jin, S. Malladi, Y. Zou, Y.H. Wen, E. Brogi, M. Smid, J.A. Foekens, and J. Massague. 2013. Selection of bone metastasis seeds by mesenchymal signals in the primary tumor stroma. *Cell*. 154:1060-1073.
- Zhao, M. 2009. Electrical fields in wound healing-An overriding signal that directs cell migration. *Semin Cell Dev Biol*. 20:674-682.
- Zhao, M., B. Song, J. Pu, T. Wada, B. Reid, G. Tai, F. Wang, A. Guo, P. Walczysko, Y. Gu, T. Sasaki, A. Suzuki, J.V. Forrester, H.R. Bourne, P.N. Devreotes, C.D. McCaig, and J.M. Penninger. 2006. Electrical signals control wound healing through phosphatidylinositol-3-OH kinase-gamma and PTEN. *Nature*. 442:457-460.
- Zheng, X., J.L. Carstens, J. Kim, M. Scheible, J. Kaye, H. Sugimoto, C.C. Wu, V.S. LeBleu, and R. Kalluri. 2015. Epithelial-to-mesenchymal transition is dispensable for metastasis but induces chemoresistance in pancreatic cancer. *Nature*. 527:525-530.